

IAEA Analytical Quality in Nuclear Applications Series No. 49

In Situ Analytical Characterization of Contaminated Sites Using Nuclear Spectrometry Techniques

Review of Methodologies and Measurements



IN SITU ANALYTICAL
CHARACTERIZATION OF
CONTAMINATED SITES USING NUCLEAR
SPECTROMETRY TECHNIQUES

The following States are Members of the International Atomic Energy Agency:

AFGHANISTAN	GEORGIA	OMAN
ALBANIA	GERMANY	PAKISTAN
ALGERIA	GHANA	PALAU
ANGOLA	GREECE	PANAMA
ANTIGUA AND BARBUDA	GUATEMALA	PAPUA NEW GUINEA
ARGENTINA	GUYANA	PARAGUAY
ARMENIA	HAITI	PERU
AUSTRALIA	HOLY SEE	PHILIPPINES
AUSTRIA	HONDURAS	POLAND
AZERBAIJAN	HUNGARY	PORTUGAL
BAHAMAS	ICELAND	QATAR
BAHRAIN	INDIA	REPUBLIC OF MOLDOVA
BANGLADESH	INDONESIA	ROMANIA
BARBADOS	IRAN, ISLAMIC REPUBLIC OF	RUSSIAN FEDERATION
BELARUS	IRAQ	RWANDA
BELGIUM	IRELAND	SAN MARINO
BELIZE	ISRAEL	SAUDI ARABIA
BENIN	ITALY	SENEGAL
BOLIVIA, PLURINATIONAL STATE OF	JAMAICA	SERBIA
BOSNIA AND HERZEGOVINA	JAPAN	SEYCHELLES
BOTSWANA	JORDAN	SIERRA LEONE
BRAZIL	KAZAKHSTAN	SINGAPORE
BRUNEI DARUSSALAM	KENYA	SLOVAKIA
BULGARIA	KOREA, REPUBLIC OF	SLOVENIA
BURKINA FASO	KUWAIT	SOUTH AFRICA
BURUNDI	KYRGYZSTAN	SPAIN
CAMBODIA	LAO PEOPLE'S DEMOCRATIC REPUBLIC	SRI LANKA
CAMEROON	LATVIA	SUDAN
CANADA	LEBANON	SWAZILAND
CENTRAL AFRICAN REPUBLIC	LESOTHO	SWEDEN
CHAD	LIBERIA	SWITZERLAND
CHILE	LIBYA	SYRIAN ARAB REPUBLIC
CHINA	LIECHTENSTEIN	TAJIKISTAN
COLOMBIA	LITHUANIA	THAILAND
CONGO	LUXEMBOURG	THE FORMER YUGOSLAV REPUBLIC OF MACEDONIA
COSTA RICA	MADAGASCAR	TOGO
CÔTE D'IVOIRE	MALAWI	TRINIDAD AND TOBAGO
CROATIA	MALAYSIA	TUNISIA
CUBA	MALI	TURKEY
CYPRUS	MALTA	TURKMENISTAN
CZECH REPUBLIC	MARSHALL ISLANDS	UGANDA
DEMOCRATIC REPUBLIC OF THE CONGO	MAURITANIA	UKRAINE
DENMARK	MAURITIUS	UNITED ARAB EMIRATES
DJIBOUTI	MEXICO	UNITED KINGDOM OF GREAT BRITAIN AND NORTHERN IRELAND
DOMINICA	MONACO	UNITED REPUBLIC OF TANZANIA
DOMINICAN REPUBLIC	MONGOLIA	UNITED STATES OF AMERICA
ECUADOR	MONTENEGRO	URUGUAY
EGYPT	MOROCCO	UZBEKISTAN
EL SALVADOR	MOZAMBIQUE	VANUATU
ERITREA	MYANMAR	VENEZUELA, BOLIVARIAN REPUBLIC OF
ESTONIA	NAMIBIA	VIET NAM
ETHIOPIA	NEPAL	YEMEN
FIJI	NETHERLANDS	ZAMBIA
FINLAND	NEW ZEALAND	ZIMBABWE
FRANCE	NICARAGUA	
GABON	NIGER	
	NIGERIA	
	NORWAY	

The Agency's Statute was approved on 23 October 1956 by the Conference on the Statute of the IAEA held at United Nations Headquarters, New York; it entered into force on 29 July 1957. The Headquarters of the Agency are situated in Vienna. Its principal objective is "to accelerate and enlarge the contribution of atomic energy to peace, health and prosperity throughout the world".

IAEA Analytical Quality in Nuclear Applications Series No. 49

IN SITU ANALYTICAL
CHARACTERIZATION OF
CONTAMINATED SITES USING NUCLEAR
SPECTROMETRY TECHNIQUES
REVIEW OF METHODOLOGIES AND MEASUREMENTS

COPYRIGHT NOTICE

All IAEA scientific and technical publications are protected by the terms of the Universal Copyright Convention as adopted in 1952 (Berne) and as revised in 1972 (Paris). The copyright has since been extended by the World Intellectual Property Organization (Geneva) to include electronic and virtual intellectual property. Permission to use whole or parts of texts contained in IAEA publications in printed or electronic form must be obtained and is usually subject to royalty agreements. Proposals for non-commercial reproductions and translations are welcomed and considered on a case-by-case basis. Enquiries should be addressed to the IAEA Publishing Section at:

Marketing and Sales Unit, Publishing Section
International Atomic Energy Agency
Vienna International Centre
PO Box 100
1400 Vienna, Austria
fax: +43 1 2600 29302
tel.: +43 1 2600 22417
email: sales.publications@iaea.org
<http://www.iaea.org/books>

For further information on this publication, please contact:

Terrestrial Environment Laboratory, Seibersdorf
International Atomic Energy Agency
2444 Seibersdorf, Austria
Email: Official.Mail@iaea.org

IN SITU ANALYTICAL CHARACTERIZATION OF CONTAMINATED SITES USING NUCLEAR SPECTROMETRY TECHNIQUES

IAEA, VIENNA, 2017

IAEA/AQ/49

ISSN 2074-7659

© IAEA, 2017

Printed by the IAEA in Austria

July 2017

FOREWORD

Past and current human activities can result in the contamination of sites by radionuclides and heavy metals. The sources of contamination are various. The most important sources for radionuclide release include global fallout from nuclear testing, nuclear and radiological accidents, waste production from nuclear facilities, and activities involving naturally occurring radioactive material (NORM). Contamination of the environment by heavy metals mainly originates from industrial applications and mineralogical background concentration.

Contamination of sites by radionuclides and heavy metals can present a risk to people and the environment. Therefore, the estimation of the contamination level and the identification of the source constitute important information for the national authorities with the responsibility to protect people and the environment from adverse health effects.

In situ analytical techniques based on nuclear spectrometry are important tools for the characterization of contaminated sites. Much progress has been made in the design and implementation of portable systems for efficient and effective monitoring of radioactivity and heavy metals in the environment directly on-site. Accordingly, the IAEA organized a Technical Meeting to review the current status and trends of various applications of in situ nuclear spectrometry techniques for analytical characterization of contaminated sites and to support Member States in their national environmental monitoring programmes applying portable instrumentation.

This publication represents a comprehensive review of the in situ gamma ray spectrometry and field portable X ray fluorescence analysis techniques for the characterization of contaminated sites. It includes papers on the use of these techniques, which provide useful background information for conducting similar studies, in the following Member States: Argentina, Australia, Brazil, Czech Republic, Egypt, France, Greece, Hungary, Italy, Lithuania, Montenegro, Spain, United States of America and Uruguay.

The IAEA wishes to thank all the participants of the Technical Meeting for their valuable contributions, in particular C. Tsabaris (Greece) and E. Margui (Spain), who assisted in the drafting and editing of this publication. The IAEA officers responsible for this publication were A. Ceccatelli and A. Pitois of the IAEA Environment Laboratories, and A.G. Karydas of the Division of Physical and Chemical Sciences.

EDITORIAL NOTE

This publication has been prepared from the original material as submitted by the contributors and has not been edited by the editorial staff of the IAEA. The views expressed remain the responsibility of the contributors and do not necessarily reflect those of the IAEA or the governments of its Member States.

This publication has not been edited by the editorial staff of the IAEA. It does not address questions of responsibility, legal or otherwise, for acts or omissions on the part of any person.

The use of particular designations of countries or territories does not imply any judgement by the publisher, the IAEA, as to the legal status of such countries or territories, of their authorities and institutions or of the delimitation of their boundaries.

The mention of names of specific companies or products (whether or not indicated as registered) does not imply any intention to infringe proprietary rights, nor should it be construed as an endorsement or recommendation on the part of the IAEA.

The contributors are responsible for having obtained the necessary permission for the IAEA to reproduce, translate or use material from sources already protected by copyrights.

The IAEA has no responsibility for the persistence or accuracy of URLs for external or third party Internet web sites referred to in this publication and does not guarantee that any content on such web sites is, or will remain, accurate or appropriate.

CONTENTS

1. INTRODUCTION.....	1
2. GENERAL CONSIDERATIONS AND STRATEGIES FOR SAMPLING, MEASUREMENT AND MAPPING USING IN-SITU METHODS.....	2
2.1. Routine outdoor environmental monitoring.....	2
2.2. Characterization of outdoor contaminated sites (Remediation monitoring).....	2
3. BASICS ON IN-SITU GAMMA-RAY SPECTROMETRY.....	5
3.1. Basic principles of the method.....	5
3.2. Available instrumentation.....	6
3.3. System calibration.....	7
3.4. Measurement and quantification procedure.....	8
3.5. Analytical applications.....	9
3.6. Uncertainty estimation.....	10
3.7. QC/QA considerations.....	11
3.8. Advantages and limitations of the method.....	12
3.9. Complementary laboratory techniques.....	12
3.10. Future developments and trends.....	13
4. BASICS ON FIELD-PORTABLE X-RAY FLUORESCENCE ANALYSIS	13
4.1. Basic principles of the method.....	13
4.2. Instrumentation: Review, current status and developments.....	14
4.3. Measurement, calibration and quantification methodology.....	16
4.4. Sample preparation.....	18
4.5. Analytical applications.....	19
4.6. Uncertainty estimation.....	20
4.7. QC/QA considerations.....	20
4.8. Advantages and limitations of the method.....	22
4.9. Complementary laboratory techniques.....	23
4.10. Future developments and trends.....	24
CONCLUSION.....	24
APPENDIX I: IN-SITU CAPABILITIES AND STUDY SITES IN COUNTRIES REPRESENTED IN THE TECHNICAL MEETING.....	25
I.1. Available instrumentation and applications.....	25
I.2. Potential sites to be surveyed by portable instrumentation.....	27
APPENDIX II: LIST OF PARTICIPANTS.....	29
REFERENCES.....	31
ANNEX: CONTRIBUTED PAPERS.....	35
Journey monitoring system, Argentina.....	35
<i>A.M. Castellanos, A. Novello, H. Blanco Bello, A. Carelli, M. Dominguez, C. Laise, H. Spinelli</i>	

Considerations for an automated system to detect ‘hot’ particles, Australia.....	41
<i>S.A. Long, L.J. Martin, E.M. Carey</i>	
An optimized NaI(Tl) multi-detector method for the determination of spatial contamination in urban areas, Brazil.....	53
<i>M.C.F. Moreira, C.C. Conti, R. Schirru</i>	
Evolution of radioactive contamination in Ploucnice river basin (Bohemia) due to uranium mining in the period 1992-2009, Czech Republic.....	59
<i>E. Hanslik, P. Simek, D. Ivanovova, M. Novak, M. Komarek</i>	
Occupational exposure for working staff in the Egyptian ceramic industry, Egypt.....	75
<i>M.R. Ezz El-Din, R.A.M. Rizk, R.M. Mohamed, H.M. Diab</i>	
In-situ methods for characterization of contaminated sites, France.....	81
<i>D. Dubot, J. Attiogbe</i>	
Fifteen year experience of the nuclear technology laboratory of the Aristotle University of Thessaloniki in the technique of in-situ gamma-ray spectrometry: Presentation of the major results, Greece.....	89
<i>A. Clouvas, S. Xanthos, G. Takoudis, M. Antonopoulos-Domis, J. Guilhot</i>	
In-situ radionuclide quantitative characterization in aquatic ecosystems using the Katerina detector, Greece.....	101
<i>C. Tsabaris, D.L. Patiris, G. Eleftheriou, M. Kokkoris, R. Vlastou</i>	
Measurement with the mobile laboratory of the Hungarian Academy of Sciences KFKI Atomic Energy Research Institute, Hungary.....	107
<i>K. Bodor, A. Nagy</i>	
Experience at the Istituto Superiore di Sanita on environmental research and monitoring with in-situ techniques, Italy.....	119
<i>C. Nuccetelli, D.M. Castelluccio, E. Cisbani, S. Frullani</i>	
Experience of investigation of contaminated sites in Lithuania, Lithuania.....	133
<i>L. Pilkyte</i>	
The effective solid angle concept and ANGLE v3.0 computer code for semiconductor detector gamma-efficiency calculations – Applicability to in-situ characterization of contaminated sites, Montenegro.....	141
<i>S. Jovanovic, A. Dlabac, N. Mihaljevic</i>	
Possibilities and drawbacks of portable XRF instrumentation for characterization of metal contaminated sites, Spain.....	159
<i>E. Margui</i>	
Environmental radioactivity monitoring plan in Uruguay, Uruguay.....	173
<i>M. del R. Odino Moure, E. Reina, L. Piuma, A. Gabrielli</i>	

Recent advances in hand-held XRF for site remediation, USA.....	183
<i>J.I.H. Patterson</i>	
CONTRIBUTORS TO DRAFTING AND REVIEW.....	189

1. INTRODUCTION

Accidental, intentional or authorized releases from past and current human activities such as mineral exploration and mining, production of electrical energy and other peaceful or military applications, can result in a legacy of contaminated land or aquatic ecosystems. The legal definition of whether an ecosystem is ‘contaminated’ varies from country to country, but at least such a definition is based on the estimation of the concentration of the contaminant present (being, for example, a metal, metalloid or a specific radionuclide). For a contaminated land, for example, the so-called Soil Screening Values (SVs) are used as generic quality standards adopted by many countries to regulate the management of contaminated land. They are usually in the form of concentration thresholds of contaminants above which certain actions are recommended or enforced. Implications of exceeding SVs vary according to national regulatory frameworks. They range from the need for further investigations to remedial actions or restrictions on land use.

In order to investigate, control and regulate a contaminated site, the direct in-situ characterization (meaning that the analytical instrument is taken to and placed over or in contact with the sampling area) is an important alternative or complement to procedures involving laboratory analysis of field samples. Direct in-situ characterization supports and improves the quality of analytical data from a contaminated site. It is adopted by many national authorities as a tool in decision-making policies through site-specific risk assessment.

In this context, the in-situ implementation of nuclear spectrometry techniques and other complementary methods has reached a high level of analytical performance and offers certain advantages over other more traditional characterization procedures of a contaminated site, including:

- Rapid determination of contaminant concentrations/activities in many spots/areas across the contaminated site without time-consuming sample collection and preparation;
- Fine-tuning of the contaminant spatial distribution, with immediate real-time identification of areas of interest (‘hot-spot’ areas), allowing further investigation of these areas with better spatial resolution;
- Cost reduction for all the stages of assessment, decommissioning and remediation processes.

This publication, which is an output from a Technical Meeting organized by the IAEA, highlights, reviews and discusses issues related to the current status and trends of various applications of in-situ nuclear spectrometry techniques for analytical characterization of contaminated sites. The advantages and limitations of employing the techniques in various fields of application are assessed in order to encourage effective support of scientific and technological development.

2. GENERAL CONSIDERATIONS AND STRATEGIES FOR SAMPLING, MEASUREMENT AND MAPPING USING IN-SITU METHODS

2.1. ROUTINE OUTDOOR ENVIRONMENTAL MONITORING

For routine outdoor environmental monitoring, systematic monitoring programmes are performed mainly based on periodical monitoring of the same points/coordinates. These points are chosen on the basis of the matrices to be analysed (air, soil, vegetation, water, seawater, river water, biota, sediment, etc) and the location and characteristics of the known or expected sources of contamination.

Routine environmental monitoring is carried out using two procedures:

- Collecting samples and measuring them in the laboratory with an appropriate analytical technique;
- Measuring directly in the field, using a monitoring equipment item (gamma-ray spectrometer, dose-rate meter, etc).

2.2. CHARACTERIZATION OF OUTDOOR CONTAMINATED SITES (REMEDIATION MONITORING)

The practical procedure for surface characterization of outdoor contaminated sites can be divided into the following phases:

- Development of an investigation plan

This includes the collection of background information on the site, selection of sampling approach and selection of measurement points. All available information that is directly or indirectly related to the contaminated site is initially collected and reviewed to support the preparation of an appropriate investigation plan, i.e. site history, site use, past studies, etc. The appropriate sampling approach among the following approaches, i.e. judgmental, random, stratified random, systematic random, systematic grid, search and transect sampling approaches [1], is then selected for representative contaminant measurements, depending upon the type and distribution of the contaminants. The systematic grid approach is often used to delineate the extent of contamination and to define contaminants' concentration gradients. It is based on the subdivision of the area of study in a geometric grid, in which the measurements are carried out at the intersections of the grid lines. The size of the area of study and the number of measurements determine the distance between measurement locations in the systematic grid. The search approach is often used to determine 'hot-spots'. The grid spacing and the number of measurements is then determined by the acceptable error of missing a 'hot-spot'. The smaller the acceptable error is, the smaller the grid spacing should be. Similarly, the smaller the 'hot-spot' is, the smaller the grid should be to locate it. The use of the search approach is illustrated in the contribution by Long et al. later in this publication.

- Measurements according to the investigation plan

Measurements along boundaries and according to the investigation plan are carried out using the appropriate in-situ analytical technique in order to delineate the extent of contamination, to define contaminants' concentration gradients and to geo-reference 'hot-spots'.

To obtain a better spatial resolution and better defined boundaries the measurement points are identified on the basis of the pre-defined grid or using a mobile laboratory/vehicle equipped with detection tools. The number of replicates at each measurement location is based on statistical and geo-statistical approaches based on estimation of the mean value and the standard deviation associated to the spatial distribution of contamination [2]. When identified, 'hot-spots' can be photographed and marked with a flag. A non-contaminated control area with similar geology and in immediate proximity of the area of study should be identified and used for evaluation of background level.

- Quality assurance of measurement results

For quality assurance purposes samples should be collected at 5 to 10% of the total measurement locations. Those samples are then brought to the laboratory for repeated or longer measurements using the appropriate laboratory analytical technique so as to get more accurate and independent measurement results. These laboratory-based measurement results are compared to the measurement results obtained in the field.

The procedure for characterizing contaminant depth profiles is defined as follows:

- Elaboration of a plan for defining the contaminant depth profile based on purpose

This includes the determination of the minimum number of points to apply a geo-statistical treatment according to the purpose and the set confidence level [3]. For example, the number of samples and the profiles' chosen characteristics will not be the same whether you build a car park on the area to rehabilitate, or a residence where a family lives. The number of samples to be analysed and the chosen depth and resolution of the profile to be sampled also depend on the contaminant type (e.g. gamma-emitter radionuclide, heavy metal or other contaminant), its migration potential in soil sub-layers and the characteristics of the analytical technique used.

- Measurement of contaminant depth profile

Measurement of contaminant depth profile is carried out to characterize depth patterns of contamination in soil. Representative samples of soil core sections need to be obtained for this purpose. Typically sampling of 20 cm soil core sections is carried out for surveys from 2 to 3 meter deep, and sampling of 50 cm to 1 meter is carried out for surveys with depths greater than 10 meters. The soil core sections are then brought to the laboratory and each core section is homogenized after removal of any extraneous material. Measurements using the appropriate laboratory analytical technique are carried out on each homogenized core section. Similarly, depth profile studies are also performed in a non-contaminated control area with similar geology and in immediate proximity of the area of study for evaluation of soil core sections' background levels. It is necessary to implement prior surveys in 'hot-spots', and increase polls density in areas where the probability of contamination is higher, or exceeds a fixed activity level. Broad experience was gained in France with the characterization of surface and depth distribution of contaminants [4].

One suitable tool for collecting depth incremental sections of soil and/or sediment with a good accuracy is the Fine Incremental Soil Collector (FISC) developed by the Soil and Water Management and Crop Nutrition Laboratory of the Joint FAO/IAEA Division of Nuclear Techniques in Food and Agriculture. The FISC system consists of a short stainless steel core tube that is inserted into the soil/sediment surface; and a tripod system to collect soil/sediment increments with the desired accuracy after the extraction of the tube [5].

The tripod includes an inner Teflon plateau extruder connected to a screw system that enables users to easily remove the material from the inside of the tube. The tube diameter can be designed according to the desired quantity of soil/sediment needed. The soil/sediment contained in the tube after field extraction can be sliced to the desired increment with a sharp plate tool and set on the tripod system for processing. The FISC is suitable to sample most mineral and organic cohesive soil/sediment types provided that they have a relatively low content of coarse particles. This tool can also be used for the characterization of top soil contamination.

- Correlations and interpretation

Correlation between depth profile and soil geology may be helpful for further data analysis and interpretation, since contaminant migration is dependent on soil type and chemical nature of the contaminant.

Information on the characterization of a contaminated area with presence of ‘hot-spots’ is presented below with a focus on the in-situ gamma-ray spectrometry technique.

- Instrumentation

To perform a first screening of the contaminated area and identify the ‘hot-spots’, a dose-rate meter is used. As, usually, high dose-rate gradients can be found around ‘hot-spots’ and it is not always possible to get close to the radioactive source, it can be necessary to apply mathematical/geometrical approaches to calculate the real distance of the source from the measurement point.

After the identification of a ‘hot-spot’, detectors such as sodium iodide NaI(Tl) spectrometers, surface contamination monitors, high-performance Germanium (HPGe) detectors or plastic scintillators can be used to get more detailed information regarding radionuclides and activity levels. Recording in real-time each measurement channel for all the detectors used and combining this information with a GPS, it is possible to obtain a large amount of data for statistical and geo-statistical analysis in order to map the resulting data stream of the screened area [3].

- Utility of mapping techniques based on mobile laboratories and vehicle detectors

Mobile laboratories and vehicle detectors allow the identification of ‘hot-spots’ in a very large area. Besides, a real-time transmission of data to other laboratories/institutions involved in decision-making process (such as national or international authorities) allows for a faster response especially in emergency situations. In case of a radiological accident a meteorological station can be included in mobile laboratories to obtain information on climate conditions. In emergency situations in-situ techniques based on mobile laboratories and/or vehicle detectors are the only ones that can provide faster responses than laboratory methods.

- Problems/difficulties in mapping procedures

One of the main problems in mapping procedures regards the non-uniformity of activity distribution with depth. Consequently, after identification of ‘hot-spots’ using a vehicle detector it is recommended to perform a repeated manual scan of the contaminated area using portable detectors. The area to be scanned can be divided in sections using a grid. In some cases, in-situ techniques are not sufficient to provide reliable results and it can be necessary to perform further measurements in the laboratory (i.e. using gamma-ray spectrometry).

Moreover, ‘hot-spot’ identification demands the use of a collimator, whose shape and size can highly affect the detector response.

Destructive measurements of sample in the laboratory can be necessary if the contaminant is not a gamma-emitting radionuclide. Alpha contamination, in particular, can only be accurately measured in the laboratory.

3. BASICS ON IN-SITU GAMMA-RAY SPECTROMETRY

3.1. BASIC PRINCIPLES OF THE METHOD

Gamma-ray spectrometry is a well-known technique for identification and quantification of the specific activity of gamma-emitting radionuclides. The basic principles of the method are based on associating detected peaks in a gamma-ray spectrum with characteristic photon energies that serve as a fingerprint for the nuclides that have been measured. Although most commonly applied to the measurement of samples in a laboratory setting, the application of gamma-ray spectrometry to measurements in the field has become increasingly prominent in later years. The most common application of in-situ gamma-ray spectrometry is the measurement of radionuclide activity levels in the ground, for example for contaminated site characterization of fallout radionuclides or surveying of naturally occurring radionuclides. However, there are countless numbers of other applications of in-situ gamma-ray spectrometry, some of which will be described in detail later in this publication.

In-situ gamma-ray spectrometry for the purpose of site characterization is most commonly performed with the detector pointing down towards the ground at 1 m height, supported from a purpose-built tripod. The detector can be collimated or uncollimated based on the size of the area that is surveyed. A gamma-ray spectrum is then accrued for a time period long enough to sufficiently quantify, or prove the absence of, the radionuclides of interest. The count rates of relevant photopeaks are then converted into activity concentration (typically Bq/kg or Bq/m²), taking into account the detector response to photon fluences from different incident angles as well as the vertical distribution of activity in the ground.

In-situ gamma-ray spectrometry was first applied to the measurement of fallout radionuclides from nuclear weapons testing as well as background radionuclides in the 1960’s [6, 7] with the first elaborate method description published in 1972 by Beck et al. [8]. Early applications of in-situ gamma-ray spectrometry were carried out using NaI(Tl) detectors, however portable HPGe gamma-ray spectrometers for in-situ applications were commercially available by the beginning of the 1980’s. Application of the method increased substantially due to the Chernobyl accident, a fact also reflected by the vastly increased number of scientific publications since that time. Updated method descriptions on in-situ gamma-ray spectrometry were published during the 1990’s through ICRU report 53 [9] and by Miller and Shebell [10] among others. The method is mentioned in IAEA-TECDOC-1017 for characterization of contaminated sites for remediation purposes [11], and in IAEA-TECDOC-1092 as a generic procedure for monitoring following a nuclear or radiological emergency [12]. In 2014, an ISO Guide for in-situ measurements of gamma-emitting radionuclides in soil was published [13]. Major advances have in later years been made to software analysis routines: various spectral methods (like unfolding, stripping, etc) have been developed for improving the analysis of gamma-ray spectra, and most traditional corrections (for example geometry and coincidence summing corrections) are now included in most commercially available software.

Additionally, codes have also been developed for simulating the in-situ instrumentation and improving their sensitivity. The evolution in the technology of computers has permitted the use of Monte Carlo simulations of counting efficiencies, making it easier to apply in-situ gamma-ray spectrometry to the measurement of a wide range of objects including barrels, pipes and contaminated equipment items.

3.2. AVAILABLE INSTRUMENTATION

A typical in-situ gamma-ray spectrometry setup consists of a detector crystal (scintillator or semiconductor type) connected to an electronics chain where signals from photon interactions in the detector crystal are reshaped, amplified, digitized and sorted into bins which comprise the final gamma-ray spectrum. Nowadays digital Multi-Channels Analyzers (MCA) (external or tube-based), incorporating all traditional electronics modules, are readily available. These instruments can be powered directly from the USB port of a laptop computer, making the systems fully portable and autonomous without the need for external power during measurements. Moreover, USB or Ethernet connectivity includes auxiliary interfaces and flexible architecture for specific in-situ and real-time applications using advanced data acquisition options. The power consumption is low (<1 W) and the systems are accompanied by gamma-ray acquisition/analysis software. In some newer units, such as the Canberra Falcon 5000 or the Ortec Detective, all necessary electronics are contained in the same unit as the detector itself.

The capability of an in-situ gamma-ray spectrometry system depends very much on the type of detector crystal. The ‘gold standard’ is the High Purity Germanium (HPGe) detector, which is widely used for radiological characterization of indoor/outdoor environments (artificial and natural radionuclides) in routine and emergency situations, and has been applied in both terrestrial and aquatic environments. High purity germanium detectors are characterized by their high energy resolution with a typical value of 1.4 keV for ^{137}Cs . Portable germanium detectors now exist with relative efficiencies $>50\%$. Specific broad energy HPGe detectors (BEGe) are also applied for the detection of low energy gamma-ray and X-ray emitting radionuclides (such as Pu isotopes, ^{210}Pb , ^{55}Fe , etc). HPGe detectors need to operate at cryogenic temperatures (-160°C or lower), temperature that has traditionally been achieved using liquid nitrogen. However, newer HPGe detection systems can now operate in portable mode with electrically-cooled systems. The presence of portable electrically-cooled systems negates the need of liquid nitrogen supplies in remote areas. The power consumption of such systems is around 100 W in cooling phase and 30 W during normal operation, with autonomous operation of 8 hours or longer using hot-swappable batteries.

Another type of semiconductor detector type used for radiation detection is Cadmium Zinc Telluride (CZT) or Cadmium Telluride (CT). These detectors can operate in direct-conversion (or photoconductive) mode at room temperature, and have a relatively high sensitivity for X-rays and gamma-rays, due to the high atomic numbers of Cd and Te, as well as better energy resolution than scintillation detectors (typically $<2\%$ for 661.6 keV). The CZT and CT detectors can be formed into different shapes for different applications, and a variety of electrode geometries, such as coplanar grids, have been developed to provide unipolar (electron-only) operation, thereby improving energy resolution. Only small volume detectors of up to about 1 cm^3 are commercially available, which means that they are most suitable for medium to high activity applications when used for in-situ gamma-ray spectrometry. CZT detectors were, for example, employed for radiological site characterization measurements following the Fukushima accident [14].

The most common type of scintillator detector for in-situ gamma-ray spectrometry is NaI(Tl). These detectors typically have dimensions of 1x1 to 3x3 inches for portable applications, however larger volume systems with a volume of several litres are often used in mobile and airborne applications. The power consumption of these detection systems is relatively low (1.5 W – 2.4 W), they are light, relatively low cost and flexible in use. The main disadvantage when NaI(Tl) operates as a spectrometer is the poor energy resolution (typically 6-8% for 661.6 keV) and spectrum instability with temperature variations. NaI(Tl) systems are also used in underwater applications for real-time monitoring of the aquatic environment. In addition, they are suitable for environmental gamma dose-rate measurements in low dose ranges from ~10 nGy/h to ~20 µGy/h.

LaBr₃ detectors offer improved energy resolution compared to NaI(Tl), fast scintillation emission, excellent stability with temperature and linearity characteristics. Typical energy resolution at 662 keV is ~3-4%, which is much lower than the one for a NaI(Tl) detector at the same energy (~6-8%). These detectors are already widely used for in-situ environmental radioactivity applications. One major disadvantage of LaBr₃ detectors is that they are internally contaminated with ¹³⁸La, which emits a gamma line at 1435.8 keV that interferes with the ⁴⁰K peak at 1460.8 keV. Recently available on the market, CeBr₃ detectors now offer similar resolution while significantly diminishing the problem of the intrinsic contamination. Both LaBr₃ and CeBr₃ detectors with dimensions of 3x3 inches are now commercially available, albeit at a significantly higher price than NaI(Tl) detectors of similar size.

Plastic scintillator crystals have been studied theoretically for in-situ applications, but are rarely used in practice. A plastic scintillator consists of a solid solution of organic scintillating molecules in a polymerized solvent. They are useful since they can be easily shaped and fabricated according to the intended application. Since they have a short decay time, on the order of a nanosecond, plastic scintillators are suitable in fast timing applications. However, the resolution is generally poor compared to the other detector types.

3.3. SYSTEM CALIBRATION

The purpose of the detector efficiency calibration is to relate the net peak count rate for a nuclide of interest to the activity concentration of the nuclide in the source or object that is measured. Efficiency calibration was, and still is, a challenging topic. There are, in principle, three approaches: empirical, mathematical and semi-empirical calibration.

The most commonly applied empirical calibration method for detectors used in in-situ gamma-ray spectrometry was first proposed by Beck et al. [8] for the measurements of radionuclides in the ground. The basic principle of the method is to separate the calibration factor into three sub-factors: normal response factor, angular correction factor and source geometry factor. The normal response and angular correction factors are based on measurements of point sources at different angles of incidence relative to the detector crystal, while the source geometry factor requires previous knowledge or qualified assumptions of the vertical activity distribution of the source. Other empirical calibration methods involve producing calibration sources which are similar to the source geometry of interest; however this method is often not practicable as it is often not feasible or even possible to produce realistic calibration sources. Calibrations can also be created or modified based on measurement results from samples taken at the measurement point. For example, core samples can be taken from a measurement site to get an indication of the vertical activity distribution in the case of in-situ gamma-ray spectrometric measurements of activity in the ground.

Mathematical (Monte Carlo) calibration is in theory statistically exact; nevertheless it requires absolute knowledge of the counting details (about the detector, source, intercepting layers and lots of nuclear, chemical and physical data). Theory was developed long ago, but practical applicability had to wait for the new computer generation. It is suited for in-situ measurements, since mathematical characterization of the actual conditions is possible. Commercial software is available for efficiency calculations in in-situ gamma-ray spectrometry. Some assume factory characterization of the detector, and offer a broad variety of measurement objects for which the efficiency calibration can be calculated. Other codes (like GEANT4, MCNP5, FLUKA, etc) are more general and require significant user input for code utilization.

Semi-empirical methods are numerous, combining advantages and minimizing drawbacks of the two previous calibrations. Typically they involve extrapolating known efficiencies from measurements of a reference source to the experimental counting geometry. These methods can be accommodated practically in any gamma-ray spectrometry counting situation. Such software is broadly applied (using both the laboratory and in-situ methods). The numerous options available for both mathematical and semi-empirical calibration approaches can sometimes appear a bit confusing and it can in some cases be difficult to know which code is most appropriate for a specific application. However, recent comparisons between the different available software packages show that there are generally only minor differences in the results calculated by different software codes [15].

A specific experimental calibration approach for the detector efficiency in water is performed in the laboratory in a water tank with stable conditions and specific dimensions dependent on the photon energies of interest. For energies up to 1460 keV the minimum radius of the tank is about 1.1 m, and is defined as the effective radius for the specific gamma-ray energy. The tank is filled with water and various certified reference sources (like ^{137}Cs , KCl , ^{111}In , $^{99\text{m}}\text{Tc}$ and others) are diluted in the tank. The acquired spectra offer the efficiency values at the emission energies of the calibration sources [16].

3.4. MEASUREMENT AND QUANTIFICATION PROCEDURE

Procedures for in-situ gamma-ray spectrometry will vary greatly based on the specific application of the method. In general, the detector should be positioned appropriately relative to the source of interest (ground, water, barrel, pipe, equipment, etc) using a collimator or filter as appropriate. Once a suitable setup has been achieved, a spectrum is acquired for a time period that gives a sufficient number of net counts in the areas of photopeaks of interest. Activity concentrations are calculated from the spectrum either manually or by using the software.

Available software for HPGe gamma-ray spectrometry generally allows for performing two types of analysis: qualitative analysis (spectroscopy) for nuclide identification, and quantitative analysis (spectrometry) for calculation of activities or activity concentrations of the identified nuclides. The latter is based on efficiency calibrations which have been previously carried out in a controlled environment, or have been generated mathematically. Spectrum analysis software is often the same for in-situ and laboratory-based gamma-ray spectrometry systems, and most of the commonly used software packages now include the possibility of doing both spectroscopy and spectrometry by taking into account efficiency calibration, nuclear data and all relevant correction factors. Additionally, some software packages offer the possibility of other spectral analyses techniques such as adding and subtracting spectra, spectrum normalization, etc.

The quantitative determination of activity concentration using in-situ gamma-ray spectrometry is not as accurate as for the laboratory-based systems due to difficulties in estimating the source geometry for the efficiency calculation/estimation. Whereas in the laboratory the efficiency is accurately and directly measured using certified reference sources, the efficiency in in-situ gamma-ray spectrometry will at least in some part be based on assumptions and approximations.

However, one significant benefit of in-situ gamma-ray spectrometry compared to laboratory analyses of samples is that in-situ gamma-ray spectrometry is much less sensitive to heterogeneities in the source distribution compared to sampling, thus gives an estimate of the average in a large volume of material. In-situ gamma-ray spectrometry and laboratory analyses of samples generally go hand in hand to provide the optimal compromise between accuracy and representativeness of the measurement results.

3.5. ANALYTICAL APPLICATIONS

The range of applications for in-situ gamma-ray spectrometry continuously keeps growing, which makes it difficult to provide an exhaustive overview. Thus, this section will focus on mentioning only the applications described later in the publication. A more general overview of some previous applications of ground-based and airborne in-situ gamma-ray spectrometry can be found in the literature [17]. Applied to marine monitoring, in-situ gamma-ray spectrometry has been used both for continuous monitoring as well as for mapping of specific aquatic sites [18-23]. Scintillation detectors have even been used for space applications [24].

Applications of in-situ gamma-ray spectrometry described later in this publication include:

- An automatic ‘hot’ particle detection system, using an array of four NaI(Tl) detectors mounted on a vehicle, was used to locate ‘hot’ particles in the Maralinga nuclear testing site in southern Australia. The detector array is connected to a single channel analyzer set to count gamma rays of approximately 60 keV, and suitable for finding Am-241 particles with an activity of 100 kBq or greater [25]. The use of fixed distance counting intervals means that the spatial relationship of the data is preserved regardless of scanning speed.
- A multiple NaI(Tl) detector array arranged in different layouts (e.g. cross or inverted T-shape) combined with Monte Carlo methods and Artificial Neural Networks (ANN) to assess the multi-directional contamination activity of urban surfaces and indication of angle of incidence has been developed in Brazil [26]. The approach can be used to indicate highly contaminated surfaces in a given area or even the direction where a radioactive source might be found, saving extra dose to the survey team and making it very useful for field surveys.
- Dedicated vehicles with comprehensive detection capabilities (VEgAS) in combination with recently developed software and the ‘KARTOTRAK’ platform have been realized at the French Alternative Energies and Atomic Energy Commission. It allows for real-time geo-referencing of results, including interpolation between measurement points, to deliver accurate and reliable maps [3, 4]. This makes the platform an important tool to facilitate the decision-making processes.

- At the Aristotle University of Thessaloniki, in-situ gamma-ray spectrometry has been used for numerous applications, including calculating photon fluences from gamma-ray spectra using Monte Carlo methods [27], computing nuclide-specific dose-rates [28], measuring gamma dose-rates in dwellings and workplaces [29-31], and detection of radioactive sources in scrap metal [32]. An overview is provided in the contribution by Clouvas et al. later in this publication.
- The ‘KATERINA’ autonomous NaI(Tl) underwater detectors, developed at the Hellenic Centre for Marine Research in Greece, are set up in a specialized frame (incorporating memory and a microcontroller) together with batteries for autonomous operation up to 3 months. Their main purpose is to characterize radioactivity levels of a specific site and detect whether increased radioactivity signals may be present, e.g. from submarine ground discharges, coastal industry, oil industry, etc [19].
- In-situ gamma-ray spectrometry is used for fast identification and quantification of environmental radionuclides as part of a suite of tools for radiological environmental monitoring in a mobile laboratory in Hungary. Measurement results are then used to support decision-making processes. This is further described in the contribution from Bodor and Nagy later in this publication.
- The ‘SNIFFER’ aerial platform for radiological emergencies has been designed and developed by Italian Universities/Research Institutes in collaboration with governmental bodies. The platform is equipped with a peculiar air sampling unit and gamma-ray detectors (NaI(Tl) and HPGe) able to give a quantitative characterization of atmospheric and ground radioactive contamination including geo-referencing [33]. There has also been an extensive work done on using in-situ gamma-ray spectrometry to calculate specific radionuclide components of the dose-rate in dwellings. This is further described in the contribution by Nuccetelli et al. later in this publication.
- In Lithuania, in-situ gamma-ray spectrometry is used to investigate and characterize different sites, including a site where the soil was contaminated with ^{226}Ra , detection of depleted uranium in debris following a fighter jet accident and investigation of plots for a new NPP. In some cases the results were also used to calculate potential dose-rates to the public due to contamination. This is further described in the contribution by Pilkyte later in this publication.
- The ‘ANGLE’ efficiency transfer software has been applied to in-situ gamma-ray spectrometric measurements. It allows for computing the efficiency of a range of different objects, including infinite slab and infinite Marinelli geometries suitable for measurements of radioactivity in the ground. In addition to the wide applicability, the software boasts high accuracy, short computing times, an intuitive and easy-to-use graphical user interface and compatibility with spectrum acquisition software [34, 35].

3.6. UNCERTAINTY ESTIMATION

The main sources of measurement uncertainty in in-situ gamma-ray spectrometry are:

- Peak counting statistics in photopeaks of interest. As for traditional gamma-ray spectrometry peak counts follow the Poisson distribution, which means that small peaks have a high relative uncertainty. This is generally associated with low radionuclide activities or short measurement times;

- Uncertainty in the peaked background correction of the net peak area, due to lack of knowledge about background levels at the measurement point, temporal or spatial variability of the background, or use of different collimators;
- Dead-time and pile-up corrections from high radionuclide activities;
- Uncertainty in the empirical or mathematical detector calibration, including discrepancies between the assumed and true source distribution (i.e. differences in geometry, density and chemical composition between calibration and sample parameters). The calculation of calibration factors and their uncertainty can also be done by employing Monte Carlo techniques [36];
- Effects of external influences such as bias voltage instability, temperature and humidity variations, radiofrequency noise, etc, which may indirectly affect the peak position and/or the peak area determination.

The estimation of the combined measurement uncertainty involves taking into account all significant uncertainty contributions according to the Guide to the Expression of Uncertainty in Measurement (GUM) [37]. The complexity of the measurement model, as well as the assumptions used for the calculation of the measurement result, may make it difficult to properly estimate the overall uncertainty. In such cases, the use of Monte Carlo uncertainty estimations [38] could be useful. In general, the overall relative uncertainty of a measurement performed using in-situ gamma-ray spectrometry is in the range of 15-30% ($k = 1$), with the main contributors being peak counting statistics and detector calibration.

3.7. QC/QA CONSIDERATIONS

Quality control (QC) for in-situ gamma-ray spectrometry is based on periodical checks similar to the ones carried out for a laboratory-based gamma-ray spectrometry system, with some slight modifications. This includes the check of zero and gain stability, energy calibration, energy resolution stability, efficiency and background stability. Relevant parameters are then evaluated by control charts. It is recommended to monitor the parameters on a regular basis, even when the detector is not in use. For HPGe detectors, parameters should be checked after any warming-up event. The energy calibration should ideally be controlled even during measurement campaigns to uncover any gain instability when moving from one measurement point to another. In order to assert the successful performance of the detector system in different possible scenarios, the detector response should be investigated as a function of varying environmental parameters (temperature, humidity) and for high count rates.

Procedures related to the calibration, operation and maintenance of systems used for in-situ gamma-ray spectrometry should be thoroughly documented in written form and organized in a quality management system. These procedures should have information related to quality assurance (QA), e.g. data recording, trackability and traceability of the measurement results. Measurement methods should be validated to ensure that they are fit for purpose. This includes evaluating the accuracy, precision, representability, repeatability, reproducibility, specificity, etc, of the method, and by comparing measurement results to those obtained by other techniques or procedures. Further quality assurance measures include participating in national or international intercomparison exercises, performing measurements at regional reference sites or of reference materials, and participating in audits and peer-reviews. More information about quality assurance and quality control programs can be found in ISO Guide 18589-7:2013 [11].

3.8. ADVANTAGES AND LIMITATIONS OF THE METHOD

In-situ techniques present the following advantages:

- In-situ techniques allow performing an exhaustive characterization of the whole surface and effective localization of ‘hot-spots’ in real-time;
- Measurements are fast and relatively low-cost;
- Compared to sampling, in-situ techniques are much less affected by heterogeneities in the source activity. This means that a result from in-situ measurements is more likely to be representative of the measurement point than the laboratory measurement result of a sample taken at the same location;
- It is possible to perform side-by-side measurements, utilizing several detectors, and comparing the measurement results;
- Measuring ranges are close to those of laboratory-based systems.

In-situ techniques present the following disadvantages/limitations:

- Efficiency calibration using in-situ systems exhibits less accuracy as compared to laboratory-based systems. Standard field calibration sources do not exist, while in the laboratory the sample may be placed and counted in a geometry for which a replicate traceable standard is available;
- The characteristics of the in-situ gamma-ray spectrometry system and its intrinsic background variability produce higher minimum detectable activity (MDA) as compared to the one obtained with a laboratory-based system;
- In emergency situation an in-situ system requires the protection of the equipment items and of the operator from contamination and physical damage;
- Climate conditions can affect the measurement process;
- Power autonomy limits long-term operations, since the batteries of some units have to be recharged. For HPGe detectors, operating time can also be limited by availability of liquid nitrogen to cool the system;
- Detectors placed in ground-based or airborne vehicles can be shielded from the source by the vehicle itself, and the correction factors for this are not well-known.

3.9. COMPLEMENTARY LABORATORY TECHNIQUES

Complementary laboratory techniques are very important to compare measurement results obtained with in-situ methods for gamma-emitting radionuclides, and essential to get accurate results for alpha- and beta-emitting radionuclides.

These complementary laboratory techniques are divided in two categories:

- Destructive techniques, such as radiochemical separation and use of alpha-particle spectrometry for the measurement of alpha-emitting radionuclides, radiochemical separation/ ^3H and ^{14}C treatment and use of liquid scintillation counting (LSC) for the measurement of beta-emitter radionuclides, use of ICP-MS, etc.

Some of those techniques can also be performed in mobile laboratories except ICP-MS, whose application in vehicle units is very limited;

- Non-destructive techniques, such as gamma-ray spectrometry, X-ray fluorescence (XRF), geophysical measurements (to get physical properties like density, grain size, humidity), geochemical measurement (to get chemical properties like acidity).

3.10. FUTURE DEVELOPMENTS AND TRENDS

Some future developments and trends related to in-situ gamma-ray spectrometry and dose-rate measurement for environmental applications are as follows:

- Further development of portable and mobile LaBr₃ and CeBr₃ autonomous detectors for in-situ gamma-ray spectrometry;
- Development of alpha and gamma cameras for in-situ applications;
- Development of sensors for chemical in-situ measurements;
- Software development for real-time automated analysis and nuclide identification;
- Survey of contaminated sites using Remote Operated Vehicles (ROV) and/or the Unmanned Aircraft Vehicle (UAV) technology to in-situ approaches;
- Use of segmented detector crystals for in-situ applications;
- Systematic studies of intercomparison exercises between various in-situ and laboratory-based systems, standardization of sampling procedures and reporting mapping results to optimize QA;
- Optimization/streamlining of the whole process to reduce the costs.

4. BASICS ON FIELD PORTABLE X-RAY FLUORESCENCE ANALYSIS (FPXRF)

4.1. BASIC PRINCIPLES OF THE METHOD

The basic physics principles of XRF spectrometry are based on energy transformation and transitions of electrons within an atom. The electrons are bound to their atom by a specific amount of energy known as binding energy or ionization energy. This is the amount of energy that is required to remove an electron from its atom.

X-rays produced by various available sources (e.g. radioisotopes, X-ray tubes or synchrotrons) with energy that exceeds ionization threshold can be absorbed by an inner-shell atomic electron (photoelectric absorption) and eject it to the continuum creating thus a corresponding inner-shell hole and an unstable excited atomic state. As the atom returns to its lowest energy state, an electron from an outer shell fills the vacancy, emitting a characteristic X-ray (or an electron, Auger process) with energy equal to the difference between the binding energies of the shells involved in the de-excitation process. The combined process that is characterized first by the X-ray induced inner-shell ionization and the subsequent fluorescent emission due to an inter-atomic electronic transition is called X-ray fluorescence [39].

Since each element has a unique set of energy levels, its X-ray emission spectrum is element specific, the so-called K-, L- or M-series of characteristic X-rays. An energy dispersive detection system can record the characteristic X-rays enabling this way the qualitative elemental analysis of the sample. In fact, energy-dispersive X-ray spectroscopy in the range between 1 and 30 keV offers the detection and quantification, with different levels of precision and accuracy, of all the elements with atomic numbers between $Z=11$ and $Z=92$, through the detection of either their K- or L-characteristic X-ray lines. The principle of the quantitative analysis originates from the mathematical relationship that associates the intensity of a characteristic X-ray line with the respective concentration of the analyte. Although the determination of unknown concentrations by measured elemental X-ray intensities is in general a rather complicated problem, the use of so-called fundamental parameter method provides iteratively a convergent solution [39, 40].

4.2. INSTRUMENTATION: REVIEW, CURRENT STATUS AND DEVELOPMENTS

The basic block configuration of XRF equipment includes an exciting X-ray source, an energy-dispersive detector, electronic modules, a CPU module, a display mechanism and various mechanical parts such as collimators, filters, positioning stage, etc. The characteristics of those components have been considerably upgraded during the past decade offering nowadays the implementation of many of the analytical features of laboratory or desktop XRF spectrometers in compact, light-weight hand-held devices (typically less than 2 kg) easily transportable on-site.

Radioactive point-like X-ray sources (such as ^{55}Fe , ^{109}Cd , ^{241}Am) were very popular in the last decades in field-portable XRF analyzers. Their small physical size (small cylinders of approximately 5 mm height and diameter), the zero power consumption and the almost monoenergetic nature of excitation supported their utilization in portable and compact devices. On the other hand, some drawbacks are the rather short half-lives of some of those isotopes (^{55}Fe -2.7 years, ^{109}Cd -453 days), the in general low strength intensity (in the order of 1-10 mC) and the need – for most of the countries – of specific regulatory requirements in transportation and field applications. However, still today they are in use for specific XRF applications (for example in screening RoHS in electronic devices and components).

The ^{57}Co , ^{241}Am and ^{109}Cd sources have been adopted by some manufacturers, in particular the first two that do not have a direct equivalent with other available portable X-ray sources. Since approximately 2000-2002, miniaturized X-ray tubes of low power consumption (compatible with battery operated instrumentation, <10 W), air-cooled, with different anode materials (Cr, Mo, Rh, Ag and W), physical principles for initiating the thermoionic emission in the cathode, different anode spot sizes and X-ray flux induced geometries (side window or end-window design) operated up to 50 kV have been developed and are commercially available nowadays.

The selection of the characteristics of a X-ray tube (maximum voltage, maximum current, beryllium window thickness, anode spot size, geometrical characteristics of the output X-ray flux, anode material, etc) can be tailored so that to be optimum either for a particular application or for a more general applicability.

The breakthrough in the X-ray instrumentation was the development of new generation compact size solid-state X-ray detectors based on Peltier cooling effect (e.g. PIN diodes and silicon drift detectors), exhibiting energy resolution and peak-to-background analytical performance competitive to the conventional liquid nitrogen cooled Si(Li) detectors. An historical step in the energy-dispersive X-ray detection was the overpass of the 200 eV FWHM barrier in 1996 by a Si(PIN) diode X-ray detector [41].

Next, this detector was selected for the Mars pathfinder mission and gained much attention when on July 7, 1997 it successfully took a XRF spectrum of a rock on the surface of Mars. Si(PIN) diodes are nowadays commercially available with a typical thickness of 500 μm and an active area of 5-25 mm^2 and FWHM at 5.9 keV down to 150 eV. In recent years, much attention has been given to the silicon drift detector (SDD). This type of detector was initially proposed by Gatti and Rehak in 1983 [42, 43]. An electric field parallel to the surface is created by many concentric ring electrodes etched into the surface. The electrons produced by the detection of a X-ray event are caused to drift towards an anode at the centre. As a consequence, a SDD has much less capacitance than a planar detector. Thus it can be operated at much shorter shaping times than a Si(PIN), with comparable resolution, whereas under optimum conditions the SDD resolution is significantly better than the Si(PIN). Furthermore, the main feature of a SDD is the possibility to record high count rates up to 100 kHz without significant deterioration of its energy resolution [44]. Typical characteristics of SDD detectors are a FWHM at 5.9 keV below 135 eV, a crystal thickness of 0.5 mm and active area dimensions up to 80 mm^2 . Special attention has been given by manufacturers to both Si(PIN) and SDD detectors to improve peak-to-background (peak-to-valley) ratio and to eliminate spectral artefacts (tails, etc). Although the performance of the best liquid nitrogen cooled Si(Li) detectors cannot be competed, Si(PIN) and SDD detectors show a remarkable improvement in their spectral characteristics. Significant efforts have been also made to develop Peltier-aided cooled detectors of higher atomic number materials so that to possibly extend the efficient detection of X-rays above 20 keV. In this context, HgI_2 (FWHM 250 eV at 5.9 keV), Cadmium-Zinc-Telluride (CZT) and more recently 1 mm CdTe Schottky diode detectors (Cadmium-Telluride, CdTe, FWHM 250 eV at 5.9 keV) have been introduced offering excellent intrinsic efficiency up to 100 keV with only the presence of the associated escape peaks to require special attention.

The parallel development of digital pulse processors (DPP), which digitize the preamplifier signal and then perform pulse shaping, peak detection, and other functions, digitally improved significantly the portability and pushed the performance of portable systems even further.

The DPP provides lower electronic noise and better stabilities than an analog system at higher count rates. It also integrates the shaping amplifier, MCA, and communication functions on a single printed circuit board not much bigger than a credit card. In addition, the digital pulse processors have more flexibility due to their powerful processing cores and could be tailored easily to any application. In combination with a SDD, the DPP optimizes the analytical performance of the XRF spectrometer in terms of both analytical range and sensitivity.

In hand-held tube-based software-controlled XRF analysers, interchangeable filters can optimize excitation conditions, whereas autonomous battery power operation is supported for a working day (4-8 h). The radiation emission complies with the IEC 61010 standard on radiation safety for benchtop instruments, however their in-situ operation may require local regulatory approval. Modern instruments incorporate a range of safety features, including key operation, relevant interlocks and contact sensors all designed to minimize the risk of significant exposure. It is essential that any operator is fully trained on these features.

Hand-held XRF equipment can analyse elements with atomic numbers even from $Z=11$ (if present in a few percent abundance) with a sensitivity for better excited elements down to the 5-10 ppm range [45-49].

4.3. MEASUREMENT, CALIBRATION AND QUANTIFICATION METHODOLOGY

The FPXRF analysis using hand-held analysers is very fast and depending on the type of the analytical information required (e.g. screening/quantitative analysis) or/and matrix analysed (e.g. metal alloy/geological material) may vary between 30 s to 2 min. Obviously, for each particular case, the measurement protocols implemented adjust the operational parameters so that to optimize excitation and measuring conditions.

For example, for the elemental analysis of a metal alloy, a unique high voltage tube and filter condition might be adequate; however, for the quantification of major, minor and trace elements in a geological sample two operational conditions are usually required for optimum analytical performance: a filtered high value of the high voltage (e.g. 40 kV) for trace elements analysis and a respective unfiltered low value (e.g. 15 kV) for major and minor elements, respectively. Modern hand-held analysers have also implemented 'smart' measurement protocols that may tune excitation conditions with the purpose to analyse optimally minor elements in specific matrices minimizing spectral interferences and background. This is usually achieved by means of proper adjustment of the high voltage setting just below or above, but close to the absorption edge of the interfering element and with the use of appropriate filters. All these features are embedded by manufacturers directly in the operational software of the hand-held instruments without the possibility to control or modify the applied settings. On the other hand, it is important for the end-users to understand the principle for the differentiation of the various measurement protocols and effort must be given towards this direction improving relevant documentation and training.

The quantitative analysis in X-ray fluorescence technique is based on the relationship between the analyte characteristic X-rays intensity and its respective concentration in the sample analysed. However, in most cases, quantification is complex and requires a careful consideration of spectral interferences, sample matrix effects including inter-element absorption of exciting and characteristic X-rays and secondary fluorescence enhancement [39, 40] and physical matrix effects related to the particle size, surface irregularity and moisture.

The big difference between controlled laboratory and uncontrolled field-portable XRF analysis is that in the first case the influence of physical matrix effects can be almost eliminated, whereas in the second case it needs to be carefully assessed and if possible quantified as explained below:

- Spectral interferences

Spectral interferences may arise from insufficient energy resolution of the detector and/or overlap of the characteristic X-ray lines of two or more elements in cases where their energies are almost identical. To deal with this kind of interferences, spectrum evaluation procedures have been developed, optimally in real-time synergy with the quantification analysis. In most of the cases, the definition and introduction of a representative matrix composition to the spectrum analysis software result in an improved accuracy in the spectrum deconvolution procedure.

- Matrix effects

Matrix effects result from the dependence of the intensity of the analyte characteristic X-rays on all the constituent elements concentration. Those effects manifest themselves as either absorption or enhancement of the measured intensity generating a non-linear intensity response versus analyte concentration. In both cases, a suitable matrix correction model has to be introduced.

- Physical matrix effects (particle size, surface irregularity and moisture)

One of the major features of X-ray fluorescence analysis is the fact that the measured analyte intensity originates from a sample information depth that is expressed in terms of the so-called critical thickness or depth (defined as the sample layer thickness from which 63.2% of the fluorescence signal originates). From this, the 99% of the analyte fluorescence intensity emanates from 4.63 times the critical depth.

In a typical soil matrix and irradiation geometry (incident/take-off angle equal to $45^\circ/45^\circ$), the critical depth varies from about 10 μm for silicon (^{55}Fe excitation) up to 200 μm for cadmium (K-shell excitation, ^{241}Am excitation). The concept of critical depth, i.e. the fact that the fluorescence intensity originates mostly from a specific thickness that depends on the energy of the exciting and detected X-rays, the sample matrix composition and set-up geometry, is of particular importance for the in-situ XRF analysis of heterogeneous samples (mineralogy effects) or of samples with surface contamination (e.g. dust). In particular, in the case of heterogeneous samples, the particles or grains, which are associated with mineral phases or individual elements, may produce a more pronounced influence to a characteristic X-ray intensity as their size is comparable or even greater than the respective critical depth of analytical information [36]. In general, if a sample contains fine particles, the XRF signal for an element will be different than for a sample containing larger grains (despite that the analyte concentration is the same in both samples). The surface irregularity of the samples is another factor that influences the detected X-ray fluorescence intensities since they can be systematically lower than those observed from flat samples, in particular for the low Z elements [49, 50]. Sample moisture contents higher than 20% may also affect the final FPXRF analytical results inducing bias especially for the elements with a characteristic X-ray below 5 keV.

For higher energies, the water dilution effect of the analysed sample might be partially or completely compensated by the corresponding change (decrease) of the sample total mass absorption coefficient. However, the sample moisture content is of great significance when analysing for instance soil or sediment saturated with water [50].

The effect of the discussed physical matrix effects could be decreased using preliminary (often simple) in-situ sample treatment procedures such as homogenization, drying and/or sieving.

For the calibration of FPXRF analysers there are two basic analytical procedures:

- The empirical approach that is based on the use of certified reference materials (CRMs) or a batch of samples very similar with the one intended to be analysed in-situ that have been ideally collected on the site of interest and characterized by independent laboratory methods. In any case, regression mathematics generate a general or site-specific calibration to incorporate the elemental response of the spectrometer and matrix effects. Empirical calibrations are incorporated in some commercial analysers, either factory-built or by the end-users.

- The Fundamental Parameter (FP) method based on a mathematic formulation that may compensate for the most important sample inter-element (matrix) effects. The FP-based calibration requires in principle only pure element or compound standards, however fine-tuning can be considerably assisted by the incorporation of multi-element Certified Reference Materials (CRMs). One of the main advantages of FP over empirical calibration is that no previously collected site-specific samples with confirmed and validated analytical results are necessary. However, the user should be aware of the limitations imposed on FP calibration since, in such method, assumptions that the sample is dried, of small particle size ($<37\ \mu\text{m}$), with an appropriate packing density, flat surface and placed on the reference plane are considered.

The quantification procedures in FPXRF analysis have been significantly improved and optimized for different types of matrices or analytical problems, but actually they are and should be compatible with the particular calibration procedures implemented eliminating to a great extent systematic errors or uncertainties in FP. A third method that is restricted to the determination of medium (generally for $26 < Z < 41$ -43) or heavy atomic number ($Z > 72$) trace elements in silicate or light elements in general matrices is the Compton normalization method. In this case, one or even more multi-element CRMs with similar matrix composition with the unknown samples are measured and the intensity of the inelastic scattering (Compton) exciting radiation (i.e. for example the Rh- $K\alpha$ Compton peak intensity in the case of the Rh-tube excitation) serves for the normalization of the trace elements' fluorescence intensities. Since the Compton peak intensity changes in different matrices almost proportionally with the fluorescence intensities, the normalization approach can reduce problems associated with varying matrix effects among samples.

4.4. SAMPLE PREPARATION

Regardless of the instrument used for the analysis, there are two methods of sample preparation that should be considered when analysing soil samples by FPXRF: in-situ and discrete sampling (physically removing a sample). Typically, both methods are employed based on the number of samples to be analysed, site/contaminant history, time allocated to conduct site activities and the proposed sampling design [51]. For in-situ analysis, first the removal of any large or non-representative debris (rocks, pebbles, leaves, etc) from the soil surface has to be performed. Then the probe is placed directly on the soil surface to perform the analysis. In-situ analysis allows rapid collection of data for a large number of sample points, eliminating physical sampling and yielding real-time data that can be used for rapid decisions in the field. However, as already stated, significant sources of error are associated to the direct analysis of the samples, above all regarding the physical matrix effects (particle size, surface irregularity and moisture).

For this reason, even though most FPXRF can measure undisturbed samples directly, a minimal sample preparation protocol is recommended to improve the analytical quality of the data (discrete sampling). In such case, the sample is usually collected from a 10 by 10 cm square that is 2.5 cm deep (soil sample of approximately 375 g or $250\ \text{cm}^3$). Then the sample is homogenized, dried, ground and packed before the FPXRF analysis. The homogeneity of the sample can be tested using a fluorescence dye.

Specified protocols regarding the sample preparation in FPXRF can be found in detail in the US EPA Method 6200 'Field Portable X-Ray Fluorescence Spectrometry for the Determination of Elemental Concentrations in Soil and Sediments' [52].

4.5. ANALYTICAL APPLICATIONS

The range of analytical applications of the FPXRF system can be classified in two major categories: a) Screening and/or determination of inorganic elemental composition in geological, environmental and/or biological samples, and b) Long-term monitoring of inorganic environmental pollutants with stationary equipment items placed on-site (particular matter in urban sites, stream waters in remote sites, occupational exposure).

In particular, different analytical applications of hand-held and portable XRF analyzers were presented that highlight the range of applicability of the in-situ XRF technology in environmental-related studies but also the benefits with respect to well-established laboratory techniques.

More specifically the following applications were presented:

- Determination of As anomalies in floodplains

The spatial heterogeneity of As concentrations in soils from an area characterized by flooding events, which led to reducing conditions and As liberation in soils, was studied. Hand-held XRF analysis was considered appropriate to analyse in-situ a high number of soil samples ($n > 100$). The sample preparation included the following steps, i.e. removal of any debris (leaves, stones, etc), loose of the soil to a depth of 1.5-2.5 cm, homogenization, drying, sieving, mixing of the loose soil, packing and finally performing the hand-held XRF analysis. The As content in most of the samples was between 6.9 and 45 mg/kg (Average: 22 mg/kg), with a detection limit for As of 6 mg/kg (120 s measuring time). This type of analysis helped to identify As 'hot-spots' present in the studied area. Additionally, the XRF analysis offered multi-elemental information that improves the understanding of the controlling factors on As mobility. More specifically it was found that As was significantly positively correlated with total Fe and Mn concentrations and it was deduced that As on the floodplain was mainly immobilized by sorption and co-precipitation processes involving Fe and Mn oxides [53].

- Environmental impact of past mining activities

A FPXRF analyser was used to evaluate metal contamination in areas affected by past mining activities (determination and distribution of metals in soils and ores) and to study remediation procedures (phytoremediation treatments) of these areas. In this way it was possible to study the distribution of regulated pollutants among different mineral phase ore veins. Besides, the evaluation of effects of metal pollution (Pb, Zn) in sediments was performed analysing core samples of metal polluted sediments to a depth of 30 cm performing 2D mappings with a spatial resolution of 600 μm [54].

The same FPXRF analyser was used for studying the potential use of sunflowers (*Helianthus annuus*) for the phytoremediation of an abandoned Pb/Zn mining area. To study in more detail the translocation of metals from the bottom to the top of sunflowers specimens, the analysis of the leaves along the length of the specimens was carried out. The analysis showed that the metals tended to accumulate with age in the basal part of the sunflowers whereas metal contents in the top part were fairly constant or decreased irregularly. It was found that the contents of Zn and Pb in the leaves nearest to the ground were up to 9 times higher than those close to the tip. It is interesting to remark that this distribution profile along the sunflower leaves was similar for both investigated sampling sites but different to that from the control area in which no significant differences were observed between Zn and Pb content in basal and the top part of vegetation specimens.

- Metal content in industrial waste water effluents

The monitoring of heavy metals in industrial waste water effluents is at present an important activity. Of special interest is the screening of elemental composition of inlet effluents and quantitative analysis of outlet effluents to study the efficiency of the chemical treatment process to eliminate metals and to comply with current established concentration limits. Commercial extraction chelating disks were used as solid sorbent to preconcentrate metals for subsequent FPXRF analysis. The limits of detection (LOD) for the following metals of interest were determined to be about 1-3 µg/L for Ni, Cu, Zn, Pb and 16 µg/L for Cd [55].

The application of portable XRF technology to support public health related issues in Jamaica and more specifically to resolve two Pb poisoning cases, was presented. In the first case, Pb contamination resulted from an old mining area (Hope river valley) that had produced waste dump in Kintyre close to a basic school yard, thus poisoning children. Elevated Pb concentrations up to about 35,000 ppm were measured in the soil. A communality-wide intervention campaign was initiated to mitigate the hazard including Pb encapsulation of the soil, nutritional enhancement and Pb-safe education. In another case, Pb soil contamination resulted from a backyard Pb smelting in Mona Commons residential community. The hand-held XRF analyser was used to measure the soil Pb concentrations and to develop a GIS map of Pb contamination in the area. The map showed that Pb contamination around the former smelter has spread over a wider area in the community and approximately one third of the residential soils were above the safe limit for Pb in soil set by the US EPA. The XRF measurement results were also used to assess the risk of Pb exposure to the residents and in particular to children, and to develop site-specific scenarii for the implementation of Pb mitigation activities.

4.6. UNCERTAINTY ESTIMATION

The total uncertainty of XRF measurements should include the contributions from the individual uncertainties introduced at all stages of the measurement process. Therefore, the total measurement variance σ_{tot}^2 can be expressed as:

$$\sigma_{\text{total}}^2 = \sigma_{\text{sample representation}}^2 + \sigma_{\text{sample collection}}^2 + \sigma_{\text{sample handling}}^2 + \sigma_{\text{sample preparation}}^2 + \sigma_{\text{analysis}}^2$$

As it is shown from the expression, the uncertainty due to the analytical stage is only one of the sources of uncertainty and may be a minor contributor to the total uncertainty of the XRF data.

The uncertainty in the measurements is caused by the precision and bias of the method. The precision can be used to quantify the random component of the uncertainty (due to geochemical variation of the sampling point and instrument deviation) and the bias to quantify the systematic component (related mostly to particle size effects, surface irregularities and moisture content).

4.7. QC/QA CONSIDERATIONS

In order to assess if the XRF methodology could be applied for the intended purpose, quality control and quality assurance (QC/QA) of the obtained measurement results are required. No measurement value could be used for decision-making unless QC tests are carried out (e.g. to run routinely a QC sample, to use method blanks) and analytical figures of merit for the methodology have been properly evaluated (e.g. limit of detection, precision, accuracy) [56].

- Performance tests and energy calibration check

For quality control assessment of the obtained data it is recommended that a QC sample is run routinely throughout the testing period, to determine if the FPXRF instrument is operating within established acceptance criteria. If required by the manufacturer, an energy calibration check can also be performed.

- Analysis of blank samples

Instrumental and method blanks should be also analysed to verify that no contamination exists in the spectrometer (probe window) and to monitor for contamination due to sample preparation, respectively. Usually, instrumental blanks are checked analysing silicon dioxide, a polytetrafluoroethylene (PTFE) block, a quartz block, clean sand and lithium carbonate. For method blank assessment, clean silica sand or lithium carbonate that undergoes the same preparation procedure as the samples are used. The frequency of the analysis of blank samples depends on the data quality objectives but it is recommended that they are analysed on each working day before and after the analyses are conducted.

- Limit of detection

The limit of detection (LOD) is defined as the lowest concentration level that can be determined using a methodology as being statistically different from an analytical blank [57]. Therefore, LODs for the elements of interest have to be carefully determined for each particular application since, depending to site action level requirements, FPXRF analysis may not be suitable. Traditionally, concentration values below the detection limit are not reported and are often not even recorded. LODs are calculated as three times the standard deviation of the results for low concentration samples (usually reference materials with a similar matrix to the analysed samples) with the concentration of the analytes being 5-10 times higher than the estimated LOD.

LODs are highly dependent on the instrument characteristics (excitation source, type of detector), on the sample matrix, on the element itself (fluorescence yield) and on the measuring time. For similar samples the individual LODs improve as a function of the square root of the testing time. For instance, measuring times lower than 50 s are used for 'hot-spot' screening but to meet higher sensitivity requirements, measuring times of 200-300 s are used. Limits of detection in the low mg/kg range (10-50 mg/kg) have been reported for the determination of metals (Zn, As, Se) in soils for testing times between 60 and 120 s [58].

- Precision

Precision refers to the degree of agreement between the results of replicate measurements and provides an estimation of the random component of the uncertainty [59]. The precision of a method is usually monitored by analysing a sample containing the target analytes at various concentration levels close to the concentration levels expected in the samples to be analysed and calculating the associated relative standard deviation (RSD, %) of the measured replicates.

The frequency of precision measurements will depend on the data quality objectives but a minimum of one precision sample should be run per day. According to US-EPA Method 6200, samples used to evaluate the precision of the results should be analysed at least 7 times in replicate and the calculated RSD should not be greater than 20% [40]. It has to be taken into account that the effective precision of the FPXRF becomes limited by the heterogeneity of the sample rather than by the noise of the analytical signal.

- Accuracy

Accuracy refers to the difference between a sample measurement result and the reference or true value [59]. One of the methods to assess accuracy or bias (related to the systematic component of uncertainty) is based on the analysis of a certified reference material (CRM) containing amounts of the elements in a representative matrix. There is, however, an important extra factor in the estimation of bias for an in-situ FPXRF method using this approach.

The CRMs are dry, very fine powders (<50 µm) that are usually prepared for XRF analysis as compressed pellets with negligible pore space between the sample grains and with a very flat surface for measurement. In contrast, in-situ measurements are performed on soils that have field moisture, heterogeneity on particle sizes and with a rough flat surface for measurement. Another more realistic way to assess the accuracy of the field measurements requires the analysis of confirmatory samples (minimum of 10% of the analysed samples) by using an approved analytical method for the determination of the target analytes in a given matrix. The confirmatory samples should be selected from the lower, middle, and upper range of concentrations measured by the FPXRF. Then, the results obtained by both methodologies should be evaluated with a least-squares linear regression analysis. Depending on the obtained regression parameters (R^2 , slope and intercept) US-EPA defined different quality levels of the obtained data regarding the purpose of the field measurement [60].

Those criteria are given in the Table 1 below.

TABLE 1. CRITERIA FOR CHARACTERIZING DATA QUALITY (ADAPTED FROM [47])

Quality level	Purpose of the field measurement	Requirement
Q1	Qualitative screening	RSD>20% $R^2<0.70$ Inferential statistics indicate that the two data sets are statistically different.
Q2	Quantitative screening	RSD<20% $R^2=0.70-1$ Inferential statistics indicate that the two data sets are statistically different, i.e. relationship $y=mx$ or $y=mx+c$ accepted.
Q3	Definitive	RSD<10% $R^2=0.85-1$ Inferential statistics (test for slope=1 and y-intercept=0) indicate that the two data sets are statistically similar.

RSD: Relative standard deviation

It is interesting to remark that, to assess a definitive analysis, usually, the sample should be dried, of small particle size (<125 µm), with a flat surface and placed on the reference plane.

4.8. ADVANTAGES AND LIMITATIONS OF THE METHOD

FPXRF analysers have proven to be a viable, cost- and time-effective approach for in-situ analysis of a variety of environmental samples. FPXRF provides both qualitative and quantitative information about site contamination. Despite the fact that FPXRF analysers have generally less sensitivity (i.e. have higher elemental detection limits) than laboratory equipment items, the obtained data are sufficient to meet site action level requirements in most cases and to map out contamination patterns and assess spatial distribution.

However, to obtain in-situ reliable analytical data, a number of factors that may affect FPXRF response must be considered (sample matrix effects, accuracy and suitability of calibration standards, sample morphology) and usually, comparison with established laboratory methods and analysis of reference materials is also necessary.

A summary of the advantages and limitations of using FPXRF for characterization of metal contaminated sites is presented below.

Advantages:

- Fast, multi-elemental and low cost analysis.
- Immediate estimation of metal contamination in-situ, enabling on-site decision (remediation strategies).
- Simple (minimal) sample preparation.
- Improved decision-making in the field.
- Possibility of implementing iterative sampling design to investigate apparent 'hot-spot' during one site visit.
- Detection limits low enough to measure in the range of screening values several metals of interest (e.g. Ba, Co, Cr, Cu, Mo, Ni, Pb, Sn and Zn).
- Good analytical precision (about 1%), but heterogeneity determines measurement precision.
- Possibility of investigating in-situ heterogeneity of metals across the site with resolution down to the centimetre scale.
- No reagents are needed to perform the analysis.
- No wastes are generated by transporting contaminated samples in the laboratory.

Disadvantages:

- In some cases, higher limits of detection than regulatory limits (case of Cd for example).
- Capital cost of equipment.
- Small depth of analysis. Very small sample size gives potentially poor representation of its real composition, lowering the measurement precision.
- Large estimates of bias in measured concentrations may arise unless corrections can be made for moisture, packing ratio (pore space volume) and surface roughness.
- Heterogeneity of sample may affect the results.
- Need for laboratory analysis check.

4.9 COMPLEMENTARY LABORATORY TECHNIQUES

In-situ FPXRF technique can be complemented by laboratory techniques for the determination of elemental composition in different kind of environmental samples. For instance, X-ray spectrometry techniques (EDXRF, WDXRF, TXRF, PIXE, PIGE), atomic spectrometry (ICP-OES, ICP-MS, ETAAS and FAAS) and INAA are commonly used for such purpose.

In addition to the elemental determination of target samples in the laboratory, determination of the distribution of metals in soil profiles can also be of great interest for the assessment of metal accumulation and mobility along the unsaturated soil zone of metal polluted areas.

4.10 FUTURE DEVELOPMENTS AND TRENDS

The portable and hand-held XRF analysers have reached nowadays a remarkable degree of design, hardware and software sophistication. However, the experience acquired up to now in the field applications has suggested certain areas for improvements that will follow progress in respective instrumentation developments. The utilization of silicon drift detectors (SDD) of larger crystal area will enable faster analysis and lower sensitivities to be attained, in particular for regulated trace elements such as Hg, Pb and As. In some cases, the need for localized analysis (at the range of 1 mm² or below) implies the incorporation in the analyser of either collimators or focusing lenses coupled with a device to inspect (visualize) and record the analysis area.

The further improvement in the embedded digital signal processing units, the larger SDD areas and the optimization of set-up parameters (windows, air distance, etc) may improve considerably the analytical range and sensitivity for light elements detection (Na, Mg, Al). This development will consequently enable a more accurate quantitative analysis of the trace contaminants by incorporating in the matrix corrections better estimated concentrations for the major and minor light elements.

The sensitivity for Cd detection requires further improvement, since it is among the most important regulated toxic contaminants. For this case, the excitation conditions (tube high voltage, filtering) and detector options may need further tuning in the respective hardware and analysis protocols.

Concerning the software for quantitative analysis based on fundamental parameters, the need for advanced algorithms that will utilize, exploit and comparatively assess the full spectrum information are more than necessary for tackling also QC/QA related issues. Obviously, the GPS mapping should be incorporated in the hand-held analyser and linked with each particular spectrum acquisition. It has been also widely recognized the need to establish regional control sites to be used for calibration and validation purposes.

CONCLUSION

The topics presented in this publication can be divided in two parts: a) the designs/developments and applications of gamma-ray spectrometry methods for environmental analysis and b) the current status on the development of hardware and software for XRF spectrometry to characterize potentially contaminated sites.

The in-situ application considered advanced methods for gamma-ray spectrometry and XRF spectrometry by improving the performances of crystals and instruments, and realizing dedicated equipment for specific monitoring purposes. In the last years each of those methods has significantly addressed issues related with calibration, design of monitoring plans and data analysis and processing.

There is a need for greater environmental contamination awareness, adoption of new or improved techniques and methodologies, as well as special training in characterization and remediation issues. It is also required a more effective transfer of technologies and knowledge, and dissemination of the methods to reduce the costs of measurement and site characterization, and improve quality of analytical results.

APPENDIX I. IN-SITU CAPABILITIES AND STUDY SITES IN COUNTRIES REPRESENTED IN THE TECHNICAL MEETING

I.1. AVAILABLE INSTRUMENTATION AND APPLICATIONS

Country	Available instrumentation	Applications
Argentina	Outdoor dose-rate meters, in-situ gamma-ray spectrometry using NaI(Tl) detectors.	Dose-rate monitoring (journey monitoring), national network of outdoor dose rates based on Reuter-Stokes.
Australia	Outdoor dose-rate meters, in-situ gamma-ray spectrometry, sampling systems.	In-situ gamma-ray mapping (vehicle configuration) and chemical analysis in the laboratory.
Brazil	In-situ gamma-ray spectrometry (NaI(Tl)) and gamma dose-rate meters: aerial, car-borne and backpack systems, in-situ gamma-ray spectrometry (HPGe). All the systems are geo-referenced.	Environmental monitoring and site characterization.
Czech Republic	Outdoor dose-rate meters, sampling grab.	Long-term in-situ radioactivity monitoring.
Egypt	Portable HPGe gamma-ray spectrometry, nuclide identifier, survey meters for dose-rate estimation, counters (gross alpha and beta), air pump and sampling equipment items, GPS vehicle and dosimeters.	Routine work and for emergency situations.
France	Mobile unit for real-time mapping, in-situ gamma-ray spectrometry, software for sampling process, indoor monitoring (gamma-ray spectrometry, spectrometry for concrete profiles to monitor ¹³⁷ Cs and uranium daughters).	Radiochemical (vehicle and laboratory for Pu and U) and chemical analysis in the laboratory.
Greece	Telemetric network for dose-rate measurements (24 stations based on Reuter-Stokes meters), in-situ gamma-ray spectrometers (HPGe and NaI(Tl) detectors), air samplers and deposition collectors, mobile laboratory, underwater spectrometers, portable dose-rate meters.	Environmental monitoring (in-situ gamma-ray spectrometry in terrestrial and aquatic environment; air, soil, seawater and surface water sampling for laboratory measurements).

Hungary	In-situ gamma-ray spectrometry system (NaI(Tl)), outdoor road monitoring system (mobile laboratory), hand-held gamma-ray spectrometry system.	Monitoring program (mobile laboratory network), outdoor radon measurements/mapping.
Italy	National dose-rate network, in-situ gamma-ray spectrometry (HPGe, NaI(Tl)), aerial platform, gamma dose-rate meter (plastic scintillators), mobile laboratories, contamination meters, air pump and sampling devices, portal system to detect scrap metal contamination.	Outdoor/indoor monitoring and environmental monitoring.
Jamaica	Hand-held XRF (soils, plants, trace elements), in-situ monitoring (alpha, beta, gamma), in-vitro lead in blood.	Natural gamma radiation monitoring, trace elements (in soils, plants, animals and humans), lead in blood of exposed children, scrap metals monitoring, biomonitoring of air pollution.
Lithuania	In-situ gamma-ray spectrometers (HPGe), mobile laboratories for gamma-ray spectrometry and dose-rate estimation (point and vehicle configuration), dose meters, radionuclide identifiers, samplers and portable contamination meters.	Radioactivity monitoring.
Montenegro	Portable gamma-ray spectrometry (HPGe), mobile unit for sampling air particulate matter, sampling equipment for extreme low activity measurements in the laboratory.	Environmental monitoring.
Spain	In-situ field-portable X-ray fluorescence systems (EDXRF, TXRF), samplers.	Metal determination in different environmental compartments (soil, sediment, vegetation, water).
Uruguay	Samplers (for soils, sediments, particulate matter, water), dose meters (alpha, beta, gamma).	Radioactivity monitoring and dosimetry.

I.2. POTENTIAL SITES TO BE SURVEYED BY PORTABLE INSTRUMENTATION

Country	Potential sites to be surveyed by portable instrumentation
Argentina	Survey of storage site after removal of nuclear waste and tailings of uranium mining, monitoring plan on the research centre EZEIZA, scrap metals.
Australia	Monitoring of nuclear test sites (Maralinga, already undertaken), uranium mining sites (already undertaken), monazite sites (already undertaken), future radioactive waste repository sites, brown coal power plants monitoring.
Brazil	Two nuclear power plants, 3 uranium mines (1 in operation, 1 being decommissioned, 1 being commissioned), 3 research reactors, NORM industries (5 fertilizers plants), copper, niobium and gold mines, oil industry, coal mining, 3 disposal sites for by-products of monazite chemical processing (1 being remediated), scrap metals, ¹³⁷ Cs disposal waste site due to an accident.
Czech Republic	Long-term monitoring of contaminated sites; environmental impact assessment of contaminated sites.
Egypt	Environmental impact assessment of fertilizer and ceramic industries, which use raw materials that contain enhanced levels of natural radionuclides above exempted levels; pre-operational radiological studies in different sites intended to be used for power plant construction.
France	One hundred sites and facilities (terrestrial and river) are planned to be surveyed by CEA-ANDRA and IRSN all around France. Defence CEA surveys by air of all the power plants in France.
Greece	Routine environmental monitoring (terrestrial and aquatic), monitoring of the environment close to NORM industries (fertilizer production industries and phosphogypsum stacks) and inspections of scrap metal loads.
Hungary	Monitoring the site of KFKI campus on which there is a research reactor and isotope factory, PAKS nuclear power plant (is operating), coal power plants, coal mines, uranium mines, ELI laser facility monitoring, depleted uranium depository, radioactivity deposits.
Italy	Monitoring natural activity (radon, radium), NORM industries (fertilizers and ceramics industries), scrap metals, phosphogypsum. Radiological survey (indoor) of 4 power plants to be decommissioned, 4 fuel fabrication and reprocessing pilot plants and routine outdoor environmental monitoring of the plants.

Jamaica	Small research nuclear reactor (SLOWPOKE2) will be decommissioned and needs monitoring, bauxite industry (red spots, red mud), oil and coal burning industry, scrap metal sites monitoring, radioactive waste from hospitals, natural radioactivity monitoring (including radon), heavy metal contaminated sites (natural and anthropogenic).
Lithuania	Project for monitoring NORM (phosphorous fertilizers), study of military bases, waste deposits, metal scrap.
Montenegro	Industrial activities (aluminium production), bauxite processing, processing and smelting plants, iron smelter, scrap metal processing (regular monitoring), abandoned military locations (jet engines with thorium and radium), depleted uranium.
Spain	Metal dispersal around mining environments (heavy metal mining: Fe, Zn, Pb).
Uruguay	Indoor/outdoor radon monitoring in the north of the country (thermal waters, morphology/mineralogy of the region), gold mining, power plants, fertilizers deposition, fertilizer industry, imported phosphate rocks need to be monitored for NORM and trace elements.

APPENDIX II. LIST OF PARTICIPANTS

TECHNICAL MEETING ON IN-SITU METHODS FOR CHARACTERIZATION OF CONTAMINATED SITES

IAEA Headquarters, Vienna, Austria

5 to 9 July 2010

Bodor, K.B.	Hungarian Academy of Sciences, Hungary
Carey, E.	Australian Radiation Protection and Nuclear Safety Agency, ARPANSA, Australia
Castellanos Macchiorlato, A.M.	Comision Nacional de Energia Atomica, Argentina
Ceccatelli, A.	International Atomic Energy Agency
Clouvas, A.	Aristotle University of Thessaloniki, Greece
Da Silva, N.C.	Commissao Nacional de Energia Nuclear, CNEN, Brazil
Diab, H.M.A.	Egyptian Atomic Energy Authority, EAEA, Egypt
Dubot, D.	French Alternative Energies and Atomic Energy Commission, CEA, France
Ferreira Moreira, M.C.	Commissao Nacional de Energia Nuclear, CNEN, Brazil
Jovanovic, S.	University of Montenegro, Montenegro
Karydas, A.G.	International Atomic Energy Agency
Lunescu, D.	ARPA Lombardia, Italy
Manes, D.	Sogin SpA, Italy
Margui, E.	University of Girona, Spain
Monken Fernandez, H.	International Atomic Energy Agency
Monteith, A.R.	International Atomic Energy Agency
Nuccetelli, C.	Istituto Superiore di Sanita, Italy
Odino Moure, M.	Ministerio de Industria, Energia y Mineria, MIEM, Uruguay
Patterson, J.	Brucker-Elemental, United States of America
Pilkyte, L.	Ministry of Health, Lithuania
Sillah, A.	Ministry of Lands, Mines and Energy, Liberia
Simek, P.	T.G. Masaryk Water Research Institute, Czech Republic
Tsabaris, C.	Hellenic Centre for Marine Research, Greece
Voutchkov, M.K.	University of the West Indies, Jamaica

REFERENCES

- [1] INTERNATIONAL ATOMIC ENERGY AGENCY, Soil sampling for environmental contaminants, IAEA-TECDOC-1415, IAEA Vienna, ISSN 1011-4289 (2004).
- [2] CHILES, J.-P., DELFINER, P., in *Geostatistics: Modeling Spatial Uncertainty*, Wiley, New York (1999).
- [3] DUBOT, D., DESNOYERS, Y., DE MOURA, P., ATTIOGBE, J., JEANNÉE, N., PÉRAUDIN, J.-J., “Characterization of radio-contaminated soils in France: challenges and outcomes”, in *Proc. Int. Conf. Intersol’*, Paris (2010).
- [4] DESNOYERS, Y., DUBOT, D., “Near real-time characterization of contaminated sites in France: Challenges, methods and outcomes”, in *Proc. Int. Conf. Intersol’*, Toronto (2011).
- [5] MABIT, L., MEUSBURGER, K., IURIAN, A.-R., OWENS, P.N., TOLOZA, A., ALEWELL, C., Sampling soil and sediment depth profiles at a fine resolution with a new device for determining physical, chemical and biological properties: the Fine Increment Soil Collector (FISC), *J. Soils Sediments* **14** (2014) 630-636.
- [6] BECK, H.L., CONDO, W.J., LOWDER, W.M., Spectrometric techniques for measuring environmental gamma radiation, HASL-150 (1964).
- [7] BECK, H.L., Environmental Gamma Radiation From Deposited Fission Products, 1960-1964, *Health Phys.* **12** (1968) 313-322.
- [8] BECK, H.L., DE CAMPO, J., GOGOLAK, C.V., In-situ Ge(Li) and Na(Tl) gamma-ray spectrometry, HASL-258 (1972).
- [9] ICRU Report N. 53 (1994).
- [10] MILLER, K.M., SHEBELL, P., In situ gamma-ray spectrometry – A tutorial for environmental radiation scientists, USDOE Report EML-557 (1995).
- [11] INTERNATIONAL ATOMIC ENERGY AGENCY, Characterization of radioactively contaminated sites for remediation purposes, IAEA-TECDOC-1017, IAEA Vienna, ISSN 1011-289 (1998).
- [12] INTERNATIONAL ATOMIC ENERGY AGENCY, Generic procedures for monitoring in a nuclear or radiological emergency, IAEA-TECDOC-1092, IAEA Vienna, ISSN 1011-4289 (1999).
- [13] INTERNATIONAL STANDARDS ORGANIZATION, Measurement of radioactivity in the environment -- Soil -- Part 7: In situ measurement of gamma-emitting radionuclides, ISO 18589-7:2013.
- [14] KOWATARI, M., KUBOTA, T., SHIBAHARA, Y., FUJII, T., FUKUTANI, S., TAKAMIYA, K., MIZUNO, S., YAMANA, H., Application of a CZT detector to in situ environmental radioactivity measurement in the Fukushima area, *Radiat. Prot. Dosimetry* **167** (2015) 348-352.
- [15] VIDMAR, T., CELIK, N., CORNEJO DIAZ, N., DLABAC, A., EWA, I.O.B., CARRAZANO GONZALES, J.A., HULT, M., JOVANOVIC, S., LEPY, M.-C., MIHALJEVIC, N., SIMA, O., TZIKA, F., JURADO VARGAS, M., VASILOPOULOU, T., VIDMAR, G., Testing efficiency transfer codes for equivalence, *Appl. Rad. Isot.* **68** (2010) 355-359.
- [16] TSABARIS, C., PROSPATHOPOULOS, A., Automated quantitative analysis of in-situ NaI measured spectra in the marine environment using a wavelet-based smoothing technique, *Appl. Radiat. Isot.* **69** (2011) 1546-1553.
- [17] TYLER, A., In situ and airborne gamma-ray, *Radioactivity in the Environment* **11** (2008) 407-448.
- [18] AAKENES, U.R., Radioactivity monitored from moored oceanographic buoys, *Chem. Ecol.* **10** (1995) 61-69.

- [19] TSABARIS, C., BAGATELAS, C., DAKLADAS, T.H., PAPADOPOULOS, C.T., VLASTOU, R., CHRONIS, G.T., An autonomous in-situ detection system for radioactivity measurements in the marine environment, *Appl. Rad. Isot.* **66** (2008) 1419-1426.
- [20] TSABARIS, C., BALLAS, D., On-line Gamma Ray spectrometry at open sea, *Appl. Rad. Isot.* **62** (2005) 83-89.
- [21] ANDROULAKAKI, E.G., TSABARIS, C., ELEFThERIOU, G., KOKKORIS, M., PATIRIS, D.L., VLASTOU, R., Seabed radioactivity based on in situ measurements and Monte Carlo simulations, *Appl. Radiat. Isot.* **101** (2015) 83-92.
- [22] WEDEKIND, C.H., SCHILLING, G., GRÜTTMÜLLER, M., BECKER, K., Gamma-radiation monitoring network at sea, *Appl. Radiat. Isot.* **50** (1999) 733-741.
- [23] OSVATH, I., POVINEC, P.P., LIVINGSTON, H.D., RYAN, T.P., MULSOW, S., COMMANDUCCI, J.-F., Monitoring of radioactivity in NW Irish Sea water using a stationary underwater gamma-ray spectrometer with satellite data transmission, *J. Radioanal. Nucl. Ch.* **263** (2005) 437-440.
- [24] QUARATI FRANCESCO, A., LaBr₃ spectrometers for space applications. PhD Thesis, Technical University of Delft (2013).
- [25] LONG, S., MARTIN, L., BAYLIS, S., FRY, J., Development and performance of the vehicle-mounted radiation monitoring equipment used in the Maralinga rehabilitation project, *J. Environ. Radioactivity* **76** (2004), 207-223.
- [26] MOREIRA, M.C.F., CONTI, C.C., SCHIRRU, R.A., New NaI(Tl) four-detector layout for field contamination assessment using artificial neural networks and the Monte Carlo method for system calibration, *Nucl. Instrum. Methods Phys. Res. A* **621** (2010) 302-309.
- [27] CLOUVAS, A., XANTHOS, S., ANTONOPOULOS-DOMIS, M., SILVA, J., Monte-Carlo based method for conversion of in-situ gamma-ray spectrum obtained with portable Ge detector to incident photon flux energy distribution, *Health Phys.* **74** (1998) 216-230.
- [28] CLOUVAS, A., XANTHOS, S., ANTONOPOULOS-DOMIS, M., Derivation of indoor gamma dose rate from high resolution in-situ gamma ray spectra *Health Phys.* **79** (2000) 274-281.
- [29] SMETANIN, M., VASILENKO, E., SEMENOV, M., XANTHOS, S., TAKOUDIS, G., CLOUVAS, A., SILVA, J., POTIRIADIS, C., Measurements and Monte Carlo calculations of photon energy distributions in Mayak PA workplaces, *Radiat. Prot. Dosim.* **131** (2008) 455-468.
- [30] CLOUVAS, A., XANTHOS, S., ANTONOPOULOS-DOMIS, M., Extended survey of indoor and outdoor terrestrial gamma radiation in Greek urban areas by in situ gamma spectrometry with portable Ge detector *Radiat. Prot. Dosim.* **94** (2001) 233-246.
- [31] CLOUVAS, A., XANTHOS, S., ANTONOPOULOS-DOMIS, M., Radiological maps of outdoor and indoor gamma dose rates in Greek urban areas obtained by in situ gamma ray spectrometry, *Radiat. Prot. Dosim.* **112** (2004) 267-275.
- [32] CLOUVAS, A., XANTHOS, S., TAKOUDIS G., POTIRIADIS, C., SILVA, J., In-situ gamma spectrometry measurements and Monte Carlo computations for the detection of radioactive sources in scrap metal, *Health Phys.* **88** (2005) 154-162.
- [33] CASTELLUCCIO, D.M., et al., SNIFFER System: A Multipurpose Aerial Platform For Large Area Radiological Surveillance, Emergency Management And Air Pollution Monitoring., In *Rapporti Istisan* 07/33, 2007.

- [34] JOVANOVIĆ, S., DLABAC, A., MIHALJEVIĆ, N., VUKOTIĆ, P., ANGLE: A PC-code for semiconductor detector efficiency calculations, *J. Radioanal. Nucl. Chem.*, **218** 1 (1997) 13-20.
- [35] JOVANOVIĆ, S., DLABAC, A., MIHALJEVIĆ, N., ANGLE v2.1 – New version of the computer code for semiconductor detector gamma-efficiency calculations, *Nucl. Instrum. Methods Phys. Res. Sect. A* **622** 2 (2010) 385-391.
- [36] BOSON, J., PLAMBOECK, A.H., RAMEBÄCK, H., ÅGREN, G., JOHANSSON, L., Evaluation of Monte Carlo-based calibrations of HPGe detectors for in situ gamma-ray spectrometry, *J. Environ. Radioactivity* **100** (2009), 935-940.
- [37] JCGM, Joint Committee for Guides in Metrology, Evaluation of measurement data – Guide to the expression of uncertainty in measurement, JCGM 100:2008, Bureau International des Poids et Mesures (BIPM), Sevres, France (2008).
- [38] JCGM, Joint Committee for Guides in Metrology, Evaluation of measurement data – Supplement 1 to the "Guide to the expression of uncertainty in measurement" – Propagation of distributions using a Monte Carlo method, JCGM 101:2008 Bureau International des Poids et Mesures (BIPM), Sevres, France (2008).
- [39] VAN GRIEKEN R., MARKOWICZ, A., in *Handbook of X-ray Spectrometry*, ISBN:0-8247-0600-5, Marcel Dekker Inc., New York (2002).
- [40] MANTLER, M., 'Quantitative Analysis', *Practical Handbook of X-Ray Spectrometry* (BECKHOFF, B., KANNGIEßER, B., LANGHOFF, N., WEDELL, R., WOLFF, H., Eds.), Springer-Verlag, Berlin (2006).
- [41] PANTAZIS, T., PANTAZIS, J., HUBER, A., REDUS, R., (2010) 90-97.
- [42] GATTI, E., REHAK, P., Silicon drift chambers - first results and optimum processing of signals, *Nucl. Instrum. Methods Phys. Res. A* **225** (1984) 608-614.
- [43] KEMMER, J., Fabrication of low noise silicon radiation detectors by the planar process, *Nucl. Instrum. Methods. Phys. Res. A* **169** (1980) 499-506.
- [44] JALAS, P., NIEMELA, A., CHEN, W., REHAK, P., CASTOLDI, A., LONGONI, A., New results with semiconductor drift chambers for x-ray spectroscopy, *IEEE Trans. Nucl. Sci.* **41** (1994) 1048-1058.
- [45] NITON: XL3t GOLD series, .
- [46] BRUKER - Elemental: Tracer III-SD or IV-SD, .
- [47] Innov-X Systems: Delta Premium Vacuum, .
- [48] CESAREO, R., X-ray physics: Interaction with matter, production, detection, *La Revista del Nuovo Cimento della Societa Italiana di Fisica*, Bologna (2000).
- [49] POTTS, P.J., WEBB, P.C., WILLIAMS-THORPE, Use of microscopic XRF for non-destructive analysis in art and archaeometry, *J. Anal. At. Spectrom.* **12** (1997) 769-778.
- [50] MARKOWICZ, A., 'Quantification and correction procedures', in *Portable X-ray Fluorescence Spectrometry, Capabilities for In-Situ Analysis* (POTTS, P.J., WEST, M., Eds), The Royal Society of Chemistry **13** (2008) 36-54.
- [51] KALNICKY, D.J., SINGHVI, R., Field portable XRF analysis of environmental samples, *J. Hazard. Mater.* **83** (2001) 93-122.
- [52] US EPA Method 6200, Field portable X-ray fluorescence spectrometry for the determination of elemental concentrations in soil and sediment, Revision 0, February (2007).
- [53] PARSON, C., The distribution and mobility of arsenic in soils: The effects of successive redox cycles, Doctoral Thesis. Université Joseph Fourier Grenoble I (2011).

- [54] GONZALEZ-FERNANDEZ, O., QUERALT, I., Fast elemental screening of soil and sediment profiles using small-spot energy dispersive X-ray fluorescence: Application to mining sediments geochemistry, *Appl. Spec.* **64** (2010) 234A-268A and 967-1071.
- [55] MARGUI, E., TAPIAS, J.C., CASAS, A., HIDALGO, M., QUERALT, I., Analysis of inlet and outlet industrial wastewater effluents by means of benchtop total reflection X-ray fluorescence spectrometry, *Chemosphere* **80** (2010) 2630-2637.
- [56] POTTS, P.J., WEST, M. (Eds.), *Portable X-ray fluorescence spectrometry. Capabilities for in situ analysis*, RSC Publishing (2008).
- [57] CURRIE, L.A., Detection and quantification capabilities and the evaluation of low-level data: Some international perspectives and continuing challenges, *J. Radioanal. Nucl. Chem.* **245** 1 (2000) 145-156.
- [58] NITON[®] XLt 700 Series Instruments. Elemental limits of detection in soils, mg/kg. NITON LLC (2004).
- [59] JCGM, Joint Committee for Guides in Metrology, *International Vocabulary of Metrology – Basic and general concepts and associated terms (VIM 2008 with minor corrections)*, Bureau International des Poids et Mesures (BIPM), Sevres, France, 100 (2008).
- [60] Quality Assurance/Quality Control guidance for removal activities. Sampling QA/QC plan and data validation procedures. EPA/540/G-90/004. OSWER Directive 9360.4-01 (1990).

ANNEX. CONTRIBUTED PAPERS

JOURNEY MONITORING SYSTEM

A.M. CASTELLANOS, A. NOVELLO, H. BLANCO BELLO, A. CARELLI, M. DOMÍNGUEZ, C. LAISE, H. SPINELLI

Comisión Nacional de Energía Atómica, Unidad Seguridad, Centro Atómico Ezeiza, Argentina

E-mail: castella@cae.cnea.gov.ar; acastella2003@yahoo.com.ar

Abstract

The methodology used to assess the environmental baseline of the Ezeiza Atomic Centre in Argentina is presented. The Ezeiza Atomic Centre, located in the Buenos Aires province of Argentina Republic, has a surface of 844 ha and is 33 km away from the Federal District of Buenos Aires. The area is divided in two parts by a road, and several facilities, which involve the management of open and sealed radioactive sources, are located on the site. Among them, there are a 10 MW research reactor for radioisotopes production, nuclear power plants, a fuel elements manufacturing plant, three radioisotopes production plants for medicine and industry, and a waste interim storage and conditioning facility. With the objective of environmental monitoring of the site, and to design the surveillance plan, the first priority, which needed to be addressed, was the assessment of the environmental baseline. The presented method emerged as one of the most suitable to carry out this task, since the method is fast, 'fit for purpose', and effective, taking into account the large areas on which measurements had to be performed. The employed method that involves the use of radiation detectors, a GPS, and free software available to all online, is presented. Thanks to its simplicity, the method can be applied to the assessment of large contaminated areas as a first monitoring of the site, and to evaluate the remediation progress or decontamination factors established by the procedures of remediation.

1. INTRODUCTION

The Ezeiza Atomic Centre is located in the Buenos Aires Province, 33 km away from the Federal District of Argentina called Buenos Aires too. The size of the site is 844 ha, which is divided in two parts by a road.

The Ezeiza Atomic Centre is a nuclear site on which several facilities operate:

- Nuclear fuels production plant;
- Facilities for wastes disposal and management;
- Nuclear science and technology research and development laboratories;
- Research nuclear reactor of 10 MW (RA-3);
- Nuclear power plants;
- Three radioisotopes production plants (^{131}I , ^{99}Mo , ^{60}Co , among others);
- Industrial irradiator for sterilization purposes;
- Cyclotron.

1.1. Brief history

The Ezeiza Atomic Centre was created in the late 50's and started with some laboratories for chemical experiments in which the scientists worked with natural uranium that was extracted from the uranium mines. A research reactor called RA-3 was built a few years later, in order to start the development of radioisotopes production for medical uses. By that time, Argentina had a significant development in certain areas of science, which was higher than for many other countries in the region, and only compared to Brazil.

Later in the 70's a first nuclear power plant called Atucha 1 (CNA-1) was started up. As a result of this development, facilities for radioisotope production for medical, and industrial applications, and different facilities of the nuclear fuel cycle, were built in a short time in different parts of the country. Standards, control and regulation of the nuclear activities were carried out by the Atomic Commission itself, and the regulatory body was inside the Atomic Commission as it was usually the model in several countries at this time. Since 1995, the regulatory body is separated from the National Atomic Energy Commission and from the operation of the nuclear power plants too [1].

The environmental monitoring of the facilities remained by that time in the hands of the regulator, but since some years, this activity is being transferred to the operator, so that it was necessary for the operator to start with the design and implementation of an environmental radiation monitoring plan at the EZEIZA Atomic Centre. The operator and the regulator carry out separately their own plan and, with different criteria, both pursue the same final goal: public protection. The operator implements its plan in order to assess its performance with regards to the rules and regulations. As the operator is the legal responsible, it is very important to have a solid record system in the environmental monitoring plan. On the other hand, the regulatory body should do the appropriate controls to verify that the operator makes all the efforts to meet the standards, licenses and constraints. Both operator and regulator have the same objective: public protection. A good relationship between regulator and operator makes it easier to achieve this shared objective.

2. OBJECTIVES

The EZEIZA environmental monitoring plan has the following goals [2]:

- To verify the compliance with safety standards and operation licenses;
- To evaluate the long-term trends and performance of the environmental protection systems;
- To control the accumulation in the environment.

Assurance of public radioprotection, in harmonization with an integrated quality management system, that includes records and accountabilities clearly established, are key elements for achieving these objectives.

3. EZEIZA ENVIRONMENTAL MONITORING PLAN

3.1. Sampling

The environmental monitoring plan will include the sampling of freshwater, drinking water, soil, sediment, air, external exposure (dose-rate/dose), and compartments of possible accumulation of contaminants, like certain foodstuffs such as milk. Those sampling areas are selected to provide the site characterization and the baseline for evaluating tendencies with a reasonable accuracy.

3.2. Baseline

In order to establish the baseline of the site, a comprehensive monitoring of dose-rates is being done among other measurements. One of the methods that are being used is the “journey” monitoring, which is currently at its testing stage.

Performing the evaluation of the current dose-rates in the site, then the identification of the sources and circumscribing their extent, is necessary to make the difference between what is “normal or abnormal” [3]. When this system started to be used, some areas into the site, with little soil contamination, product of old practices that by the time they were done, had been performed in a way according to the “state-of-the-art” but that nowadays is not accepted by the current environmental protection practices, could be discovered. Most of the ‘hot-spots’, which were found, have been already removed and the rest of them are being used as controlled laboratory for testing of remedial methods.

4. USED MATERIALS

The materials employed for the “journey” monitoring are the radiation detector (RADEYE model PRD) as well as a homemade plastic holder. Those are shown in Fig. 1.



FIG.1. Materials employed in “journey” monitoring.

They were adapted to a vehicle for the journey, as shown in Fig. 2.



FIG.2. Working with the system.

In addition to the system described above, the vehicle had the following equipment items for the proper recording of the dose-rate data:

- GPS;
- RS232 adaptor + USB RS232 adaptor;
- Laptop and wireless internet adaptor;
- Software available:
 - Radeye-PRD;
 - Google Earth;
 - Screen Video Capturer.

Typical dose-rate and location recording display during “journey monitoring” is illustrated in Fig. 3.

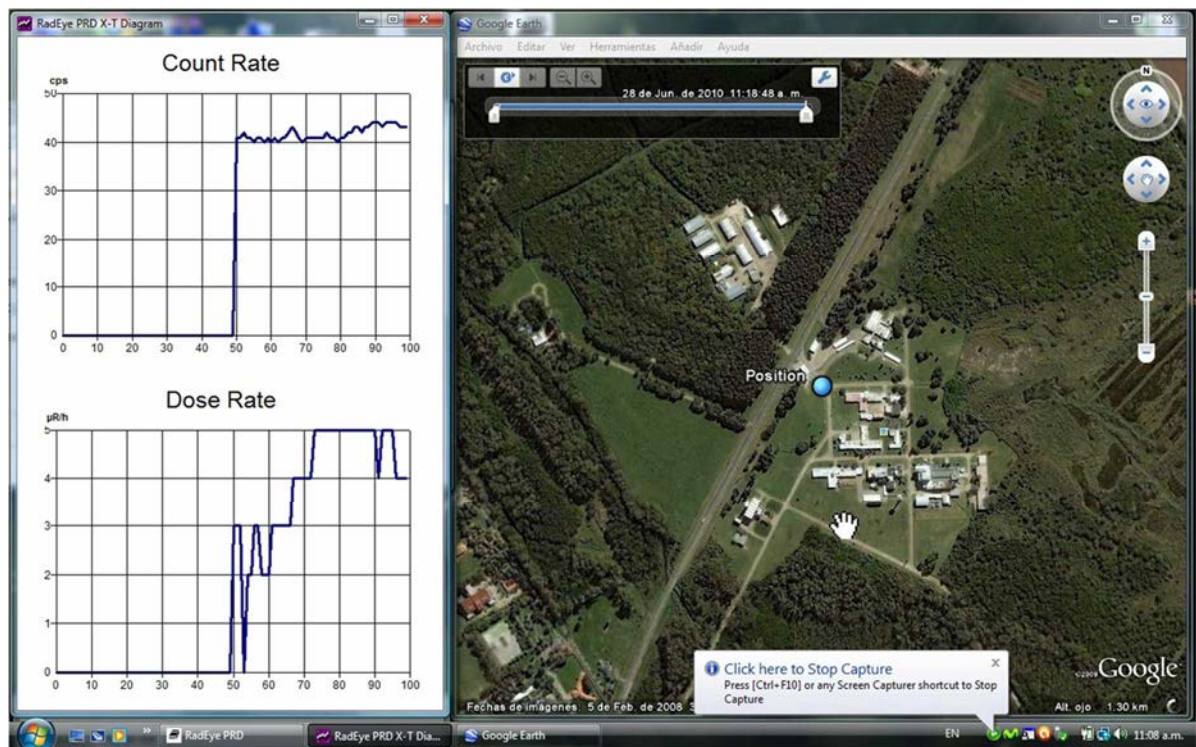


FIG.3. Display during a “journey” monitoring.

5. ADVANTAGES

The developed system presents the following advantages:

- Low cost;
- May use existing adapted equipment items;
- Offers a graphical user interface of the information (analogical vs. digital);
- Is suitable to record information;
- Is fast, and therefore can evaluate large areas in a short time period;
- Can give instantaneous information of abnormal deviations to allow taking early measures if necessary;
- Works on-line/in-situ;
- Is portable;
- Does not need to be operated by specialized personnel;
- Help in first steps of remediation of contaminated sites to evaluate decontamination factors.

6. DISADVANTAGES

The developed system has however the following two disadvantages:

- Manual link between geo-reference and dose-rate;
- Depends on the internet communication.

It has to be noticed that the link between geo-reference and dose-rate may be made automatic with additional effort.

7. CONCLUSIONS

“Journey” monitoring may be one of the methods to be used for establishing the baseline for the beginning of an environmental monitoring plan. It may also be a suitable method for the sampling of dose-rates in routine samples of the plan, taking into account that the measurements remain recorded as the “fingerprint” of the site.

It has been demonstrated that the developed system would be also useful for other purposes such as the searching of lost or hidden sources, and remediation evaluations. It is necessary to improve the link between the information related with the geo-references that is provided by the GPS and the results of dose-rate provided by the radiometer; this can however be solved by software programmers.

REFERENCES

- [1] Ley 24804 Nacional de la Actividad Nuclear.
- [2] DOMINGUEZ, M., Plan de Vigilancia Radiológica ambiental del CAE, Informe de BECA (2008).
- [3] ENGELBRECHT, R., SCHWAIGER, M., State-of-the-art of standard methods used for environmental radioactivity, Appl. Rad. Isot. **66** (2008) 1604.

CONSIDERATIONS FOR AN AUTOMATED SYSTEM TO DETECT ‘HOT’ PARTICLES

S.A. LONG, L.J. MARTIN, E.M. CAREY

Australian Radiation Protection and Nuclear Safety Agency (ARPANSA), 619 Lower Plenty Road
Yallambie, Victoria, Australia

Email: Emma.Carey@arpansa.gov.au

Abstract

As the radiological auditor for the Maralinga Rehabilitation Project, the Australian Radiation Protection and Nuclear Safety Agency (ARPANSA) was required to ensure that the remediated areas did not contain any particles highly contaminated with plutonium and that the numbers of moderately contaminated particles met the criterion set for the project. In order to examine a land area exceeding 2,500,000 m², it was necessary to develop an automated system for detecting ‘hot’ particles. The technical aspects considered when developing this system are discussed. In particular, the basis for optimizing the counting interval and an improved counting methodology are discussed and compared with alternatives. The performance of the system under the conditions found at Maralinga is also described.

1. INTRODUCTION

1.1. British Government nuclear weapons tests

The British Government detonated seven nuclear weapons at Maralinga, South Australia, between 1956 and 1957 (indicated as ‘major trial sites’ in Fig. 1) and the contamination resulting from these tests has largely decayed and no longer poses a health risk. However, the British Government also conducted many ‘minor trials’ at Maralinga between 1959 and 1963. These trials were safety tests and other experiments designed to develop the components of a nuclear weapon, and involved the dispersal of various radionuclides using conventional explosives. Most of these radionuclides were short-lived but four sites (TM100, TM101, Wewak and Taranaki) were still contaminated with plutonium (mainly ²³⁹Pu with smaller amounts of ²³⁸Pu, ²⁴⁰Pu and ²⁴¹Pu) some thirty years later.

1.2. The aim of the Maralinga Rehabilitation Project

The aim of the Maralinga Rehabilitation Project was to remediate the plutonium contamination to the extent that the site could be safely returned to its traditional owners. To this end, highly contaminated soil was excavated and buried on site, while moderately contaminated areas were made subject to restrictions on land use. Planning of the project began in 1993 and the remediation was completed in 2000.

The ‘minor trials’ not only dispersed finely divided contamination over large areas, as shown in Fig. 1, they also dispersed larger, highly contaminated particles to distances of a few hundred metres at each site. While these ‘hot’ particles were less than a few millimetres in size, and often smaller than the surrounding grains of sand, they could incorporate MBq quantities of plutonium. Since such highly contaminated particles pose a serious ingestion hazard, or worse, had the potential to contaminate a wound, it was essential that they be removed during the rehabilitation project.

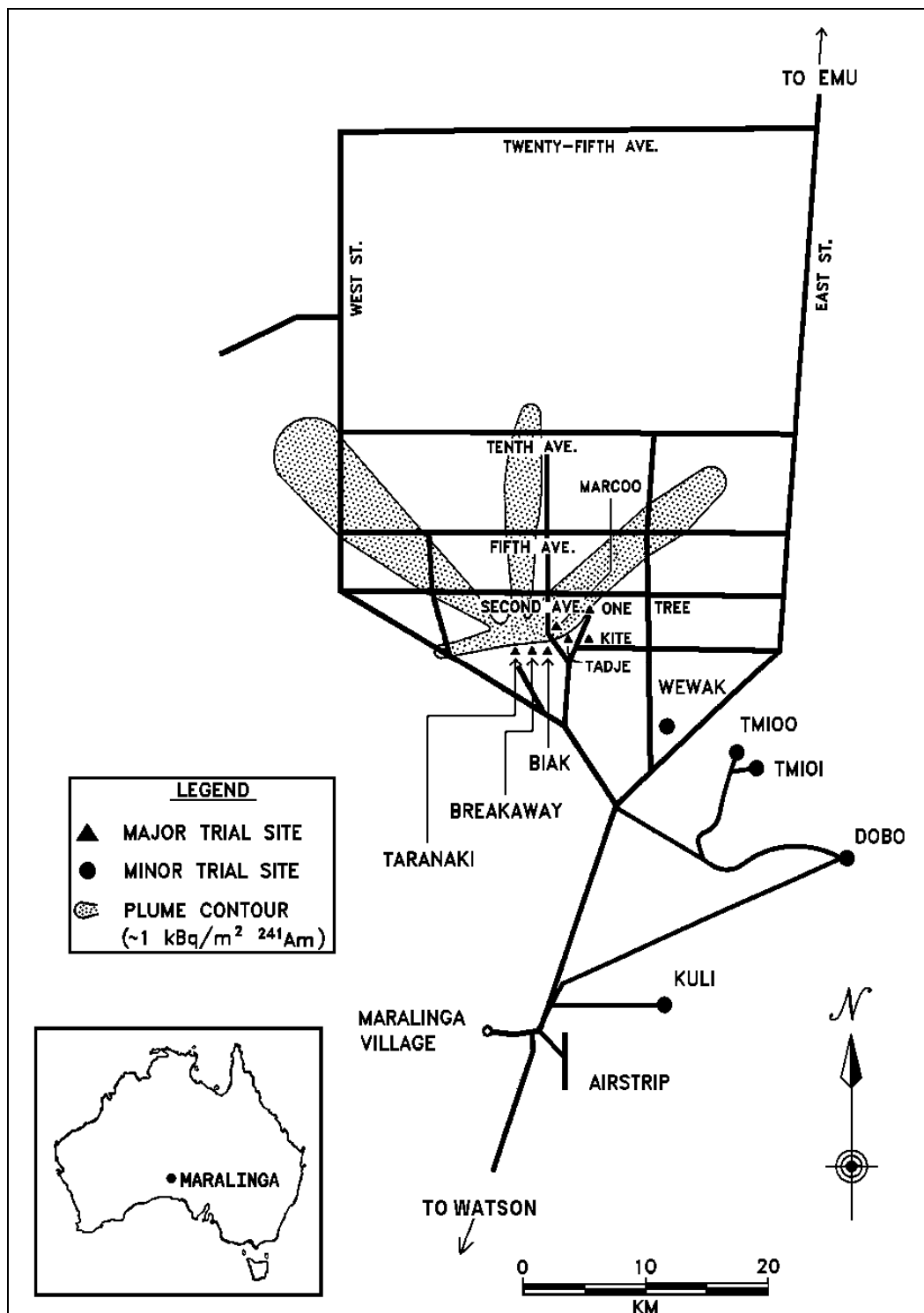


FIG. 1. Maralinga test sites detailing the names and locations of the major and minor trial sites.

1.3. ARPANSA's role in the Maralinga Rehabilitation Project

ARPANSA, as the radiological auditor, was required to ensure that the remediated areas did not contain any highly contaminated particles and that the density of moderately contaminated particles was within the criterion set for the project, i.e.:

- that all particles exceeding 700 kBq of ^{239}Pu activity were removed.
- that the density of particles exceeding 140 kBq of ^{239}Pu was less than 1 in 10 m².

ARPANSA was required to ensure that these criteria were met within a total area of 2,500,000 m².

While ^{239}Pu does not emit any gamma rays with sufficient intensity to permit practical measurements in the field, a minor constituent of the plutonium, ^{241}Pu , is relatively short-lived ($T_{1/2} = 14$ years) and decays to ^{241}Am which, although an alpha-particle emitter, emits an easily detected gamma ray. Given an empirical ratio of ^{239}Pu to ^{241}Am , the quantitative detection of this gamma ray may be used as a surrogate in the measurement of plutonium contamination levels.

To achieve the necessary measurements within the time permitted, ARPANSA was required to develop equipment items capable of surveying 10,000 m² in less than two hours, and able to detect all particles that exceeded 100 kBq of ^{241}Am (700 kBq ^{239}Pu).

Some of the technical aspects that were considered when designing this system are discussed and the optimisation of the counting interval and an improved counting methodology are also detailed. The solution developed by ARPANSA is compared to other systems and the performance of the ARPANSA system is also discussed.

2. GENERAL CONSIDERATIONS FOR A PARTICLE DETECTOR

Many issues need to be considered before a system to automatically detect 'hot' particles can be designed. These issues fall into three basic categories:

1. Regulatory issues that form the basic requirements of the task to be performed;
2. Practical issues that primarily involve the physical environment in which the survey is to be conducted;
3. Technical issues that involve the physical design of the detection system.

The regulatory and practical issues are generally beyond the control of the designer but have a considerable impact on the design of the system.

In the case of the Maralinga Rehabilitation Project, the regulatory and practical criteria were:

- The location of all particles exceeding 100 kBq of ^{241}Am activity must be determined within a metre to enable later verification and removal;
- Actual activity and location of a high activity particle could be determined by subsequent measurement with other instruments;
- The occasional indication of a 'hot' particle by the system, where none existed (false-positive identification), was acceptable;

- Areal density of particles exceeding 20 kBq of ^{241}Am had to be estimated but individual particles did not have to be located;
- Particles with activities less than 20 kBq ^{241}Am activity didn't need to be detected;
- Detectors must cover 100% of the area to be surveyed;
- Terrain could contain rocks or other obstacles up to 20 cm diameter;
- The surface may be slightly contaminated at levels up to 3 kBq/m² of dispersed ^{241}Am activity and would also emit higher energy gamma rays from naturally occurring radionuclides;
- The developed system should be capable of surveying areas at an average rate >1 m²/s;
- The developed system should be capable of operating for extended periods of time in temperatures regularly exceeding 35°C;
- The system must be easily serviceable in a remote field location.

The required regulatory and physical criteria suggest that the surveying system should be vehicle mounted to provide both speed of measurement and operator comfort. The system should incorporate a high-precision Global Positioning System (GPS) to enable the unambiguous location of particles. A detection system sensitive to gamma rays of 60 keV should be used and these detectors should not be closer to the ground surface than 25cm. The surveying system should also be automated to cope with the relatively high data rate and to enable accurate and complete records to be maintained.

3. TECHNICAL CONSIDERATIONS

General considerations for the design of a particle detection system were acceptable; however, careful consideration of the physics of the system enabled a significant refinement of the initial design.

3.1. Selection of the detector system

As described earlier, the detectors chosen had to be sensitive to the 60 keV gamma rays emitted by ^{241}Am , but they were not required to be sensitive to gamma rays at other energies. This immediately suggests the utilisation of an energy-dispersive detector and energy-discriminating electronics. The energy resolution of such a detector is important as one of the factors reducing the effect of background radiations. Taken into account the need for both high detection efficiency and robustness of the system, a scintillation detector and a Single Channel Analyser (SCA) to produce signals only if the energy is deposited in the detector at 60 keV are chosen for the surveying system.

Higher energy gamma rays may also deposit a 60 keV event in the detector if they deposit this energy through inelastic scattering. Compton scattering events such as those will contribute to the background signal in the system. The amount of Compton background is proportional to the detector volume. However, low-energy gamma rays are quickly absorbed by materials and the detection efficiency for such gamma rays is primarily determined by the detector area facing the source. Therefore, a thin but large area detector, such as the Bicron G5 detectors, chosen by ARPANSA for this project, would maximize the signal from ^{241}Am while minimizing the background from other sources.

The basic design of the surveying system is, therefore, to have one or more Bicron G5 detectors mounted on a vehicle which can be driven systematically over the area to be surveyed. As the detector passes over a particle, the count rate observed in an energy window set to about 60 keV will increase. The increase in count rate would be recorded by the electronics attached to the detector output. The count rate and GPS coordinates would be stored for subsequent analysis.

3.2. Optimization of the counting interval

The electronics monitoring the detector signal do not actually record the observed count rate, but rather acquire the number of counts over a specified counting interval. If this interval happens to be one second, then the acquired number of counts is equivalent to the count rate. However, a counting interval of one second may not be appropriate for the system.

If one examines the geometry of the system set-up as shown in Fig. 2, then one can determine that, for moderate values of H and O , the count rate observed by a thin detector moving at speed V , at a height H above the ground surface, at a longitudinal distance x and a lateral offset O from the particle is:

$$R = \frac{E \cdot S \cdot H}{4 \cdot \pi \cdot (x^2 + H^2 + O^2)^{3/2}} + B$$

Where,

$E = a \cdot \beta$ is the emission rate of the particle, with activity a and emission probability β ;

$S = A \cdot \varepsilon$ is the Effective Frontal Area (EFA) of a planar detector of area A and intrinsic efficiency ε ,

B is the contribution to the count rate due to sources other than the ‘hot’ particle (background contribution).

The count rate, as a function of longitudinal position, is shown in Fig. 3 where:

- The lateral offset is 25 cm;
- The height is 30 cm;
- The EFA of the detector is 100 cm²;
- The activity of a ²⁴¹Am particle is 100 kBq.

Background contribution to the count rate is a constant 15 counts per second (CPS), as shown in Fig. 3.

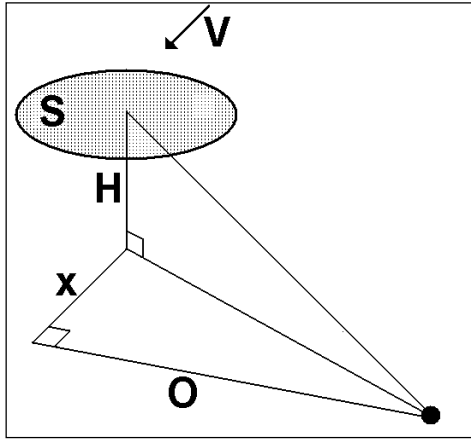


FIG. 2. The 'hot' particle – detector geometry.

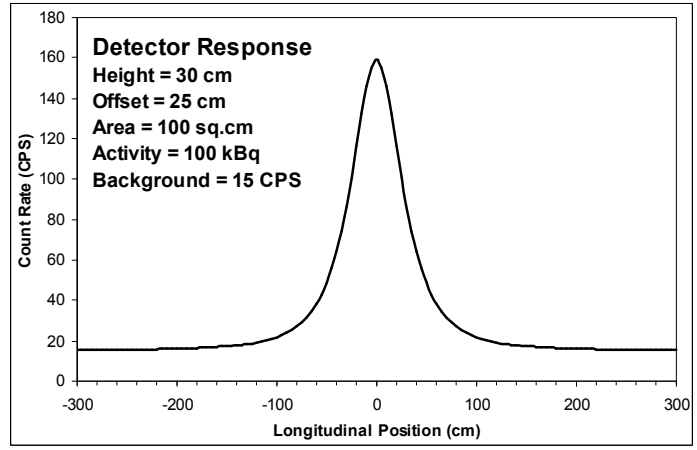


FIG. 3. Count rate as a function of longitudinal position.

It should be noted that the peak shown in Fig. 3 becomes narrower as the lateral offset is decreased and the response decreases considerably with increasing lateral offset. Consideration of these effects leads to the decision that an array of Bicron G5 detectors should be used, arranged 50 cm apart in order that the lateral offset is limited to 25 cm. The vehicle used would then have to be driven in such a way that the separation of the outer detectors on subsequent passes would be no more than 50 cm.

The total count recorded by the system is proportional to the area under the curve as shown in Fig. 3. Figure 3 clearly shows that, if the counting interval extends more than 100 cm beyond the location of the 'hot' particle, the increase in the area under the curve is most likely to be due to the background, rather than to the 'hot' particle. Further investigation on the effect of the counting interval requires the examination of the integral of the count rate:

$$C = \int_{t_1}^{t_2} R dt = \int_{x_1}^{x_2} R \cdot \frac{1}{V} dx$$

$$C_P = \frac{E \cdot S \cdot H}{4 \cdot \pi \cdot V} \cdot \frac{1}{H^2 + O^2} \cdot \left[\frac{x_2}{\sqrt{x_2^2 + H^2 + O^2}} - \frac{x_1}{\sqrt{x_1^2 + H^2 + O^2}} \right]$$

$$C_B = \frac{B \cdot (x_2 - x_1)}{V}$$

Where:

C_P are the counts due to the 'hot' particle;

C_B are the counts due to the background;

x_1 and x_2 are the longitudinal positions of the detector relative to the particle at the start and end of the counting interval.

To further illustrate the effect of the counting interval, Fig. 4 shows the integrated counts as a function of the counting interval for a 'hot' particle located at the centre of the interval, and those from other sources. Figure 4 shows that increasing the counting interval beyond 150 cm (75 cm either side of the 'hot' particle) significantly increases the background count rate but does not appreciably increase the count rate due to the 'hot' particle.

Figure 5 shows the ratio of counts due to a ‘hot’ particle to those due to the background, as a function of counting interval. Figure 5 shows that if the counting interval is made as small as possible, most of the acquired counts will be due to the particle. However, it should be noted that, as the counting interval is decreased, the total number of counts acquired is also decreased.

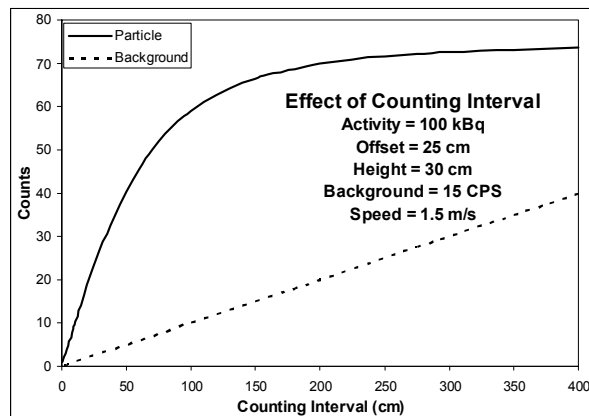


FIG. 4. Integrated counts as a function of counting interval.

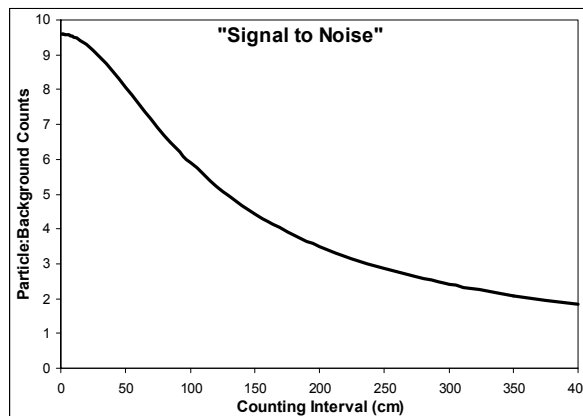


FIG. 5. Ratio of counts due to a particle to those due to other sources, as a function of counting interval.

Figure 6 shows that the relative uncertainty in the acquired counts due to the random nature of radioactive decay remains fairly constant with a decreasing counting interval until the interval is reduced to about 75 cm; after this, the uncertainty in the count rate increases rapidly. Increased uncertainty in the integrated counts will lead to an increase in the risk that a ‘hot’ particle will not be detected by the system. Clearly, a balance must be found between maximizing the ‘signal-to-noise’ ratio and minimizing the uncertainty. In the case of the system used at Maralinga, this balance dictates that a counting interval of between 50 cm and 80 cm would be optimum for the successful performance of the survey. Note that at a surveying speed of approximately 5 km/h, this counting interval corresponds to the detectors counting continuously for a period between 0.3 s and 0.6 s.

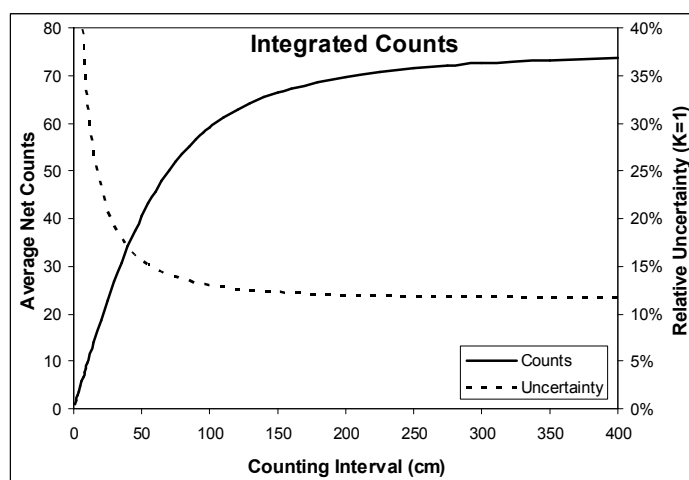


FIG. 6. Integrated counts as a function of counting interval. The net counts are shown as the solid line using the left axis. The relative uncertainty in these counts is shown as the dotted line using the axis on the right.

The equations show that the optimum counting interval is actually defined in terms of distance rather than time. Therefore, ARPANSA sought a method of generating a signal defining the counting period in terms of distance. It was noted that most modern vehicles use a Hall effect sensor on the tail shaft of the vehicle to produce the signals used to operate the speedometer and odometer. It was experimentally determined that a pulse was produced by this sensor every 21.3 cm travelled by the vehicle used at Maralinga. It was decided that the counting interval would be determined by three pulses from this unit, defining the interval to be 64 cm. It is worth noting that this signal was also used to drive a high-resolution speedometer, enabling the driver to more easily maintain the constant, slow speed required.

3.3. An improved counting methodology

The preceding discussion assumed that the particle was centrally located in the counting interval. As the location of the ends of the counting intervals and the location of the ‘hot’ particles are independent of each other, ‘hot’ particles would be randomly distributed across the counting intervals in which they are detected.

Figure 7 shows ‘hot’ particles randomly located in consecutive counting intervals. For ‘hot’ particles of equal activity, the equation for the integrated counts shows that the observed count rate in interval 3 or interval 4 would be 71% of that in interval 1. In order to account for such a large variation in count rate, one would have to accept a higher rate of ‘false-positive’ detections so as not to miss ‘hot’ particles located at the edges of counting intervals.

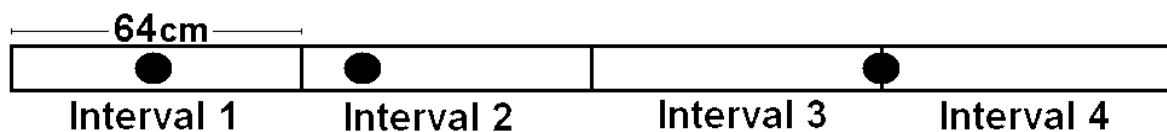


FIG. 7. ‘Hot’ particles, shown as black dots, located randomly in counting intervals.

It was realized that the large variation in count rate due to particle position could be minimized by utilizing overlapping counting intervals. It was relatively simple to define sub-intervals terminated by a single pulse from the odometer sensor and use the running sum of the counts from three consecutive sub-intervals as the total counts for the counting intervals. This is illustrated in Fig. 8.

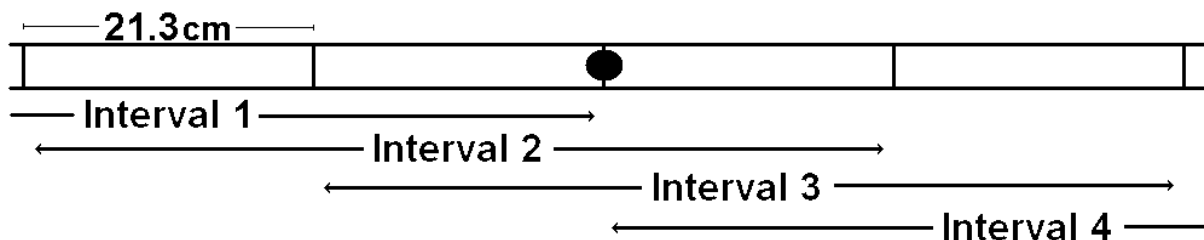


FIG.8. Overlapping counting intervals defined by three consecutive sub-intervals.

As can be seen in Fig. 8, while the particle is on the edge of intervals 1 and 4, it is near the centre of intervals 2 and 3. Indeed, the use of overlapping intervals means that the particle can be no further than 11 cm off-centre, resulting in a maximum variation of 3% in the count rate due to the position of the ‘hot’ particle in the counting interval.

By minimizing the variation with position, one is maximizing the number of counts recorded in the interval and, hence, the detection efficiency of the system. Figure 9 shows the Poisson probability that a ‘hot’ particle, placed in the worst possible position relative to the detector, will produce fewer than 20 counts during the counting interval. Figure 9 shows the probability that a ‘hot’ particle will not be detected by the system if the threshold for detection is 20 counts. Figure 9 clearly shows the superiority of using the overlapping counting intervals.

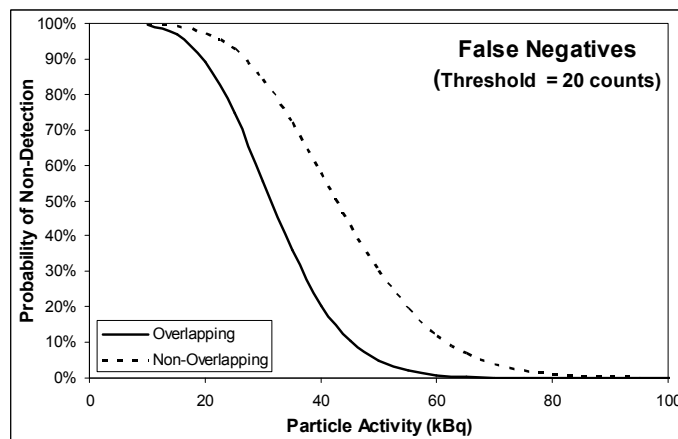


FIG. 9. Probability of a ‘hot’ particle not being detected, as a function of the ‘hot’ particle activity.

4. SYSTEM PERFORMANCE

The final design [2] of the ‘hot’ particle detection system is shown below in Fig. 10. The system consists of an array of four 12.5 cm diameter by 1.6 mm thick NaI(Tl) detectors mounted on the bull bar of a light four-wheel-drive vehicle. These detectors were each connected to a single-channel analyser set to count gamma rays of ~60 keV. The single-channel analysers were interfaced with a laptop computer so that the signals could be recorded and analysed.

The detectors were mounted at a nominal height of 30 cm above the ground surface with their centres 0.5 m apart. This allowed the systems to effectively survey a 2 m wide track, and by driving at a speed of 5-6 km/h, individual particles and fragments with an activity of 20 kBq could be detected with approximately 50% efficiency. All particles and fragments with an activity of 100 kBq or greater are detected within a 2 m track of such a system. By this procedure, the vehicle was able to thoroughly survey a hectare in 1-2 hours.

The vehicle was also fitted with a differential GPS (DGPS) system that was also interfaced with the computer so that the entire area covered by the searching process was accurately recorded. The position of all positive signals from any of the four detectors was also recorded to an accuracy of 1 m.

This system was used to survey the entire area of 250 hectares from which soil had been removed. This area had typically been surveyed by another particle detection system before being surveyed by the ARPANSA system. Nonetheless, the ARPANSA system located 121 ‘hot’ particles with activities exceeding 100 kBq of ^{241}Am activity. The system was also able to estimate the number of particles exceeding 20 kBq of ^{241}Am activity in a particular area through statistical analysis of the data stored during the survey.

The preceding discussion has concentrated on minimizing the probability that a high-activity particle will not be detected by the system and has assumed the worst-case scenario for geometrical efficiency. It can be shown that this worst-case scenario produces approximately half the counts compared with the best-case scenario, in which the 'hot' particle is immediately below the detector when the detector is in the centre of the counting interval. It means that a 50 kBq particle in the best-case scenario appears the same as a 100 kBq 'hot' particle in the worst-case scenario. Therefore, while the system will reliably detect all high-activity particles, it will also indicate the presence of many more such particles than they are really present. The actual calibration factor used to convert counts to activity meant that all particles that the system identified as having an activity above 70 kBq had to be investigated. This resulted in over 300 putative particles requiring investigation.

This system was also used to survey the perimeters of the three soil removal areas to ensure that no high-activity particles remained. While the terrain in the soil removal areas consisted of cleared, rocky ground, levelled to a fairly smooth surface, the terrain in the 120 hectares of this perimeter consisted of uneven ground sparsely covered with vegetation. Nonetheless, the system was able to attain at least 70% coverage of these perimeter areas. During these perimeter surveys, the system located a further 85 high-activity particles. All of those particles were located within 50 m of the soil removal boundary, but further than 50 m from the survey perimeter.

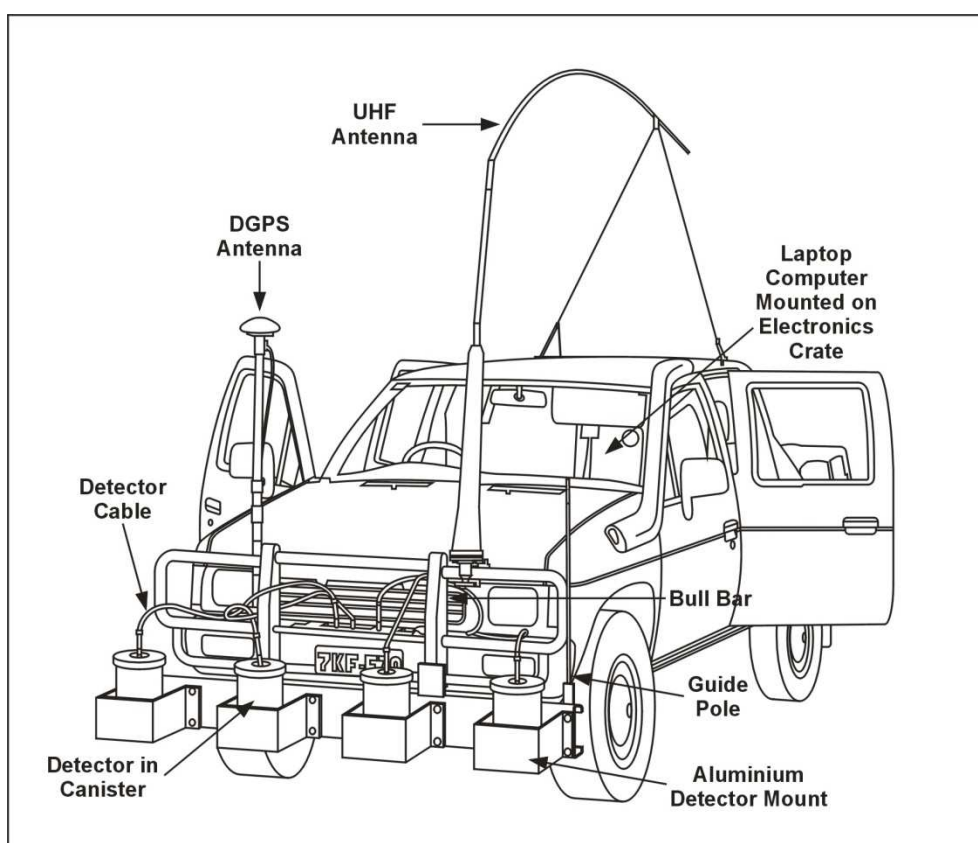


FIG. 10. The 'hot' particle detection system used at Maralinga.

5. CONCLUSIONS

The proper consideration of both the specific task to be performed and the technical aspects of ‘hot’ particle detection enabled significant optimization of the design of the particle detection systems. In particular, optimization of both the counting interval and counting methodology provided significant improvements over systems that use non-overlapping counting intervals of fixed time duration.

The designs of the ARPANSA systems were proven during the Maralinga Rehabilitation Project. In particular, the use of overlapping counting intervals defined by distance proved to be a very efficient method of locating ‘hot’ particles. This system was able to locate 121 particles, exceeding the defined criteria, and which had not been located by another system that had not been optimized for the task.

REFERENCES

- [1] “Rehabilitation of Former Nuclear Test Sites at Emu and Maralinga (Australia)”, in Report by the Maralinga Rehabilitation Technical Advisory Committee, Department of Education Science and Training, Canberra (2003).
(http://www.radioactivewaste.gov.au/framework/publications/store_and_maralinga_publications.htm)
- [2] LONG, S., MARTIN, L., BAYLIS, S., FRY, J., Development and performance of the vehicle-mounted radiation monitoring equipment used in the Maralinga rehabilitation project, J. Environ. Radioactivity **76** (2004), 207-223.

AN OPTIMIZED NaI(Tl) MULTI-DETECTOR METHOD FOR THE DETERMINATION OF SPATIAL CONTAMINATION IN URBAN AREAS

M.C.F. MOREIRA^{*1,2}, C.C. CONTI¹, R. SCHIRRU²

¹ Instituto de Radioproteção e Dosimetria, CNEN/IRD, Av. Salvador Allende s/nº, P.O. Box 37750, 22780-160 Rio de Janeiro, Brasil (Radiation Protection and Dosimetry Institute, CNEN/IRD)

² Universidade Federal do Rio de Janeiro, COPPE, Programa de Engenharia Nuclear, Laboratório de Monitoração de Processos, P.O. Box 68509, 21941-972 Rio de Janeiro, Brasil (Federal University of Rio de Janeiro, COPPE, Nuclear Engineering Program, Process Monitoring Laboratory)

Abstract

A four NaI(Tl) three-inches detectors arranged in a cross-shaped layout combined with Monte Carlo method and Artificial Neural Networks (ANN) has been proposed to assess the multi-directional contamination activity of urban surfaces following a radioactive release, for ground natural radiation mapping and/or to search for radioactive sources. This methodology has been optimized to a three 3"×3" NaI(Tl) detector arranged in a T-shaped layout asymmetrically shielded providing easier handling and reducing costs, weight and analysis time. The detectors' responses to the contaminated surfaces were simulated using Monte Carlo calculations. A very simple model of a street with a wall on either side was used to simulate the urban environment. Training and production datasets for the three detectors with lead shielding with the thicknesses of 2.5, 5.0, 7.5 and 10 cm were obtained with the Monte Carlo calculations. These datasets were used to train and test an ANN, which was chosen in a previous work. This approach can be used to indicate highly contaminated surfaces in a given area or even the direction where a radioactive source might be found, saving extra dose to the survey team. The results showed that trained ANN can accurately predict the contamination on urban surfaces and that the thickness of 5.0 and 7.5 cm present slightly better results. The proposed setup, its calibration and the calculations are a powerful tool for use in field surveys.

Keywords: in-situ radiation measurements, NaI(Tl) detectors' calibration, Monte Carlo simulations, neural networks, surface contamination assay.

1. INTRODUCTION

The dispersal of radioactive isotopes in the environment due to a nuclear or radiological accident at a large scale would cause the deposition of radioactive materials in different urban or semi-urban areas. This contamination dynamics is of complex modelling and, in many cases, based on models of atmospheric dispersion and on models of deposition on the surfaces according to weather conditions.

Some studies of Conti, Jacob, and Sachett [1-4] proposed in-situ gamma-ray measurements associated with mathematical models to assess the dose at a given point in space due to contamination on urban and flat surfaces. They use the Monte Carlo (MC) method to calculate the photon fluency at a given point in space, to assess the geometry of the detector, or even to compare with experimental values. In the cases studied up to now, just a single detector (target) was modelled and the geometry of the source was an approach to a semi-infinite plane with correction for finite geometry. The studies considered the radioactive material to be deposited on the soil surface or homogeneously distributed in the soil or distributed in the soil as a function of depth [3, 5]. Those are the three distributions considered to represent the soil contamination by radioactive materials.

* Corresponding author.

Tel.: +55 21 21732904 . Fax.: +55 21 24422530

Email: marcos@ird.gov.br

Address: Av. Salvador Allende s/n, 22631-450 Rio de Janeiro, RJ, Brasil

A recent work of Moreira et al. [6] using a NaI(Tl) four-detector setup and the Monte Carlo method (MC) to generate the detectors' data to train Artificial Neural Networks (ANNs) proved to be a suitable technique to assess the spatial contamination of urban and semi-urban surfaces. The single detector technique approaches this three-dimensional problem by a one-dimensional perception of the environment. The one-detector approach does not give any information on the photon's angle of incidence or origin.

The methodology proposed by Moreira et al. [6] has been optimized and a three NaI(Tl) detector arranged in a T-shaped layout asymmetrically shielded was studied. Lead shielding thicknesses of 2.5, 5.0, 7.5 and 10 cm were also tested in this work. The objective is to propose an optimized layout that provides easier handling and reduced costs, weight and analysis time.

The quantity of photons that reaches a certain detector in a multi-detector arrangement will be the result of the combination of the different concentrations on the contaminated surfaces. The overall assessment of the amount of photons that reach any of the three or four detectors can lead to the radionuclide concentration on each of the three different surfaces.

As in the previous work [6], the dimensions of the simulated surface were chosen to account for most of the photons that could reach the detectors in free air [5] and its total area is 200 m². The MC method was used to generate each detector's response dataset to three contaminated surfaces for the photon energy of 662 keV. In this study the Monte Carlo N-Particle Code MCNP5, worldwide validated [7-9], was used to obtain each detector's response to the three combined contaminated surfaces [10, 11]. A feedforward ANN using the backpropagation learning algorithm [12] was used to assess the response of this detector's arrangement for varying levels of surface contamination. The ANNs were implemented using the NeuroShell2 code.

2. EXPERIMENTAL SETUP

2.1. Detectors' layout and simulated environment

The present work studied the simulated contamination of two walls and of the ground for the energy of 662 keV, which is equivalent to the major yield gamma energy of ¹³⁷Cs. The surfaces of the walls considered were 5 m high by 10 m long. The surface area of the ground was 10 m wide by 10 m long. The chosen values for the dimensions of the surface of walls and ground were the same as in the previous work and aimed to take into account a typical urban area and the small contribution of the photons originated at distances greater than 10 m.

The detectors' layout consists of three 3"×3" NaI(Tl) detectors arranged in a T-shaped layout as shown in Fig. 1. A top view of the array can be seen in the schema (a) and a vertical cross section in schema (b). As in the four detector arrangement, this layout was proposed to favor the number of photons striking the detector from the unshielded directions and to reduce the influence of photons from other areas.

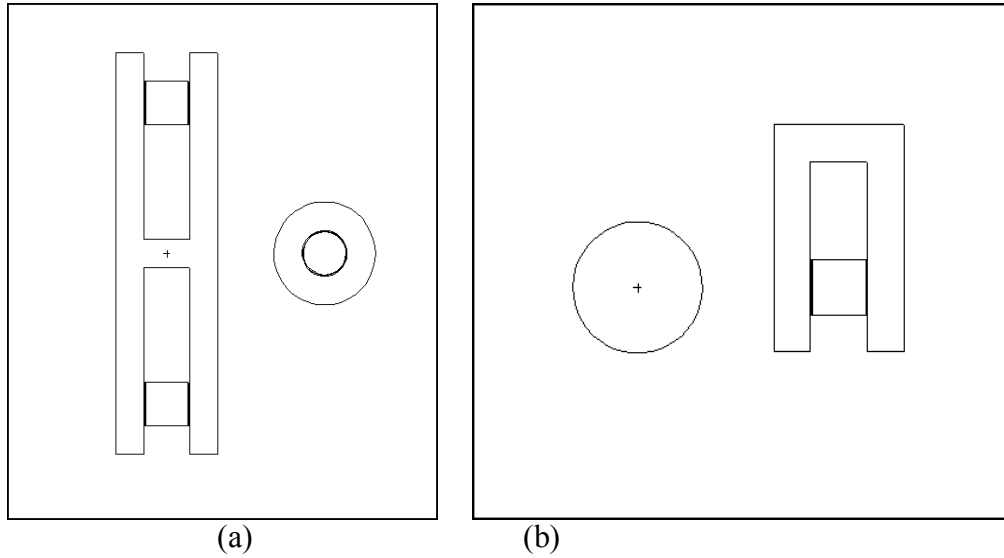


FIG. 1. Schematic view of the array of three NaI(Tl) detectors. A top view of the array can be seen in the schema (a) and a vertical cross section in schema (b). The numbers represent the surfaces and cells of the MC file.

The computer code MCNP5 – Monte Carlo N-Particle Code developed at Los Alamos National Laboratory [13] – was used to obtain the detectors' response datasets due to the contaminated surfaces. The Monte Carlo method simulates the transport of photons or particles in matter. The path of the photon or particle from its origin to the target is commonly referred as the photon or particle history. The average concentration values are determined by the simulation of a large number of cases [11, 14, 15].

The MCNP5 computer code is widely used in calculations of transport of photons and particles, as can be seen in the work of Jacob [16]. It was then used to simulate the three-dimensional geometry of this work. As in the previous work, the simulation consisted of photons being emitted from the surfaces with the number of photon histories ranging from $1\text{E}+05$ to $8\text{E}+09$ photons followed up by the code till they reach the target. The higher numbers of photon histories were reached by dividing the surfaces into smaller areas contaminated with $1\text{E}+09$ photons (MCNP5 limitation) and summing up the contribution from each of these areas.

2.2. Artificial neural network topologies

The NeuroShell2 computer code [17] was used to train, test, and implement the proposed artificial neural network. This code mimics the human capacity to solve complex problems of classification and estimated values using previous experience through the use of artificial neural networks. Several network topologies based on backpropagation learning can be used. In this work, a specific ANNs' topology called WARD was used. It was previously selected by Moreira et al. [6] as the most suitable topology for the four-detector layout. This is a feedforward ANNs' topology with the backpropagation learning algorithm. This topology is suitable to solve problems of detecting the characteristics of the dataset.

Two very important parameters used in this work during the network learning phase are the momentum factor $\alpha = 0.5$ and the learning rate. The criteria to stop the learning process were the minimum value of the mean squared error of $1\text{E-}07$ and the maximum number of epochs elapsed since the last minimum value of mean squared error of $1\text{E+}05$. All those parameters were adjusted to the same values as used in the previous work.

3. RESULTS

3.1. The training dataset

The datasets for each wall and ground surfaces were obtained by Monte Carlo calculations using the MCNP5 computer code for the following number of photon histories: $1\text{E+}07$, $5\text{E+}07$, $1\text{E+}08$, $5\text{E+}08$, $1\text{E+}09$ and $5\text{E+}09$ photons emitted from the surface. The Monte Carlo calculation uncertainty was kept below 2%.

It was demonstrated that the number of photons that reach each detector was proportional to the number of emitted photons from each surface, allowing the use of a base value from each surface with errors below 2% [6]. Each surface was divided in four parts and four simulation runs with $1\text{E+}09 \text{ } \gamma/\text{m}^2$ were done, the mean value of the four parts was used as the base value to derive the other values.

Training datasets of 343 elements were generated for the values of $1\text{E+}05$, $5\text{E+}05$, $1\text{E+}06$, $5\text{E+}06$, $1\text{E+}07$, $5\text{E+}07$, $1\text{E+}08$, $5\text{E+}08$, $1\text{E+}09$ and $8\text{E+}09 \text{ } \gamma/\text{m}^2$ of contamination for each surface and the correspondent numbers of photons that reached the detectors. Four different datasets were generated to the lead shielding thicknesses of 2.5, 5.0, 7.5 and 10 cm. For this work, only the energy of 662 keV was used.

Two different datasets with 30 elements each, called productions datasets, were produced using the base values and pseudo-random values ranging from $1\text{E+}05$ to $5\text{E+}09 \text{ } \gamma/\text{m}^2$ for each surface for the first dataset and from 0 to $1\text{E+}10$ for each surface for the second dataset. The first production dataset aims to test a range of values equivalent to the training data and the second production dataset aims to test the generalization capability of the chosen ANNs to values that are not present in the training dataset.

3.2. The parameter of the artificial neural network

For this study, the WARD ANN topology was used. Three neurons were used for input and output layers corresponding to the dimensions of the input and output vectors with the activation functions of hyperbolic tangent and logistics respectively. The neurons at the input layer represent the number of photons that reach each detector, and the neurons at the output layer represent the number of photons (contamination) on each surface.

The WARD ANN with three hidden layers with 20 neurons in each layer was implemented with the following activation functions: Gaussian, Gaussian complementary and hyperbolic tangent. This topology showed the best results for this problem.

The NeuroShell2 code automatically and randomly chose 20% of the training dataset and uses it as a calibration dataset. It was chosen to present the data randomly to the ANN, providing that this is not a time series problem, and the order in which the values are presented to the ANN should not be considered in the learning process.

3.3. Training results

Table 1 presents the results for the four different thicknesses of the lead shielding. The training process was stopped when a mean squared error less than or equal to $1.00\text{E-}07$ was achieved or when more than 100,000 epochs occurred after the last mean squared error was achieved. An epoch is defined as a complete pass through the ANN of the entire set of training patterns [17].

The following parameters were used to assess the different thicknesses and the three-detector layout: R^2 (coefficient of multiple determinations), r^2 (determination coefficient) and the correlation coefficient. The parameter R^2 , squared multiple correlation coefficient, is a statistical indicator normally applied to the multiple regression analysis. It compares the accuracy of the value of the model to the accuracy of another model of which the predicted value is the average of all values [17]. The correlation coefficient r was used to measure the degree to which the predicted values obtained from each studied network varies from the values of the MCNP simulated data. The parameter r^2 is simply the square of the correlation coefficient, also known as the determination coefficient, and it is a measurement of the variance of a predictable variable from the other variable.

TABLE 1. R^2 , r^2 E CORRELATION COEFFICIENT FOR THE THREE-DETECTOR LAYOUT USING THE WARD ANN TOPOLOGY, FOR THE TRAINING AND PRODUCTION DATASETS FOR THE 4 STUDIED THICKNESSES

Lead shielding thickness		2.5 cm			5 cm			7.5 cm			10 cm		
		Detector 1	Detector 2	Detector 3	Detector 1	Detector 2	Detector 3	Detector 1	Detector 2	Detector 3	Detector 1	Detector 2	Detector 3
Training data set	R^2	1.0000E+00	1.0000E+00	1.0000E+00	1.0000E+00	1.0000E+00	1.0000E+00	1.0000E+00	1.0000E+00	1.0000E+00	1.0000E+00	1.0000E+00	1.0000E+00
	r^2	1.0000E+00	1.0000E+00	1.0000E+00	1.0000E+00	1.0000E+00	1.0000E+00	1.0000E+00	1.0000E+00	1.0000E+00	1.0000E+00	1.0000E+00	1.0000E+00
	r	1.0000E+00	1.0000E+00	1.0000E+00	1.0000E+00	1.0000E+00	1.0000E+00	1.0000E+00	1.0000E+00	1.0000E+00	1.0000E+00	1.0000E+00	1.0000E+00
Production data set (inside range)	R^2	9.9210E-01	9.3760E-01	9.9960E-01	9.8400E-01	9.9840E-01	9.9880E-01	9.8340E-01	9.9010E-01	9.9830E-01	9.5340E-01	9.8920E-01	9.9790E-01
	r^2	9.9340E-01	9.5810E-01	9.9980E-01	9.8530E-01	9.9870E-01	9.9910E-01	9.9070E-01	9.9530E-01	9.9940E-01	9.7760E-01	9.9520E-01	9.9920E-01
	r	9.9670E-01	9.7880E-01	9.9990E-01	9.9260E-01	9.9940E-01	9.9960E-01	9.9540E-01	9.9760E-01	9.9970E-01	9.8870E-01	9.9760E-01	9.9960E-01
Production data set (outside range)	R^2	0.0000E+00	0.0000E+00	9.5000E-02	0.0000E+00	6.7800E-02	2.2000E-02	1.4760E-01	3.9300E-02	1.7190E-01	0.0000E+00	0.0000E+00	1.1900E-02
	r^2	3.7790E-01	1.9500E-02	1.8430E-01	2.6220E-01	2.6020E-01	4.0040E-01	6.8220E-01	4.1030E-01	4.3380E-01	4.1720E-01	5.2050E-01	4.5910E-01
	r	6.1480E-01	1.3950E-01	4.2930E-01	5.1210E-01	5.1010E-01	6.3280E-01	8.2600E-01	6.4050E-01	6.5860E-01	6.4590E-01	7.2150E-01	6.7760E-01

It can be seen from the data presented in Table 1 that the ANN showed slightly better values for the thicknesses of 5 and 7.5 cm for the training and production (inside range) datasets, but in all cases the values are closer to the unity showing good agreement between simulated and predicted values. For the production dataset (outside range) no agreement is shown.

4. DISCUSSION

The data presented in Table 1 shows that NaI(Tl) three-detector array with 5 cm thick lead shielding have attained values for R^2 , r^2 and correlation coefficients equal to 1 for the training datasets. For the production dataset with values inside the training range, the values are very close to the unity. For the production dataset with values outside the training range, very low results or even zero showed that no correlation or agreement was observed for this dataset.

Table 1 also shows that the different shielding thickness cases produced no greater difference for the R^2 , r^2 and correlation coefficient value. For the training datasets all of them are equal to the unity and for the production dataset (inside range) the values are very close to the unity with slightly better values for the thicknesses of 5 cm and 7.5 cm. The production dataset (outside range) values were very low, close to zero in some cases.

5. CONCLUSION AND RECOMMENDATIONS

The three 3"×3" NaI(Tl) detector T-shaped layout and the calibration methodology presented have proven to be adequate to determine the spatial contamination in urban and semi-urban areas. Lead shielding thicknesses of 2.5, 5.0, 7.5 and 10.0 cm show good results and can be used. The thicknesses of 5.0 and 7.5 cm present slightly better results.

As the ANNs were tested only with the described ANN topology for the energy of 662 keV, the study of this technique for higher energies (3,000 keV) has to be completed and compared with these results for better layout evaluation.

REFERENCES

- [1] CONTI, C.C., et al., Air Kerma Above Environmental Radiometric Calibration Facility For field Equipmant, V Encontro Nacional de Aplicações Nucleares : s.n. (2000).
- [2] CONTI, C.C., et al., Ge detectors calibration procedure at IRD/CNEN for in situ measurements, International Symposium on Technologically Enhanced Natural Radiation, Rio de Janeiro (1999).
- [3] JACOB, P., PARETZKE, H.G., Gamma-ray exposure from contaminated soil, Nuclear Science and Engineering **93** (1986) 155.
- [4] SACHETT, I.A., Caracterização da radiação gama ambiental em área urbana usando uma unidade móvel de rastreamento, Tese de Doutorado, D.Sc. Rio de Janeiro, RJ, Brasil : IBRAG – UERJ (2002).
- [5] MOREIRA, M.C.F., Padronização de um método para espectrometria gama in situ com detector de Germânio. Dissertação de Mestrado, M.Sc. Rio de Janeiro, RJ, Brasil : COPPE – UFRJ (1990).
- [6] MOREIRA, M.C.F., CONTI, C.C., SCHIRRU, R., A new NaI(Tl) four-detector layout for field contamination assessment, Nucl. Instrum. Methods Phys. Res. Sect. A. **621** (2010) 302.
- [7] SAITO, K., MORIUCHI, S., Monte Carlo calculation of accurate response functions for a NaI(Tl) detector for gamma rays, Nucl. Instrum. Methods **185** (1981) 299.
- [8] HENDRICKS, P.H.G.M., MAU, M., MEIJER, R.J., MCNP Modelling of Scintillation-Detector Gamma-Ray Spectra From Natural Nuclides, Appl. Radiat. Isot. **57** (2002) 449.
- [9] RIEPPO, R., VANSKA, R., Efficiency calibration of a 4" x 4" face-type NaI(Tl) double crystal gamma-ray spectrometer, Nucl. Instrum. Methods **155** (1978) 459.
- [10] KALOS, M.H., WHITLOCK, P.A., Monte Carlo Methods, Wiley - Interscience publication, New York (1986).
- [11] RUBINSTEIN, R.Y., Simulation and the Monte Carlo Method, John Wiley & Sons, Inc., New York (1981).
- [12] FAUSETT, LV., Fundamentals of Neural Networks'Architeture, Algorithms and Applications. s.l., Prentice Hall (1994).
- [13] MCNP - A General Monte Carlo n-particle transporte code: Overview and theory, Los Alamos National Laboratory (2003).
- [14] SALINAS, I.C.P., Determinação dos fatores de blindagem para construções tipicamente brasileiras, Tese de Doutorado, D.Sc. Rio de Janeiro, RJ, Brasil : s.n., UFRJ - COPPE (2006).
- [15] SALINAS, I.C.P., CONTI, C.C., LOPES, R.T., Effective density and mass attenuation coefficient for building material in Brazil, Appl. Radiat. Isot. **64** (2006) 13.
- [16] JACOB, P., MECKBACH, R., Shielding Factors and External Dose Evaluation, Radiat. Prot. Dosim. **21** (1987) 79.
- [17] Ward Systems Group Inc. NeuroShell II Manual (1993).

EVOLUTION OF RADIOACTIVE CONTAMINATION IN PLOUČNICE RIVER BASIN (BOHEMIA) DUE TO URANIUM MINING IN THE PERIOD 1992-2009

E. HANSLÍK, P. ŠIMEK, D. IVANOVÁ, M. NOVÁK, M. KOMÁREK

T.G.M. Water Research Institute, Public Research Institution, Czech Republic

Email: eduard_hanslik@vuv.cz

Abstract

Since the end of the 60's, both the classical underground mining and in-situ acid leaching have been used to exploit uranium in Stráž pod Ralskem locality in Northern Bohemia. Before putting a central decontamination station into operation in 1989, the Ploučnice river was contaminated by waste waters, which contained ^{226}Ra and uranium. During high flows, sediments and suspended solids from the river polluted also the flood plain areas. The uranium mining was terminated in 1994 and subsequently a programme was established for monitoring of the changes in the basin contamination by radioactive substances. The river bottom sediments were sampled in the longitudinal profile of the Ploučnice river with the frequency of one sample in a year in the period 1994-1999 and subsequently the sampling interval was reduced to five years. The gamma-ray spectrometric analysis of the samples was focused on determination of the concentrations of ^{226}Ra and ^{228}Ra . The flooded areas were also monitored by in-situ measurements of gamma radiation at the height of one meter above the ground. The measurements were carried out simultaneously with sediment sampling. The results of the analyses of riverbed sediments showed that their contamination by the radionuclides, particularly by ^{226}Ra , was decreasing as well as the gamma radiation in the flood plain areas.

1. INTRODUCTION

Since the end of the 60's, both the classical underground mining and in-situ leaching have been used to exploit uranium in Stráž pod Ralskem locality. The underground mining was accompanied by extraction of high amount of mine water (in a rate of about 500 L/s). This water contained high concentrations of ^{226}Ra and uranium, particularly in dissolved form. Before putting a central decontamination station into operation in 1989, the Ploučnice river was contaminated by the waste waters. The uranium mining was terminated in 1994 and the chemical extraction, which did not have impact on water radioactivity in the Ploučnice river, in 1996. Since 1996, the impacted localities have been gradually restored. Since the beginning of the uranium mining until 1999, the hydrosphere was permanently monitored for its contamination by radioactive substances, particularly by ^{226}Ra . The main results of the monitoring of the impacts of the uranium ore mining on hydrosphere are described in research reports of the T.G.M. Water Research Institute [1-4]. In July 1981, an extreme flood of the Ploučnice river caused contamination of its flooded area by riverbed sediments. A monitoring system was consequently established to monitor the changes in the hydrosphere contamination in the Ploučnice river basin by radioactive substances, particularly in relation to high flows. The riverbed sediments were sampled in 7 sites located in the reach along the Ploučnice river between Noviny and Děčín, and also in the Svitávka river at Zákupy reference river site, which was not contaminated. The sampling was performed with a frequency of one sample in a year in the period 1994-1999 and subsequently the interval was reduced to 5 years. The intention was also to perform the sampling after a possible flood with return period of 5 years or more, but no flood of such magnitude occurred during the period 1994-2009. The gamma-ray spectrometric analysis of the samples was focused on determination of the concentrations of ^{226}Ra and ^{228}Ra . The flooded areas were also monitored at 8 sites by in-situ measurements of gamma radiation at the height of one meter above the ground. The measurements were carried out simultaneously with sediment sampling. The last measurement was carried out in 2009 and this measurement included reed sampling at sediment sampling sites [5].

2. METHODS

2.1. Gamma radiation

The monitored cross-sections were fixed by using granite blocks (at Hradčany site, the monitoring sites were signed on a bridge). The gamma radiation was monitored between the blocks in the selected river cross-sections. The location of the cross-sections is shown in Fig. 1 (D1 Mimoň and D2 Mimoň (left and right bank), D3 Hradčany inflow and D4 Hradčany outflow, D5 Boreček and D6 Brenná, D7 Žizníkov and D8 Žizníkov). The in-situ measurements of gamma radiation were performed at fixed sites of the cross-sections at the height of one meter above the ground. The gamma radiation was measured by using TESLANB 3201 device during a time period of 10 s subsequently for three times in pGy/s and for graphical interpretation the results were converted to $\mu\text{Gy/h}$. The relative standard deviation at 95% level of confidence was 15.6% for values around 30 $\mu\text{Gy/h}$, 3.9% for 130 $\mu\text{Gy/h}$ and 2.8% for 300 $\mu\text{Gy/h}$.

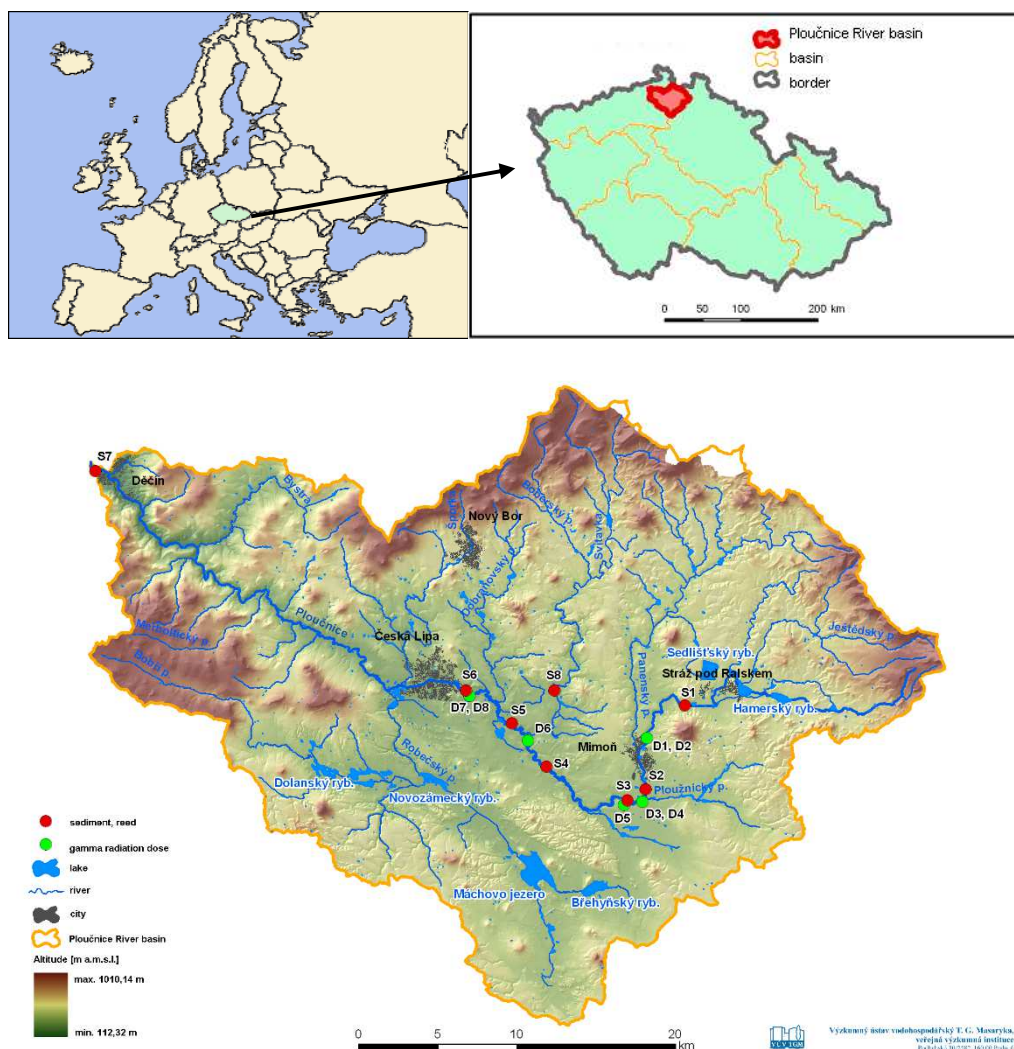


FIG. 1. Locations of cross-sections for monitoring of gamma radiation (D1 to D7) and sampling of sediments and reed (S1 to S7) in the Ploučnice river basin.

2.2. Sampling and gamma-ray spectrometric analysis of sediments and biomass

The sampling was performed at 7 river sites - S1 Noviny, S2 Mimoň laguny, S3 Boreček, S4 Veselí, S5 Vlčí Důl, S6 Žizníkov and S7 Děčín Zámecký rybník. The Svitávka river at Zákupy was chosen as reference river site (not contaminated). The locations of the S1 to S8 river sites are shown in Fig. 1. The sediment samples were taken from the depth of 10 cm below the ground surface and homogenized by their mixing in a plastic box. Some of the samples were used for grain size analysis performed by ARCADIS Geotechnika a.s. Praha Laboratories (formerly Geotechnika a.s. Praha) [6, 7]. The grain size of all the samples was below 2 mm. In the laboratory, the samples were dried at a temperature of 105°C to their constant weight and located into Marinelli containers, whose volume was 450 mL. The covers of the containers were hermetically sealed using silicone lubricant. For reaching radioactive equilibrium between the radionuclides of uranium and thorium series, the samples were subsequently located in a dustless ventilated room for a period of 30 days.

The reed was sampled at sediment sampling sites S1 to S6, S8 and at the mouth of the Ploučnice river (the reed did not grow at S7 Děčín Zámecký rybník river site) at the boundaries between water and banks. In the laboratory, the reed samples were dried at a temperature of 105°C and located into Marinelli containers, whose volume was 450 mL. Activities of the radionuclides emitting gamma radiation were determined using methods specified in the ČSN ISO 10703 standard on "Water quality – Determination of radionuclide activities by spectrometric measurement of gamma radiation with high resolution". Gamma-ray spectrometry with REGe (N-type) semiconductor germanium detector (GR 3018 model), whose relative efficiency is 30% and FWHM resolution is 1.8 keV for ^{60}Co peak with energy of 1,332 keV, was used for their determination. For energetic and efficiency calibration, etalon of ^{152}Eu from ČMI IIZ type MBSS 1, with an activity of 2,240 kBq and a geometry of 450 mL Marinelli container, was used. The measurement duration t was from 4 to 12 h. The minimum detectable activity a_{ND} , specified for level of significance $\alpha = \beta = 0.05$, was 0.5 Bq/kg for ^{137}Cs in samples of sediment and reed and measurement duration of 8 h. Genie 2000 software was used for the analysis. The results of the gamma-ray spectrometric analysis were specified in Bq/kg of dry matter with a measurement uncertainty of 2 sigma.

3. ASSESSMENT OF RESULTS AND DISCUSSION

3.1. Gamma radiation in the flooded area

The results of the gamma radiation monitoring were interpreted graphically. An example of the results for a contaminated site (D5 Boreček) and for an uncontaminated site (D8 Žizníkov) are given in Figs. 2 and 3. The gamma radiation values for 2009 were compared with minima and maxima values from the period 1992-2004. In the contaminated site (D5 Boreček, Fig. 2), the results for 2009 in the area of the first maximum at the distance between 6 m and 22 m were moderately below the minimum values from the preceding period. In the other observation sites, the gamma radiation values were at the level of lower range or moderately below this level in the whole length of the cross-section. The radiation level as specified for landfills in a Decree of the State Office for Nuclear Safety No. 307/2002 [8] was exceeded at the distance between 2 m and 22 m from the bank of the Ploučnice river. This criterion, originally specified for landfills, was also used for the assessment of the gamma radiation in the flooded areas.

The observed values in Gy were considered to be identical with the input of dose equivalent in Sv (§ 57, point e of the decree of the State Office for Nuclear Safety [8]), which specifies that deposited material meets the requirement stipulated in point a), it does not cause an increase in the radiation equivalent by more than $0.1 \mu\text{Sv/h}$ (as compared to the original value) at the distance of 1 m from the landfill surface and that the input of the dose equivalent does not exceed $0.4 \mu\text{Sv/h}$.

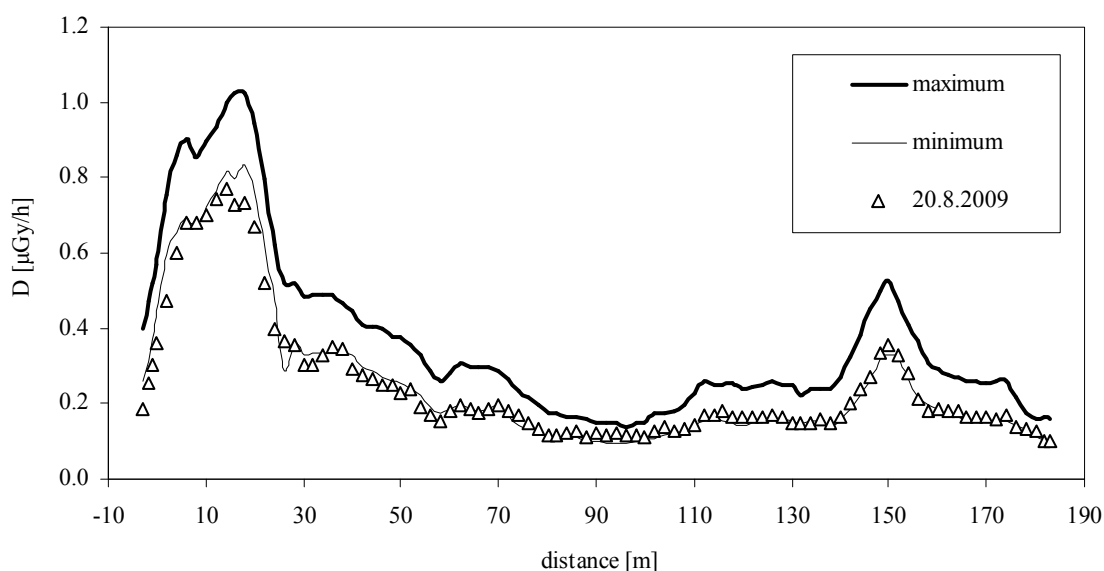


FIG. 2. Gamma radiation in 2009 in an interval of maxima and minima from 1992 to 2004 at D5 Boreček cross section.

All of the values of the gamma radiation from 2009 in the uncontaminated site (D8 Žízníkov) were within the minimum and maximum limits from the period 1994-2004. The value of $0.1 \mu\text{Sv/h}$ was not exceeded at any observation site in the cross-section.

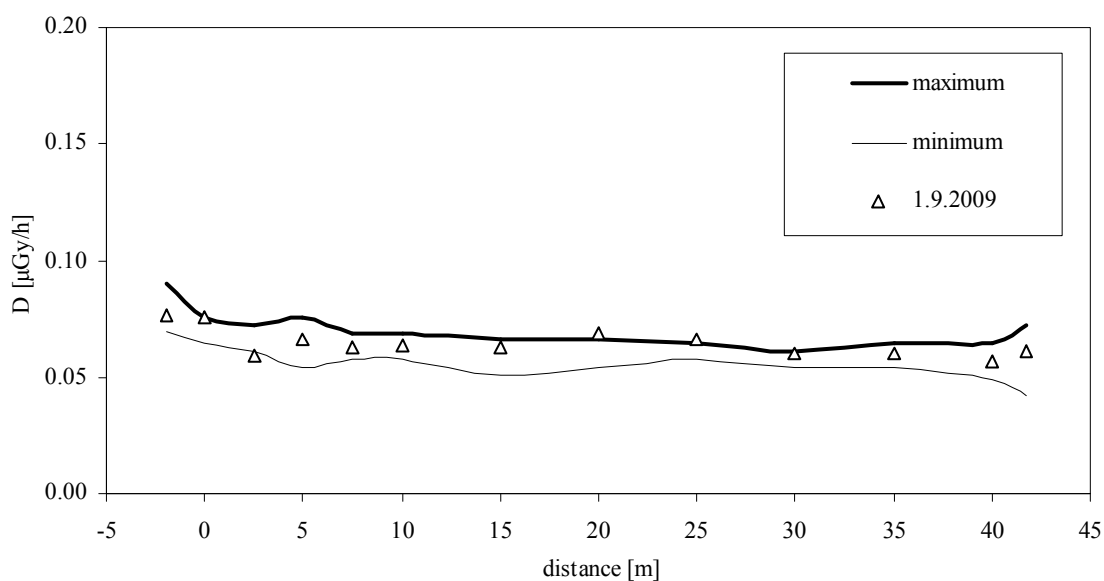


FIG. 3. Gamma radiation in 2009 in an interval of maxima and minima from 1994 to 2004 at D8 Žízníkov cross-section.

3.2. Gamma radiation in the selected sites of the monitored cross-sections

The data from the period 1994-2004 were analysed in terms of their time variability at D4 Hradčany outflow, and D5 Boreček and D6 Brenná cross-sections. The analysis was performed for two of the observation sites selected at certain distances from the zero point in the flooded areas along each of the cross-sections. The observed data were interpolated by using logarithmic, linear and exponential functions. Coefficients of correlation exhibited the best fit for the logarithmic function at 3 sites, the linear function at 2 sites and the exponential function at 3 sites. The logarithmic function was used in the form of a kinetic equation of the first order:

$$\ln D_{i,j} = -\lambda_{ef,i,j} \times t + q_{i,j} \quad (1)$$

Where:

$D_{i,j}$ is the gamma radiation at selected monitoring site j of cross-section i in $\mu\text{Gy/h}$;

$\lambda_{ef,i,j}$ is the effective ecological (observed) constant that describes decrease in the radiation at cross-section i , site j , in $1/\text{year}$;

t is the time in year;

$q_{i,j}$ is the parameter of the kinetic equation at cross-section i , site j , in $1/\text{year}$.

The constant $\lambda_{ef,i,j}$ was used for the calculation of the effective ecological half-life using the equation as follows:

$$T_{ef,i,j} = \frac{\ln 2}{\lambda_{ef,i,j}} \quad (2)$$

Where $T_{ef,i,j}$ is the observed effective ecological half-life of the gamma radiation at cross-section i , site j , in year.

For the description of the half-life of the radiation component relevant to the former uranium ore mining, the total radiation was corrected by subtracting its background level:

$$D_{i,j}' = D_{i,j} - D_b \quad (3)$$

Where $D_{i,j}$ is the gamma radiation at selected monitoring site j of cross-section i in $\mu\text{Gy/h}$ corrected using the background radiation D_b , which was substituted by the mean radiation calculated for the Žízníkov uncontaminated site in $\mu\text{Gy/h}$.

The corrected constant $\lambda_{ef,i,j}'$ and effective ecological half-life $T_{ef,i,j}'$ were calculated by substituting $D_{i,j}'$ for $D_{i,j}$ in Eq. (1). Figs. 4 to 7 show time changes in the gamma radiation, which is interpolated using a logarithmic function. The graphical interpretation shows that the gamma radiation was decreasing during the whole period 1992-2009. The coefficients of correlation r of the decrease interpolated by the logarithmic function were in the range 0.49-0.95, by the linear function in the range 0.48-0.96 and by the exponential function in the range 0.56-0.84. Analogically, for the corrected values of the gamma radiation, the correlation coefficients were 0.49-0.94, 0.48-0.96 and 0.57-0.81 respectively.

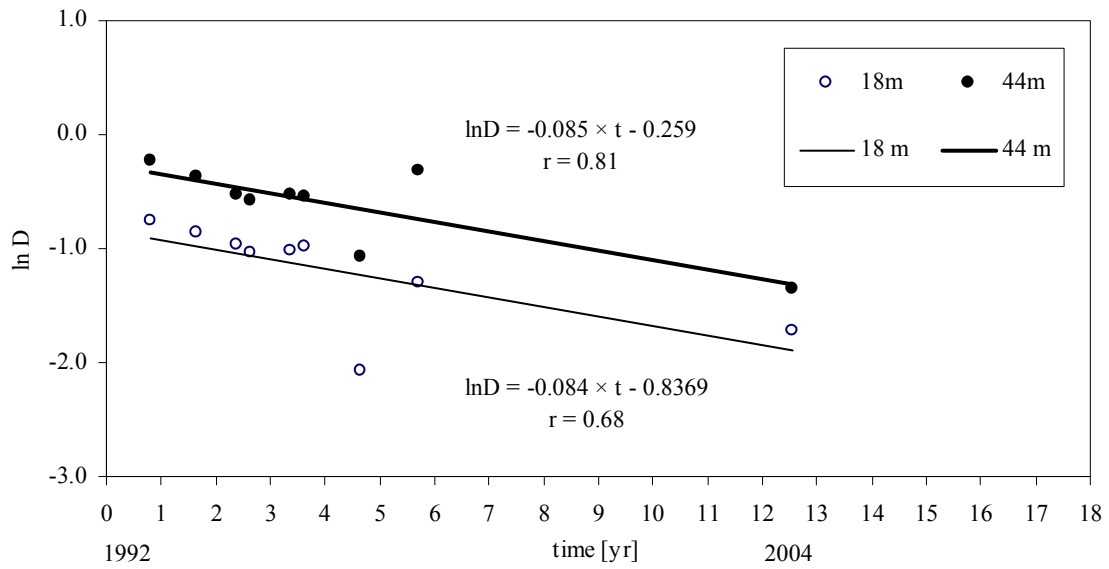


FIG. 4. Time development of gamma radiation (D) at distances of 18 m and 44 m at D3 Hradčany inflow cross-section for the period 1992-2004.

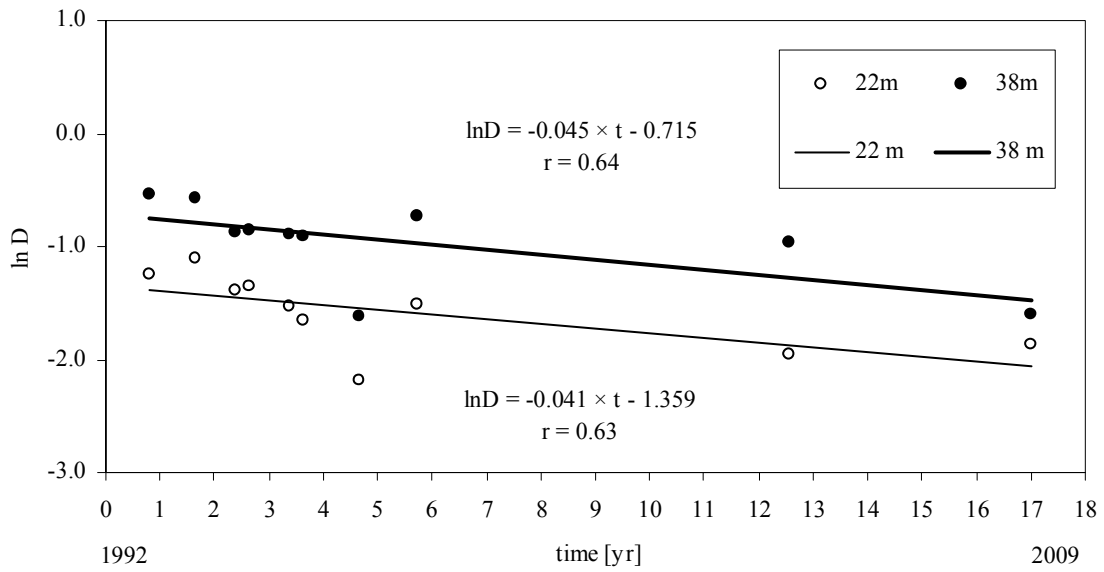


FIG. 5. Time development of gamma radiation (D) at distances of 22 m and 38 m at D4 Hradčany outflow cross-section for the period 1992-2009.

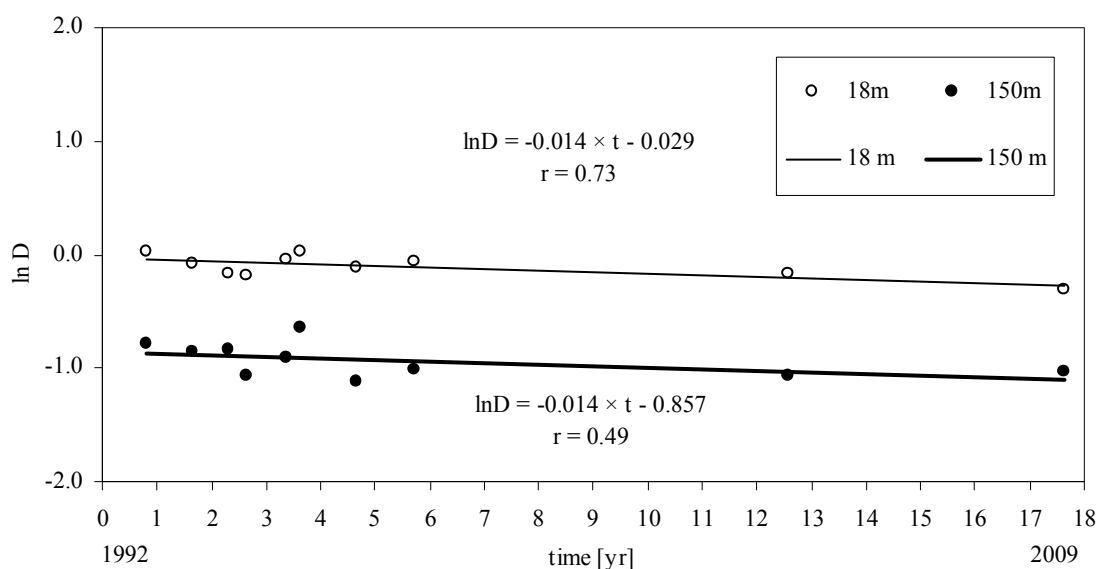


FIG. 6. Time development of gamma radiation (D) at distances of 18 m and 150 m at D5 Boreček cross-section for the period 1992-2009.

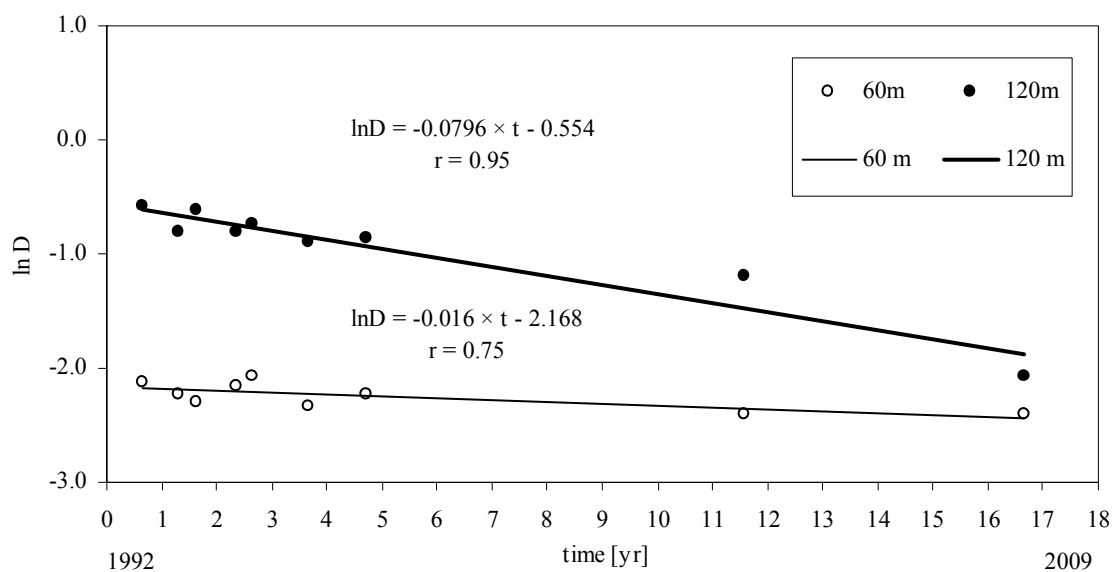


FIG. 7. Time development of gamma radiation (D) at distances of 60 m and 120 m at D6 Brenná cross-section for the period 1993-2009.

Table 1 gives the values of the effective ecological constants, effective ecological half-times of the gamma radiation and their corrected values. The values of λ_{ef} and T_{ef} substantiate that the gamma radiation (contamination) was decreasing most rapidly in D3 Hradčany inflow and D4 Hradčany outflow cross-sections, where the effective ecological half-life was 8.2 years.

Boreček cross-section exhibited the smallest decrease in the gamma radiation with effective ecological half-lives of 49.2 years and 49.5 years. The corrected half-lives were decreasing more slowly as compared to the uncorrected values. The half-lives in the identical cross sections were 6.3 years (6.9 years), 45.6 years and 42 years respectively.

TABLE 1. CONSTANTS OF GAMMA RADIATION DECREASE AND EFFECTIVE ECOLOGICAL HALF-LIVES BEFORE AND AFTER SUBTRACTION OF THE BACKGROUND RADIATION SELECTED SITES OF THE MONITORING CROSS-SECTIONS

Profile in Ploučnice river		l	λ_{ef}	T_{ef}	λ_{ef}'	T_{ef}'
		(m)	(1/year)	(year)	(1/year)	(year)
Mimoň	D1	12	0.019	37.3	0.029	23.6
		22	0.046	15.2	0.057	12.1
Hradčany - vtok	D3	18	0.084	8.2	0.11	6.3
		44	0.085	8.2	0.1	6.9
Hradčany - výtok	D4	22	0.041	16.9	0.059	11.7
		38	0.045	15.3	0.056	12.3
Boreček	D5	18	0.014	49.2	0.015	45.6
		150	0.014	49.5	0.017	42
Brenná	D6	60	0.016	42.3	0.042	16.6
		120	0.08	8.7	0.108	6.4

3.3. Contamination of river sediments by radioactive substances

The results of the monitoring of ^{226}Ra activities in bottom sediments that were sampled in a network of cross-sections S1 to S8 in the period 1994-2009 are shown in Fig. 8. The range of the ^{226}Ra activities in the bottom sediments from the cross-sections of the Ploučnice river was relatively wide. The lowest values were detected for S1 Noviny and S6 Žízníkov cross-sections while during the whole observation period the highest values exhibited in S3 Boreček cross-section located in the area of a central landfill. A decreasing trend in the activities of ^{226}Ra was detected for S4, S5 and S6 cross-sections while the radium activity was increasing at S7 Děčín Zámecký pond, which is the most downstream cross-section. The differences in ^{226}Ra activities between the cross-sections are attributable to different granularity of the sediment samples.

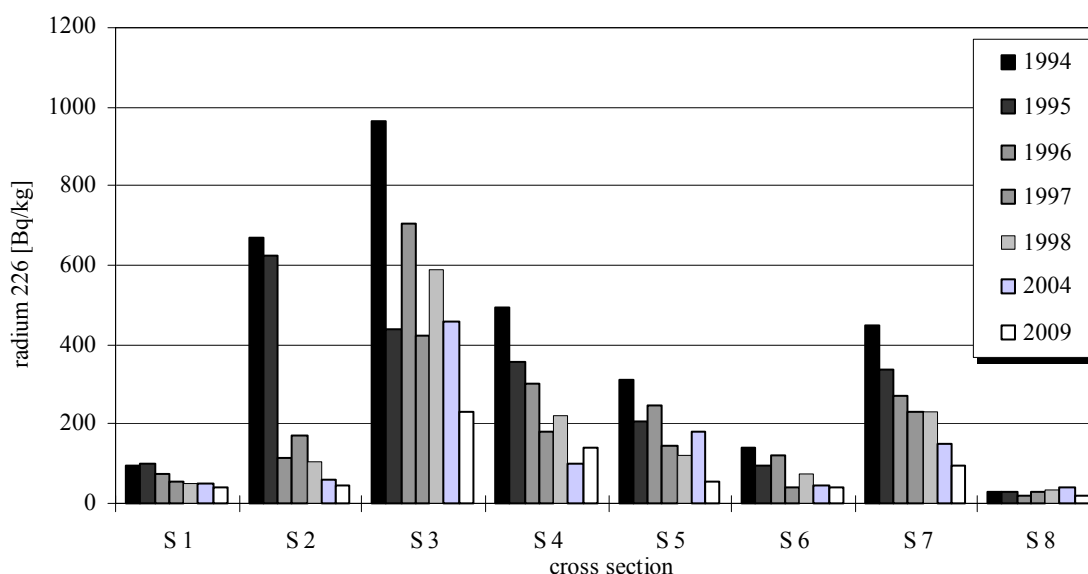


FIG. 8. ^{226}Ra activities in bottom sediments from the Ploučnice river (S1 to S7 cross-sections) and from the uncontaminated cross-section of the Svitávka River (S8) for the period 1994-2009.

In the period 1994-2009, the mean grain size of the samples S1–S7 at 50% of a sample weight was 1.09 mm, 0.36 mm, 0.14 mm, 0.30 mm, 0.24 mm, 0.23 mm and 0.05 mm, respectively. The lowest activity of ^{226}Ra at S8 Svitávka Zákupy reference cross-section was detected for a mean grain size of 0.54 mm.

In the period 1994-2009, the gamma activities in the individual cross-sections exhibited a decreasing trend, with exception of S8 reference section. A certain variability is probably attributable to differences in grain size between the individual cross-sections and other factors associated with sampling. A monotonous trend in ^{226}Ra activity was detected for sediments that were sampled from Děčín Zámecký pond cross-section.

The results of the monitoring of the ^{226}Ra activities in the sediment samples for the period 1994-2009 showed that the activities in S1 cross-section, which is located closely downstream from the waste water outflow from uranium ore mining at Stráž pod Ralskem, were relatively small as compared to those at the remaining cross-sections. This fact can be explained by the highest grain sizes of the sediments from this section. The graphical interpretation of the results suggests that the sediments in upstream reaches were transported and subsequently deposited in the area between S2 Mimoň and S5 Vlčí Důl cross-sections. During the whole observation period, the highest activities of ^{226}Ra were detected in sediment samples from S3 Boreček cross-section. It could be generally concluded that the ^{226}Ra activities were significantly decreasing during the whole monitoring period 1994-2009.

During the first year (1994), the highest ^{226}Ra activities were in the range from 700 to 1,000 Bq/kg. Subsequently, the highest activities were mostly detected in S3 Boreček cross-section. 592 Bq/kg was detected as maximum in 1998, 457 Bq/kg in 2004 and 231 Bq/kg in 2009. In 2009, the lowest ^{226}Ra activities in S1, S2 and S6 were in the range 41-48 Bq/kg, which is at the level of the whole country mean of 48 Bq/kg derived from the monitoring network of sediments not affected by the activities of the uranium industry [5]. In S5 cross-section, it was 56 Bq/kg and 97 Bq/kg was detected for S7 Děčín Zámecký pond closing cross-section.

Graphical interpretation of the ^{228}Ra activities in the sediments sampled at S1 to S8 cross-sections in the period 1994-2009 is given in Fig. 9.

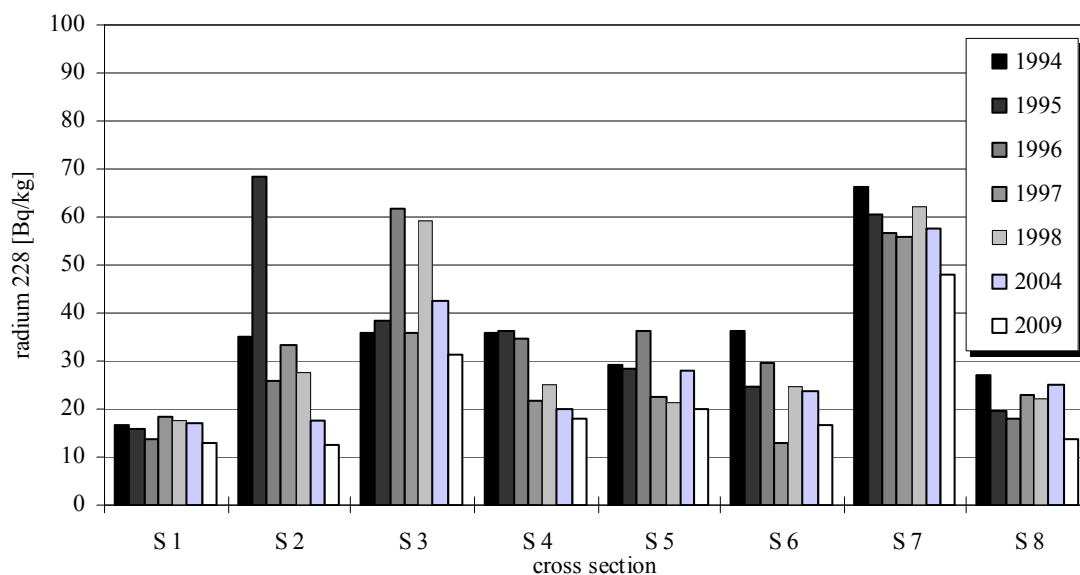


FIG. 9. ^{228}Ra activities in bottom sediments from the Ploučnice river (S1 to S7 cross-sections) and from the uncontaminated cross-section of the Svitávka River (S8) for the period 1994-2009.

The results show that the activities of ^{228}Ra were significantly below those of ^{226}Ra . In average, the highest ^{228}Ra activities were detected in sediments from S7 Děčín Zámecký pond cross-section while the lowest values were derived for S1 Noviny cross-section. These values were even slightly below those from the S8 Svitávka Zákupy reference cross-section. Variability in the ^{228}Ra activities between the cross-sections can be explained by different grain sizes of the samples because high activities were detected from samples whose granularity was small. Examples can be given in the ranges of the ^{228}Ra activities in 1998, i.e. 17-62 Bq/kg, in 2004, i.e. 17-58 Bq/kg and in 2009, i.e. 13-48 Bq/kg.

The trends in the ^{226}Ra and ^{228}Ra activities were assessed by using logarithmic, linear and exponential functions. For these functions, the correlation coefficients derived for ^{226}Ra were in the range of 0.72-0.96, 0.70-0.87 and 0.79-0.99, respectively. The ^{228}Ra activities corrected using the results from S8 Svitávka Zákupy reference cross-section exhibited correlation coefficients in the range of 0.72-0.88, 0.70-0.78 and 0.78-0.96, respectively. The coefficients of correlation derived for the corrected values of ^{228}Ra activities were in the range of 0.37-0.88, 0.29-0.80 and 0.16-0.91, respectively. The logarithmic function, which is applicable for derivation of effective ecological half-lives, was used for subsequent analysis (in spite of its lower correlation coefficients as compared to those derived for the exponential function).

The decrease in the activities of ^{226}Ra and ^{228}Ra was assessed using a kinetic equation of the first order as follow:

$$\ln a_i = -\lambda_{ef,i} \times t + q_i \quad (4)$$

Where:

a_i is the ^{226}Ra (respectively ^{228}Ra) activity in cross-section i in Bq/kg of dried matter;
 $\lambda_{ef,i}$ is the effective ecological (observed) constant that describes the decrease in activities in sediments at the monitored cross-section i in 1/year;
 t is the time in year;
 q_i is the parameter of the kinetic equation.

The constant $\lambda_{ef,i}$ was used for derivation of the effective ecological half-life using the following equation:

$$T_{ef,i} = \frac{\ln 2}{\lambda_{ef,i}} \quad (5)$$

Where $T_{ef,i}$ is the effective ecological (observed) half-life of a decrease in activity in sediments at selected sampling site i in year.

For the description of the decrease in the activities of ^{226}Ra (respectively ^{228}Ra) relevant to the contamination from the former uranium industry, these activities were corrected using the background values as follows:

$$a_i' = a_i - a_b \quad (6)$$

Where a_i' is the the activity in sediments at sampling site i corrected using the ^{226}Ra (respectively ^{228}Ra) activity detected for the S8 Svitávka Zákupy unaffected cross-section in Bq/kg.

After substituting a_i' for a_i in the Eq. (4), the corrected values of $\lambda_{ef,i}'$ and effective ecological half-life $T_{ef,i}'$ were calculated using Eq. (5). The results are summarized in Table 2.

TABLE 2. CONSTANTS OF GAMMA RADIATION DECREASE AND EFFECTIVE ECOLOGICAL HALF-LIVES BEFORE AND AFTER SUBTRACTION OF THE BACKGROUND RADIATION AT SELECTED SITES OF THE MONITORING CROSS-SECTIONS

Profile at Ploučnice river		radionuclide	λ_{ef} (1/year)	T_{ef} (year)	λ_{ef}' (1/year)	T_{ef}' (year)
Noviny	S1	^{226}Ra	0.052	13.3	0.11	6.3
		^{228}Ra	0.012	57.3	-*)	-*)
Mimoň laguny	S2	^{226}Ra	0.158	4.4	0.222	3.1
		^{228}Ra	0.084	8.3	0.417	1.7
Boreček	S3	^{226}Ra	0.064	10.8	0.07	9.9
		^{228}Ra	0.015	45	0.035	20
Veselí	S4	^{226}Ra	0.08	8.6	0.095	7.3
		^{228}Ra	0.046	15	0.366	1.9
Vlčí Důl	S5	^{226}Ra	0.082	8.4	0.117	5.9
		^{228}Ra	0.019	35.7	0.213	3.3
Žizňikov	S6	^{226}Ra	0.069	10	0.133	5.2
		^{228}Ra	0.027	26	0.205	3.4
Zámecký rybník	S7	^{226}Ra	0.089	7.8	0.107	6.5
		^{228}Ra	0.015	46.2	0.025	28.3

*) Not assessed, the ^{228}Ra activities in S8 Svitávka Zákupy reference cross-section exceeded those in given section.

The calculated values of the effective ecological half-life of ^{226}Ra were in the range of 4.4-13.3 years. The activities of ^{226}Ra were decreasing most rapidly at S2 Mimoň laguny cross-section and most slowly at S1 Noviny section, which was less affected by the contamination. The decrease in the activities of ^{228}Ra was significantly smaller. Its half-life was in the range of 8.3-57.3 years. It is assumed that the component of ^{228}Ra relevant to the uranium mining is substantially smaller as compared to that of ^{226}Ra . The values of the effective ecological half-life that were derived from the activities of ^{226}Ra in the sediments corrected using the results from S8 Svitávka Zákupy cross-section are shorter as compared to those derived from the uncorrected values. Their range was from 3.1 years derived for S2 Mimoň laguny cross-section to 9.9 years at S3 Boreček section. The values of the corrected effective ecological half-life of ^{228}Ra are associated with higher uncertainty because of relatively high background concentrations of ^{228}Ra in sediments as compared to its total concentration. Another problem is in the fact that the background activities derived for a selected cross-section are not necessarily sufficiently representative for the other sites. This applies also to ^{226}Ra . Substantial is however the fact [9] that the half-life of ^{228}Ra (5.76 years) is much shorter as compared to that of ^{226}Ra (1600 years).

Subsequent analysis was focused on the ratio of the activities of ^{226}Ra and ^{228}Ra in the sediment samples. The results of the calculation of this ratio, which could be considered to be an indicator of the impact of uranium ore mining and processing, are given in Fig. 10.

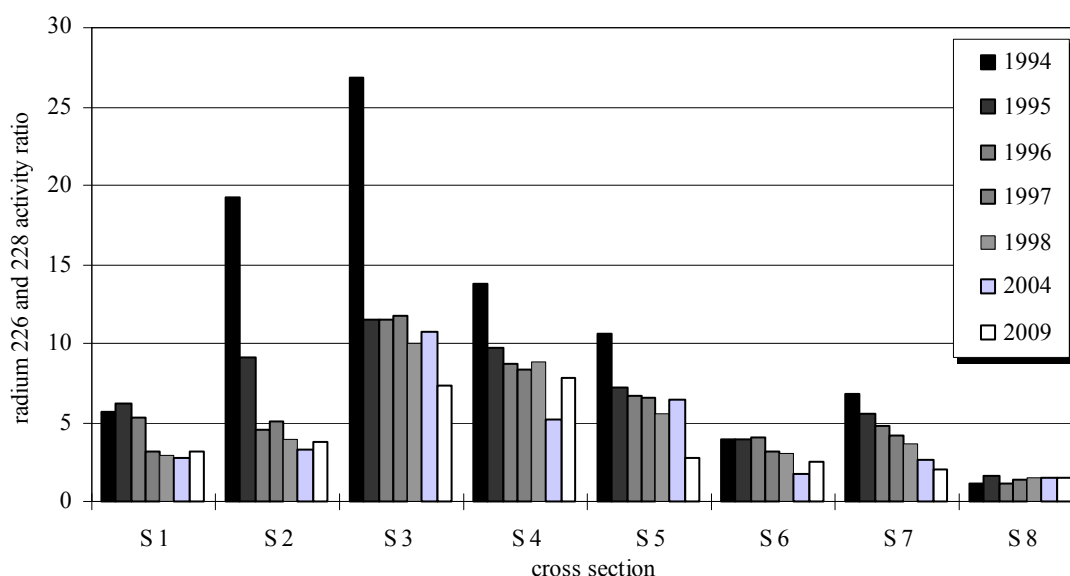


FIG. 10. Ratio of the activities of ^{226}Ra and ^{228}Ra in bottom sediments of the Ploučnice river (S1 to S7 cross sections) and in S8 Svitávka Zákupy uncontaminated section for the period 1994-2009.

The mean value of the ratio of ^{226}Ra and ^{228}Ra in the contaminated cross-sections S1 to S7 on the Ploučnice river was 11.9 in 1994, 7.8 in 1995, 6.2 in 1996, 5.9 in 1997, 5.3 in 1998, 4.7 in 2004 and 4.2 in 2009. The mean value of this ratio in uncontaminated river sediments in the Czech Republic is 1.0. This ratio can also substantiate the decrease of the sediment contamination by ^{226}Ra along the Ploučnice River.

For the uncontaminated cross-section, the S8 Svitávka Zákupy, the mean ratios in the specified years were 1.2, 1.6, 1.1, 1.4, 1.5, 1.5 and 1.6, respectively, with a mean value of 1.4. The mean value is relevant to the first class specified for contamination of river sediments by ^{226}Ra [10, 11]. The range of the ratios of ^{226}Ra and ^{228}Ra at the S8 reference locality can be attributed to uncertainties in determination of low values of ^{226}Ra and ^{228}Ra respectively.

The results of previous studies, which were focused on the determination of this ratio at localities that were used for landfilling of waste from uranium ore mining and processing [9, 11-13], show that the ratio of ^{226}Ra and ^{228}Ra indicates a contamination of the sediments if it exceeds 1.5.

3.4. Reed

Reed was sampled in 2009 at sampling localities of sediments. This plant did not grow at S7 Děčín Zámecký pond locality and therefore it was sampled at the mouth of the Ploučnice river at Děčín, where also the granularity of the sediments was relevant to that at the original sampling site.

^{226}Ra activities (related to dried matter) at S1 to S6 (and Děčín) cross-sections were in the range from 4 to 36 Bq/kg. At Žízníkov and Děčín cross-sections, the activities of ^{226}Ra were at the levels of background values that were derived for Svitávka Zákupy reference cross-section. For the S1 to S5 cross-sections, the ^{226}Ra activities were in the range from 14 to 36 Bq/kg, which does not differ significantly from the reference levels. ^{228}Ra activities were mostly below the detection limit, with the exceptions of 5 Bq/kg and 7 Bq/kg derived for S2 and S5 cross-sections, respectively. In spite of the fact that the activities of ^{226}Ra are small, the ratio between the activities of ^{226}Ra and ^{228}Ra for the detectable sites was 5 and 6, which shows that reed is a good bioindicator for detection of the persisting contamination stemming from uranium ore mining at Stráž pod Ralskem.

4. CONCLUSIONS AND RECOMMENDATIONS

This study assesses changes in the contamination of a flooded area by radioactive substances using the results of gamma radiation monitoring systems and those from the monitoring of ^{226}Ra and ^{228}Ra activities in bottom sediments sampled at selected cross-sections of the Ploučnice river during the period 1992-2009. In 2009, the sediment sampling was extended with reed samples.

The results of the gamma radiation monitoring in the period 1992-2009 showed that the contamination by the radioactive substances was decreasing. The decrease can be described by an equation, which is used for the description of a kinetic of first order. The effective ecological (observed) half-lives were derived in the range from 8.2 to 49.5 years. The gamma radiation was decreasing most rapidly in D3 Hradčany and D4 Hradčany cross-sections, where the effective ecological half-life was 8.2 years. D5 Boreček cross-section exhibited the smallest decrease in the gamma radiation with effective ecological half-lives of 49.2 years. After correcting the results by subtracting the background activities derived from D8 Žízníkov uncontaminated cross-section, the effective ecological half-lives were shorter, in the range 6-45.6 years.

The results of the monitoring of the bottom sediments substantiated that the activities of both radionuclides were decreasing. The range of the ^{226}Ra activities in bottom sediments from the cross-sections of the Ploučnice river was relatively wide. The lowest values were detected for S1 Noviny and S6 Žízníkov cross-sections while during the whole observation period the highest values exhibited S3 Boreček cross-section located in the area of a central landfill.

The calculated values of the effective ecological half-life of ^{226}Ra were in the range of 4.4-13.3 years. The activities of ^{226}Ra were decreasing most rapidly at S2 Mimoň laguny cross-section and most slowly at S1 Noviny section. The decrease in the activities of ^{228}Ra was significantly smaller. Its half-life was in the range of 8.3-57.3 years. It is assumed that the component of ^{228}Ra relevant to the uranium mining is substantially smaller as compared to that of ^{226}Ra . The values of the effective ecological half-life that were derived from the activities of ^{226}Ra in the sediments corrected using the results from S8 Svitávka Zákupy cross-section are shorter as compared to those derived from the uncorrected values. Their range was from 3.1 years derived for S2 Mimoň laguny cross-section to 9.9 years at S3 Boreček section. The values of the corrected effective ecological half-life of ^{228}Ra are associated with higher uncertainty because of the relatively high background concentrations of ^{228}Ra in sediments as compared to its total concentration. Substantial is however the fact that the half-life of ^{228}Ra (5.76 year) is short.

In 2009, the sediment monitoring was extended with reed samples. The results showed that reed is a good bioindicator for detection of the persisting contamination stemming along the Lužnice River from uranium ore mining at Stráž pod Ralskem. The results of the monitoring indicate that a control measurement should be repeated in 2014 or after a flood, whose return period would exceed 5 years.

REFERENCES

- [1] HANSLÍK, E., MOUCHA, V., NEZNAL, M., Contamination of littoral range along the Ploučnice river by radioactive substances (in Czech), Rep. T.G.M. WRI Prague (1990).
- [2] HANSLÍK, E., et al., Migration of radionuclides in the Ploučnice river basin (in Czech), Rep. T.G.M. WRI Prague (1991).
- [3] HANSLÍK, E., et al., Changes in gamma radiation at cross sections in the flooded area of the Ploučnice river in 1998 (in Czech), Rep. T.G.M. WRI Prague (1999).
- [4] HANSLÍK, E., MANSFELD, A., JUSTÝN, J., MOUCHA, V., ŠIMONEK, P., Impact of uranium ore mining on contamination of hydrosphere of the Ploučnice river in the period 1966 – 2000 (in Czech), Výzkum pro praxi, Vol. 45, T.G.M. WRI, Prague (2002).
- [5] HANSLÍK, E., Assessment of the contamination of Ploučnice river basin by radioactive substances (in Czech), Rep. T.G.M. WRI, Prague (2009).
- [6] KŘÍŽOVÁ, H., Report on the results of the geotechnical laboratory analyses (in Czech), SG Geotechnika Prague (1997).
- [7] KŘÍŽOVÁ, H., Protocols of the results of laboratory analyses, ARCADIS Geotechnika Prague (2009).
- [8] Decree of State Office for Radiation Protection No. 307/2002, on protection against radiation as amended by a Decree of State Office for Radiation Protection No. 499/2005 (in Czech).
- [9] LEDERER, C.M., SHIRLEY, V.S., Table of isotopes, 7th ed., Wiley-Inter-science Publication, New York (1978).
- [10] HANSLÍK, E., Radioactive substances, Information bulletin of Project No. 14 Elbe (in Czech), T.G.M. WRI Prague (1997).
- [11] HANSLÍK, E., et al., Radium isotopes in river sediments of Czech Republic, *Limnologica* **35** (2005) 177.
- [12] HANSLÍK, E., KALINOVÁ, E., JEDINÁKOVÁ-KŘÍŽOVÁ, V., Activity ratio $^{226}\text{Ra}/^{228}\text{Ra}$ as indicators of river bottom sediment radioactive contamination due to uranium mining and milling in Czechia, 8th Int. Conf. Biochemistry of Trace Elements, Adelaide, Australia (2005).
- [13] HANSLÍK, E., RŮŽIČKA, J., Ecological problems of chemical treatment plants for uranium ore (in Czech), *Vodní hospodářství* **41** 7 (1991) 240.

OCCUPATIONAL EXPOSURE FOR WORKING STAFF IN THE EGYPTIAN CERAMICS INDUSTRY¹

M.R.EZZ EL-DIN, R.A.M. RIZK, R.M. MOHAMED, H.M.DIAB

Radiation Protection Department, National Center for Nuclear Safety and Radiation Control, Atomic Energy Authority, Physics Department, Faculty of Science, Helwan University, Egypt

Email: hnndiab@yahoo.co.uk

Abstract

Non-nuclear industries use raw materials containing significant levels of radionuclides; the processing of those materials can expose workers and people living and working near such sites to radiation levels well above the natural background. Zircon sands processing falls within this category. Zircon sands are mainly made of zirconium silicate (ZrSiO_4) or baddeleyite (ZrO_2) with natural radioactivity content exceeding by one or two orders of magnitude the one present on average in the earth's crust. This is due to the fact that, during zircon crystals formation owing to magma masses cooling, uranium and thorium atoms get trapped into the crystal structure. This study deals with the determination of occupational exposure due to natural ionizing radiation in some ceramic companies involved in industrial materials processing and storage in the surrounding.

Keywords: Occupational exposure, zirconium silicate, dust concentration

1. INTRODUCTION

Zircon sand can be found as natural raw materials and as by-product of heavy mineral sand mining and processing. Important zircon minerals are zircon (ZrSiO_4) and baddeleyite (ZrO_2). Sorting discriminates these minerals from other heavy minerals or simple silica. The processing involves procedures such as sieving, washing, drying and grinding. These processes do not produce any specific waste products [1]. At present, Australia, South Africa, United States of America, Ukraine, India, China, Brazil and Sri Lanka are the largest exporters of Zirconium minerals [2]. Mostly, the zircon sands are used as refractories, foundry sands and in ceramic industry. In Egypt, around 42 kilotons of zircon sands go into the ceramic markets. It is imported mainly from Italy (Australia export zircon to Italy), but sometimes, it is also imported from Germany, Spain or the Netherlands.

Working with materials not usually radioactive but which contain naturally occurring radionuclides may cause a significant increase in the exposure of workers and member of the public. The term "Occupational exposure" has been used to refer to the exposure of workers that is committed during a period of work. One of such exposures given in the Basic Safety Standards (BSS) is from unmodified concentrations of radionuclides in raw materials [3]. Occupational dose to workers during the storage of the raw materials and production have been measured using a thermoluminescent dosimeter (TLD) card. Comprehensive study of external gamma radiation, airborne radioactive dust and surface contamination levels were conducted. The risk hazard due to increase of occupational exposure to workers during the routine work was evaluated.

¹ Part of the work is published in the Egyptian Journal of Radiation Sciences and Applications **19** (2006) 233-241.

2. EXPERIMENTAL WORK

The occupational radiation doses received by the workers in ceramic factories were calculated as follow according to the Basic Safety Standard 115 [3]:

$$E = E_{\text{ext}} + \sum_j h(g)_{j, \text{ing}} J_{j, \text{ing}} + \sum_j h(g)_{j, \text{inh}} J_{j, \text{inh}}$$

Where,

E_{ext} is the external exposure in a year;

$h(g)_{j, \text{ing}}$ and $h(g)_{j, \text{inh}}$ are the committed effective dose per unit intake for ingestion and inhalation of radionuclide j (Sv/Bq) by the group of age g ;

$J_{j, \text{ing}}$ and $J_{j, \text{inh}}$ are the relevant intake via ingestion or inhalation of radionuclide j in a year (Bq).

The personal dose equivalent was measured using a TLD card. The effective dose for inhalation was obtained by summing the dose derived from dust inhalation and the dose due to the inhalation of radon released by zircon sands due to uranium decay. The effective dose for ingestion may be considered negligible due to the type of activity carried out and since the work methods were adapted.

2.1. Determination of external dose using TLD

Both external and internal exposures may result from naturally occurring radionuclides coming from industrial activities. Radiation monitoring of workers in ceramic factories with different activities is important to demonstrate if operational radiation protection measures apply, or further measures should be considered. Assessment of environmental radiation dose-rate was evaluated. Thermoluminescent detectors were used to determine the effective dose from external exposure. Five locations were chosen for area monitoring according to the activity of work (storage, grinding and production). The TLD dosimeters consist of two parts, a TLD card and a holder. The TLD card consists of four hot-pressed LiF-100 (LiF: Mg, Ti) thermoluminescent chips of $3 \times 3 \times 0.38 \text{ mm}^3$ encapsulated between two sheets of Teflon, which are 10 mg/cm^2 thick and mounted on an aluminum substrate. The holder is made of durable, tissue-equivalent, ABC plastic, and is sealed to retain the card in a light and moisture-free environment. It also protects the card from environmental damage and retains the filtration media. A Harshow 6600 reader was used in this study.

2.2. Determination of internal dose from inhaled dust

Internal exposures arise from the intake of radionuclides by inhalation and ingestion. Doses by inhalation result from the presence in air of dust particles containing radionuclides of the ^{238}U and ^{232}Th decay chains. The dominating component of inhalation exposure is the short-lived decay products of radon. To determine the occupational dose due to dust inhalation, air samples were collected by an electrical pump positioned away from walls and 1 m above the floor [3]. Samples locations, time duration and flow rate were adjusted in the grinding department. High-efficiency filter papers were used. Samples filters were stored in protective envelopes before and after use. The annual dust content inhaled by workers was calculated by considering 8 working hours for 250 days a year, with a breathing rate equal to $1.25 \text{ m}^3/\text{h}$ and a breathable fraction equal to 1 [4].

2.3. Determination of internal dose from inhaled radon

Radon measurements were conducted using the scintillation cell method (Lucas method). The air samples were collected for 5 min at a flow rate of about 2.4 L/min on a high-efficiency filter paper (Millipore, diameter 2.5 cm), followed by alpha-particle counting after a delay time of about 5 min. The period of delay was selected to minimize the error resulting from variations in radon daughter ratios. The filter papers were counted using a EDA type counting system (RAD-200 radon daughter detector, EDA Instrument Inc.) by placing the filter paper on a scintillation tray coated with silver-activated zinc sulphide. For a 5 min counting time measurements, a radon concentration can be measured with a reproducibility of $\pm 15\%$ [5]. The radon concentration expressed as Working Level (WL), was calculated using the following equation:

$$WL = R/E.v.t.F$$

Where,

R is the alpha-particle count rate in count/min;

E is the counting efficiency;

v is the volumetric sampling rate in L/min;

t is the sampling time in min; and

F is a conversion factor.

2.4. Gamma-spectrometric analysis

Several samples of zircon silicate were provided from main local manufactures in Egypt. All samples were prepared in 100 mL Marinelli beakers, weighted and sealed to avoid radon exhalation. Radioactivity measurements were conducted after a period of at least 28 days for secular equilibrium between ^{222}Rn and its short-lived decay products [6]. A HPGe gamma-ray spectrometer with a 40% efficiency and a 2.0 keV resolution at 1.33 Mev photons, shielded by 4 inches Pb, 1 mm Cd and 1 mm Cu linked up to a multichannel analyser, were used for the measurements. The system was calibrated and the calibration quality control was carried out by using the Certified Reference Materials of soil IAEA-226 and IAEA-375 whose concentration of natural radioactivity are certified by the IAEA. Activity concentrations of ^{238}U and ^{232}Th were determined.

3. RESULTS

The external radiation dose was measured using a TLD card at five locations in each factory. The mean external dose at each site was 0.2 mSv/y in the grinding area, 0.3 mSv/y in the production area and 1.25 mSv/y in the storage area. Figure 1 represents the external radiation dose measured in each factory.

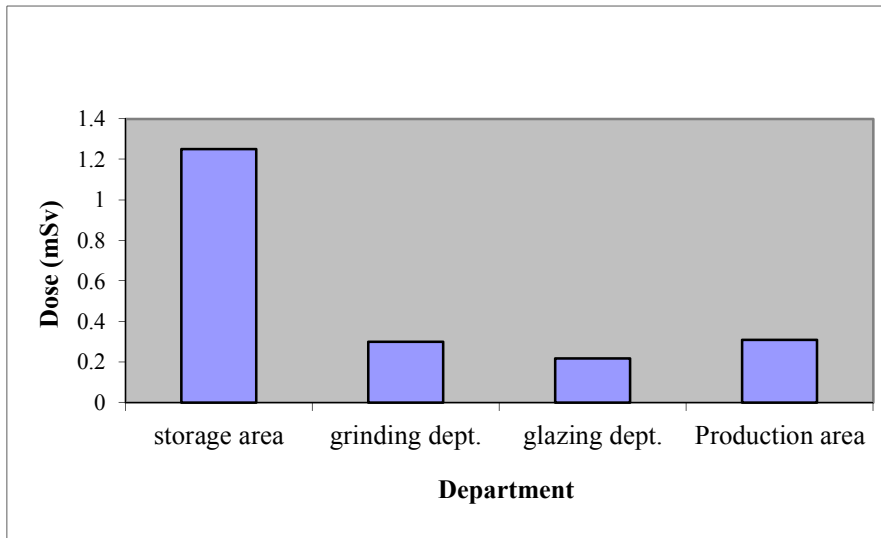


FIG. 1. Annual external dose in mSv.

The average dust concentration in the grinding department was varying from 0.3 to 0.7 mg/m³. In calculating the intake value for inhalation, the dust concentration was adapted to 0.5 mg/m³. The concentration of radioactivity of inhaled dust was assumed to be equivalent to the activity concentration measured in raw materials samples using gamma-ray spectrometry. The activities concentrations of the radionuclides from the ²³⁸U and ²³²Th chains were determined in zircon silicate and their values ranged from 1,500 to 2,000 Bq/kg with an average of 1,800 Bq/kg and from 390 to 600 Bq/kg with an average of 500 Bq/kg, respectively. The ⁴⁰K was not detected.

The intake value for inhalation of the radionuclide j over one year ($J_{j,inh}$) can be calculated using the following parameters: dust concentration, FGR 11 dose factors [4], and assumptions: the worker breathing rate is 1.2 m³/h, the duration of exposure is 2,000 h, the particle size is 5 µm and there are no respiratory protections [7]. The committed effective dose for inhalation of dust resulted to be 0.2 mSv/y. Figure 2 represents the annual internal dose due to dust inhalation.

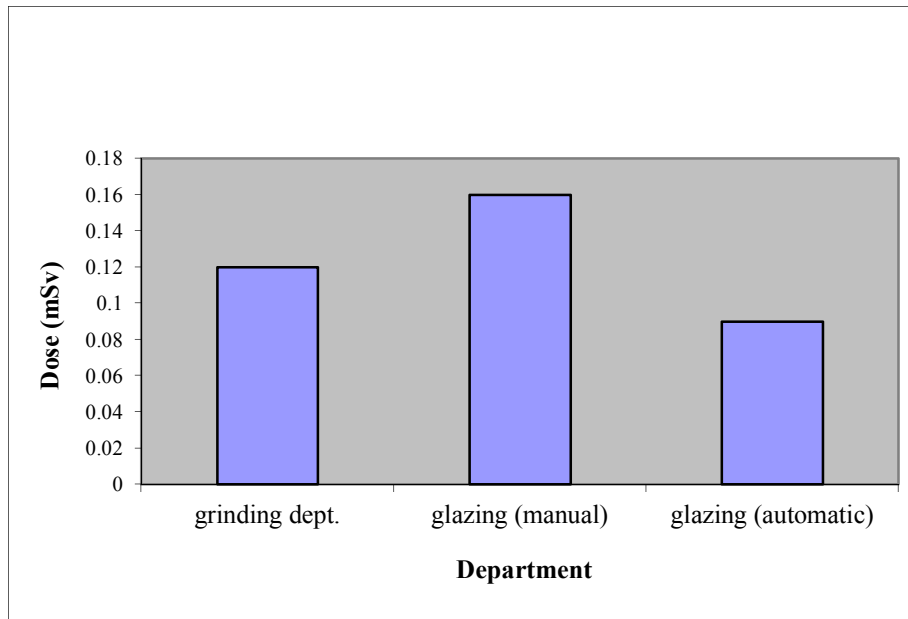


FIG.2 Annual internal dose due to dust inhalation.

The effective dose for radon inhalation in mSv/y was determined using the ^{222}Rn decay products in working level unit. Figure 3 represents the annual internal dose due to radon inhalation. The occupational exposure dose has been calculated according to the BSS as the summation of the three main contributions. The total exposure dose for workers resulted to be more than 1.5 mSv/y, which falls within the exposure limit for workers (20 mSv/y) and is less than the value given in [4].

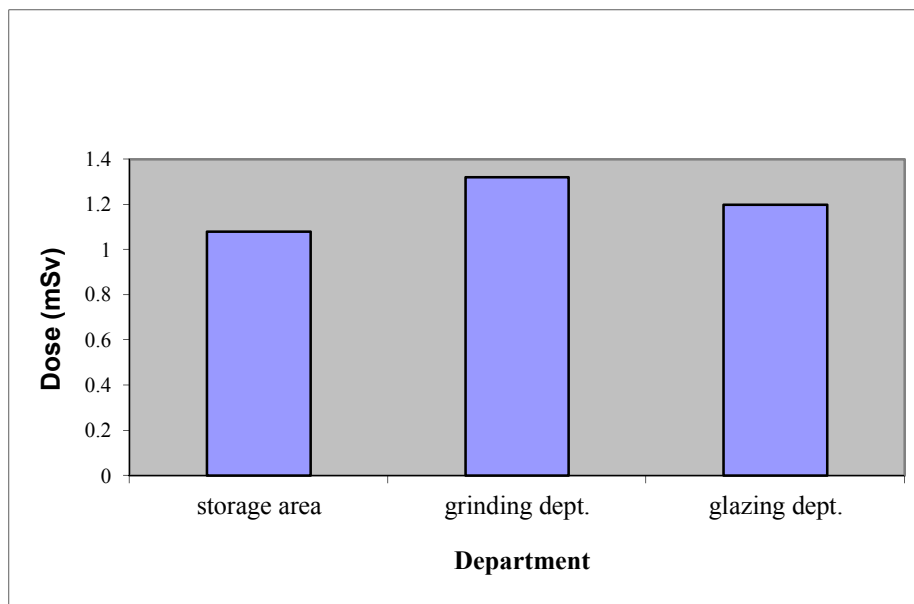


FIG.3. The annual internal dose due to radon inhalation.

4. CONCLUSION

The occupational radiation exposure in the Egyptian ceramics factories is one of the major aspects at the National Center for Radiation Safety and Control of the Atomic Energy Authority. This study relates to the regulations and measures needed for workers dealing with zirconium materials. From an occupational point of view, simple precautions are generally sufficient to minimize the external radiation exposure (job rotation of workers). Proper industrial hygiene rules are sufficient to avoid internal contamination resulting from zircon silicate (use of dust masks) and efficient ventilation is very important in grinding and glazing preparation areas.

REFERENCES

- [1] UNITED NATIONS FOR SCIENTIFIC COMMITTEE ON THE EFFECTS OF ATOMIC RADIATION, Sources effects and ionizing radiation, United Nation Scientific Committee on the effects of Atomic Radiation. United Nations, New York, USA (1988).
- [2] NATIONAL RADIOLOGICAL PROTECTION BOARD, Working with Zircon Sands, NRPB Publications, United Kingdom (1993).
- [3] INTERNATIONAL BASIC SAFETY STANDARDS FOR PROTECTION AGAINST IONIZING RADIATION AND FOR THE SAFETY OF RADIATION SOURCES, Safety Series No. 115, IAEA.
- [4] RIGHI, S., SIMONETTO, C., GUERRA, R., BRUZZI, L., Occupational Exposure to natural radiation at a zircon sand processing plant, Italy, International Research Center for Environmental Science (2002).
- [5] KHATER, A.E., HUSSEIN, M.A., HUSSEIN, M.I., Occupational exposure of phosphate mine workers, J. Environ. Radioact. **75** (2004) 47.
- [6] MOLLAH, A.S, RAHMAN, M.M., HUSAIN, S.R., Distribution of gamma emitting radionuclides in soil at the atomic energy research establishment, Bangladesh, J. Health Phys. **50** (1986), 835.
- [7] INTERNATIONAL ATOMIC ENERGY AGENCY, Safety Standards series, Assessment of occupational exposure due to intake of radionuclides, RS-G-1.2 (1984).

IN-SITU METHODS FOR CHARACTERIZATION OF CONTAMINATED SITES

D. DUBOT¹, J. ATTIOGBE²

¹ CEA, French Alternative Energies and Atomic Energy Commission, France, Email: didier.dubot@cea.fr

² GEOVARIANCES, France, Email: attiogbe@geovariances.com

1. INTRODUCTION

The establishment of radiological maps for the appraisal and for the monitoring of any work in nuclear environment is a crucial issue to deal with. Radiological evaluations have to be performed before and after the decontamination process, thanks to an optimized amount of samplings and radiological and chemical analysis. Thanks to the experience feedback, sampling and optimized amount of sample protocols have been established, as well as data analysis and modelling tools. In order to address these various operations, the French Alternative energies and Atomic Energy Commission (CEA) has been the very first institute to implement over the last 10 years an innovative methodology aiming at characterizing radiological contaminations of its sites. This center was set up in 1946 in the Fort of Châtillon, located in Fontenay-aux-Roses, 7 km south from Paris. After implementation of programs related to evacuation of nuclear materials, a remediation plan of the whole site was elaborated in 1995. Today, the facilities are going through a remediation program that will allow setting up buildings for new research activities. The goal of this methodology relies on various tools such as expertise vehicles with comprehensive detection performances (VEgAS) and a recently developed software platform called Kartotrak. A Geographic Information System (GIS) tailored to the radiological needs constitutes the heart of the platform; it is complemented by several modules aiming at sampling optimization, data analysis and geostatistical modeling, real-time acquisition and validation of cleanup efficiency. The use of all of these tools allows optimizing volumes and cost of the remediation process.

2. CLEANUP METHODOLOGY

In parallel to the dismantling of various facilities, outdoor contaminated parcels are also considered for remediation. The CEA formalized for the Nuclear Safety Authority, in 2000, its decontamination methodology that was already applied for years on CEA centers. This methodology is partly based on the guide entitled “Managing places potentially contaminated by radioactive substances” [1]. In this way, the CEA initiated the radiological characterization of the whole Fontenay-aux-Roses site many years ago. This approach is based on several steps. The historical investigations [2] aim at understanding the radiological past of the target area, which is fundamental to calibrate/orientate the subsequent characterization. This includes gathering information from archives, operational characteristics, materials handled, measurement results, accidents, interviews (workers, residents), maps and aerial views, records about former characterization or remediation activities. The assumption of a contaminated area uses a radiological control with a simple radiation detector to show high level of radioactivity in some areas. The contamination must be confirmed with additional measurements. If a contamination is confirmed, the dose limits for people may be exceeded and a level of protection necessary for workers undertaking further characterization activities is determined.

The surface characterization provides a detailed map of the radiological activity and is established thanks to surface measurements using, for example, in-situ gamma-ray spectrometry of soil surface samples. The risks to the environment can thus be identified.

The in-depth characterization consists in a campaign of drill holes indicating the contamination depth in the ground. The drilling samples should also go through chemical analysis to complete the detailed evaluation. Any potential transfer towards the groundwater has to be considered. The remediation method of the contaminated area is then being set up, actions are carried out in order to excavate and leave a satisfactory residual activity. The waste zoning is established thanks to the previous characterization (2D maps, 3D volumes).

Together with the removal of the contaminations, a survey of the operations is performed to guarantee the safety of the workers. Some measurements are carried out to validate the achievement of the remediation (end-point dose assessment) and to follow up the radiological status of the area for any future use.

3. THE EXPERTISE VEHICLES

The CEA has developed three vehicles dedicated to expertise and investigation. The second of them, LAMAS II, contributes to perform 2D site cartography using measurements by in-situ gamma-ray spectrometry. The LAMAS II vehicle also includes a radiochemistry laboratory for the measurement of alpha-emitting radionuclides (U, Pu) with low detection limits. The final prototype, called VEGAS, is equipped with the same measuring devices required for the 2D cartography [3]. One of the main innovations of this vehicle is the installation of DSP10 detectors, newly used in the field of radiological characterization. This vehicle can cover about 1 ha per hour for exhaustive measurements on practicable ground. The DSPs detect most radionuclides usually found on sites that are contaminated by industrial and nuclear research activities. Their detection limits are given in Table 1 [4].

TABLE 1. DETECTION PERFORMANCES OF THE DSP DETECTORS

Radio-nuclides	TAR ROADS (Pollution of 1 m ² area)				GROUNDS (Pollution of 1 m ² area and 5 cm thick)			
	Detection Limits (kBq.m-2)				Detection Limits (Bq.kg-1)			
	0 km/h	2,6 km/h	5 km/h	10 km/h	0 km/h	2,6 km/h	5 km/h	10 km/h
137-Cs	3	3.7	5	9	57	70	95	168
60-Co	1.6	1.9	2.7	4.8	30	36	50	90

4. THE SOFTWARE PLATFORM

Kartotrak [5] is a Geographic Information System (GIS) developed by the CEA in 2004 and available since 2010 as a final product thanks to a 10-year partnership with the Geovariances company. Kartotrak is a comprehensive software solution designed for radiological characterization projects. The integrated workflow, shown in Fig. 1, guides the user through each step of the study.

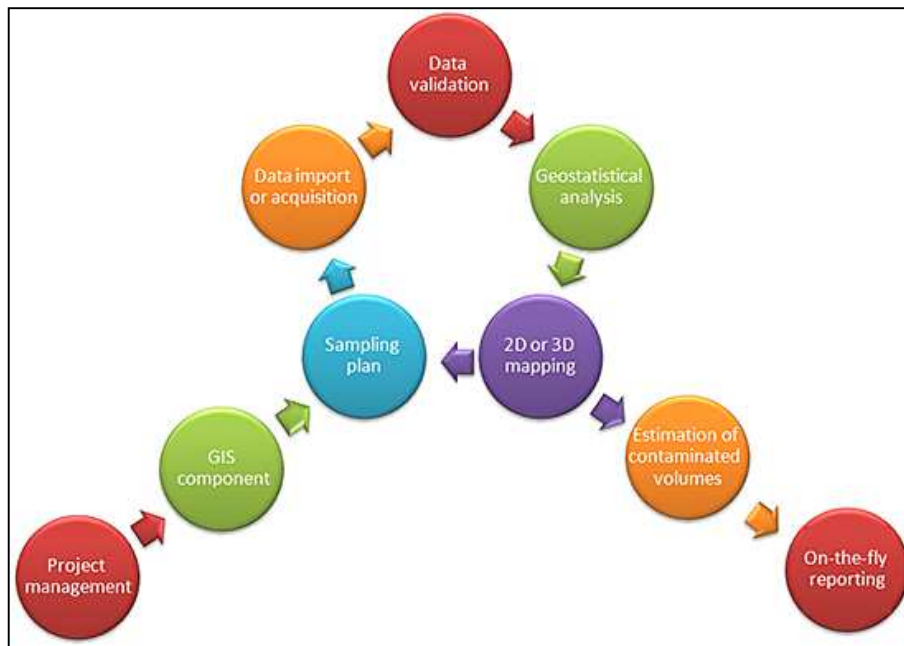


FIG.1. Integrated workflow of Kartotrak.

The GIS functions allow integrating and displaying any spatial information on the contamination vicinity in overlaid vector map layers: aerial photos, buildings, facilities, lands or communication axes, historical or geophysical survey data, computed maps. Preparing the in-situ operations, measuring lengths and surfaces are easily performed in any geographical system able to position data (WGS84, Lambert, etc). The displays can be enhanced with vector or raster images, or even using imported scanned paper maps or maps from internet that can be geolocalized later on in the project. A view of the display is shown in Fig. 2.

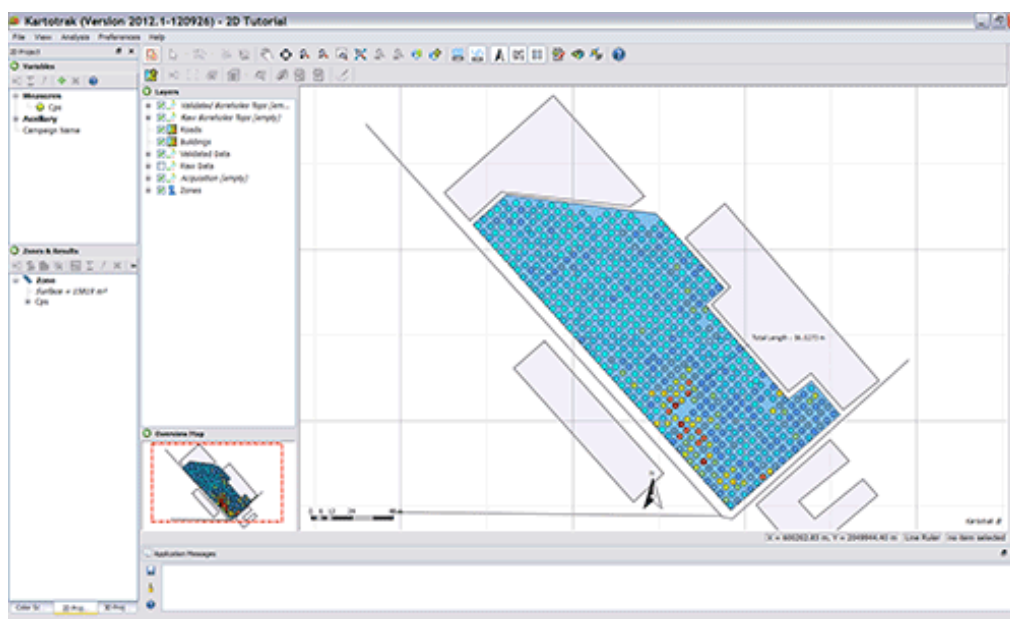


FIG.2. Global view of the interface with various layers and data points.

When preparing the in-situ operations, the user can optimize the sampling strategy using the information provided by the sampling acquisition [6] and the analysis module, which represent a considerable part of the site characterization budget. Kartotrak gives the ability to wisely prepare the sampling strategy in order to maximize information while minimizing investigation costs.

It offers tools to design sampling plans in an optimal way, as illustrated in Fig. 3:

- Range of sampling plan pattern from sampling over a regular grid (rectangular, triangular or circular mesh [7]) to random sampling.
- Range of statistical tests (WRS test, sign test, Wilks formula) for mesh size optimization.
- Interactive definition of sample location.

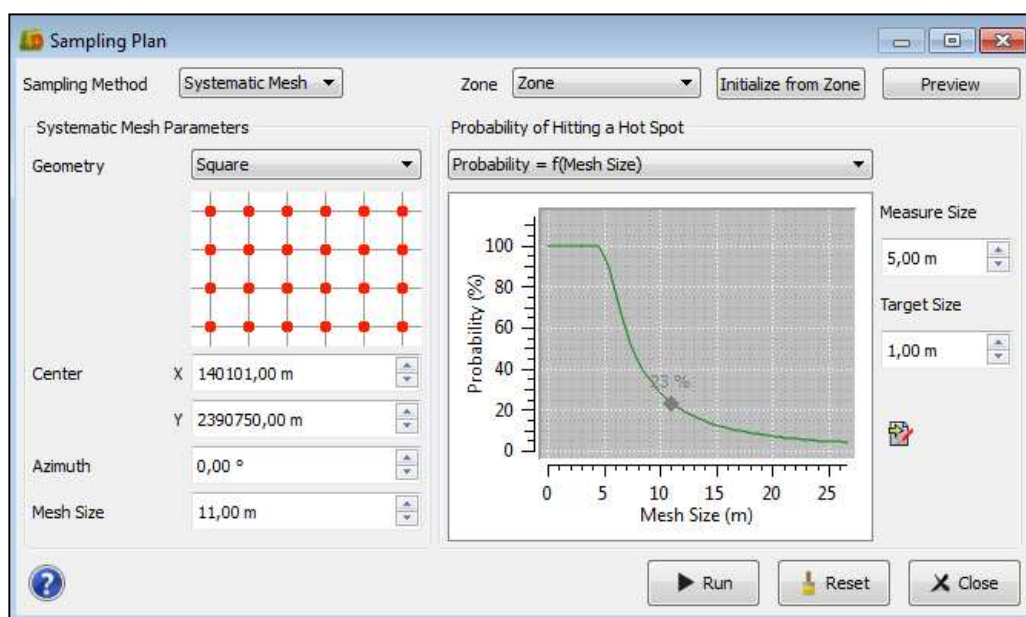


FIG.3. Sampling plan interface.

Kartotrak can be efficiently used on-site for real-time data acquisition to achieve a quick radiological characterization. This is easily performed when the software is connected to a GPS and various measuring devices allowing a real-time monitoring of areas, for a quick and non-destructive survey, as illustrated in Fig. 4.

The user is then able to:

- Manage the characterization project daily with an iterative update of the sampling plan [8, 9].
- Highlight potential issues and position additional investigation.
- Iteratively reduce the surface to be thoroughly characterized.



FIG.4. Real-time data acquisition path.

Kartotrak offers high-value exploratory data analysis tools with interconnected statistical representations. The user can interactively check the data, analyse their spatial behaviour and assess the correlation with other variables. The software delivers accurate and reliable interpolated maps with information on their reliability. Results also help in identifying areas which are sub-sampled or inside which contamination levels are highly variable.

The software focuses on fast and simplified geostatistical workflows, as shown in Figs 5 and 6:

- Accurate and reliable 2D or 3D interpolated maps (ordinary Kriging).
- Variance indicator maps, providing information on maps quality and reliability.
- Estimation computed either on points or over volumes (3D block kriging) so that the average contaminant concentration can be obtained on a volume corresponding to the sampling support size.

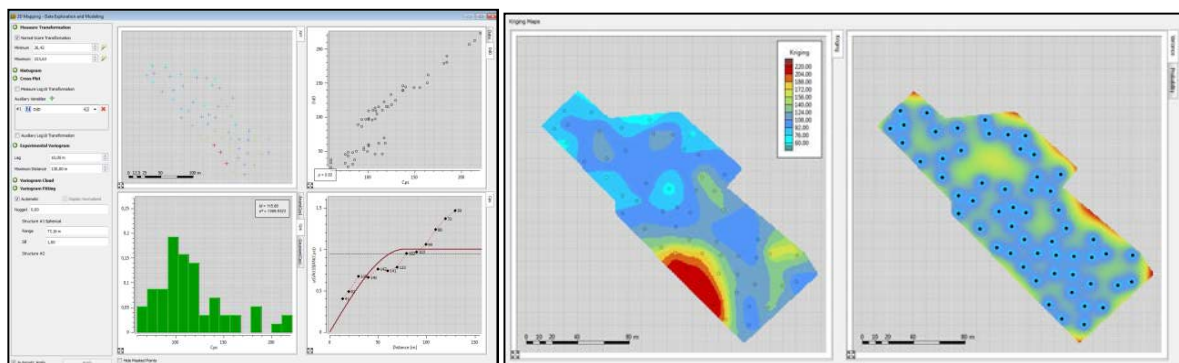


FIG.5. Successive steps in geostatistical data processing for final 2D interpolation.

Kartotrak provides decision-makers with the tools required for efficient risk assessment:

- Probability map of exceeding user-specified contamination thresholds.
- Probability map of having contamination values smaller than the values of the map.
- Confidence interval map, particularly useful to highlight areas where the confidence is low.

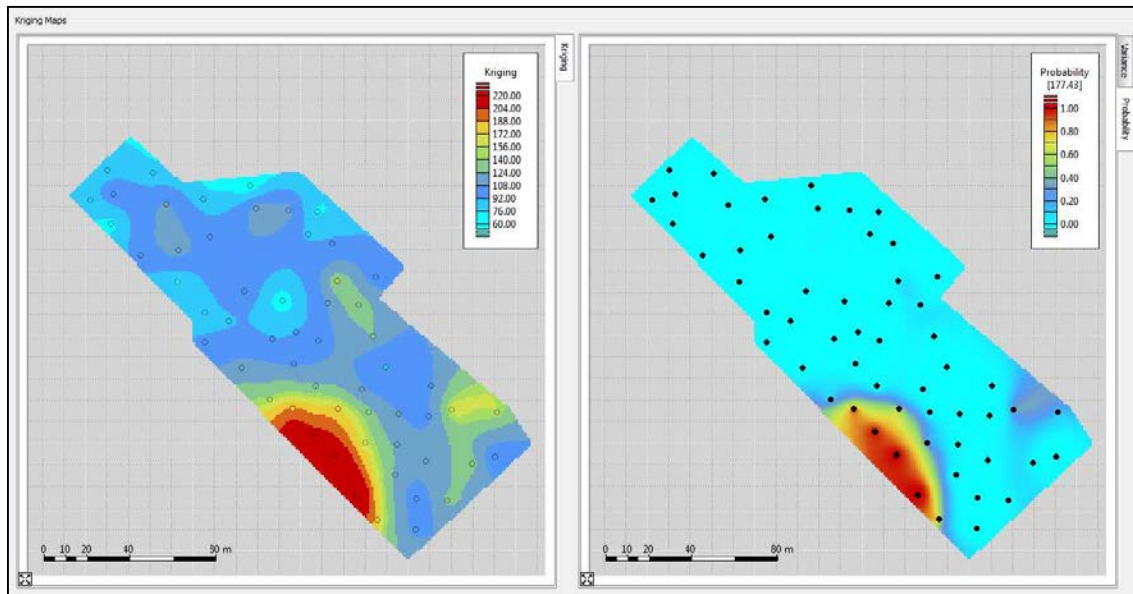


FIG.6. Kriging result and risk analysis result.

Furthermore, distribution curves of the contaminated land volumes or masses according to the specified contamination threshold are available for volume estimation. Kartotrak computes the contaminated land volume distribution from the probability of exceeding a user-defined threshold or from geostatistical simulation results, as shown in Fig. 7.

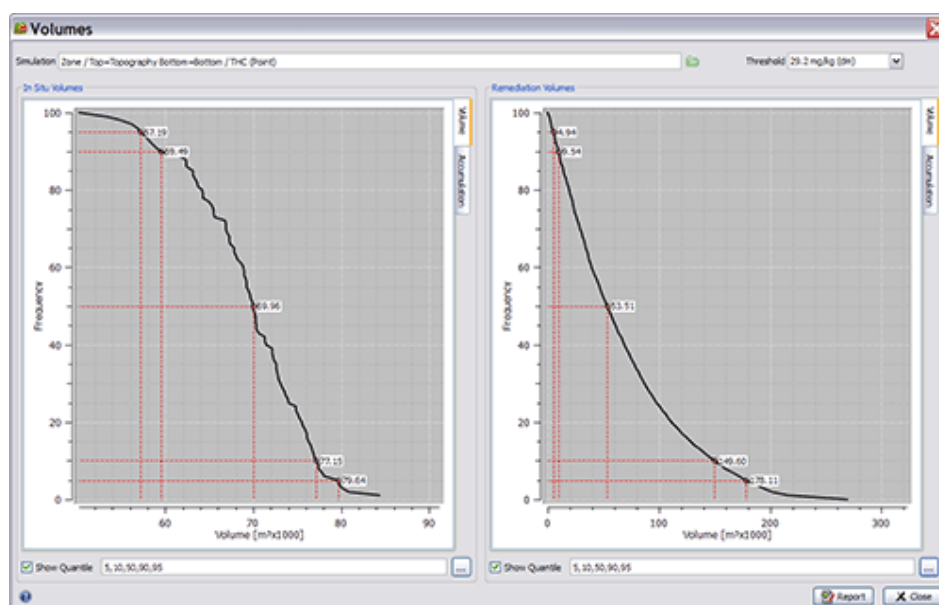


FIG.7. Volume estimation within confidence interval.

Through its 3D viewer, Kartotrak strengthens the understanding of the contamination by displaying any relevant environmental information: boreholes, sample points, topography or lithologic surfaces and 3D computed maps in a single view. This feature is illustrated in Fig. 8. When coupled with historical information, the viewer strengthens the understanding of the contamination to eventually define scoping sampling design in a wiser way.

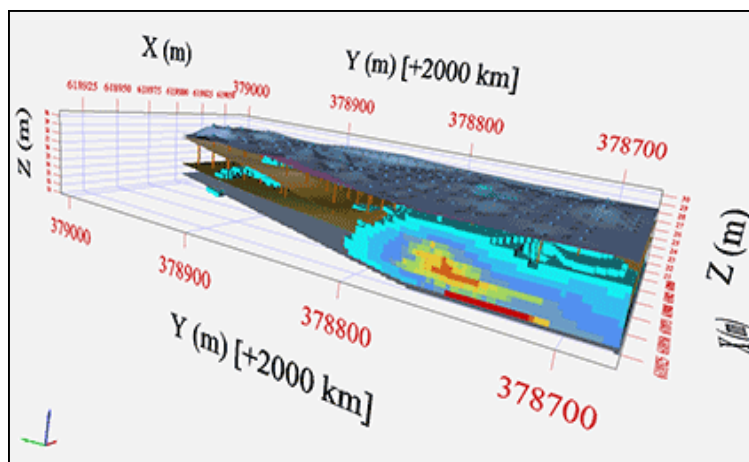


FIG.8. 3D interpolation based on results from drillhole samples.

5. CONCLUSION

In order to address the decontamination of the Fontenay-aux-Roses Center, one of the missions of the CEA has consisted of the development of methodology and setting up measuring devices (VEgAS) and innovative software, improving the process of characterizing the wastes before their removal. The detection performances of the new detectors allow to measure while driving, in order to quickly highlight contaminated areas in addition to those identified during the analysis of the historical activities. The identified contaminated areas will go through further radiological evaluation. The Kartotrak platform is now suited to manage globally and achieve a cleanup project. It has become an important tool for project managers to take decisions and to respect costs and deadlines. All these developments, as well as their concrete applications on various sites in France, contribute to the acknowledged know-how of the CEA center of Fontenay aux-Roses for radiological characterization and remediation of radioactively contaminated soils. The transfer of the methodology and related software platform to nuclear facilities is under process, aiming at providing a suitable framework to address a tremendously increasing demand about the characterization of contaminated concrete structures and facilities. The first developments have now grown from prototypes to industrial products, ready to be used for many sites.

REFERENCES

- [1] IRSN, Managing places potentially contaminated by radioactive substances. Version 0, Guide DPPR-BRGM (2001).
- [2] DUBOT, D., VACHERON, M., Radiological state of the CEA of Fontenay-aux-Roses audit environment (2006).
- [3] ATTIOGBE, J., Radiological evaluation of contaminated sites and soils. Vegas: an expertise and investigation vehicle (2011).

- [4] FAURE, V., Technical report: Detection limits and performances of scintillation plastic of VEGAS to measure in while driving (2009).
- [5] ATTIOGBE, J., Technical note of the GIS Kartotrak and data treatment software Krigéo. Technical note CEA/FAR, reference SIT-NT 06 03 (2006).
- [6] DESNOYERS, Y., Decision-making aid module STRATEGE dedicated to sampling for radiological characterization and evaluation by statistics. Technical note CEA/FAR, reference SIT-NT 07 03 (2007).
- [7] DUBOT, D., Results of the measures collected before the decontamination of Pech Rouge. SPRE 2003 / 517 / DDU (2003).
- [8] GÉOSIPOL, Practical contributions from geostatistics for the characterization and management of contaminated sites (2005).
- [9] JEANNÉE, N., Geostatistical characterization of industrial pollutions of soils. PhD thesis, Ecole des Mines de Paris (2001).

FIFTEEN YEAR EXPERIENCE OF THE NUCLEAR TECHNOLOGY LABORATORY OF THE ARISTOTLE UNIVERSITY OF THESSALONIKI IN THE TECHNIQUE OF IN-SITU GAMMA-RAY SPECTROMETRY: PRESENTATION OF THE MAJOR RESULTS

A. CLOUVAS, S. XANTHOS*, G.TAKOUDIS**, M. ANTONOPOULOS-DOMIS, J. GUILHOT

Nuclear Technology Laboratory, Department of Electrical and Computer Engineering, Aristotle University of Thessaloniki, 54124 Thessaloniki, Greece

Email: clouvas@eng.auth.gr

* present position : Alexander Technological Education Institute , 54700 Thessaloniki, Greece.

** present position : Joint Research Center (JRC), Ispra Italy.

Abstract

The members of the Nuclear Technology Laboratory of the Aristotle University of Thessaloniki in Greece have performed extensive research in the field of in-situ gamma-ray spectrometry during the last fifteen years. The major results are presented and discussed.

1. INTRODUCTION

The members of the Nuclear Technology Laboratory of the Aristotle University of Thessaloniki in Greece have performed extensive research in the field of in-situ gamma-ray spectrometry during the last fifteen years. Most of the work was performed with portable Ge detectors. In a few cases plastic detectors were also used.

The major results of the following studies are presented:

- Monte Carlo based method for conversion of in-situ gamma-ray spectrum obtained with portable Ge detector to incident photon fluence rate energy distribution;
- Derivation of indoor gamma dose-rate from high-resolution in-situ gamma-ray spectra;
- Extended survey of indoor and outdoor terrestrial gamma radiation in Greek urban areas by in-situ gamma-ray spectrometry with portable Ge detector;
- Radiological maps of outdoor and indoor gamma dose-rates in Greek urban areas obtained by in-situ gamma-ray spectrometry;
- Contribution of ^{137}Cs to the total absorbed gamma dose-rate in air in Greek forest ecosystems deduced by in-situ gamma-ray spectrometry measurements and Monte Carlo computations;
- A combination study of indoor radon and in-situ gamma-ray spectrometry measurements in Greek dwellings;
- Simultaneous measurement of indoor radon, radon-thoron progeny and high-resolution in-situ gamma-ray spectrometry in Greek dwellings;
- Twenty year follow-up study of radiocesium migration in soil;

- In-situ gamma-ray spectrometry for the determination of absorbed dose-rate in air following myocardial perfusion scintigraphy with ^{201}Tl ;
- Measurements and Monte Carlo calculations of photon energy distributions in MAYAK Production Association workplaces;
- In-situ gamma-ray spectrometry measurements and Monte Carlo computations for the detection of radioactive sources in scrap metal;
- Spatial and spectral gamma-ray response of plastic scintillators used in portal radiation detectors: Comparison of measurements and simulations;
- Determining minimum alarm activities of orphan sources in scrap loads: Monte Carlo simulations validated with measurements;
- ‘Exotic use’ of Ge detectors: Measurement of ionizing cosmic radiation (muons) dose-rates with portable Ge detector.

2. PRESENTATION OF THE MAJOR RESULTS

The major results of each study mentioned in the introduction are presented.

- Monte Carlo based method for conversion of in-situ gamma-ray spectrum obtained with portable Ge detector to incident photon fluence rate energy distribution [1].

A Monte Carlo based method for the conversion of an in-situ gamma-ray spectrum obtained with a portable Germanium detector to photon fluence rate energy distribution is proposed. The spectrum is first stripped of the partial absorption and cosmic-ray events leaving only the events corresponding to the full absorption of a gamma ray. Applying to the resulting spectrum the full absorption efficiency curve of the detector determined by calibrated point sources and Monte Carlo simulations, the photon fluence rate energy distribution is deduced. The events corresponding to partial absorption in the detector are determined by Monte Carlo simulations for different incident photon energy and angles using the CERN’s GEANT code. Using the detector's characteristics given by the manufacturer as an input it is impossible to reproduce experimental spectra obtained with point sources. A transition zone of increasing charge collection efficiency has to be introduced in the simulation geometry after the inactive Ge layer (dead layer) in order to obtain good agreement between the simulated and experimental spectra. The functional form of the charge collection efficiency is deduced from a diffusion model. This result, at the time this work was presented, was new and perhaps it is still interesting for industries constructing Ge detectors. The stripping method can be easily adapted to any available commercial portable Ge detector. The values of the parameters needed by the program are written in an ordinary text file. The principal geometrical characteristics are given only as default values so the user can change them without program rebuilding.

- Derivation of indoor gamma dose-rate from high-resolution in-situ gamma-ray spectra [2].

The dose build up factor B related to the ratio of primary to scattered gamma radiation in indoor environment was calculated with Monte Carlo simulations using the MCNP code for different indoor geometries and gamma source distributions. The main conclusion is that the B factor does not depend strongly on parameters such as dimensions of the rooms, the thickness of walls, the density of the building materials, and the gamma source geometry. If only approximate results are desired it is possible to use those factors derived for a half-space geometry also for the indoor environment. The calculated dose build up factors were used within the framework of the full absorption peak analysis method in order to deduce the dose-rates in air from about 100 indoor in-situ gamma-ray spectrometry measurements performed at the town of Thessaloniki, Greece. A spectral “stripping method”, which has been previously developed [1], was applied to the same 100 gamma-ray spectrometry measurements.

The comparison between the 100 indoor absorbed gamma dose-rates in air deduced a) by the full spectrum analysis using the calculated build up factors and b) by the “stripping method” indicated that there is a good linear correlation between the results of the two methods. The mean difference in the dose-rates deduced by the two methods is of the order of 17%, which is reasonable, if it is taken into account that the uncertainty associated to each method is estimated to be about 20-30%.

- Extended survey of indoor and outdoor terrestrial gamma radiation in Greek urban areas by in-situ gamma-ray spectrometry with portable Ge detector [3].

The results obtained from more than 1,000 indoor and outdoor in-situ gamma-ray spectrometry measurements in 41 towns (from all geographic subdivisions) of the Greek mainland (not islands) were presented and discussed. To our knowledge this is the first national ground survey in urban areas performed in the world based on high-resolution gamma-ray spectrometry with portable Ge detector. The absorbed dose-rate in air due to the Uranium series, Thorium series, ^{40}K , and ^{137}Cs , could be derived from the in-situ gamma-ray spectra.

The mean total outdoor and indoor absorbed gamma dose-rate in air for the different towns varies between 17-88 nGy/h and 20-101 nGy/h respectively. The cities with relatively higher mean total absorbed dose-rates are located in Northern Greece. On the contrary in Southern Greece, and particularly in Athens and surroundings, where 33% of the Greek population lives, the values of the mean total outdoor and indoor absorbed gamma dose-rates are between 22 and 24 nGy/h, meaning among the smallest mean values measured in the Greek towns. The Greek population-weighted average for the outdoor and indoor gamma dose-rates is 31 and 36 nGy/h respectively. Assuming that 80% of people's time is spent indoor, a mean annual effective dose of 0.54 mSv from the gamma radiation can be deduced.

The indoor gamma dose-rate is almost always higher than the outdoor gamma dose-rate. This is due to the fact that most of the buildings and houses of Greece are made of brick and concrete. In this case the gamma rays emitted outdoors are efficiently absorbed by the walls, and the indoor absorbed dose-rate depends mainly on the activity concentrations of natural radionuclides in the building materials. Under these circumstances, the indoor-outdoor ratio of absorbed dose-rates in air is higher than 1 as a result of the change in source geometry.

The indoor and outdoor absorbed dose-rates in air are mainly due to natural emitters. The mean contributions of the Uranium series, Thorium series, ^{40}K and ^{137}Cs to the total dose-rate are 28.5% for U, 34% for Th, 37% for ^{40}K for the indoor measurements and 28% for U, 33% for Th, 31.5% for ^{40}K for the outdoor measurements, respectively. The mean contribution of ^{137}Cs from the Chernobyl accident to the total indoor dose-rate for the different Greek towns is negligible (always smaller than 1%). On the contrary, the mean contribution of ^{137}Cs to the total outdoor dose-rate for the different Greek towns is small but not negligible. For the buildings and houses constructed before the Chernobyl accident the actual indoor ^{137}Cs gamma radiation is only due to the presence of ^{137}Cs from the Chernobyl accident in the nearby outdoor environment. The attenuation of the outdoor radiation observed at 661.6 keV due to the shielding of the houses was at least 90% and up to 100%. For houses and buildings that were under construction in 1986, ^{137}Cs acts also as an indoor source term, however with only small contribution to the total dose-rate.

- Radiological maps of outdoor and indoor gamma dose-rates in Greek urban areas obtained by in-situ gamma-ray spectrometry [4].

In the present work 254 in-situ gamma-ray spectrometry measurements with a portable Germanium detector and 707 total gamma dose-rate measurements with a NaI(Tl) detector were performed in towns of 16 Greek islands.

The main conclusions of this experimental work are the following:

1. The mean total outdoor and indoor absorbed gamma dose-rate in air for the different islands varies between 22 and 108 nGy/h, and between 26 and 83 nGy/h respectively. The relatively most populated islands, with population more than 100,000 inhabitants (Kriti, Evia, Rhodes and Corfu), have the relatively lower mean total absorbed gamma dose-rates. The two islands, Lesbos and Limnos, which are in Northern Greece and belong to the Prefecture of Lesbos, have the relatively higher outdoor gamma dose-rates in air. The islands of volcanic origin have higher outdoor gamma dose-rates in air compared to the nearby islands, which are not of volcanic origin.
2. The indoor and outdoor absorbed gamma dose-rates in air are mainly due to natural emitters. The mean contribution of ^{137}Cs from the Chernobyl accident to the total outdoor and indoor gamma dose-rate for the different Greek islands is negligible (always smaller than 3% for the outdoor environment and 0.5% for the indoor environment).
3. The relative contribution of the different natural gamma emitters (Uranium series, Thorium series and ^{40}K) to the total gamma dose-rate varies from island to island. Depending on the island, the contribution of the Uranium series to the total outdoor gamma dose-rate can be a factor of two smaller or higher than the contribution of Thorium series to the total gamma dose-rate. Due to the variability of the relative contribution of the different natural emitters (Uranium series, Thorium series and ^{40}K) to the total gamma dose-rate, in-situ gamma-ray spectrometry can give general information about the origin of the building materials. In particular in some cases it can indicate if the building materials used in an island are of local origin.
4. The good correlation between the total gamma absorbed dose-rates measured with the NaI(Tl) and HPGe detectors indicates that, within 10% error, NaI(Tl) detector can also be used in field for total gamma dose-rate measurements.

The obtained results in conjunction with those previously reported [3] were used for the realization of a complete indoor and outdoor gamma radiation map of Greek urban areas obtained by in-situ gamma-ray spectrometry with portable Ge detector. To our knowledge, these are the first national radiological maps performed in the world based on high-resolution in-situ gamma-ray spectrometry with a portable Ge detector.

- Contribution of ^{137}Cs to the total absorbed gamma dose-rate in air in Greek forest ecosystems deduced by in-situ gamma-ray spectrometry measurements and Monte Carlo computations [5].

The absorbed gamma dose-rate in air at 1 m above soil due to natural gamma emitters and ^{137}Cs from the Chernobyl accident was determined inside a *Quercus conferta* Kit ecosystem in Northern Greece by combination of Monte Carlo simulations with the MCNP code and in-situ gamma-ray spectrometry measurements. The total absorbed gamma dose-rate in air is about 64 nGy/h, where 40% of this value is due to ^{137}Cs and 60% is due to natural gamma emitters. The Monte Carlo simulations indicated that the gamma absorbed dose-rate in air due to ^{137}Cs is mainly (70%) due to unscattered radiation and to a lesser extent (30%) to the scattered radiation. The results obtained with the Monte Carlo simulations for the unscattered radiation were in very good agreement with the experimental values deduced by in-situ gamma-ray spectrometry measurements. From the combination of the Monte Carlo simulations and in-situ gamma-ray spectrometry measurements a conversion factor $C=1 \text{ nGy.m}^2/\text{kBq.h}$ was deduced for ^{137}Cs . This factor is of the same order of magnitude as that obtained in [6], i.e. $C=0.82 \text{ nGy.m}^2/\text{kBq.h}$, for totally different forest ecosystem (Allepo pine) in Northern Greece. Therefore, even though the above-mentioned conversion factors must be used with caution and only for similar forest sites, for a rapid estimation of ^{137}Cs gamma dose-rates inside a forest ecosystem a conversion factor of $0.9 \text{ nGy.m}^2/\text{kBq.h}$ can be adopted.

- A combination study of indoor radon and in-situ gamma-ray spectrometry measurements in Greek dwellings [7].

The aim of this study was to investigate a possible correlation between indoor radon and indoor gamma dose-rates deduced by in-situ gamma-ray spectrometry measurements by using a portable Ge detector. Indoor radon and high-resolution in-situ gamma-ray spectrometry measurements were performed in 60 apartments in Thessaloniki, the second largest city of Greece. Geometric mean radon concentration is 52 Bq/m^3 . The mean total absorbed dose-rate in air due to gamma radiation is $56 \pm 9 \text{ nGy/h}$. The contribution of the different radionuclides to the total indoor gamma dose-rate in air is 41% due to ^{40}K , 36% due to the Thorium series and 23% due to the Uranium series. No correlation was found between indoor gamma dose-rate due to the Uranium series and indoor radon for ground and first floor apartments. For upper floor apartments (above second floor) a weak correlation is observed. The mean annual effective dose due to radon is 1.15 mSv, i.e. more than four times higher compared to the effective dose due to gamma radiation (0.27 mSv).

- Simultaneous measurement of indoor radon, radon-thoron progeny and high-resolution in-situ gamma-ray spectrometry in Greek dwellings [8].

Simultaneous indoor radon, radon–thoron progeny and high-resolution in-situ gamma-ray spectrometry measurements with portable high-purity Ge detector were performed in 26 dwellings of Thessaloniki, the second largest town of Greece, during the period March 2003-January 2005. The radon gas was measured in each of the 26 dwellings with an AlphaGUARD ionisation chamber every 10 min, for a time period between 7 and 10 days. Most of the values of radon gas concentration were between 20 and 30 Bq/m³, with an arithmetic mean of 34 Bq/m³. The maximum measured value of radon gas concentration was 516 Bq/m³.

The comparison between the radon gas measurements performed with AlphaGUARD and short-term electret ionisation chamber shows very good agreement, taking into account the relative short time period of the measurement and the relative low radon gas concentration. Radon and thoron progeny were measured with a SILENA instrument (model 4s). From the radon and radon progeny measurements, the equilibrium factor *F* could be deduced. Most of the measurements of the equilibrium factor are within the range 0.4–0.5. The mean value of the equilibrium factor *F* is 0.49 ± 0.10 , i.e. close to the typical value of 0.4 adopted by UNSCEAR. The mean equilibrium equivalent thoron concentration measured in the 26 dwellings is $EEC_{\text{thoron}} = 1.38 \pm 0.79$ Bq/m³. The mean equilibrium equivalent thoron to radon ratio concentration, measured in the 26 dwellings, is 0.1 ± 0.06 . The mean total absorbed dose-rate in air, owing to gamma radiation, is 58 ± 12 nGy/h. The contribution of the different radionuclides to the total indoor gamma dose-rate in air is 38% due to ⁴⁰K, 36% due to Thorium series and 26% due to Uranium series. The annual effective dose, due to the different source terms (radon, thoron and external gamma radiation), is 1.05, 0.39 and 0.28 mSv, respectively.

- Twenty year follow-up study of radiocesium migration in soil [9].

The profile of ¹³⁷Cs present in undisturbed soil due to the Chernobyl accident was measured repeatedly for approximately 20 years.

The main conclusions of this work are the following:

- Vertical migration of ¹³⁷Cs in soil is a very slow process. The mean vertical migration velocity is estimated to ~0.1–0.2 cm/y.
- The form of the ¹³⁷Cs profile in the soil has changed over the years. During the period 1987–94, the ¹³⁷Cs distribution was reproducible by a sum of two exponentials. In contrast, during 2005, the ¹³⁷Cs distribution can be described well by a single exponential function.
- A method based on in-situ gamma-ray spectrometry measurements and Monte Carlo computations was investigated in order to estimate the profile of ¹³⁷Cs without performing soil sampling analysis. Despite the fact that this method cannot provide the precise profile of ¹³⁷Cs in the soil, it can still yield useful information since it distinguishes between fresh deposition (surface contamination) and old deposition, which is important in the case of a radiological emergency.
- In-situ gamma-ray spectrometry for the determination of absorbed dose-rate in air following myocardial perfusion scintigraphy with ²⁰¹Tl [10].

The time dependence of the absorbed gamma dose-rate in air at a distance of 1 m from a patient who was undergoing myocardial perfusion scintigraphy with ^{201}Tl was measured. The absorbed gamma dose-rate was deduced by in-situ gamma-ray spectrometry using a 'calibrated' portable Ge detector which allows the direct measurement of spectral dose-rate distribution in the surroundings of a source without any assumption about the source geometry. The decrease of the absorbed dose-rate over time can be expressed by a single exponential decay. The effective and biological half-lives of ^{201}Tl were estimated to be 63 h and 20 days respectively. The effective dose received by the persons (i.e. relatives) in the nearby environment (1 m distance) of the patient is smaller than 0.03 mSv.

The maximum value of 0.03 mSv corresponds to the unrealistically pessimistic assumption of a continuous presence of a person at 1 m from the patient. The value of 0.03 mSv is small as compared to the arithmetic annual mean worldwide, weighted for population, effective dose due to terrestrial gamma rays (0.46 mSv) and cosmic rays (0.38 mSv).

- Measurements and Monte Carlo calculations of photon energy distributions in MAYAK Production Association workplaces [11].

Photon energy distributions were measured in different workplaces of the Mayak Production Association (MPA), which was the first plutonium production plant in the former Soviet Union. In-situ gamma-ray spectrometry measurements were performed with a portable germanium detector. The spectral stripping method is used for the conversion of the in-situ gamma-ray spectra to photon fluence rate energy distribution. This method requires the simulation of the portable germanium detector, which has been performed based on the MCNP code of the Los Alamos National Laboratory in the United States. Measured photon fluence rate energy distributions were compared with calculated photon energy distributions (with the MCNP code) in two different workplaces: in the first workplace the geometry exposure was known; on the contrary, in the second workplace, as in most workplaces of MPA, the exposure geometry was unknown.

The main conclusions of this work are:

1. The portable germanium detector used for the in-situ gamma-ray spectrometry measurements was successfully simulated. A very good agreement between the experimental and calculated efficiency curves was achieved.
2. Photon radiation energy distributions in the MPA workplaces may vary within wide ranges.
3. The good agreement between the experimental and calculated photon fluence rate energy distributions in a MPA workplace, where the radiation source term and the geometry were well defined, demonstrates the correctness of the stripping routine procedure used for the conversion of an in-situ gamma-ray spectrum to photon fluence rate energy distribution.
4. In MPA workplaces where the radiation source geometry is in general unknown, it is difficult to compare directly the experimental and calculated photon fluence rate energy distributions. However, it is possible, under certain conditions, to deduce useful information about the contribution of the different radiation source terms to the total photon fluence rate energy distribution from the comparison between the experimental and calculated photon fluence rate energy distributions.

- In-situ gamma-ray spectrometry measurements and Monte Carlo computations for the detection of radioactive sources in scrap metal [12].

A very limited number of field experiments have been performed to assess the relative radiation detection sensitivities of commercially available equipment items used to detect radioactive sources in recycled metal scrap. Such experiments require the cooperation and commitment of considerable resources from the vendors of the radiation detection systems and the cooperation of a steel mill or scrap processing facility.

The results will unavoidably be specific to the equipment item tested at the time, the characteristics of the scrap metal involved in the tests, and to the specific configurations of the scrap containers. Given these limitations, the use of computer simulation for this purpose would be a desirable alternative. With this in mind, this study sought to determine whether Monte Carlo simulation of photon fluence rate energy distributions resulting from a radiation source in metal scrap would be realistic. In the present work, experimental and simulated photon fluence rate energy distributions in the outer part of a truck due to the presence of embedded radioactive sources in the scrap metal load were compared. The experimental photon fluence rates were deduced by in-situ gamma-ray spectrometry measurements with portable Ge detector and the calculated ones by Monte Carlo simulations with the MCNP code. The good agreement between simulated and measured photon fluence rate energy distributions indicated that the results obtained by the Monte Carlo simulations are realistic.

- Spatial and spectral gamma-ray response of plastic scintillators used in portal radiation detectors: Comparison of measurements and simulations [13].

Portal radiation detectors are commonly used by steel industries in the probing and detection of radioactivity contamination in scrap metal. Furthermore, a large number of portal monitors are installed at the border crossings to prevent illegal radioactive material trafficking. These portal detectors typically consist of either PS (polystyrene) or PVT (polyvinyltoluene) plastic scintillating detectors. Through the electronic circuit of the detector, an energy region-of-interest (ROI) window can be determined in order to focus on the detection of certain radionuclides. In this study, the spatial response of a portal PS scintillator to a ^{137}Cs and a ^{60}Co source for various energy ROI windows is presented. Furthermore, a number of measured spectra for different source positions on the surface of the scintillating detector are shown. The measured spatial response showed a quantitative and qualitative dependence on the energy window used each time. In addition, measured spectra showed energy shifts for different positions of the two sources on the detector surface. The aforementioned phenomena could not be adequately explained and modelled using gamma-particle transport Monte Carlo simulation tools, such as the MCNP4C2 code. In order to fully explain these phenomena, optical simulations modelling the transport of the light yield within the detector were carried out using Gate v3.0.0 with GEANT 4.8.0p01 of CERN. As a conclusion, a detailed analysis and simulation of PS plastic scintillators has been conducted. A set of spectra taken for different source positions on the surface of the scintillator has shown differences that depend on the scintillator's optical properties and explain its different responses for different energy ROI windows. These observations have been backed up by simulations and can be referred to as a guideline for later works.

- Determining minimum alarm activities of orphan sources in scrap loads: Monte Carlo simulations validated with measurements [14].

Portal monitoring radiation detectors are commonly used by steel industries in the probing and detection of radioactivity contamination in scrap metal. These portal monitors typically consist of polystyrene (PS) or polyvinyltoluene (PVT) plastic scintillating detectors, one or several photomultiplier tubes (PMT), an electronic circuit, a controller that handles data output and data manipulation linking the system to a display or a computer with appropriate software and usually, a light guide. Such a portal used by the steel industry was opened and all principal materials were simulated using a Monte Carlo simulation tool (MCNP4C2).

Various source-detector configurations were simulated and validated by comparison with corresponding measurements. Subsequently an experiment with a uniform cargo along with two sets of experiments with different scrap loads and radioactive sources (^{137}Cs , ^{152}Eu) were performed and simulated. Simulated and measured results suggested that the nature of scrap is crucial when simulating scrap load-detector experiments. To conclude, an accurate simulation of the portal monitoring detectors was achieved using MCNP. The ‘scintillator-source’, ‘portal monitor-source’ and long distance source measurements showed good agreement with the corresponding simulations, validating the simulated geometry. Furthermore, the homogenous load simulation was validated by measurements, showing that a detector-truck simulation is pragmatic. Simulating measurements with scrap loads though, is more complex and scrap type dependent. This was obvious in the ‘old scrap E1’ experiments. In some cases there were differences between portal monitor measurements with almost the same measuring geometry. Additionally, similar outputs from measurements with completely different geometries were recorded. The aforementioned illustrates the degree of inhomogeneity of the specific scrap type load (‘old scrap E1’). The greatest deviations between measured and simulated values appeared when the source was placed in the middle of the load, while the differences were smaller for outer source positions; in these positions, the source-detector geometry appears to be more important than the type of scrap. Apparently, in this case (‘old scrap E1’ scrap load) the measured values cannot be approximated by simulation. Nevertheless the minimum alarm activities yielding from simulations would be higher than the ones derived from measurements, erring on the safe side. In the inner or middle parts of the load, where a non-detectable source is more likely to be found, the shredded (more ‘homogeneous’) scrap measurements showed better agreement with the analogous simulations. The quantitative difference observed was significantly smaller than in the previous case (‘old scrap E1’). After a sensitivity analysis using the mean scrap density as a free parameter, it was found that a slightly higher simulated density could give a better match between measurements and simulations. It should be beared in mind that both the actual and the simulated scrap densities (1.006 g/cm^3 and 1.3 g/cm^3) represent a small fraction of iron’s density (13% and 16.5% of 7.87 g/cm^3), therefore the mean scrap density does not necessarily represent the scrap density in the different locations of the scrap load. Based on the simulated results, a series of minimum alarm activity calculations for ^{137}Cs , ^{60}Co and ^{192}Ir sources were performed. It was found that the height of the least detectable source varied with the mean scrap density and the gamma-ray emitting energies of the radionuclide. Higher mean scrap densities and/or lower gamma-ray energies suggested positions of least detectable sources towards the centre of the load. Lower mean scrap densities and nuclides with higher emitting gamma-ray energies pointed to the top of the trailer as being the most unfavourable place for source detection. Finally, the highest values of calculated minimum alarm activities along with the corresponding source positions for each case were presented.

- ‘Exotic use’ of Ge detectors: Measurement of ionizing cosmic radiation (muons) dose-rates with portable Ge detector [15]

The present work shows how portable Ge detectors can be useful for measurements of the dose-rate due to ionizing cosmic radiation. The proposed methodology converts the cosmic radiation induced background in a Ge crystal (energy range above 3 MeV) to the absorbed dose-rate due to muons, which are responsible for 75% of the cosmic radiation dose-rate at sea level. The key point is to observe in the high energy range (above 20 MeV) the broad muon peak resulting from the most probable energy loss of muons in the Ge detector. This can be done by applying an attenuation gain in the amplifier by an external simple voltage divider.

This is important, as in standard gamma-ray spectrometry systems, the lowest amplifier gain is still too high for observing the muon peak. An energy shift of the muon peak was observed, as expected, for increasing dimensions of three Ge crystals (10%, 20%, and 70% relative efficiency). Taking into account the dimensions of the three detectors the location of the three muon peaks was reproduced by Monte Carlo computations using the GEANT code. The absorbed dose-rate due to muons has been measured in 50 indoor and outdoor locations at Thessaloniki, the second largest town of Greece, with a portable Ge detector and converted to the absorbed dose-rate due to muons in an ICRU sphere representing the human body by using a factor derived from Monte Carlo computations. The outdoor and indoor mean muon dose-rate was 25 nGy/h and 17.8 nGy/h, respectively. The shielding factor for the 40 indoor measurements ranges from 0.5 to 0.9 with a most probable value between 0.7 and 0.8.

3. CONCLUSIONS AND FINAL REMARKS

A summary of the work performed in the last fifteen years by the members of the Nuclear Technology Laboratory of the Aristotle University of Thessaloniki in the field of in-situ gamma-ray spectrometry was presented. In most of the research work a portable Germanium detector was used. In few studies plastic detectors were used. Different applications of in-situ gamma-ray spectrometry were investigated: metrology (simulation of Germanium detectors or plastic detectors), environmental radioactivity, measurements in contaminated sites (MAYAK Production Association), industrial applications (scrap), medical applications, and cosmic radiation measurements with portable Ge detector. This research was published in 2 Doctorate theses and in 15 publications in international scientific journals, as reported in the list of references. Most of the work was supported by the European Commission (DG-RESEARCH and DG-ENVIRONMENT), by the Greek Secretary of Research and Technology (GSRT), by Greek municipalities and by industry (SIDENOR STEEL FACTORY). Last but not least, the authors would like to thank all the colleagues and friends who contributed to this work and in particular Jorge Silva from the University Paris VI in France, Costas Potiriadis from the Greek Atomic Energy Commission, Evgeni Vasilenko and Michail Smetanin from the MAYAK Production Association.

REFERENCES

- [1] CLOUVAS, A., XANTHOS, S., ANTONOPOULOS-DOMIS, M., SILVA, J., Monte-Carlo based method for conversion of in-situ gamma-ray spectrum obtained with portable Ge detector to incident photon flux energy distribution, *Health Phys.* **74** 1 (1998) 216-230.
- [2] CLOUVAS, A., XANTHOS, S., ANTONOPOULOS-DOMIS, M., Derivation of indoor gamma dose rate from high resolution in situ gamma ray spectra, *Health Phys.* **79** 3 (2000) 274-281.

- [3] CLOUVAS, A., XANTHOS, S., ANTONOPOULOS-DOMIS, M., Extended survey of indoor and outdoor terrestrial gamma radiation in Greek urban areas by in situ gamma spectrometry with portable Ge detector, *Radiat. Prot. Dosimetry* **94** (2001) 233-246.
- [4] CLOUVAS, A., XANTHOS, S., ANTONOPOULOS-DOMIS, M., Radiological maps of outdoor and indoor gamma dose rates in Greek urban areas obtained by in situ gamma ray spectrometry, *Radiat. Prot. Dosimetry* **112** (2004) 267-275.
- [5] CLOUVAS, A., XANTHOS, S., ANTONOPOULOS-DOMIS, M., ALIFRAGIS, A., Contribution of Cs-137 to the total absorbed gamma dose rate in air in a Greek Forest ecosystem: Measurements and Monte Carlo computations, *Health Phys.* **76** 1 (1999) 36-43.
- [6] CLOUVAS, A., XANTHOS, S., ANTONOPOULOS-DOMIS, M., ALIFRAGIS, A., Radiocesium gamma dose rates in a Greek pine forest: Measurements and Monte Carlo computations, *Radioactivity in the Environment* **7** (2005) 1155-1166.
- [7] CLOUVAS, A., XANTHOS, S., ANTONOPOULOS-DOMIS, M., A combination study of indoor radon and in situ gamma spectrometry measurements in Greek dwellings, *Radiat. Prot. Dosimetry* **103** (2003) 363-366.
- [8] CLOUVAS, A., XANTHOS, S., ANTONOPOULOS-DOMIS, M., Simultaneous measurements of indoor radon, radon-thoron progeny and high resolution gamma spectrometry in Greek dwellings, *Radiat. Prot. Dosimetry* **118** (2006) 482-490.
- [9] CLOUVAS, A., XANTHOS, S., TAKOUDIS, M., ANTONOPOULOS-DOMIS, M., ZINOVIADIS, G., VIDMAR, T., LIKAR, A., Twenty-year follow-up study of radiocesium migration in soil, *Radiat. Prot. Dosimetry* **124** (2007) 372-377.
- [10] CLOUVAS, A., XANTHOS, S., ANTONOPOULOS-DOMIS, M., Gamma ray spectrometry for the determination of absorbed dose rate in air following a myocardial perfusion scintigraphy with Tl-201, *Radiat. Prot. Dosimetry* **74** (1997) 97-101.
- [11] SMETANIN, M., VASILENKO, E., SEMENOV, M., XANTHOS, S., TAKOUDIS, G., CLOUVAS, A., SILVA, J., POTIRIADIS, C., Measurements and Monte Carlo calculations of photon energy distributions in Mayak PA workplaces, *Radiat. Prot. Dosimetry* **131** (2008) 455-468.
- [12] CLOUVAS, A., XANTHOS, S., TAKOUDIS, G., POTIRIADIS, C., SILVA, J., In situ gamma spectrometry measurements and Monte Carlo computations for the detection of radioactive sources in scrap metal, *Health Phys.* **88** 2 (2005) 154-162.
- [13] TAKOUDIS, G., XANTHOS, S., CLOUVAS, A., ANTONOPOULOS-DOMIS, M., POTIRIADIS, C., SILVA, J., Spatial and spectral gamma-ray response of plastic scintillators used in portal radiation detectors; comparison of measurements and simulations, *Nucl. Instrum. Methods Phys. Res. Sect. A* **599** (2009) 74-81.
- [14] TAKOUDIS, G., XANTHOS, S., CLOUVAS, A., POTIRIADIS, C., Determining minimum alarm activities of orphan sources in scrap loads; Monte Carlo simulations, validated with measurements. *Nucl. Instrum. Methods Phys. Res. Sect. A* **614** (2010) 57-67.
- [15] CLOUVAS, A., XANTHOS, S., ANTONOPOULOS-DOMIS, M., SILVA, J., Measurements with a Ge detector and Monte Carlo computations of dose rate yields due to cosmic muons, *Health Phys.* **84** 2 (2003) 274-281.

IN-SITU RADIONUCLIDE QUANTITATIVE CHARACTERIZATION IN AQUATIC ECOSYSTEMS USING THE KATERINA DETECTOR

C. TSABARIS¹, D.L. PATIRIS¹, G. ELEFThERIOU^{1,2}, M. KOKKORIS², R. VLASTOU²

¹ Hellenic Centre for Marine Research, Institute of Oceanography, Attica, Greece

² National Technical University of Athens, Faculty of Applied Mathematics and Physics, Athens, Greece

Abstract

A new detection system, named 'KATERINA', based on NaI(Tl) crystal has been developed and applied for in-situ measurements of radioactivity in aquatic ecosystems. The detection system is designed for qualitative and quantitative radionuclide detection (gamma-ray emitters) in any aquatic environment (sea, groundwater, lakes, etc) with a maximum depth of deployment up to 400 m. It offers volumetric activities in absolute units (Bq/m³ or Bq/L) for all gamma-ray emitters in the energy range from the threshold energy of 50 keV up to 3,000 keV. The efficiency calibration in aquatic environment was first realized by dilution of three reference sources (^{99m}Tc, ¹³⁷Cs and ⁴⁰K) inside a special tank filled with water and then it was simulated using the GEANT4 code. The system could be deployed immersed in two ways. Powered by batteries, it incorporates special memory and microcontroller operating autonomously in-situ as stand-alone unit acquiring and buffering data for periods up to three months without any maintenance. Alternatively, it can be installed into supporting floating stations (buoys) for longer period performing continuous in-situ measurements at sites where contamination by artificial and/or natural occurring radioactive materials could be observed (i.e. in regions with enhanced industrial fertilizer activities or other 'hot-spot' areas). Unlike laboratory methods, its continued operation into supporting floating stations makes it ideal to monitor radioactivity in real-time, enabling early warning in the case of a contamination event. Till nowadays, the detector has been deployed in autonomous mode, acquiring radon's daughters (²¹⁴Pb and ²¹⁴Bi) concentrations in several coastal regions around the Mediterranean Sea where submarine groundwater is discharged and also, over submarine magmatic regions of the Adriatic Sea, monitoring natural radioactivity. During these studies inter-comparison exercises were performed with standard laboratory methods (i.e. germanium detector techniques) obtaining satisfactory results.

1. INTRODUCTION

The most common method for radioactivity measurements in the environmental sciences is the gamma-ray spectrometry. There are two main approaches, the sampling methods which are based on collecting masses of material (water, soil, etc) consequently processed using laboratory equipment items and/or using portable instruments on site. On the other hand there is the in-situ approach, which is based on specially designed detection equipment items capable to acquire and buffer or transmit data operating exactly on the point of interest. Regarding aquatic ecosystem studies, the 'traditional' sampling approach is often implemented by collecting significant water quantities analysed by time-consuming techniques, which demand special facilities and know-how for the chemical treatment of the samples. This technique introduces various uncertainties due to the tracer reference data and half-life limitations. The application of in-situ detection systems on aquatic environment demands durable constructed equipment items providing corrosion and pressure resistance, ensuring operational stability and minimal gamma-ray attenuation. Additionally, special attention has to be paid on reliable marine efficiency calibration procedures.

In-situ detection systems are very scarce concerning their applicability in aquatic ecosystems. Despite their modest energy resolution, NaI(Tl) crystals are the most common detection material for long-term measurements due to low consumption, good efficiency and low cost.

During the last decades, such crystals accompanied by electronic modules have been used as integrated units inside special housing apparatus in many aquatic applications supported by floating measuring stations (buoy) for marine radioactivity monitoring [1-5] and autonomously (without supporting station) for seabed mapping [6, 7] and seawater measurements [8, 9]. Other scintillation crystals have also been applied (YAP-Ce) for radon measurements [10] investigating environments of geophysical interest found in geothermal and volcanic areas. Also, detectors of semi-conductor HPGe crystals were applied in aquatic environments for seabed studies [8], but the enhanced cooling needs of the crystal could not make such detectors applicable for long-term measurements.

Along with the implementation of NaI(Tl) based detection systems for in-situ measurements there has been considerable effort in developing algorithms capable to simulate and analyse the recorded spectra. As those crystals have lower energy resolution compared to HPGe detectors, various emissions from naturally occurring radionuclides may produce overlap photopeaks resulting in serious uncertainties on radioisotopes' concentration estimations. Various methods, based on Monte Carlo techniques, have been proposed [11, 12] aiming to reliable simulated spectra of NaI(Tl) crystals taking into account their low energy resolution and the absorption of gamma rays from the seawater. Recently, using the GEANT4 code, a new method has been published [13], where the concept of a marine efficiency coefficient, according to the gamma-ray energy, was introduced and estimated both by computer code and experimental procedure.

In the present work the detection system KATERINA is briefly presented. It could be applied in a variety of radionuclides' studies involving naturally occurring (^{238}U daughters, ^{232}Th daughters, ^{235}U and ^{40}K), cosmogenic (^{207}Bi) and anthropogenic (^{137}Cs , ^{134}Cs , $^{95}\text{Zr}/^{95}\text{Nb}$, ^{106}Ru and ^{60}Co) radionuclide detection. The system could be applied either as autonomous stand-alone unit or with the support of a floating station. Its deployment at several places around the Mediterranean and Adriatic Seas, mainly for radon daughters' concentration measurements, provided the opportunity for inter-calibration exercises with standard laboratory methods (i.e. HPGe techniques) with satisfactory results.

2. MATERIAL AND METHODS

The detection system KATERINA consist of a 3"×3" NaI(Tl) scintillation crystal, connected in succession with a photomultiplier tube, a preamplifier and a power supply unit, along with electronics for signal amplification, data acquisition and storage. The power consumption has been kept low enough (~1.2-1.4 W) resulting in the autonomous operation of the system for several months supplied by a special gel-type battery pack. The crystal and all the electronic modules are specially assembled to fit inside a water-tight cylindrical enclosure (85×550 mm). The enclosure was designed to offer continuous functionality up to 400 meters water depth and continuous operation. The enclosure's material was chosen (among Al, Fe, Acetal, and POM) according to minimal gamma-ray absorption, long corrosion resistance and reliable pressure tolerance. Detailed technical specifications of the KATERINA detection system are given elsewhere [14].

The system is calibrated (energy, energy resolution and efficiency) in the energy range of 50 keV to 3,000keV and its stability has been tested for water temperature variations (from 10 to 35°C). Measurements of the absolute detector marine efficiency (in m³) have been performed in the water environment. For this purpose, a calibration tank of 5.5 m³ volume filled with water has been used. The detector was mounted in the middle of the tank in order to be surrounded by one meter of water, which is enough to simulate the high attenuation of gamma rays (for $E_\gamma < 1,100$ keV). At the bottom of the tank, an electric pump was used to continually circulate the water, mixing three reference sources (^{99m}Tc, ¹³⁷Cs and ⁴⁰K) and keeping homogenous conditions. The system was also inter-calibrated during field deployments by comparing acquired data of radon's daughters (²¹⁴Pb and ²¹⁴Bi) concentrations with results from water samples measured by HPGe techniques.

3. DEPLOYMENTS AND RESULTS

The system installed in a special frame along with battery packs has been deployed in various regions in the Mediterranean Sea for autonomous in-situ operations on submarine groundwater discharges (SGD) into the coastal zone [15]. During those deployments, a CTD (conductivity, temperature and density) unit was also used in order to specify the optimum location for the establishment of the detection system according to minimum values of water's salinity. KATERINA was positioned 1 m above the seabed and via a connection with a simple accompanying mobile computer data in real-time was obtained (on-line mode). An indicative spectrum of detected gamma rays acquired during the deployment in Evoikos Gulf in Greece is shown in Fig. 1. Significant radionuclides' concentrations were measured due to the discharging of radon-rich groundwater.

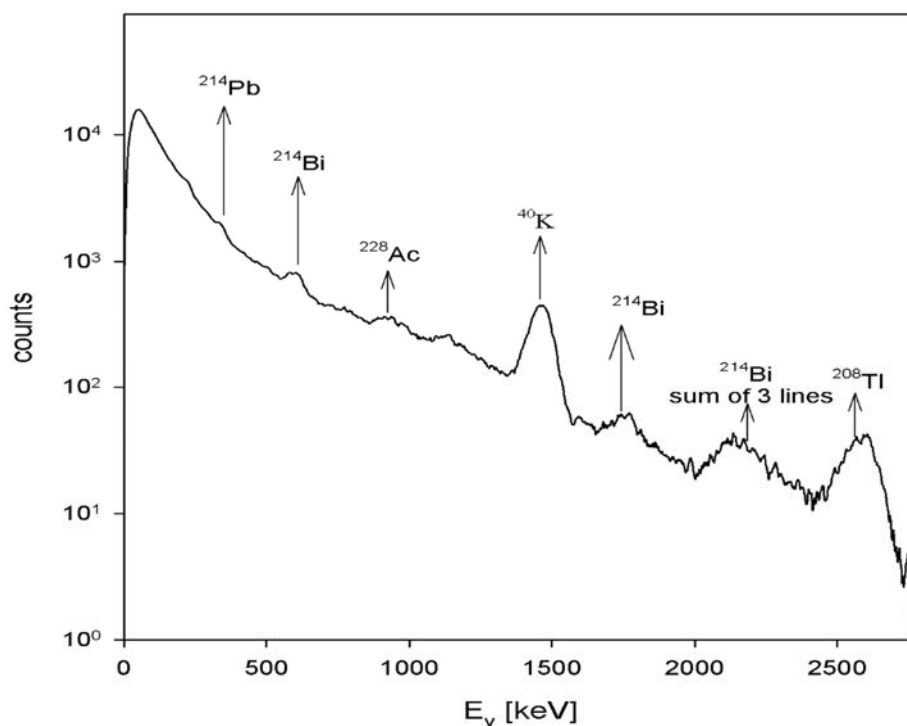


FIG 1. A typical gamma-ray spectrum obtained in-situ by KATERINA detector at SGD location in Evoikos Gulf in Greece [15].

Additionally, the system was applied in two regions of the Adriatic Sea measuring radionuclides in water masses close to magmatic regions [16]. The significant contribution of ^{232}Th daughters was clearly observed during the measurement performed in Vis Island in Croatia. More specifically, ^{232}Th daughter, ^{212}Pb , exhibits at 238 keV an activity concentration of 220 Bq/m^3 . Also, ^{208}Tl was observed at two energy peaks (583 keV and 2,614 keV) and the measured concentrations obtained from these two photopeaks were found in good agreement (76 Bq/m^3 and 82 Bq/m^3 , respectively). Furthermore, the concentrations of ^{222}Rn daughters (^{214}Pb and ^{214}Bi) were measured between 115 Bq/m^3 and 120 Bq/m^3 . All natural radionuclide activity concentration was found enhanced as compared with those from open sea measurements due to the magmatic origin of the studied region.

During the deployments at another SGD location at South Peloponnesus in Greece (region of Stoupa), the system's results for the concentration of radon daughters were inter-compared with results obtained by laboratory-based HPGe technique, measuring samples taken from the same water masses. The samples were collected at the deployment point by divers with Niskin bottles, were stored in a sealed glass bottle and they were transported directly to the laboratory. The activity concentration using HPGe technique was estimated to $1.1 \pm 0.2 \text{ Bq/L}$ for ^{214}Pb and to $1.2 \pm 0.2 \text{ Bq/L}$ for ^{214}Bi , while the analysis of KATERINA spectra exhibited similar results, i.e. $1.0 \pm 0.1 \text{ Bq/L}$ and $1.3 \pm 0.1 \text{ Bq/L}$ respectively.

In the future, the system, along with studies in more aquatic ecosystems, is planning to be developed as tool method for seabed and beach sand mapping. It will be deployed at coastal regions with enhanced NORM and TENORM, while at the same time core analysis and measurements of granulometry, geochemistry, mineralogy and organic carbon will be implemented. From such studies KATERINA will be involved for radionuclide characterization of sediments and beach sand using the grid-based method. By this time a preliminary application in the region of Sounio in Greece has occurred placing the in-situ detection system 5 cm above the seabed. Additional measurements are in progress as well as analysis of surface and core samples. Further investigation and systematic study are needed in order to have quality assurance using comparison between in-situ and laboratory-based techniques.

REFERENCES

- [1] AAKENES, U.R., Radioactivity monitored from moored oceanographic buoys, *Chem. Ecol.* **10** (1995) 61.
- [2] SOUKISSIAN, T.H., CHRONIS, G.T., NITTIS, K., POSEIDON: operational marine monitoring system for Greek seas, *Sea Technol.* **40** (1999) 31.
- [3] WEDEKIND, C., SCHILLING, G., GRUTTMULLER, M., BECKER, K., Gamma-radiation monitoring network at sea, *Appl. Radiat. Isot.* **50** (1999) 733.
- [4] TSABARIS, C., BALLAS, D., On line gamma-ray spectrometry at open sea. *Appl. Radiat. Isot.* **62** (2005) 83.
- [5] OSVATH, I., POVINEC, P.P., LIVINGSTON, H.D., RYAN, T.P., MUSLOW, S., COMMANDUCCI, J.-F., Monitoring of radioactivity in NW Irish Sea water using a stationary underwater gamma-ray spectrometer with satellite data transmission, *J. Radioanal. Nucl. Chem.* **263** (2005) 437.
- [6] MAUCEC, M., DE MEIJER, R.J., RIGOLLET, C., HENDRICKS, P.H.G.M., JONES, D.G., Detection of radioactive particles offshore by gamma-ray spectrometry Part I: Monte Carlo assessment of detection of depth limits, *Nucl. Instrum. Methods Phys. Res. A* **525**, (2004) 593.

- [7] OSVATH, I., POVINEC, P.P., Seabed gamma-ray spectrometry applications at IAEA-MEL, *J. Environ. Radioact.* **53** (2001) 335.
- [8] POVINEC, P.P., OSVATH, I., BAXTER, M.S., Underwater gamma spectrometry with HpGe and NaI(Tl) detectors, *Appl. Radiat. Isot.* **47** (1996) 1127.
- [9] van PUT, P., DEBAUCHE, A., DE LELLIS, C., ADAM, V., Performance level of an autonomous system of continuous monitoring of radioactivity in seawater, *J. Environ. Radioact.* **72** (2004) 177.
- [10] PLASTINO, W., DE FELICE, P., DE NOTARISTEFANI, F., Radon gamma-ray spectrometry with YAP:Ce scintillator. *Nucl. Instrum. Methods Phys. Res. A* **486** (2002) 146.
- [11] VLASTOU, R., NTZIOU, I.T., KOKKORIS, M., PAPADOPOULOS, C.T., TSABARIS, C., Monte Carlo simulation of γ -ray spectra from natural radionuclides recorded by a NaI detector in the marine environment, *Appl. Radiat. Isot.* **64** (2006) 116.
- [12] VLACHOS, D.S., TSABARIS, C., Response function calculation of an underwater gamma ray NaI(Tl) spectrometer, *Nucl. Instrum. Methods Phys. Res. A* **539** (2005) 414.
- [13] BAGATELAS, C., TSABARIS, C., KOKKORIS, M., PAPADOPOULOS, C.T., VLASTOU, R., Determination of marine gamma activity and study of the minimum detectable activity (MDA) in 4pi geometry based on Monte Carlo simulation. *Environ. Monit. and Assess.* **165** (2010) 159.
- [14] TSABARIS, C., BAGATELAS, C., DAKLADAS, T., PAPADOPOULOS, C.T., VLASTOU, R., CHRONIS, G.T., An autonomous in situ detection system for radioactivity measurements in the marine environment, *Appl. Radiat. Isot.* **66** (2008) 1419.
- [15] TSABARIS, C., SCHOLTEN, J., KARAGEORGIS, A.P., COMANDUCCI, J.-F., GEORGOPOULOS, D., KWONG, L., PATIRIS, D.L., PAPATHANASSIOU, E., Underwater in situ measurements of radionuclides in selected submarine groundwater springs-Mediterranean Sea, *Rad. Prot. Dosim.* **142** (2010) 273.
- [16] PETRINEC, B., FRANIC, Z., LEDER, N., TSABARIS, C., BITUH, T., MAROVIC G., Gamma Radiation and dose rate investigations on the Adriatic islands of magmatic origin, *Rad. Prot. Dosim.* **139** (2010) 551.
- [17] TSABARIS, C., PATIRIS, D.L., IOANNIDES, K., KARAGEORGIS, A.P., STAMOULIS, K., ELEFThERIOU, G., GEORGOPOULOS, D., PAPATHANASSIOU, E., "Radio Isotopes as Tracers for the study of the Submarine Groundwater Discharge of Kalogria Bay, SW Peloponnissos, Greece", paper presented at 39th CIESM Congress, Venice, Italy (2010).

MEASUREMENTS WITH THE MOBILE LABORATORY OF THE HUNGARIAN ACADEMY OF SCIENCES KFKI ATOMIC ENERGY RESEARCH INSTITUTE

K. BODOR, A. NAGY

Hungarian Academy of Sciences KFKI Atomic Energy Research Institute, Budapest, Hungary

Email: bodor.karoly@energia.mta.hu

Abstract

The different kinds of measurements carried out with the mobile laboratory of the Hungarian Academy of Sciences KFKI Atomic Energy Research Institute are reviewed. The mobile laboratory of the Atomic Energy Research Institute, whose development started in 1990, was the first mobile laboratory in Hungary. The equipment items of the mobile laboratory enable reliable measurements. The mobile laboratory is an appropriate tool for effective radiological environmental monitoring and it can be used in cooperation with other mobile laboratories and with the army. The mobile laboratory's measurements results support decision-making processes.

1. REQUIREMENTS FOR EFFECTIVE RADIOLOGICAL ENVIRONMENTAL MONITORING

The mobile laboratory is an appropriate tool for ensuring an effective radiological environmental monitoring. It has portable instruments and provides a fast reaction time. The different measurement tools available in the mobile laboratory provide wide measuring ranges and reliable measurements, since radioactivity levels can be determined with different measuring instruments. The mobile laboratory's measurements results support decision-making processes.

2. THE MOBILE LABORATORY OF THE ATOMIC ENERGY RESEARCH INSTITUTE

The mobile laboratory of the Atomic Energy Research Institute, whose development started in 1990, was the first mobile laboratory in Hungary. The mobile laboratory is a Transporter with SYNCRO (4 wheels) inclination, and it has one extra battery for the instruments. The engine charges the batteries; alternatively, the batteries can also be charged from the main electricity network. The mobile laboratory is shown below in Fig. 1.



FIG. 1. The mobile laboratory of the Atomic Energy Research Institute.

1. EQUIPMENT ITEMS OF THE MOBILE LABORATORY

The mobile laboratory is equipped with:

- GPS;
- Three notebooks;
- Inspector;
- Canberra 2020 HPGe detector;
- Iodine measuring system;
- BNS 98 dose-rate meter;
- NanoSPEC hand-held gamma-ray spectroscopy system;
- UMO dose-rate and surface contamination meter;
- Air sampling system;
- Soil sampling kit;
- Emergency hat.

With these equipment items the mobile laboratory is able to make route monitoring using dose-rate measurements, in-situ gamma-ray spectrometry, sampling (soil, plant, liquid), assay with in-situ gamma-ray spectrometry, atmospheric radioactive concentration measurements and personal dosimetry.

3.1. Measurements with the nanoSPEC instrument, a hand-held gamma-ray spectroscopy system

The nanoSPEC is a complete gamma-ray spectroscopy system, including multi-channel analyser, amplifier, high voltage power supply, memory and an integral pin scintillation detector. Before the measurements, the scintillation detector has to be calibrated. The energy calibration is easy with the built-in library, a ^{137}Cs source is used for calibration. A calibration library was made out by measuring different radioactive sources to cover the whole energy and channel range of the spectrum.

The following parameters can be measured using the nanoSPEC instrument:

- Dose-rate;
- Count rate;
- Live spectrum display;
- Nuclide identification.

3.2. Route monitoring

The BNS 98 dose-rate meter is located in the front right of the mobile laboratory, as shown in Fig. 2. The BNS 98 dose-rate meter measures the actual dose-rate and the GPS allocates the position of the mobile laboratory. The data transferred to the main control system of the mobile laboratory and the route monitoring programme represent the position and the actual dose-rate. An example of dose-rate map is shown in Fig. 3.

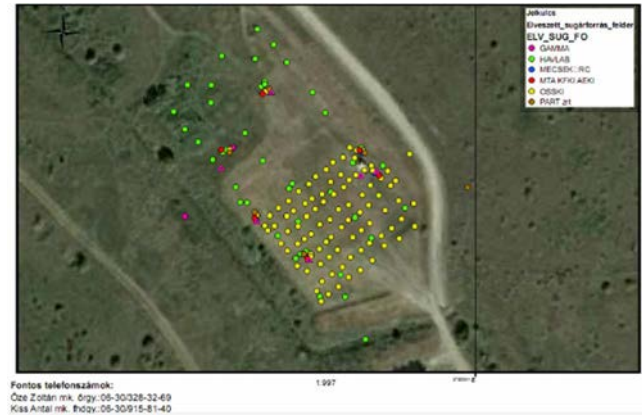


FIG. 2. The BNS 98 dose-rate meter.

FIG. 3. Example of dose-rate map.

3.3. Lost radioactive source exploration exercise in the KFKI campus

A lost radioactive source exploration exercise was made on the KFKI campus in 2009. The task was to find, allocate the position and provide the dose-rate of the radioactive material. After one circle in the north side of the campus in a byway, the dose-rate level was increased rapidly from the normal level (~ 100 nGy/h) to a much higher level (1152 nGy/h). The accurate position of the radioactive material was allocated using the triangulation method. This method is illustrated in Fig. 4.

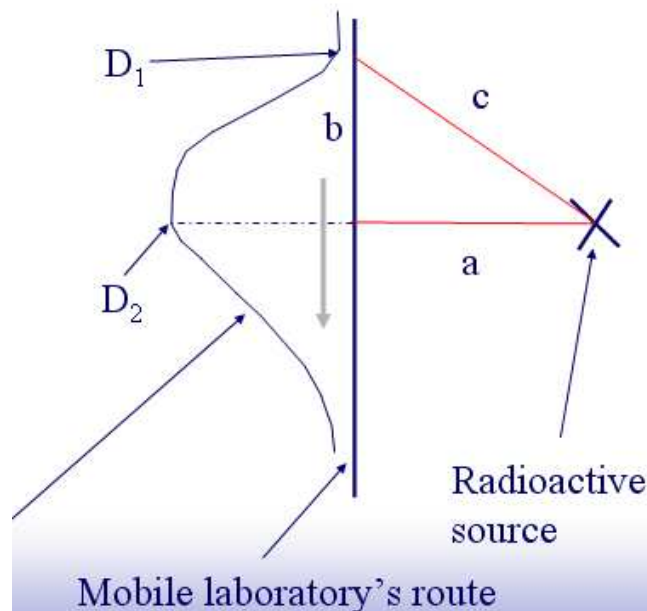


FIG. 4. The triangulation method.

The dose-rate levels and the distance between the two points were measured.

Using this commensurable parameters the real distance of the radioactive material was assigned using the following equation:

$$a=[b^2/(D_2/D_1-1)]^{1/2} \quad (1)$$

where:

D_1, D_2 are dose-rate levels;

b is the distance between D_1 - D_2 points;

a is the real distance of the radioactive source from the mobile laboratory.

In case the radioactive material is buried, then the maximum dose-rate above the ground is used to allocate the depth of the source; this maximum dose-rate can be determined using a dose-rate meter. Dose-rate measurements had to take place at two heights (d_1, d_2) at that point. The method used to locate a buried radioactive material is illustrated in Fig. 5.

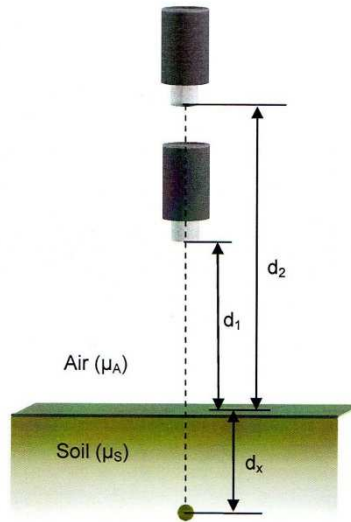


FIG. 5. Measuring positions in the case of a buried radioactive material.

From these parameters the depth of the source can be calculated using the following equation:

$$d_x=[d_2-d_1 \times (N_1/N_2)^{1/2}]/(N_1/N_2)^{1/2}-1 \quad (2)$$

where:

d_x is the depth of the radioactive material in the soil;

d_1 and d_2 are the measured height positions;

N_i is the net count rate at position i .

It is therefore fast and simple to identify the radioactive material with the nanoSPEC gamma-ray spectroscopy system using route monitoring and the triangulation method. The radioactive material can be identified by measuring the spectrum with the nanoSPEC. The activity of the source can then be easily calculated.

3.4. Calibration and determination of the angle dependence of the BNS 98 dose-rate meter

The calibration and determination of the angle dependence and mobile laboratory shielding of the BNS 98 was made using a ^{137}Cs radioactive source at different distances and angles. The reference instrument was a calibrated UMO dose-rate meter. The sensible part of the BNS 98 dose-rate meter is on the right hand side of the instrument. The highest efficiency shielding effect of the mobile laboratory is on the back left side of the van. As expected approximately 75% of the radiation is shielded in this position. The shielding effect of the mobile laboratory and the angle dependence of the BNS 98 dose-rate meter are illustrated in Fig. 6.

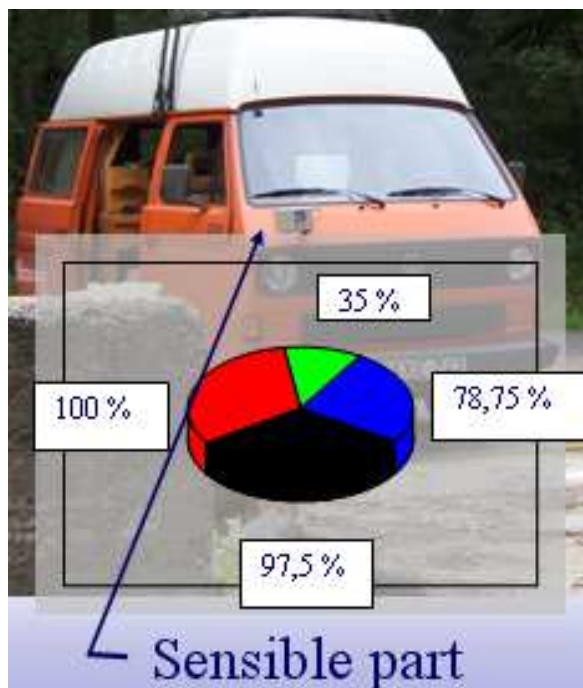


FIG. 6. The shielding effect of the mobile laboratory and the angle dependence of the BNS 98 dose-rate meter.

3.5. The latest on-line route monitoring developments

A new central environment control system has been developed at the Environmental Protection Service (EPS). One of the goals of this development is to simultaneously display the BNS 98 dose-rate meter data and the data provided by the non-mobile stations. This development is made possible by a wireless internet connection between the main server and the mobile laboratory. The main task of the mobile laboratory is to locate and identify radioactive sources in case a radioactive material is lost or an emergency situation occurs. With the help of this new complex environment control system wirelessly connected to the BNS 98 dose-rate meter of the mobile laboratory the route and measured data of the mobile laboratory will be traceable on the main screen of the EPS. A snapshot of the new central environment control system monitor is shown in Fig. 7.

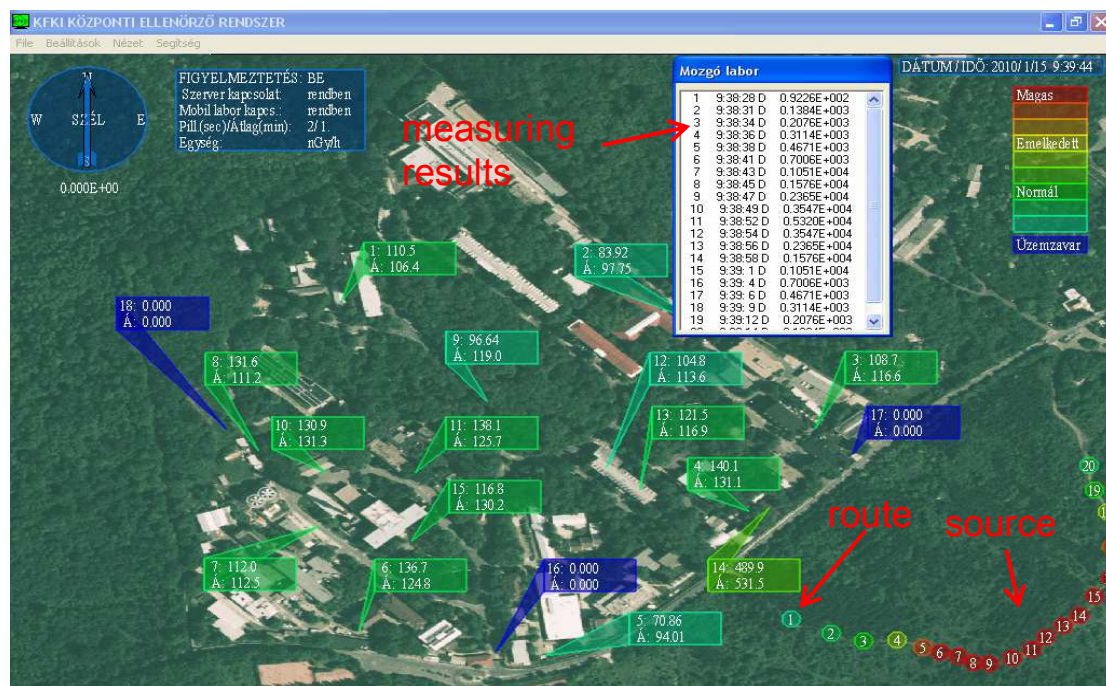


FIG. 7. Snapshot of the new central environment control system monitor (Stations 16 to 18 are not connected). On the figure the route (coloured dots 1 to 20) and the dose-rates measured along this route are demonstrated in the case of a hypothetical radioactive orphan source placed in the location marked on the picture.

3.6. In-situ gamma-ray spectrometry

In-situ gamma-ray spectrometry is a useful equipment item for fast qualitative and quantitative assay of the environmental radiation level. The gamma-ray spectrum can be easily evaluated and the radionuclide concentration can be calculated using a specially developed spreadsheet table that contains the conversion factors and the fallout radioactive contamination depth distributions in the soil.

The in-situ gamma-ray spectrometry system contains the following instruments:

- Inspector (analysing instrument);
- Canberra 2020 GeLi detector;
- $V_{\text{active}} = 93 \text{ cm}^3$;
- Relative efficiency: 22,2% (1,333 keV);
- Resolution: 1,89 keV;
- Software: GENIE 2000;
- Liquid N_2 as refrigerant.

The in-situ gamma-ray spectrometry system is shown in Fig. 8. The spreadsheet used for the calculation of the radionuclide concentration is given in Fig. 9.



FIG. 8. In-situ gamma-ray spectrometer.

Izotóp	Konc.	Hiba	Dózistelj.	Hiba	Eloszlás	Energia	Beütés	Hiba	Konv. fakt.	Konc.	Hiba	Dóziskonc.	Dózistelj.	Hiba
	Bq/kg	Bq/kg	nóyh	nóyh		keV	%	cps/Bq/kg	Bq/kg	Bq/kg	nóyh/Bq/kg	nóyh	nóyh	
K-40	729,88	13,87	31,39	0,60	Egyenletet	1460,8	2780	1,9	0,00212	729,889	13,868	0,043	31,385	0,596
U-Ra sor	40,72	0,59	18,08	0,43	Egyenletet	295,2	588	11,3	0,00878	37,193	4,203			
						352,0	1100	6,8	0,01560	39,427	2,681			
						1120,3	266	10,5	0,00338	43,747	4,893			
						1764,6	215	2,7	0,00291	41,004	1,107			
									Átlag	40,716	0,972	0,444	18,078	0,431
Th sor	29,16	1,27	19,12	0,83	Egyenletet	583,1	512	7	0,00973	29,240	2,047			
						911,1	422	8	0,00719	32,607	2,609			
						964,969	263	7,6	0,00541	27,008	2,053			
									Átlag	29,184	1,267	0,655	19,115	0,830
Felületi konc.	Hiba	Dózistelj.	Hiba	Eloszlás	Energia	Beütés	Hiba	Konv. fakt.	Konc.	Hiba	Dóziskonc.	Dózistelj.	Hiba	
	Bq/cm ²	Bq/cm ²	nóyh	nóyh		keV	%	cps/Bq/cm ²	Bq/cm ²	Bq/cm ²	nóyh/Bq/cm ²	nóyh	nóyh	
Ag-110m	0,000	0,000	0,00	0,00	Modeexp3	657,8		2,539	0,000	0,000	117	0,00	0,00	
Ce-144	0,000	0,000	0,00	0,00	Modeexp3	133,5		0,439	0,000	0,000	0,599	0,00	0,00	
Co-60	0,000	0,000	0,00	0,00	Modeexp3	1173,2		2,221	0,000	0,000	101	0,00	0,00	
Cs-134	0,000	0,000	0,00	0,00	Modeexp3	804,7		2,795	0,000	0,000	68,1	0,00	0,00	
Cs-137	0,036	0,008	0,89	0,21	Modeexp3	661,7	145	24	2,280	0,036	0,008	25,1	0,88	0,21
Mn-54	0,000	0,000	0,00	0,00	Modeexp3	834,8		2,480	0,000	0,000	36,5	0,00	0,00	
Ru-106	0,306	0,032	2,67	0,28	Modeexp3	511,9	339	10,6	0,617	0,306	0,032	8,76	2,67	0,28
Sb-125	0,000	0,000	0,00	0,00	Modeexp3	427,9		0,956	0,000	0,000	18,6	0,00	0,00	
Cs-137	0,036	0,008	0,89	0,21	Modeexp3	661,7		2,280	0,036	0,008	25,1	0,88	0,21	
Természeti dózistelj. mGy/h												68,58		
Mesterséges dózistelj. mGy/h												3,58		
Teljes dózistelj. mGy/h												72,14		

FIG. 9. Spreadsheet for activity calculation.

The fundamental quantities used for in-situ gamma-ray spectrometry include the full absorption peak count rate (N), the fluence rate (Φ), and the source activity (A). In practice, one would like a single factor to convert from the measured peak count rate in a spectrum to the source activity level in the soil or the dose-rate in air.

This factor can be calculated as follows from three separately determined terms:

$$N/A = (N/N_0) \times (N_0/\Phi) \times (\Phi/A) \quad (3)$$

where:

N/A is the full absorption peak count rate at a specific energy;

N_0/Φ is the full absorption peak count rate per unit fluence for a plane parallel beam of photons at a specific energy;

N/N_0 is the correction factor for the detector response at a specific energy;

Φ/A is the fluence rate at a specific energy.

The measurement time is usually 2,000 s.

The evaluation is fast using the GENIE 2000 software.

The software shows the following parameters:

- Nuclide name;
- Energy;
- Activity concentration;
- Dose-rate;
- Measurement failure.

The activity concentrations, activity concentration failures, dose-rates and dose-rate failures are calculated from the peak area and the measurement failure data using a specially developed spreadsheet table.

3.6.1. Efficiency determination of the in-situ gamma-ray spectrometer

The efficiency determination of the in-situ gamma-ray spectrometer was carried out using a ^{131}I radioactive source at different distances, as illustrated in Fig. 10.

The dose-rate was calculated using the following equation:

$$D = \text{DCF}_{^{137}\text{Cs}} \times A / r^2 \quad (4)$$

where:

D is the dose-rate;

DCF is the dose conversion factor;

A is the activity;

r is the distance.

The decreasing dose-rates are the same in percentage as the measured peak areas. The decreasing dose-rate has r^{-2} characteristics, as shown in Fig. 11.

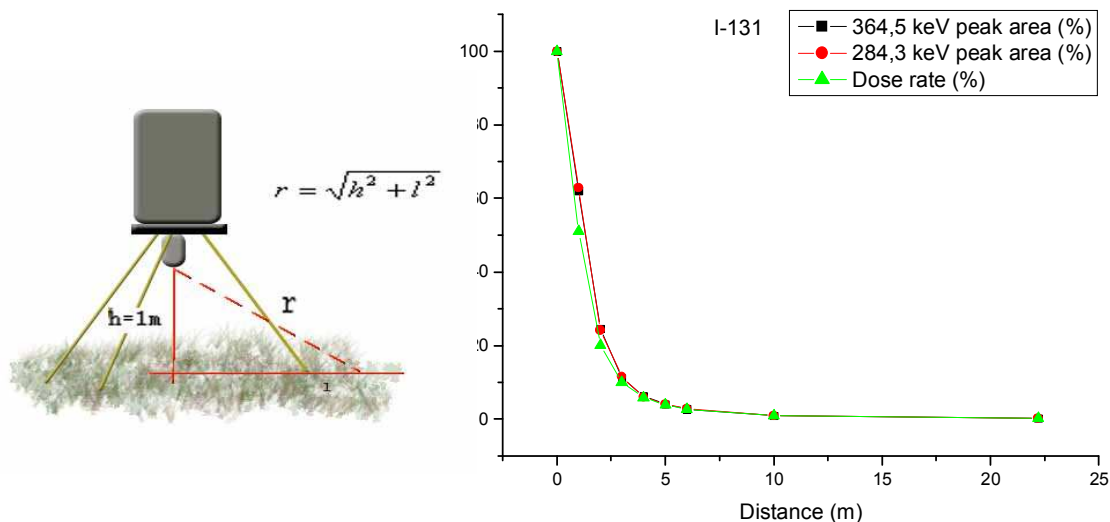


FIG. 10. Efficiency determination methodology.

FIG. 11. Dose-rate as a function of distance.

3.6.2. Semiconductor versus scintillation detector, smuggling trends

The smugglers can mix (put together) illegal radioactive materials to the legal radioactive carriages. If the plutonium is mixed with ^{133}Ba or ^{131}I , the scintillation detectors are not able to detect the low yield gamma lines of the plutonium [2], as shown in Fig. 13. On the contrary, the modern portable semiconductor gamma-ray spectrometers can detect the plutonium, as also shown in Fig. 12.

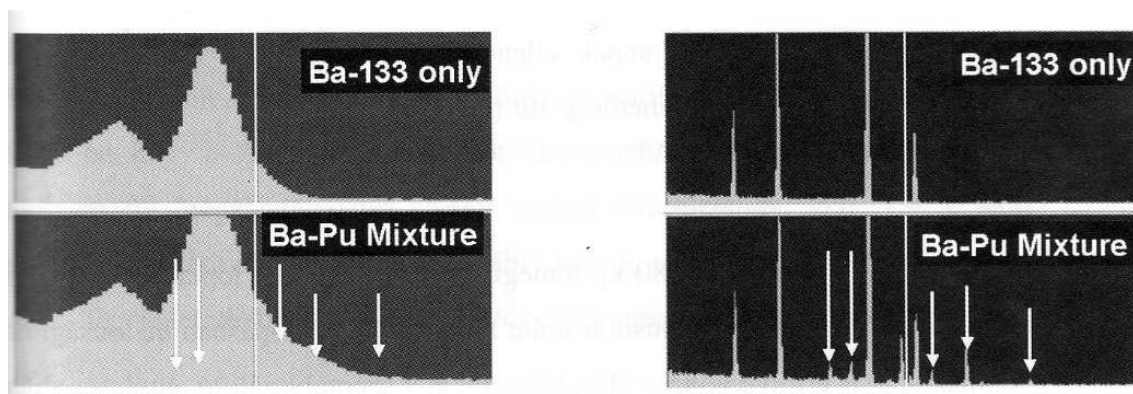


FIG. 12. Scintillation detector ^{133}Ba and Ba-Pu mix spectrum;
Semiconductor detector ^{133}Ba and Ba-Pu mix spectrum.

3.7. Sampling

The environmental samples can be assayed using in-situ gamma-ray spectrometry. The gamma-ray spectrometry system (HPGe) has lead shielding, as shown in Fig. 13. For the laminated soil sampling, special tools and instruments are used as shown in Fig. 14. The samples are collected according to the SIRA recommendations.

3.7.1. Atmospheric radioactive concentration measurements

The mobile laboratory is equipped with an air sampling system, which allows the continuous air sampling in a contaminated area. The air samples are taken from the external air space using a combined filter, as shown in Fig. 15. The filter can separate the organic and the aerosol-bound radioactive iodine. After the sampling, the aerosol filter is measured using gamma-ray spectrometry in a lead shielded area.



FIG 13. Lead shielding. FIG. 14. Soil sampling kit.

FIG. 15. Air sampling system.

3.8. Personal dosimetry

The staff members of the mobile laboratory are using thermoluminescent dosimeters (TLD) for personal dosimetry purpose. The used TLD dosimeters are shown in Fig. 16. After the measurement period, the TLD dosimeters are read using a TLD reader, and results are evaluated. The whole body counter of the Environmental Protection Service is used for detecting any incorporation of radioactive material. The used whole body counter is shown in Fig. 17. The in-situ personal radioactive loading can be detected with the PorTL system that was developed at the Atomic Energy Research Institute.

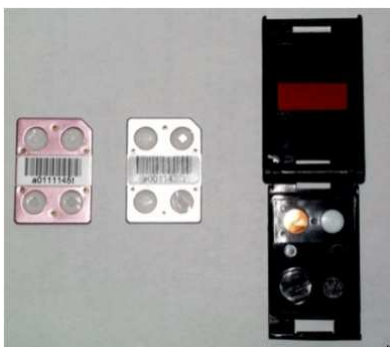


FIG 16. TLD-100 and TLD 7776 cards.



FIG. 17. Whole body counter of the EPS.

3.9. In-situ radioactive Iodine measurements in the human thyroid gland

The radioactive Iodine can be released into the atmosphere from the Budapest Research Reactor and from the Institute of Isotopes Co., Ltd. The human body accumulates the radioactive Iodine into the thyroid gland, as shown in Fig. 18. To take samples from the nose is the first step to determinate the Iodine incorporation, the Iodine incorporation can be detected with the Iodine measurement system, which is unique in Hungary. This system is shown in Fig. 19. With stable Iodine feeding – after Iodine contamination – the accumulation to the thyroid gland and the dose can be reduced as illustrated in Fig. 20 [3].

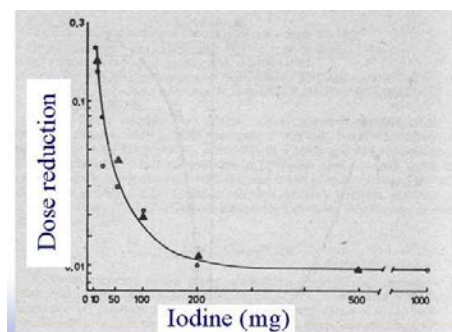
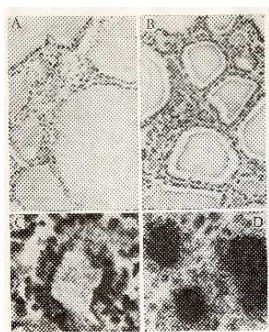


FIG. 18. Iodine capitation. FIG. 19. In-situ radioactive Iodine measurements. FIG. 20. Iodine profilaxis.

3.10. Determination of NORM contamination in the environment from the Hungarian Coal Power Plants

The NORM (Naturally Occurring Radioactive Material) can be produced by coal-powered plants. The coal that burns in the power plant naturally contains radioactive material. The amount of the radioactive material can be higher for mined coal surrounded with Uranium, Thorium and its daughter elements. The coal burns in the stokehold, the radioactive material and the ash are concentrated by filtering the stack gas. The filtered out radioactive material is placed into the slurry near the coal power plants. The radioactivity level of the slurry can be much higher than naturally present in the surrounding places.

Measurements were taken near the Hungarian coal power plants, as shown in Fig. 21 [1]. Samples were collected from the slurry and the soil was measured with the nanoSPEC instrument and the in-situ gamma-ray spectrometer. The dose-rate level was generally three times higher than the average, the maximum value was 510 nSv/h. The outmost activity concentration levels were measured near the coal power plant of Pécs, as shown in Table 1. The coal that burns in the coal power plant of Pécs was mined in the Mecsek mountains. The coal contains Uranium and its daughter elements, because Uranium mines were situated near the coal mining areas.



FIG. 21. In-situ measurement and soil sampling positions near the coal power plants.

TABLE 1. IN-SITU MEASUREMENT RESULTS NEAR THE COAL POWER PLANTS

	^{40}K (Bq/kg)	U-Ra-chain (Bq/kg)	Th-chain (Bq/kg)	^{106}Ru (Bq/cm ²)
Mátfa	439.73	16.77	0.92	0.258
Pécs	729.89	40.72	29.18	0.305
Lőrinc	328.19	26.58	17.81	0.257

REFERENCES

- [1] ELEMÉR, V., GYÖRGY, P., in Atomtechnology and Environmental Protection, Budapest (1986).
- [2] JÁNOS, S., in Cases, radiation accidents, Veszprém (2008).
- [3] BÉL, A K., in Radioecology and environmental radiation protection, Veszprém (2004).

EXPERIENCE AT THE ISTITUTO SUPERIORE DI SANITÀ ON ENVIRONMENTAL RESEARCH AND MONITORING WITH IN-SITU TECHNIQUES

C. NUCCETELLI, D.M. CASTELLUCCIO, E. CISBANI, S. FRULLANI

Department of Technology and Health, Istituto Superiore di Sanità, Viale Regina Elena 299 00161
Roma, Italy

Email: cristina.nuccetelli@iss.it

Abstract

Since the 80's the former Physics Laboratory of the Istituto Superiore di Sanità has been using gamma-ray spectrometry to perform research activity, particularly in in-situ conditions on natural radioactivity (^{238}U and ^{232}Th series and ^{40}K in soil and water, disequilibrium in the radioactive chains, etc) and radiological emergencies involving large areas (uncontrolled nuclear satellites re-entering in the atmosphere, Chernobyl accident). Afterwards, this technique was used to study the contribution of natural radionuclides in building materials to the indoor radon, thoron and gamma dose-rate. Moreover, a method to estimate the radionuclide activity concentration in building materials and a procedure to evaluate gamma dose-rate indoors from outdoor measurements were developed. At the same time, in collaboration with the Italian Fire Brigades, Civil Protection and Environment Ministry and groups from Universities and Research Institutes, the 'SNIFFER' aerial platform for radiological emergencies has been designed and developed. The platform is equipped with a peculiar air sampling unit and gamma detectors able to permit a quantitative characterization of the atmospheric and ground radioactive contaminations.

1. INTRODUCTION

The Istituto Superiore di Sanità (Italian National Institute of Health), research and advisor body of the National Health Service, has been involved in the study of environmental radioactivity as an important source of population exposure.

There were two main lines:

1) In-situ gamma-ray spectrometry is a powerful tool to provide rapid and spatially representative estimates of environmental radioactivity. For this reason since the 80's the Radioactivity and Health Effect unit of the Istituto Superiore di Sanità has been using this technique to perform research activity, particularly on natural radioactivity (^{238}U and ^{232}Th series and ^{40}K in soil and water, disequilibrium in the radioactive chains, etc) and radionuclide distribution of Chernobyl fallout in soil. In the 90's this experience was transferred to many other Italian laboratories by publication of protocols and organization of theoretical and experimental courses. Afterwards, the research activity on the use of in-situ gamma-ray spectrometry was devoted to the study of the contribution of natural radionuclides in building materials to the indoor gamma dose-rate and a method to estimate the radionuclide activity concentration in building materials of natural and industrial (NORM) origin was developed. Also in this frame, expertise on addressing problems arising from in-situ analysis of natural materials and NORM has been improved.

2) After several years of research and development, the Istituto Superiore di Sanità (the National Institute of Health in Italy) in collaboration with the Ministry of Environment has implemented and is now commissioning the 'SNIFFER' system, a multi-purpose air sampling platform based on fixed wing aircraft. The 'SNIFFER' consists of two air sampling lines: one is dedicated to the identification and measurement, in isokinetic condition, of the atmospheric aerosol radioactive contamination and the other one to the quantitative monitoring of organic compounds and aromatic hydrocarbons. The sampled data are combined with environmental (temperature, pressure, air density and speed) and geo-location information for a full characterization of the sampling conditions and their temporal and geographical location. Radiological surveillance, quantitative assessment (since the early phase of a radiological emergency) and air quality monitoring on large areas represent the main target applications of the 'SNIFFER'. The system is described from its motivations to the main design issues and some details of its implementation.

2. IN-SITU GAMMA-RAY SPECTROMETRY INDOORS

In-situ gamma-ray spectrometry is a well-known and widely utilized tool to determine the outdoor gamma dose-rate from the soil and to calculate the natural and artificial radionuclide concentration and their contribution to the dose-rate [1]. Early investigations regarding the indoor application of this technique started in the 80's [2, 3] and other methods and developments appeared in the 90's. At present, with different approaches called "integrated" [7] – elaboration of spectra [4-6], computation plus room model – the use of in-situ gamma-ray spectrometry indoors allows the evaluation of the gamma dose and the relative contribution of the various nuclides to the total gamma dose-rates. In some countries an indoor methodology was also applied to perform surveys in order to get information on population exposure from building materials. Indoor applications of in-situ gamma-ray spectrometry can also provide interesting information about building materials as sources of radon, thoron and gamma rays [7] and supply quantitative estimates about the activity concentrations of radionuclides in building materials. Finally, on the basis of average spectrometry information on building materials, a methodology was developed to estimate the indoor gamma dose-rate from measurements on the external wall of a building. This method, called "IN-OUT", is in validation phase after very encouraging preliminary results.

2.1. An integrated method to characterize building materials in-situ

The rough application of in-situ gamma-ray spectrometry in indoor environments cannot supply quantitative information about activity concentration of radionuclides in building materials [2, 3]. Indeed, only estimation of the dose-rate contribution to the gamma dose-rate indoors from U chain, Th chain and ^{40}K is possible. However this technique can provide interesting information about building materials as a radon source. In fact, a method based on analyses of gamma-ray spectra data has been developed by the authors to provide, in the field, quantitative estimation of activity concentration ratios of ^{238}U and ^{232}Th . Moreover, disequilibrium in ^{226}Ra sub-chain due to ^{222}Rn exhalation was evaluated [4-6]. The method was applied to data of gamma-ray spectrometry measurements carried out with HPGe detector (26%) in seven dwellings and one office in Rome. The first results of the data analysis showed that, as regards to especially the ^{226}Ra sub-chain disequilibrium, different building materials (tuff, concrete, etc) can have very different characteristics, as shown in Table 1.

TABLE 1. FIRST RESULTS OF THE APPLICATION OF THE ‘INTEGRATED METHOD’

dwelling	building material	Dose-rate HPGe nGy/h	Dose-rate RS* nGy/h	% dose-rate contribution			activity concentration ratio $^{226}\text{Ra}/^{228}\text{Ac}$	activity concentration ratio $^{226}\text{Ra}/^{214}\text{Pb}$
				U	Th	K		
A	tuff	401 ± 12	398 ± 13	22.8	62.0	15.2	0.67 ± 0.08	1.31 ± 0.15
B	tuff	237 ± 10	258 ± 11	25.2	57.4	17.4	0.76 ± 0.08	1.28 ± 0.14
C	tuff	355 ± 10	340 ± 12	24.0	62.0	14.0	0.66 ± 0.07	1.23 ± 0.15
D	tuff	335 ± 12	323 ± 12	23.3	64.5	12.2	0.65 ± 0.10	1.31 ± 0.17
E (office)	tuff	288 ± 11	294 ± 12	25.3	58.4	16.4	0.78 ± 0.08	1.31 ± 0.14
F	concrete	161 ± 10	155 ± 10	25.4	52.6	21.8	0.62 ± 0.10	1.00 ± 0.13
G	concrete	278 ± 11	253 ± 11	25.7	57.6	16.7	0.65 ± 0.08	1.07 ± 0.12
H	concrete	300 ± 12	271 ± 11	24.5	60.0	15.5	0.62 ± 0.07	1.06 ± 0.12

If, in addition to the spectrometric data, other indoor environment parameters (indoor gamma dose-rates, room dimensions, wall thickness, etc) are utilized in a room model, an in-situ evaluation of ^{226}Ra , ^{228}Ac and ^{40}K activity concentration and an indication of the exhalation features, by means of estimation of exhaled ^{222}Rn activity concentration, can be achieved.

The method, described in detail elsewhere [6, 7], was tested in two test rooms of which we had a sample of the material they were built with, i.e. tuff. The results obtained are shown in Table 2. The agreement between the activity concentration estimates obtained with the ‘integrated method’ and the laboratory gamma-ray spectrometry system was very good.

TABLE 2. ACTIVITY CONCENTRATIONS OF ^{232}Th , ^{226}Ra , AND ^{40}K IN THE WALLS OF THE TWO TEST ROOMS, ESTIMATED WITH TWO DIFFERENT METHODS

Method of evaluation	Test room 1			Test room 2		
	$C_{\text{Th-232}}$	$C_{\text{Ra-226}}$	$C_{\text{K-40}}$	$C_{\text{Th-232}}$	$C_{\text{Ra-226}}$	$C_{\text{K-40}}$
	Bq/kg	Bq/kg	Bq/kg	Bq/kg	Bq/kg	Bq/kg
integrated method	190	110	890	350	260	2040
Gamma-ray spectrometry on sample*	187 ± 4	109 ± 2	956 ± 13	339 ± 8	254 ± 14	2166 ± 35

*Concentration with total uncertainty (1 σ).

Encouraged by these results, the method was applied to other dwellings [7]. With in-situ gamma-ray spectrometry the ratio between radon decay products (RnDp) and ^{226}Ra , i.e. the emanation fraction in the building materials, and the relevant exhalation rate E , could be estimated as well. From these parameters it was also possible to calculate the contribution of building material to the estimated ^{222}Rn activity concentration C_{Rn} [8].

Table 3 shows the results obtained in eight dwellings in Rome. It is worth noting that only in dwelling n°4, built with tuff and on the ground floor, the contribution of Rn from the soil appears to be significant and computable by the difference between the estimated values, obtained by accounting for only the building material contribution CRn estimated, and the total CRn measured value.

TABLE 3. ESTIMATES OF EMANATION, EXHALATION RATE AND BUILDING MATERIAL CONTRIBUTION TO INDOOR RADON IN SEVEN DWELLINGS AND ONE OFFICE IN ROME

dwelling	level	building material	RnDp	E (Bq/m ² h)	C _{Rn} exhaled (Bq/m ³)	C _{Rn} measured (Bq/m ³)
1	5 th	tuff	0.31	179	116	124
2	5 th	tuff	0.26	196	89	135
3	5 th	tuff	0.25	217	104	140
4	ground	tuff	0.29	254	161	338
office	1 st	tuff	0.29	301	158	130
5	4 th	concrete	0.05	3	2	40
6	3 rd	concrete	0.15	33	15	58
7	4 th	concrete	0.18	30	21	86

2.2. ‘IN– OUT’ method

When it is impossible to enter a dwelling to measure the indoor gamma dose-rate, as it can happen in epidemiological studies and surveys on randomly selected dwellings, if inhabitants refuse the measurement, or the dwellings are not currently occupied, it would be very useful to obtain an accurate and precise estimate of indoor gamma dose-rate. The so-called ‘IN-OUT’ method was set up to estimate the indoor gamma dose-rate attributable to building materials [9]. With this method the indoor gamma dose-rate is estimated from the gamma dose-rate measurements performed on an external wall [9, 10]. The method consists of the evaluation of ²²⁶Ra, ²²²Rn, ²²⁸Ac and ⁴⁰K activity concentrations of the building materials, with an ad-hoc algorithm, using the external wall measurements and data from in-situ gamma-ray spectrometry, from which radiation field characteristics are derived. Since spectrometry parameters are fairly constant for the same kind of building material and same kind of buildings, in this case masonry [4, 5, 11, 12], spectrometry data we already had for some dwellings in Rome were used. With the radionuclide content data, it was possible to estimate the indoor gamma dose-rate by applying a room model [13], which needs information on the geometry and structure of the dwelling. After a feasibility study performed on few dwellings [11], a systematic collection of experimental data to validate the ‘IN-OUT’ method was carried out within the framework of the ‘SETIL’ project, the Italian epidemiological study on the etiology of childhood leukemia, lymphoma and neuroblastoma. Indeed, the data consisting of actual indoor dose-rate measurements and detailed dwelling information, contained in questionnaires collected during the indoor measurements, were used, and personnel involved in the survey was requested to measure the gamma dose-rate at contact with the external wall of the building. Table 4 shows the results obtained in the first 91 dwellings enrolled in the ‘SETIL’ survey in two District, Latium and Campania [9]. The crude ratio of the outdoor and indoor measured value is reported in comparison with the ratio of the ‘IN-OUT’ model estimate and indoor measured value.

The table shows that, on average, the outdoor measured value is an accurate estimate of the indoor value, but with a low precision, as given by the coefficient of variation (COV), which is 30% for the complete set. In comparison, the ‘IN-OUT’ method represents a great improvement in the precision: the overall COV decreases to 11%.

TABLE 4. SUMMARY OF PRELIMINARY RESULTS OF THE ‘IN-OUT’ METHOD

District	Building material	No. of dwellings	Measured gamma dose-rate (nGy/h)				Outdoor value Indoor value		‘IN-OUT’ estimate Indoor value	
			Indoor		Outdoor		AM	COV	AM	COV
			AM	SD	AM	SD				
Latium	Tuff/stone	26	227	60	254	91	1.12	30%	0.99	8%
	Concrete/bricks	22	133	52	138	50	1.11	40%	1.07	13%
	All	48	186	72	201	94	1.12	34%	1.03	12%
Campania	Tuff/stone	19	188	24	193	28	1.04	17%	1.02	10%
	Concrete/bricks	24	143	37	145	37	1.04	25%	1.04	10%
	All	43	163	39	166	41	1.04	22%	1.03	10%
Total	Tuff/stone	45	210	52	228	77	1.09	26%	1.00	9%
	Concrete/bricks	46	138	44	142	43	1.07	33%	1.05	12%
	All	91	176	49	184	76	1.08	30%	1.03	11%

AM = Arithmetic Mean, SD = Standard Deviation, COV = Coefficient of Variation = SD/AM

Afterwards, to improve the method and validate its robustness, the number of sampled dwellings was extended and another District, Piedmont, was involved. At the moment, the final elaboration of data, concerning a total of 212 dwellings distributed in Latium, Campania and Piedmont, is in progress with a new version of the ‘IN-OUT’ method. This new release is much more independent from details of dwellings than the previous ones. An exhaustive description of this last approach can be found in other publications [14, 15]. In Table 5 a summary of results can be found. The power of the ‘IN-OUT’ method to make accurate and precise estimates stems from the ratios between estimated and measured values of gamma dose-rate. Therefore, this method can be very useful in epidemiological studies or surveys, when it is impossible to perform direct measurements, and it is critical to obtain an estimate of the indoor gamma dose-rate with adequate accuracy and precision

TABLE 5. SUMMARY OF FINAL RESULTS OF THE ‘IN-OUT’ METHOD

Building material	No. of dwellings	Measured gamma dose-rate (nGy/h)				Outdoor value Indoor value		‘IN-OUT’ estimate Indoor value	
		Indoor		Outdoor		AM	COV	AM	COV
		AM	SD	AM	SD				
Tuff/stone	67	204	49	220	80	1.08	28%	1.0	17%
Concrete/bricks	145	113	52	122	72	0.85	37%	0.99	21%
All	212	142	66	151	87	0.92	36%	1.00	20%

3. AERIAL PLATFORM FOR OUTDOOR RADIATION MONITORING

In the late 70's, the Cosmos 954 spy satellite with nuclear reactor disintegrated in the atmosphere during an uncontrolled re-entering in the atmosphere; the nuclear fuel (30.8 kg of ^{235}U) scattered on an area of 120,000 km² of the north-west territories of Canada. This was the most famous and potentially dangerous accident of the 8 (known) uncontrolled nuclear-powered spy satellites re-entered into the earth atmosphere from the 70's to the 90's. It demonstrated unequivocally the need of a system for radioactivity monitoring and surveillance on large areas. In fact, in the early 80's the Cosmos 1402 satellite with nuclear reactor likely fell down in the Atlantic Ocean, 20 minutes before its orbit passes over most of Italy and the central Europe-East Europe. Triggered by these events, in 1983, the former Physics Laboratory of the Italian National Institute of Health in collaboration with the Laboratory of Atomic Defence of Centre of Studies and Experiences of the Italian Fire Brigades began a research and development program on the feasibility of a system for the monitoring of radioactivity by sensors on an aerial platform. The main goal of the program was the definition of the optimal instrumentation for the measurement of (beta and gamma) radioactivity to face large (spatial) scale emergency events in short time in order to provide useful information to the authorities that manage the emergency.

The program considered 3 specific emergencies:

1. Search and localization of radioactive sources scattered on large areas (e.g. for mine prospect);
2. Measurement of contamination on extended territories, on ground (e.g. nuclear power plant contamination);
3. Sampling and characterization of radioactive clouds (e.g. radioactive fallout at high altitude from nuclear explosions).

The aerial platform represents the unavoidable choice that can fulfil all the above points. The first proposed solution was a matrix of NaI(Tl) scintillators, which offer high gamma efficiency, good signal-to-noise ratio and moderately low energy resolution. A first prototype of the proposed system: a single large NaI(Tl) crystal (40×10×10 cm³) was installed on an anti-vibration platform hosted by an Agusta-Bell 412 helicopter. The control and acquisition system was quite sizeable (about 60×60×120 cm³) at that time able to store up to 38 ADC spectra of 4,000 bits each. The system was characterized and tuned by dedicated campaigns [16]; sensitivity was studied in terms of altitude, aircraft speed, integration time and size of the detector.

The sensitivity S , as minimum detectable ground radioactivity, was found related to the altitude h (for fixed source) by:

$$S \approx \exp(0.0475 h + 8.64) \quad (1)$$

with S the sensitivity in Bq/m² and h the altitude in meter.

It is worth noting that the above expression is valid in the hypothesis that the radioactivity in the atmosphere is negligible or well-known. In the general case, the radioactivity measured on board of the aircraft is the weighted sum of 3 contributions at least: ground, atmosphere and craft fuselage radioactivity (where the contamination dissolved in air is accumulated), and therefore a quantitative estimation of the ground contamination may require the measurement of the atmospheric one (and the residual contamination accumulated on the aircraft fuselage).

Such quantitative estimation needs a proper sampling of the atmosphere particulates and in particular the flux of the sampled air must be known. This is achievable in the so-called 'isokinetic condition' that is keeping the speed of the air entering the sampler (vector) equal to that of the air in the atmosphere right before the inlet orifice such that the sampling efficiency is close to 1. This condition cannot be easily achievable on aircraft with moveable wings such as helicopters, which on the other hand is the most flexible aircraft platform for search of radioactive sources.

3.1. Chernobyl Accident

In April 1986 while the above program was going on, the worst accident of the nuclear civil history occurred in the nuclear power plant of Chernobyl. The radioactive gases and powders released by the reactor number 4 scattered all around the European continent as shown in Fig. 1.

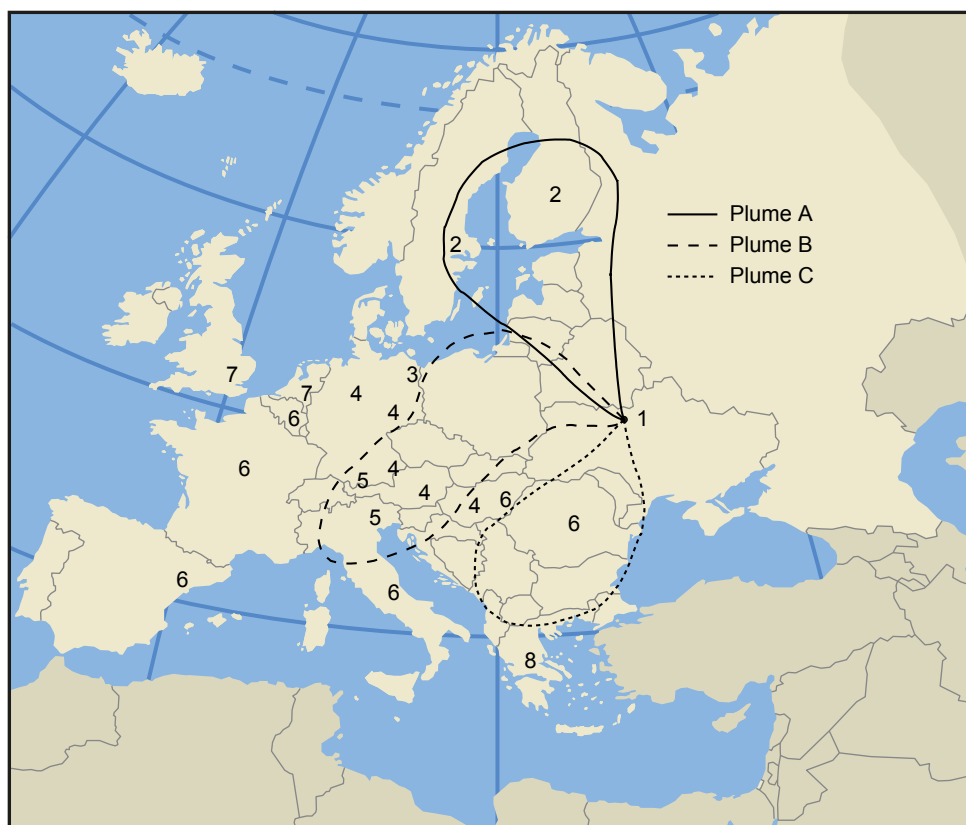


FIG. 1. Development of the radioactive clouds from the Chernobyl plant. Numbers represent the first day of observation of radioactivity excess in the atmosphere (1=April 26, 2=April 27 and so on up to 8=May 3); the three lines identify the radioactive plume development (Plume A= April 26, Plume B= April 27-28, Plume C = April 29.30)

The helicopter-based NaI(Tl) system was used for a series of mission in the centre and south of Italy: the helicopter flew at a 100 m altitude with a 110 km/h speed and integrated gamma-ray spectra every 4 km. These measurements, whose summary is shown in Fig. 2, provided semi-quantitative information on the ground and atmospheric contamination, and demonstrated the conclusion reported in the previous section: the presence of atmospheric contamination prevented the validity of the expression reported previously and in addition the contamination accumulated on the aircraft fuselage compromised the extraction of the ground contamination.

Moreover, the energy resolution of the NaI(Tl) was not enough for a quantitative identification of all radioisotopes. Ultimately, a significant measurement of the ground contamination was achieved only after 1 month since the accident, when the atmospheric radioactivity was negligible.

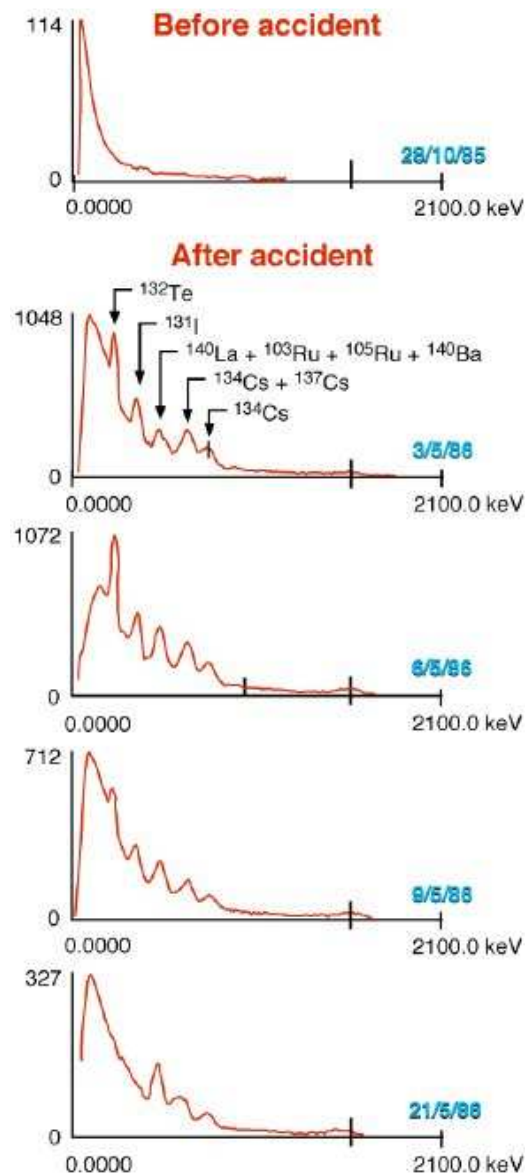


FIG. 2. Gamma-ray spectra of the NaI(Tl) before and right after the Chernobyl accident, acquired on the Augusta/Bell helicopter described in the text; data from reference [16].

3.2. The ‘SNIFFER’ Project

From the above limitations, in 1989 the Civil Protection Department funded a project devoted to the feasibility study of an aerial sampling line for particulates able to characterize the gamma-ray emitting radionuclides composition by means of a HPGe detector. The project ended up with a multi-functional system on aerial platform, named ‘SNIFFER’, designed for quantitative sampling of particulates in a radioactive cloud (in both configurations near- and far-field) obtained in the isokinetic condition.

The payload was originally designed for the Alenia Partenavia Observer P68 [17], then adapted to the more compact and flexible Sky Arrow 650 by Iniziative Industriali Italiane with the addition of an independent sampling line (funded by the Italian Ministry of Environment) for the monitoring of air pollution by Volatile Organic Compounds (VOC) and Polycyclic Aromatic Hydrocarbons (PAH) induced by the ground transportation at low altitude [18]. Thus, the original system became an integrated unit for radiological and air pollution surveillance on extended areas.

The Sky Arrow fixed wing aircraft is able to take off and land on small distance; it can operate on a large range of altitudes from few tens of meters to few kilometers at speed ranging from 60 to 90 nodes (constrained by the Italian Aviation Authority – ENAC). In this respect, the Sky Arrow resembles the flexibility of a helicopter, with the unavoidable limitation imposed by a fixed wing craft.

The ‘SNIFFER’ payload is made of the following subsystems:

1. The isokinetic sampling line, which integrates the compact radiation detectors: a small BGO crystal for beta- and gamma-rays, a small Geiger counter and a high-energy resolution HPGe gamma-ray spectrometer;
2. The NaI(Tl) crystal and attached photon detector inside the aircraft (similar to the helicopter system described above);
3. Environmental sensors for in/out temperatures, pressures, air flow, sitting along the sampling line, inside and outside the aircraft; a GPS receiver completes the sensor for precise geo-location;
4. A second, independent sampling line for the ground transportation pollution monitoring, as mentioned above;
5. A dedicated, low consumption, control and acquisition systems.

Those subsystems are shown in Fig. 3.

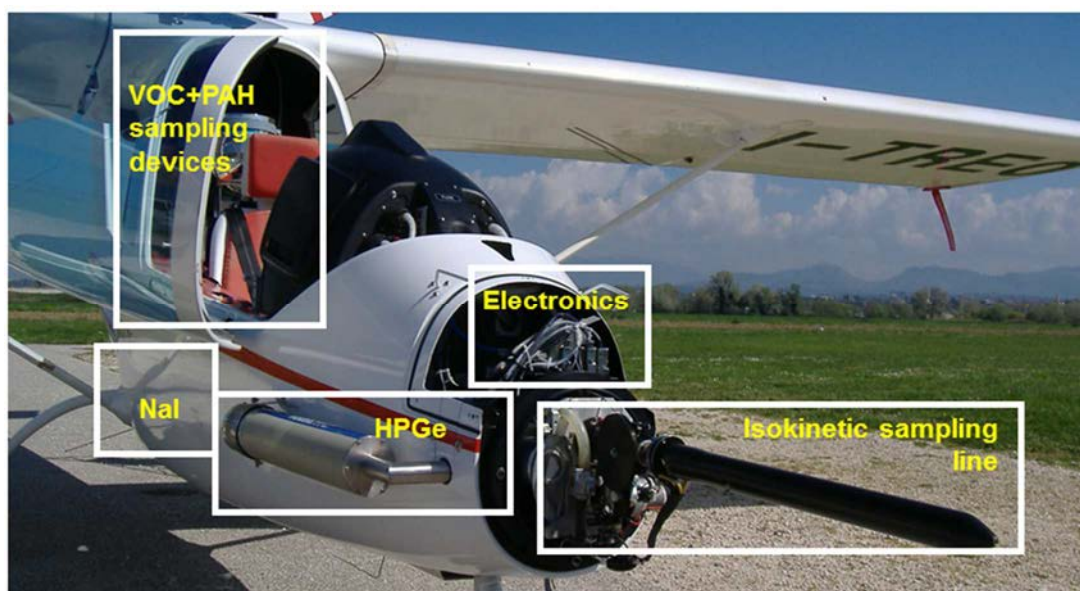


FIG. 3. The 'SNIFFER' aerial platform with the main subsystems.

The sampling line probably represents the most original part of the system; hosted on the front part of the fuselage (which has been properly adapted for that purpose), the isokinetic sampling line, schematically presented in Fig. 4, consists of a 450 mm long nose of 15 mm diameter, heated by a resistive coil to avoid condensation. The aerosol flowing along the nose is sampled on one out of the 4 Teflon filters housed on a disk remotely controlled. Beyond the filter there are 2 small detectors of 1 cm diameter each, a chamber in Geiger regime and a BGO crystal coupled to a photodiode. The main purpose of those detectors is the integral information on the presence of beta- and gamma-ray emitter contamination (sort of alarm sensor). The control system automatically reads the environmental sensors along the line and regulates a needle valve after the detectors to keep the isokinetic condition. Eventually the high-energy resolution HPGe detector, facing the last exposed filter, permits the gamma-ray spectrometry of the sampled aerosol in quasi real-time.

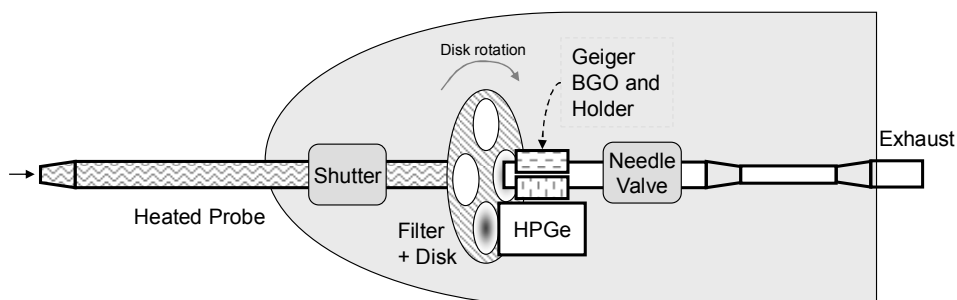


FIG. 4. Schematic view of the 'SNIFFER' sampling line. Temperature, pressure and flow sensors are not shown.

The compact control system, shown in Fig. 5, is based on the PC104 industrial standard, and consists of 2 microprocessor boards which interface the sensors, actuators and the detectors; the acquired data are geo-located by the above mentioned GPS receiver.

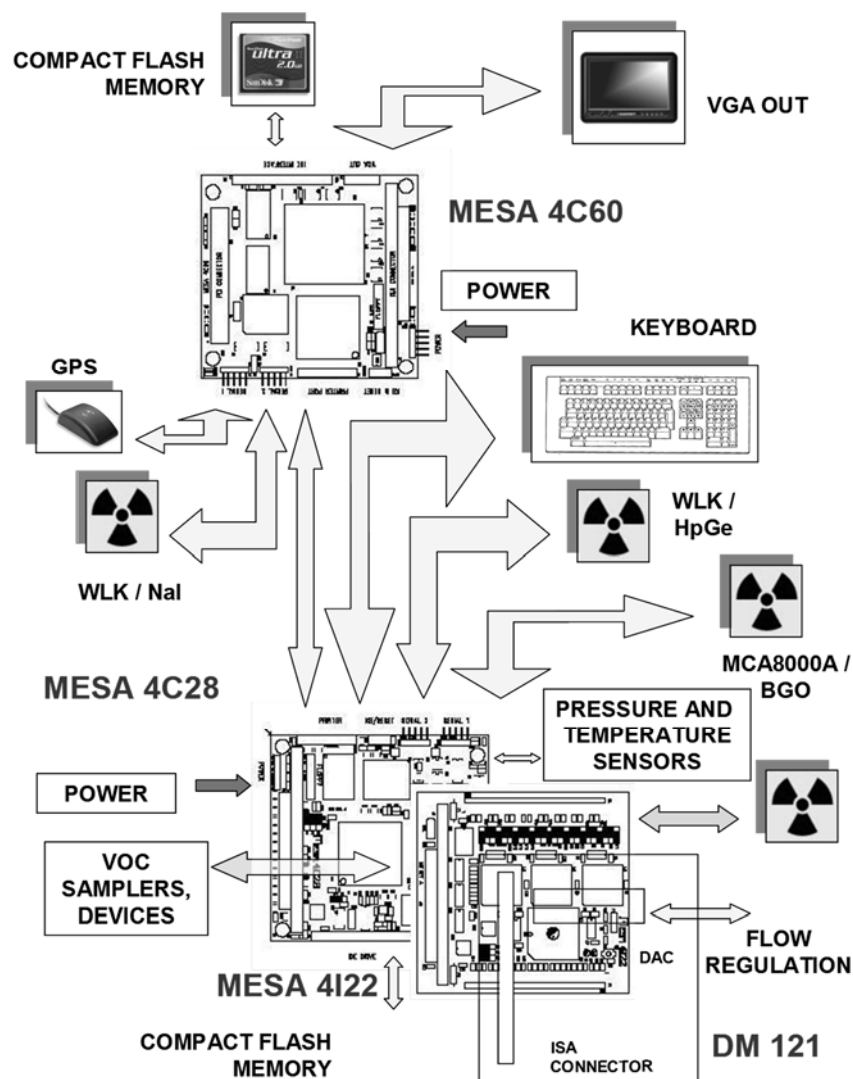


FIG. 5. The 'SNIFFER' control system, schematic view.

The 'SNIFFER' platform has obtained the ENAC certification and thereafter it performed quite a few measurement campaigns in 2007 and early 2008.

3.4. Future Development

The 'SNIFFER' system is ready to become operational; relatively minor improvements may however get the system significantly more valuable, i.e. bi-direction air-ground transmission in order to get the acquired data readily available to the emergency team that manages the situation and permits the real-time re-programming of the mission according to the analysed data; this represents a small improvement and technology is widely available.

The Sky Arrow has proven to operate as an unmanned vehicle. The platform can therefore be adapted to operation without human pilot on board. This would permit the 'SNIFFER' to fly directly into a potentially dangerous radioactive cloud.

REFERENCES

- [1] BECK, H.L., DE CAMPO, J., GOGOLAK, C., In-situ Ge (Li) And NaI(Tl) gamma-ray spectrometry, report HASL-258, U.S. Atomic Energy Commission, New York (1972).
- [2] MILLER, K.M., A spectral stripping method for a Ge spectrometer used for indoor gamma exposure rate measurements, Report EML-419, Environmental Measurement Laboratory, USDOE, New York (1984).
- [3] MILLER, K.M., BECK H.L., Indoor gamma and cosmic ray exposure rate measurements using a Ge spectrometer and pressurised ionisation chamber, *Radiat. Prot. Dosim.* **7** (1984) 185
- [4] BOCHICCHIO, F., CAMPOS VENUTI, G., FELICI, F., GRISANTI, A., GRISANTI, G., KALITA, S., MORONI, G., NUCCETELLI, C., RISICA, S., TANCREDI, F. Characterisation of some parameters affecting the radon exposure of the population *Radiat. Prot. Dosim.* **56** (1994) 137.
- [5] BOCHICCHIO, F., CAMPOS VENUTI, G., NUCCETELLI, C., RISICA, S., TANCREDI, F., Indoor measurements of ^{222}Rn and ^{220}Rn and their decay products in a Mediterranean climate area, *Environ. Int.* **22** 1 (1996) 633.
- [6] NUCCETELLI, C., BOLZAN, C., GRISANTI, G., RISICA, S., Building Materials as a Source of Gamma Radiation and Radon Concentration: Tests and Improvement of Experimental Methods, In: Proceedings of the 10th International Congress of the International Radiation Protection Association, May 14-19 2000 Hiroshima, Japan, P-1b-19 (CD - ROM).
- [7] NUCCETELLI, C., BOLZAN, C., In-situ gamma spectroscopy to characterize building materials as radon and thoron sources, *Sci. Total Environ.* **272** (2001) 355.
- [8] NUCCETELLI, C., BOLZAN, C., RISICA, S., A new method to evaluate the building material contribution to indoor radon concentration. In: Proceedings of Third Eurosymposium on Protection against Radon. Liege 10-11 May 2001, 123-126.
- [9] BOCHICCHIO, F., NUCCETELLI, C., SETIL WORKING GROUP, A method to evaluate the building material contribution to indoor gamma dose rate through outdoor measurements: preliminary results, *Radiat. Prot. Dosim.* **111** (2004) 413.
- [10] NUCCETELLI, C., BOLZAN, C., BOCHICCHIO, F., SETIL WORKING GROUP, A tentative method to evaluate the building material contribution to indoor gamma dose rate, *The Natural Radiation Environment VII*, Elsevier's "Radioactivity in the Environment" Book Series, Vol.7, Elsevier, Amsterdam (2005) 85
- [11] CLOUVAS, A., XANTHOS, S., ANTONOPOULOS-DOMIS, M., Monte Carlo based method for conversion of in-situ gamma-ray spectra obtained with a portable Ge detector to an incident photon flux energy distribution. *Health Phys.* **74** (1998) 216.
- [12] CLOUVAS, A., XANTHOS, S., ANTONOPOULOS-DOMIS, M., Derivation of indoor gamma dose rate from high resolution in-situ gamma-ray spectra. *Health Phys.* **79** (2000.) 274.
- [13] MARKKANEN, M.. Radiation dose assessment for materials with elevated natural radioactivity. Report STUK-STO 32, Finnish Centre for Radiation and Nuclear Safety, Helsinki (1995).

- [14] NUCCETELLI, C., BOCHICCHIO, F., MENGHI, E., SETIL WORKING GROUP, A Computational Study To Evaluate Indoor Gamma Dose-Rate On The Basis Of Outdoor Measurements. In Proc. of the Second European Congress of the International Radiation Protection Association Radiation protection - From knowledge to action. Paris, 2006 CD-ROM.
- [15] NUCCETELLI, C., BOCHICCHIO, F., SETIL WORKING GROUP, Further development of a computational method to evaluate indoor gamma dose-rate from building materials using external wall measurements. In Proc. of the 12th International Congress of the International Radiation Protection Association, Buenos Aires 2008 CD-ROM.
- [16] BERTOCCHI, A., BERTOCCHI, A., CRATERI, R., FRULLANI, S., GADDINI, M., GARIBALDI, F., GIULIANI, F., GRICIA, M. MASELLO, R., MONTELEONE, G., MAZZINI, F., NADDEO, C., SALUSEST, B., SANTAVENERE, F., TACCONI, O., VISCHETTI, M., Remote Sensing Of Fission Products Gamma Rays Radioactive Contamination. In Proceedings of Conference 'Physics In Environmental and Biomedical Research', World Scientific, 1986, p. 361-366.
- [17] CISBANI, E., et al., Aerial Platform for In-Plume Sampling and On-Line Measurements in the emergency early phase. In Proceedings of the International Congress on Radiation Protection (IRPA9), volume 2 (1996) p. 666-671.
- [18] CASTELLUCCIO, D.M., et al., SNIFFER System: A Multipurpose Aerial Platform For Large Area Radiological Surveillance, Emergency Management And Air Pollution Monitoring., In Rapporti Istisan 07/33, 2007.
<http://www.iss.it/publ/?lang=1&id=2128&tipo=5>

EXPERIENCE OF INVESTIGATION OF CONTAMINATED SITES IN LITHUANIA

L. PILKYTĖ

Radiation Protection Centre, Kalvariju 153, 08221 Vilnius, Lithuania

Email: lpilkyte@rsc.lt

Abstract

Cases of investigations of contaminated sites in Lithuania and evaluation of exposure doses are presented. For every case a plan for investigation was created using available information. Sampling and measurement methods were chosen, scenarios for calculations of exposure doses were created. After dose-rate screening a spot of contaminated soil was detected in one of the former Soviet military bases. Due to military human driven activities soil was contaminated with radium. Subsequent measures were recommended and analysed from the point of view of optimization of radiation protection. Urgent dose-rate scanning of land where Russian fighter crashed was done and widely spread metal sticks were found. Dose-rate meter identified ^{238}U . Sticks were analysed by gamma-ray spectrometry and MGAU code, and it was shown that it was depleted uranium. Radiological assessment of site with stored sewage sludge from Visaginas city where workers of Ignalina NPP live was performed. The optimization of the number of samples to be sampled was performed using the program Environ-Calc. Concentrations of the ^{60}Co and ^{137}Cs in the sewage sludge were determined by gamma-ray spectrometry. Remedial actions were recommended. Effective doses to the members of reference groups were assessed. In-situ gamma-ray spectrometric measurements of two plots were done for construction of a new nuclear power plant. Plots under investigations were in the vicinity of Ignalina NPP. Measurements were done by an in-situ gamma-ray spectrometer fixed on a tripod holder; detector without collimator was directed downwards, 1 m above the ground. Geometry for efficiency calibration was characterized by thickness of layer of soil and area of soil. Density of contamination of soil with radionuclides was recorded in Bq/m^2 , though these radionuclides were distributed in the layer of some thickness.

1. INTRODUCTION

Radiation Protection Centre is a regulatory authority with well-defined responsibilities of licensing, inspections, enforcement, registration of sources and doses, and emergency preparedness. An equal attention is paid to the development of radiation protection expertise and to radiological investigations. It was found that the regulatory authority should have possibilities for assessment of radiation and radiation protection related situations, evaluating doses, making prognosis, giving advice [1]. Radiation Protection Centre has an accredited laboratory and has experience in the investigation of contaminated sites in Lithuania using available techniques. A few different cases are illustrated.

2. METHODS

For the investigation of contaminated sites gamma dose-rate measurements are very important. It must be decided, before investigation, how to organize the dose-rate measurements combined with sampling and in-situ gamma-ray spectrometry. Dose-rate measurements in the areas are performed at the height of 1 m and values are recorded. Radiation Protection Centre also has certified working instructions for 'Measurements of equivalent dose-rate of ionizing radiation'. Dose-rate scanning of site is done using the certified instruction for 'Scanning of site for search of ionizing radiation'. It is used to find places with higher gamma dose-rate. Dose-rate meters like Target FieldSpec and Canberra Inspector1000 with NaI(Tl) detectors are used for the identification of radionuclides on the site.

Sampling under field conditions are done depending on the task of every investigation. Samplers with fixed surface area and for vertical distribution are used. Samples after preparation are measured in the laboratory. Results also can be compared with in-situ gamma-ray spectrometric measurements.

Measurements of concentrations of radionuclides are performed by gamma-ray spectrometry. Gamma-ray spectrometry at Radiation Protection Centre is an accredited method. Four HPGe gamma-ray spectrometers are available in the laboratory. One of them is a broad energy Ge detector (20-2,000 keV) with carbon epoxy window. Other gamma-ray spectrometers are calibrated in the energy range from 59 keV (^{241}Am) to 1,836 keV (^{88}Y). Two of them have low background shielding. Different reproducible geometries of samples are used for the measurements. Reference sources and mathematical calibration ISOCS/LABSOCS are used for efficiency calibration of the gamma-ray spectrometers. Canberra software Genie 2000 is used for the analysis of the spectra. The relative efficiency of the gamma-ray spectrometers is in the range of 20.6-27.3% at 1,332 keV.

On-site measurements of soil contamination are carried out using in-situ gamma-ray spectrometry. The detector used in in-situ gamma-ray spectrometry is a high-purity germanium crystal (diameter – 63.5 mm, length – 64.4 mm). Calibration is done in the energy range from 59 keV (^{241}Am) to 1,836 keV (^{88}Y). Calibration standard is a mixture of 10 radionuclides in the Marinelli beaker. Analysis of spectra is done by the software Genie 2000. The efficiency of the in-situ gamma-ray spectrometer is calibrated using the ISOCS software.

When the techniques of ISOCS are used it is necessary to have some information on the geometry of the source (the volume of soil, from which gamma photons are recorded by the detector). This geometry is characterized by the thickness of layer of soil and by the area of soil. If assumption is made that the surface of the soil is flat, this area has the shape of a circle. Soil density is also an important factor. Density of contamination of soil with radionuclides is recorded in Bq/m^2 , though these radionuclides are distributed in the layer of some thickness.

Measurements of contaminated site are done by an in-situ gamma-ray spectrometer fixed on a tripod holder; the detector without collimator is directed downwards. The geometry of the measurements is a circle of 20 m diameter and 20 cm thickness; the detector is situated 1 m above the ground. The location for the measurement is as flat as possible and similar to the geometry of calibration. A thickness of 20 cm is selected on the basis of previous investigations of depth distribution of ^{137}Cs in soil. It has been determined that ^{137}Cs was distributed down to 20 cm of depth and its radiation was recorded from 20 cm thick layer depending on the type of soil. The distribution of ^{137}Cs in soil is close to an exponential one in undisturbed soil; however, its concentrations in different depths are very different. Before in-situ measurements an actual distribution of the artificial radionuclides was unknown, therefore the measurement geometry characterized above was used. The resolution of the in-situ gamma-ray spectrometer is high (0.91 keV FWHM at 122 keV and 1.86 keV FWHM at 1,332 keV), therefore, all the radionuclides in the calibrated energy range might be identified.

Radon measurements in soil air have been performed according to the working instructions 'Measurements of radon concentrations in soil air' of RSC Quality Manual. Measurements are performed using an instrument MARKUS 10 (manufactured by Gammadata in Sweden). Soil air is sucked through the tube from the depth of 0.7 to 1 m into the measuring chamber. Radon and its daughters decay in the chamber and alpha particles under electrical field inside the chamber are deposited on the surface of an Ortec Ultra silicon detector having a resolution <16 keV and an area of 100 cm². The pulses from the detector are amplified and filtered. An analyser records pulses only due to radiation of polonium (²¹⁸Po) because the half-life (3 min) of ²¹⁸Po is the shortest among the alpha daughters of radon, therefore, its activity changes rapidly and a new measurement might be started quickly. These measurements were done when the site was contaminated with ²²⁶Ra.

3. INVESTIGATIONS OF CONTAMINATED SITES

3.1. Investigation of site contaminated due to past activities

The investigation of an area located in Panevėžys, Skaistakalnis Park, where soil was contaminated with radium, has been performed. The contaminated area was approximately 76 m². It was a former Soviet military base. It was known from archives that the radioactive waste from the Soviet military base was transported by soviet military units to Russia in 1985. After Lithuania regained its independence the assessment of chemical and radioactive contamination was performed in all the areas which were left by the soviet military units. The radioactive contamination of the above-mentioned area was detected in August 1993 when the increased radiation level was recorded in the territory of repairs shop of the military air force unit. Soil wooden floor (approximately 4 m³) and vessel with 400 litres of radioactive liquid used for washing of engines were taken by air to Russia.

According to the prepared plan the Radiation Protection Centre performed dosimetric measurements in this site and identified location of contaminated spot. Vertical distribution sampling was performed. It was found by gamma-ray spectrometric measurements that the soil was contaminated with ²²⁶Ra. Measurements of concentrations of this radionuclide in soil, radon concentration in soil, air and closest water bodies were performed. Since radium is very radiotoxic the measurements of total alpha and beta activities in drinking water and water from the river were also carried out.

The samples of soil were taken in locations where the gamma dose-rate was the highest. In order to determine the distribution of radium in soil the samples were taken by layers. ²²⁶Ra concentration was between 0.1 Bq/g and 54 Bq/g. The results of the spectrometric measurements showed that the concentrations of ²²⁶Ra in the upper layers of soil are higher than the ones deeper and that these concentrations decrease rapidly with depth, but not always. The contamination is not homogeneous in depth and in area, it is like small spots. Examples of distribution of ²²⁶Ra by depth are given in Fig. 1.

Radon concentration in soil was between 13 kBq/m³ and 79 kBq/m³, the average being 37 kBq/m³. Those are not high concentrations, they are similar to the concentrations measured in Lithuanian soil. Since radon is a decay product of ²²⁶Ra it is clear that a relatively small amount of soil is contaminated.

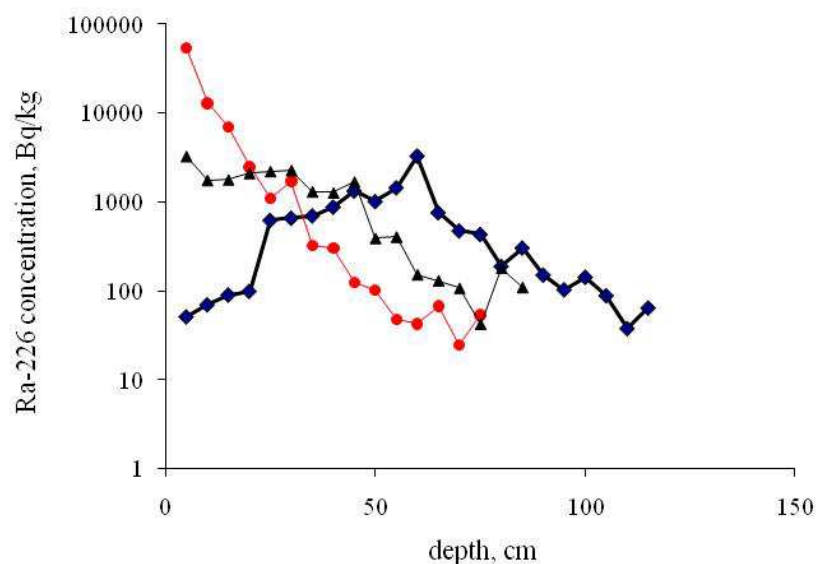


FIG. 1. Distribution of ^{226}Ra at different points (each curve represents the distribution at the points).

The possible doses and resources needed for protective measures shall be taken into account for the selection of optimized radiation protection measures. After the analysis of the measurement results and assessment of the potential doses, recommendations were prepared and were given to the Panevėžys municipality on how this area should be managed.

Three possible measures were identified: to transfer 30 cm of top layer of contaminated soil to a repository of radioactive waste, not to take any measures or to cover the contaminated soil with clean one. The last option has been suggested as the most optimized.

3.2. Investigation of site after emergency

A Russian fighter crashed on Lithuanian territory. Due to the possibility of sealed sources of ionising radiation being on board, gamma dose-rate measurements were conducted at the crash location [3]. It was detected that the dose-rate near the metal sticks on the ground was higher than background level. The sticks were spread around and many of them were bent. All these sticks were collected with gamma dose-rate meters. Dose-rate meter detected ^{238}U . Detailed investigation was done at the laboratory of the Radiation Protection Centre. Sticks were of equal mass (12.63 ± 0.06) g and volume (36.4 ± 0.8) mL; due to the strike they were differently deformed. No information from Russia was available.

Sticks were measured with a HPGe gamma-ray spectrometer. Spectra were analysed with MGAU code (Multiple Group Analysis for Uranium) to find uranium enrichment [4]. MGAU code was received from EC JRC Institute for Transuranium Elements. Now MGAU code is part of the S507C of Canberra software Genie 2000. The code is capable to analyse the part of spectra containing low energies registered by high-resolution Ge detector. Using this code there is no need to calibrate the efficiency of the spectrometer for geometry of measurement. The method for determination of uranium enrichment is quick, precise and reliable. The composition of uranium was determined as follows ^{235}U – (0.325 ± 0.004)% and ^{238}U – (99.674 ± 0.004)%. It was depleted uranium. Dose-rate scanning of site was repeated several times. Sticks were collected and Russia took them back. These depleted uranium sticks were ballast material from bombs carried by the fighter. At the moment of the crash some of the bombs broke and sticks spread around.

3.3. Radiological assessment of site and dose evaluation

Temporary storage of sewage sludge of Visaginas city was in a quarry, in Karlu village, Ignalina district. Workers of Ignalina nuclear power plant live in Visaginas. Waste from Ignalina NPP could get into storage.

Assessment of doses was done from investigation results [5]. Using the software Environ-Calc from the American Chemical Society the number of samples needed to be sampled was optimized. The area of the site was 1 hectare. Layer of sludge was between 1 m and 1.5 m. 38 sludge samples from different depth (5-90 cm) were collected. Round area was divided to 8 equal parts. Samples were taken on radii every 10-15 m. Gamma-ray spectrometry measurements of fresh samples were done. Two artificial radionuclides ^{60}Co and ^{137}Cs were found. Average activity concentration of ^{60}Co for the fresh weight in the samples was (42 ± 8) Bq/kg (range 1.4-135 Bq/kg) and for ^{137}Cs – (10 ± 4) Bq/kg (range 1.2-25 Bq/kg). These radionuclides are indicators of Ignalina NPP discharge. The ^{137}Cs concentration in the sewage sludge is close to the concentrations in Lithuanian soil. The distributions of the samples as a function of ^{60}Co and ^{137}Cs concentrations are shown in Fig. 2.

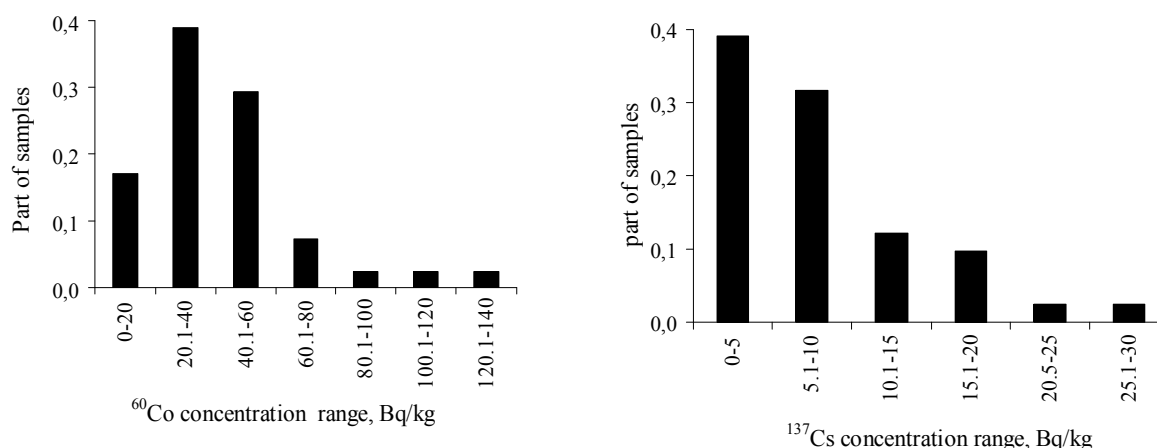


FIG. 2. Distribution of samples as a function of ^{60}Co concentration (left), and ^{137}Cs concentration (right).

A general dose model was used for conservative evaluation [6]. Two potential exposure pathways for the radionuclides in the sewage sludge were considered and two scenarios descriptions were made. The first scenario is when the sludge is used for fertilization and the second one when the sludge is covered with soil. Clearance levels are used for waste from regulatory activities. Clearance level can be applied, when radionuclides are identified, activity concentration measured and annual effective dose to reference group less than $10 \mu\text{Sv}$.

The effective dose using the first scenario for a 1 year child would be $12 \mu\text{Sv}$, and for an adult $9.4 \mu\text{Sv}$. In another scenario effective doses for the workers in the sewage storage were estimated to be 0.76 mSv . The lowest doses would be when the sewage storage is covered using soil.

3.4. Investigation plots for a new NPP

Potential plots for a new nuclear power plant in the vicinity of Ignalina NPP (RBMK type reactor) were investigated [7]. Dose-rate, radon concentrations in soil air, activities of radionuclides using in-situ gamma-ray spectrometry, activity concentrations of strontium (^{90}Sr), plutonium and transuranium elements in soil samples, were measured. The plot I for construction of a new nuclear power plant has an area of 36.92 hectares. The third reactor of Ignalina Nuclear Power Plant (INPP) has been under construction in the plot, later it was pulled down to fundament. The constructions of forced concrete have been dismantled down to 1 m of depth. The area has been re-cultivated.

The plot II for the construction of a new nuclear power plant has a plot of 37.51 hectares. The electricity distribution installations have been constructed on the plot. Later the above-ground constructions were dismantled, fundament remains. Since the same measurements and their volumes were planned for both plots the strategy of planning of investigations and sampling was the same in both cases. Sampling points in each plot were located homogenously in the whole area of the plot. The area has been divided into parts. Their number was equal to the number of samples (measurements). The plan was prepared for each type of measurements and sampling of soil. Sampling of soil, measurements of radon concentrations in soil air and determination of activities of radionuclides using in-situ gamma-ray spectrometry were carried out at the same points. Measurements using in-situ gamma-ray spectrometry were performed at the same points as the sampling in the place.

Since plots under investigation were in the vicinity of the Ignalina NPP, the results on activities of reactor radionuclides ^{60}Co and ^{137}Cs were presented. In the cases they were not identified, the minimum detection levels were given. Minimum detection level depends on the gamma-ray spectrometric system, the duration of the measurement and the energy of gamma photons.

The ^{137}Cs radionuclide appeared in the environment from global contamination due to atmospheric tests of nuclear weapons and Chernobyl fallout as well. Natural radionuclides are present everywhere in soil. For efficiency calibration of the in-situ gamma-ray spectrometer assumption was made that ^{137}Cs and ^{60}Co are homogenously distributed in area and depth.

Efforts were made to find a place as similar to the calibration geometry as possible. If it was impossible to avoid trees and water bogs, uncertainties are involved. Comparison of results from in-situ measurements and laboratory gamma-ray spectrometric investigations were done. Measurements by in-situ gamma-ray spectrometry are performed at the same points as soil sampling. Radiation Protection Centre for in-situ gamma-ray spectrometric measurements has a certified working instruction for 'In situ gamma spectrometric investigations'.

Soil samples were taken in the area where in-situ gamma-ray spectrometric measurements were done. 'Envelope' method was used for sample collection (side – 10 m, diagonal – 15 m). Soil sample ring (square – 0.015 m^2 , depth – 5 cm) was used. Investigations of the concentrations of gamma-emitter radionuclides in soil samples were performed using laboratory gamma-ray spectrometry. Analysed samples were placed in Marinelli beakers. The results were compared with in-situ gamma-ray spectrometry measurements. The concentrations of ^{137}Cs measured using laboratory gamma-ray spectrometry are close to the ones measured from in-situ measurements.

Though during in-situ measurements it was assumed that ^{137}Cs and ^{60}Co are homogeneously distributed in layer of 20 cm depth and circle of 314 m² square (volume – 63 m³) and measurements were done at the same humidity, the whole environment was analysed. Soil sample for measurements of concentrations of ^{137}Cs and ^{60}Co was taken from 5 volumes much smaller (769 cm³) at a depth of 0-5 cm, but after it was dried and analysed for a longer time, lower concentrations could be measured. No ^{60}Co and other artificial gamma-emitter radionuclides (except ^{137}Cs) were detected in any of the soil samples analysed using gamma-ray spectrometry and in any spectrum recorded by in-situ gamma-ray spectrometry. ^{137}Cs concentrations (from MDA till $(3.1 \pm 0.4) \text{ kBq/m}^2$) were found at a few parts of plot II. Low ^{137}Cs concentrations ($(0.3 \pm 0.2) \text{ Bq/kg}$ – $(0.6 \pm 0.1) \text{ Bq/kg}$) were found using laboratory gamma-ray spectrometry, when it was less than the minimum detectable activity using in-situ gamma-ray spectrometry measurement at plot I. It is also because soil samples are measured in low background shielding and in-situ gamma-ray spectrometry is in open air.

Values of dose-rate recorded in the areas of plots under investigations were in the range of background radiation in Lithuania. No significant dose-rate increase, which might be related with source of ionizing radiation or contaminated area, was recorded.

4. CONCLUSIONS

Radiation Protection Centre makes efforts in optimizing use of available resources in order to characterize contaminated sites and identify radiation protection measures.

REFERENCES

- [1] LADYGIENĖ, R., MORKŪNAS, G., PILKYTĖ, L., Regulatory and scientific aspects of environmental studies, Health Sciences **14** (2004) 2.
- [2] Investigation of contaminated site with radium in Panevezys city after recovery works, Radiation Protection Centre report to Panevezys municipality (2004).
- [3] Investigation of site and radioactive material after fighter crash, Radiation Protection Centre Annual report, Vilnius (2006). <http://www.rsc.lt/index.php/pageid/331>
- [4] International workshop on gamma evaluation codes for plutonium and uranium isotope abundance measurements by high-resolution gamma spectrometry: current status and future challenges, book of abstracts, EC JRC Institute for Transuranium Elements, ITU (2005).
- [5] LADYGIENĖ, R., PILKYTĖ, L., MORKŪNAS, G., Assessment of doses due to radionuclides in sewage sludge for different scenario of its use, Health Sciences **13** (2003) 54.
- [6] Generic Models for Use in Assessing the Impact of Discharges of Radioactive Substances to the Environment, Safety Reports Series No. 19, IAEA, Vienna (2001).
- [7] Report on Investigations of Contamination with Radionuclides of Potential Plots for a New Nuclear Power Plant, Radiation Protection Centre report, Vilnius (2009).

THE EFFECTIVE SOLID ANGLE CONCEPT AND ANGLE v3.0 COMPUTER CODE FOR SEMICONDUCTOR DETECTOR GAMMA-EFFICIENCY CALCULATIONS – APPLICABILITY TO IN-SITU CHARACTERIZATION OF CONTAMINATED SITES*

S. JOVANOVIC, A. DLABAC, N. MIHALJEVIC

University of Montenegro, Centre for Nuclear Competence and Knowledge Management (UCNC),
G. Washington Blvd.2, 81000 Podgorica, Montenegro

Emails: bobo_jovanovic@yahoo.co.uk , adlabac@t-com.me

Abstract

The ANGLE software for semiconductor detector efficiency calculations in its various forms has been in use for now 20 years in numerous gamma-ray spectrometry based analytical laboratories all around the world. Its purpose is to allow for the accurate determination of the activities using gamma-ray spectrometry of samples for which no 'replicate' standard exists, in terms of geometry and matrix. ANGLE employs a semi-empirical 'efficiency transfer' approach, which combines advantages of both absolute (Monte Carlo) and relative (traceable source based) methods to determine sample activity by gamma-ray spectrometry, while reducing the practical limitations of the latter methods and minimizing potential for systematic errors in the former. The physical model behind is the concept of effective solid angle – a parameter calculated upon the input data on geometrical, physical and chemical (composition) characteristics of (i) the source (including its container vessel), (ii) the detector (including crystal housing and end-cap) and (iii) counting arrangement (including intercepting layers between the latter two). The program can be applied to practically all situations encountered in gamma-ray spectrometry practice, e.g. for environmental monitoring, radioactivity control, Neutron Activation Analysis, scientific research applications, etc. Point, disc, cylindrical or Marinelli geometries, small or large, of any matrix composition, measured on coaxial, planar or well-type detectors, HPGe or Ge(Li) can be treated. No standards are required, but a start-up 'reference efficiency curve' must be obtained, generally as a one-time procedure. Latest ANGLE v3.0 version is presented. Besides its (i) wide range of applicability, (ii) high accuracy, (iii) ease-of-use, (iv) short computation times, (v) flexibility in respect with input parameters and output data, (vi) easy communication with another software and (vii) suitability for teaching/training purposes, ANGLE architecture offers potential for (viii) accommodating other efficiency calculation methods of semi-empirical or absolute (Monte Carlo) type and for (ix) expanding its current scope of applicability to further/particular user's needs and/or fields of interest. A key aspect and difference from other approaches, which greatly enhances practicality, is that (x) no 'factory characterization' of the detector response is required – any detector may be used as long as some basic knowledge concerning its construction is available. Besides the years of practical utilization, accuracy of the software has been recently successfully tested in an IAEA-organized intercomparison exercise – ANGLE scored 0.65% average deviation from the exercise mean for $E_\gamma > 20$ keV energies. Applicability of ANGLE to in-situ radioactivity measurements, including surface and in-depth contamination, is straightforward. It goes simply about defining 'counting geometry' as either (i) an infinite slab, when detector is placed above the surface, or (ii) an infinite Marinelli source, when put into a hole digged in the soil, so as to increase detection efficiency and reduce counting times. ANGLE is commercially distributed by AMETEK/ORTEC, U.S.A.

*Published in part in: S. Jovanovic et al., Nucl. Instr. Meth. Sect. A, **662** 2 (2010) 385

1. INTRODUCTION – THEORETICAL BACKGROUND

The concept of *effective solid angle* ($\overline{\Omega}$) was introduced in gamma-ray spectrometry so as to deal with determination of the full-energy-peak efficiency (ϵ_p) of a semiconductor detector for the sample counted. Given a gamma-source (S) and a detector (D), the effective solid angle is defined as:

$$\overline{\Omega} = \int_{V_S, S_D} d\overline{\Omega} \quad (1)$$

with V_S being the source volume and S_D the detector surface exposed to the source ('visible' by the source).

Illustration of the definition of the *effective solid angle* is given in Fig. 1.

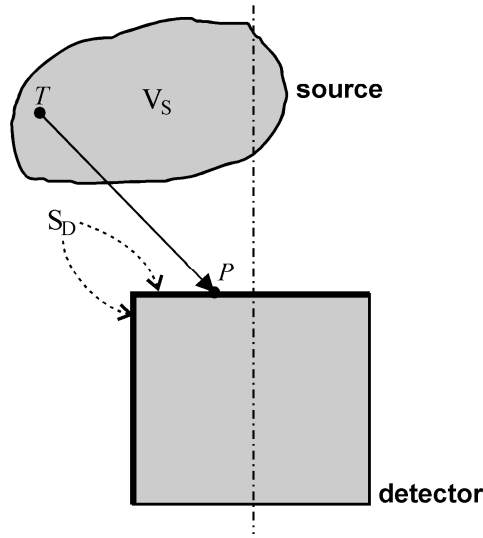


FIG. 1. Definition of the effective solid angle ($\overline{\Omega}$).

From Eq. (1), it follows that:

$$d\overline{\Omega} = \frac{F_{att} \cdot F_{eff} \cdot \vec{TP} \cdot \vec{n}_u}{|\vec{TP}|^3} d\sigma \quad (2)$$

In this equation, T is a point varying over V_S , P a point varying over S_D , and \vec{n}_u is the external unit vector normal to the infinitesimal area $d\sigma$ at S_D . Equation (1) is thus a fivefold integral. Factor F_{att} accounts for gamma attenuation of the photon following the direction \vec{TP} out of the detector active zone, while F_{eff} describes the probability of an energy degradable photon interaction with the detector material (i.e. coherent scattering excluded), initiating the detector response. The two factors include therefore geometrical and composition-related parameters of the materials traversed by the photon [1].

To assume that the virtual peak-to-total ratio is an intrinsic characteristic of the detector crystal (depending on the energy of the gamma ray only) [1, 2] means that ε_p is proportional to $\overline{\Omega}$. This very important assumption enables conversion from any chosen reference geometry (accurate and reliably determined) (index ‘ref’) to that of the actual sample, which is the basis of the ‘efficiency transfer’ (ET) principle.

$$\varepsilon_p = \varepsilon_{p,ref} \frac{\overline{\Omega}}{\overline{\Omega}_{ref}} \quad (3)$$

Efficiency transfer factor is thus the ratio of the actual to reference efficiency at a given gamma energy. The ET approach is extremely useful – offering (i) practically unlimited flexibility in sample type and size, matrix composition, detector choice and source-detector counting arrangement and, crucially, (ii) cancelling out much of the impact of input data uncertainties (especially those of the detector) on final ε_p calculation result. This implicit latter ‘ET error compensation’ gives to ET an important advantage over purely mathematical (Monte Carlo) efficiency calculation approaches [3-6].

For the characterization of contaminated sites, disc, large cylinder and Marinelli sources are of particular interest. The following is obtained when applying Eqs. (1) and (2) [7].

a) For cylindrical sources:

$$\begin{aligned} \overline{\Omega} &= \int_{V_1, S_1} d\overline{\Omega} + \int_{V_2, (S_1+S_2)} d\overline{\Omega} = \\ &= \frac{4}{r_o^2 L} \int_0^L (d+l) dl \int_0^{r_o} r dr \int_0^\pi d\phi \int_0^{R_o} \frac{F_{att} \cdot F_{eff} \cdot R dR}{[R^2 - 2Rr \cos \phi + r^2 + (d+l)^2]^{3/2}} + \\ &+ \frac{4R_o}{(r_o^2 - R_o^2)L} \int_0^L dl \int_{R_o}^{r_o} r dr \int_0^{\phi_o} d\phi \int_{-H}^0 \frac{F_{att} \cdot F_{eff} \cdot (r \cos \phi - R_o) dh}{[R_o^2 - 2R_o r \cos \phi + r^2 + (d+l-h)^2]^{3/2}} \end{aligned} \quad (4)$$

with

$$\phi_o = \phi_o(r) = \arctg \frac{\sqrt{r^2 - R_o^2}}{R_o}$$

b) Disc sources are calculated from Eq. (4) as well, with the source height equal to L=0.

c) Marinelli sources:

$$\begin{aligned}
\overline{\Omega} = & \int_{(V_1+V_2), S_1} d\overline{\Omega} + \int_{V_2, S_2} d\overline{\Omega} + \int_{V_3, S_1} d\overline{\Omega} + \int_{(V_3+V_4), S_2} d\overline{\Omega} + \int_{V_5, (S_2+S_3)} d\overline{\Omega} = \\
= & \frac{4}{r_o^2 L + (r_o^2 - r_\phi^2) L_\phi} \int_0^L (d+l) dl \int_0^{r_o} r dr \int_0^\pi d\phi \int_0^{R_o} \frac{F_{att} \cdot F_{eff} \cdot R dR}{[R^2 - 2Rr \cos \phi + r^2 + (d+l)^2]^{3/2}} + \\
& + \frac{4R_o}{r_o^2 L + (r_o^2 - r_\phi^2) L_\phi} \int_0^L dl \int_{R_o}^{r_o} r dr \int_0^{\phi_o} d\phi \int_{-H}^0 \frac{F_{att} \cdot F_{eff} \cdot (r \cos \phi - R_o) dh}{[R_o^2 - 2R_o r \cos \phi + r^2 + (d+l-h)^2]^{3/2}} + \\
& + \frac{4}{r_o^2 L + (r_o^2 - r_\phi^2) L_\phi} \int_0^d l dl \int_{r_\phi}^{r_o} r dr \int_0^\pi d\phi \int_0^{R_o} \frac{F_{att} \cdot F_{eff} \cdot R dR}{(R^2 - 2Rr \cos \phi + r^2 + l^2)^{3/2}} + \\
& + \frac{4R_o}{r_o^2 L + (r_o^2 - r_\phi^2) L_\phi} \int_{d-L_\phi}^d dl \int_{r_\phi}^{r_o} r dr \int_0^{\phi_o} d\phi \int_{-H}^0 \frac{F_{att} \cdot F_{eff} \cdot (r \cos \phi - R_o) dh}{[R_o^2 - 2R_o r \cos \phi + r^2 + (l-h)^2]^{3/2}} + \\
& + \frac{-4}{r_o^2 L + (r_o^2 - r_\phi^2) L_\phi} \int_{d-L_\phi}^{-H} (l+H) dl \int_{r_\phi}^{r_o} r dr \int_0^\pi d\phi \int_0^{R_o} \frac{F_{att} \cdot F_{eff} \cdot R dR}{[R^2 - 2Rr \cos \phi + r^2 + (l+H)^2]^{3/2}}
\end{aligned} \tag{5}$$

The cylindrical and Marinelli sources are described in Figs. 2 and 3, respectively.

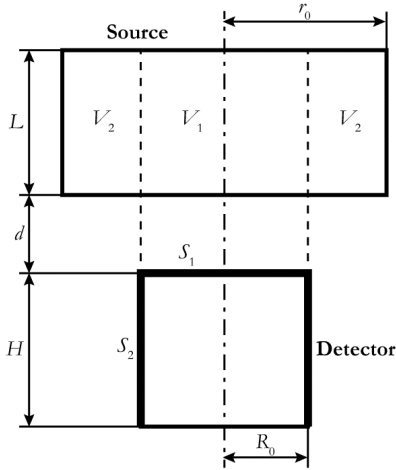


FIG. 2. Cylindrical source ($r_o > R_o$).

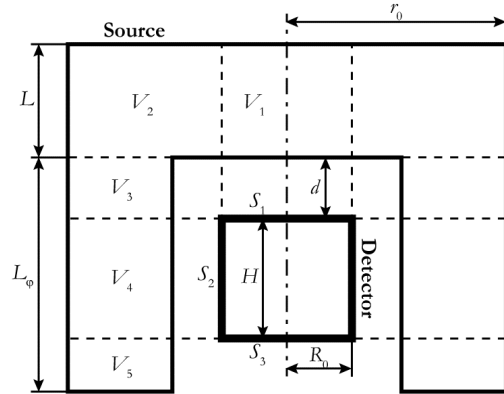


FIG. 3. Marinelli geometry.

2. ANGLE v3.0 – SHORT DESCRIPTION

ANGLE v3.0 calculates full energy peak efficiencies (ε_p) and effective solid angles ($\overline{\Omega}$) for given source-detector configuration and chosen gamma energies, as described above [8]. The main screen is designed to be self-explanatory to the user: five principal windows define ‘Detector’, ‘Source’, source ‘Container’, counting ‘Geometry’ and ‘Other’ parameter data. Each one may be selected/manipulated easily from its respective drop-down menu. The main menu enables easy data input, storage, reviewing or editing, aided with graphical illustrations, so as to help user familiarity and to prevent data entry errors. The current data selection appears highlighted on the screen and can be used for immediate calculations or stored for later usage. Single calculations can be performed or grouped into batch jobs.

Output results can be easily transferred to other software e.g. spreadsheet or word processing programs. Thus, ANGLE is suitable for integrating into more complex programs, which make it useful in a wide variety of situations. The ANGLE main screen is shown in Fig. 4.

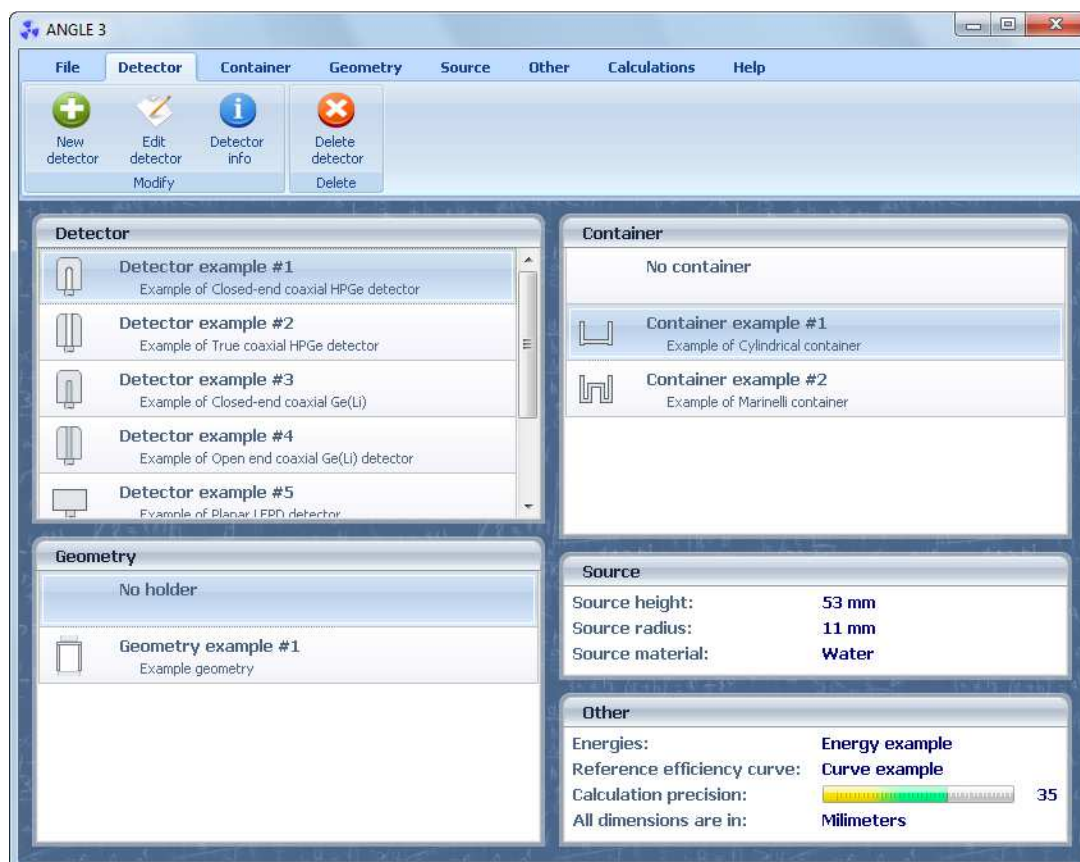


FIG. 4. ANGLE main screen (Reproduced courtesy of AMETEK/ORTEC).

A few examples of screens are given in Figs. 5-8. With ANGLE being user-friendly software, the screens tend to be self-explanatory for those basically familiar with semiconductor detector gamma-ray spectrometry programmes. For instance, detector data are managed as shown in Fig. 5, while Fig. 6 illustrates handling of reference efficiency curve and characterizing reference (calibration) counting arrangement. Figure 7 gives an example of the complexity/versatility of data input, while maintaining simplicity and clearness of the communication with the user – this figure shows one particular layer, namely the possibility to change e.g. chemical composition of one intercepting layer, ‘source support’ in this case, traversed by the photons on their way from the source to the detector. Results are found within the ‘Calculation’ menu, and are given in the form of ϵ_p (and/or $\overline{\Omega}$) versus E_γ tables, as shown in Fig. 8. These can readily be transferred to another application for further analyses or for graphical presentation.

New detector

Detector | End-cap window | Antimicrophonic shield | End-cap | Vacuum | Housing

Detector name: SCD317

Detector type: Closed-end coaxial HPGe

Detector height: 45.2 mm

Detector radius: 24.8 mm

Bulletizing radius (0 = none): mm

Core top type: ☐ Rounded ☐ Flat

Core height: mm

Core radius: mm

Inactive Ge top thickness: mm

Inactive Ge side thickness: mm

Contact top thickness: mm

Contact side thickness: mm

Contact material:

Contact pin radius: mm

Contact pin material:

Detector description:

OK Cancel Help

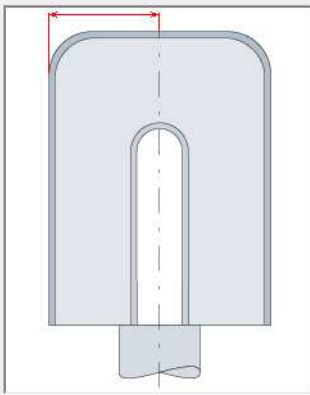


FIG. 5. Entering the data for a new detector (Reproduced courtesy of AMETEK/ORTEC).

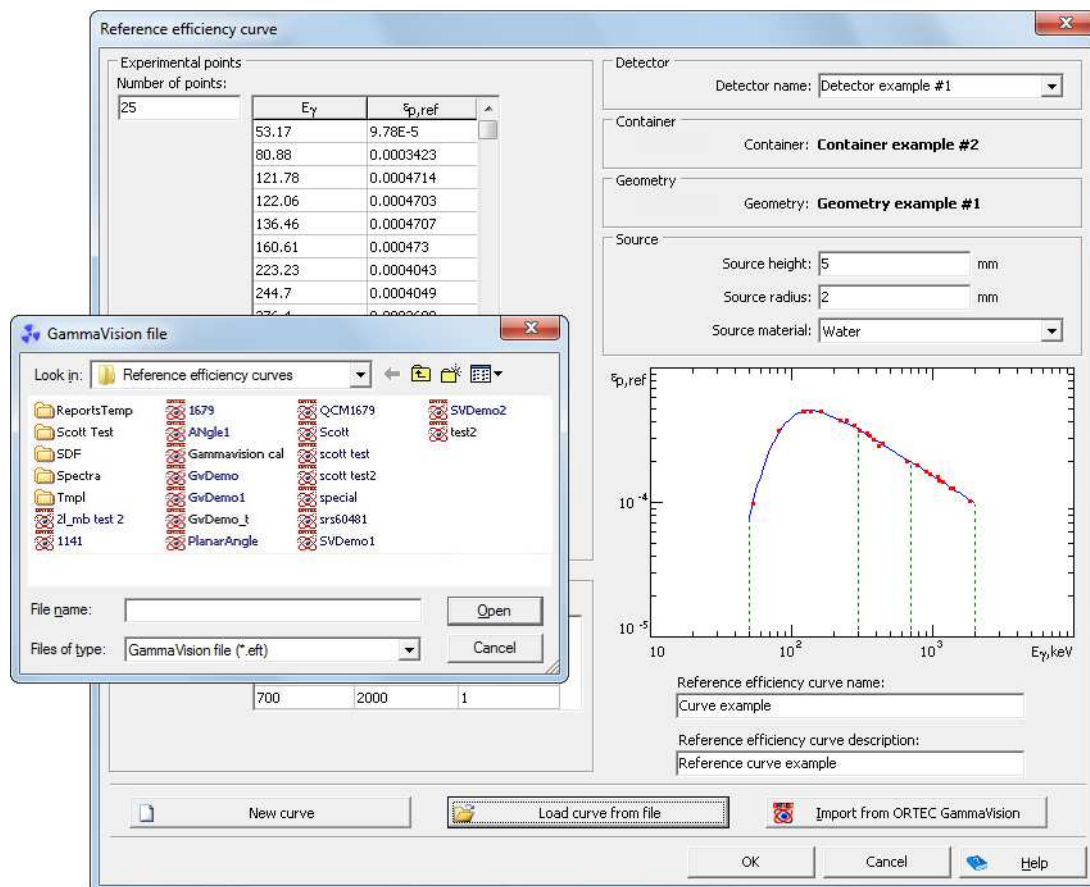


FIG.6. Reference efficiency curve (Reproduced courtesy of AMETEK/ORTEC).

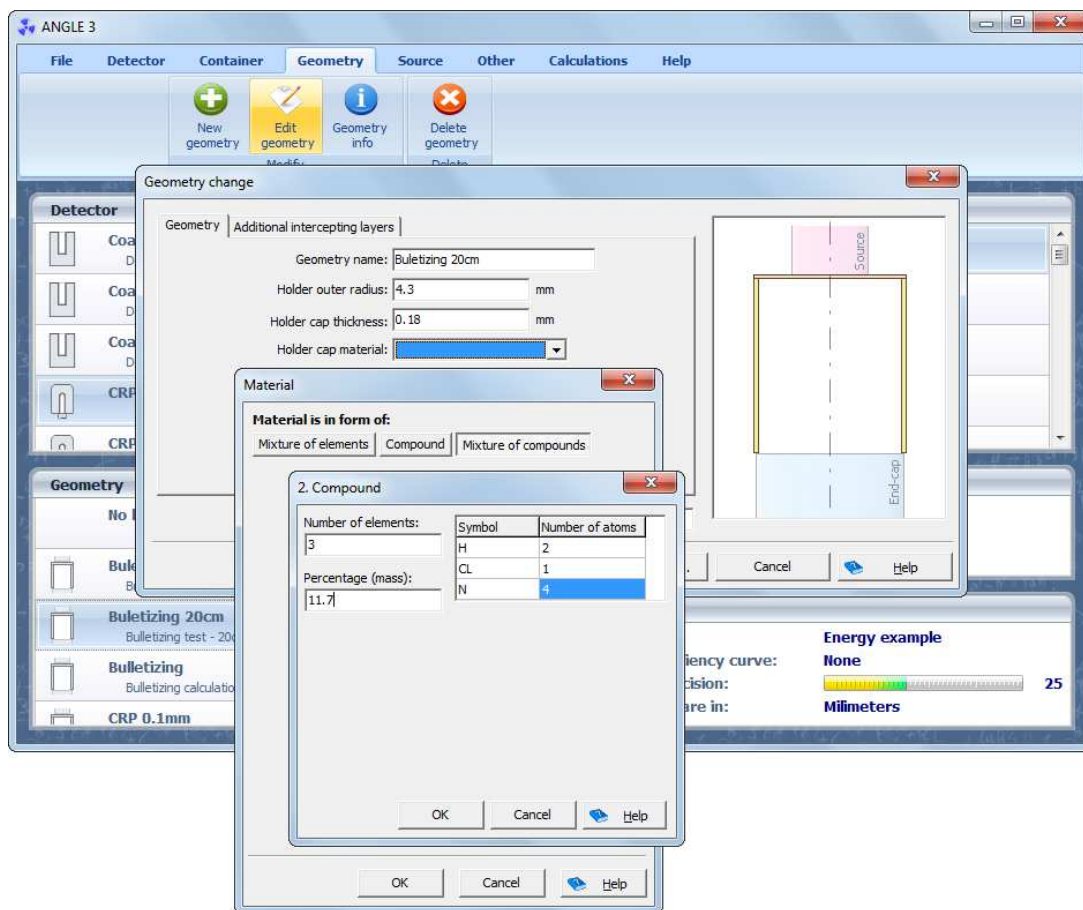


FIG. 7. Changing source support composition data – an example of defining a particular parameter (Reproduced courtesy of AMETEK/ORTEC).

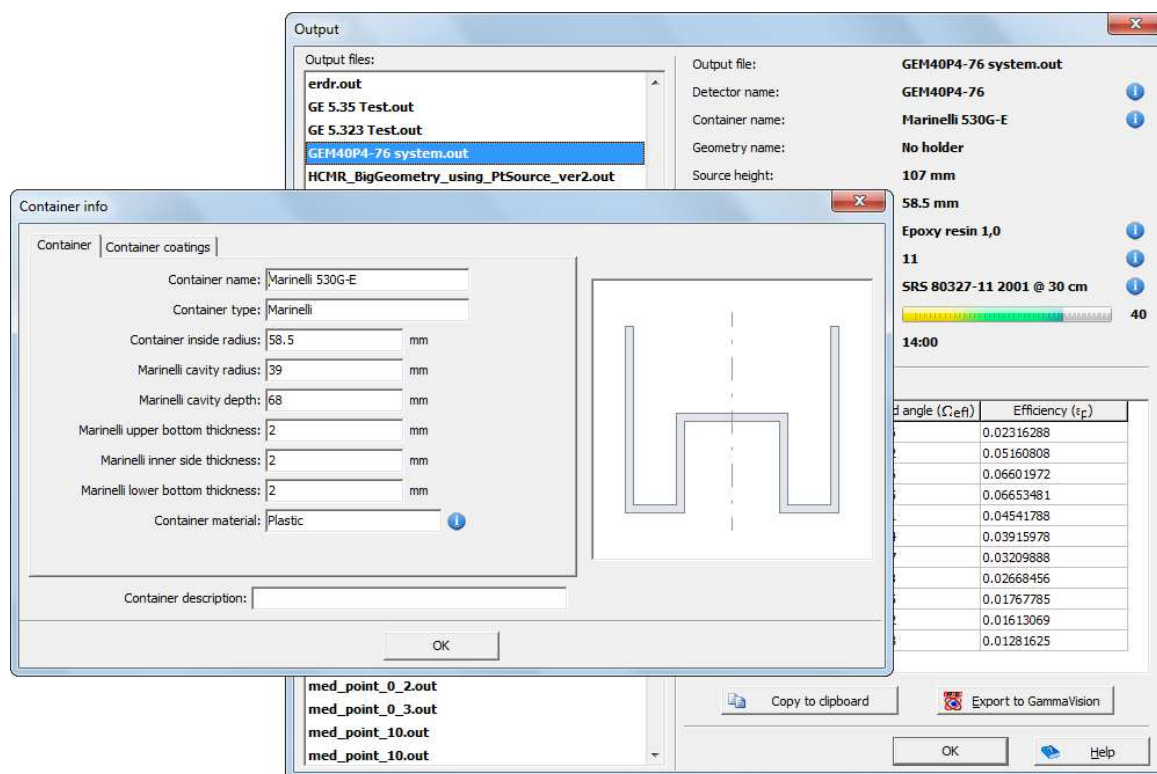


FIG. 8. A typical ANGLE output (Reproduced courtesy of AMETEK/ORTEC).

ANGLE is a commercial software distributed by AMETEK/ORTEC, U.S.A. [9]. Free demo version is available on request, allowing unrestricted data input try-out and limited number of calculation cycles. Detailed user's manual is available therein. As a matter of fact, ANGLE is compatible with ORTEC's GammaVision software for spectra elaboration, as shown in Fig. 9.

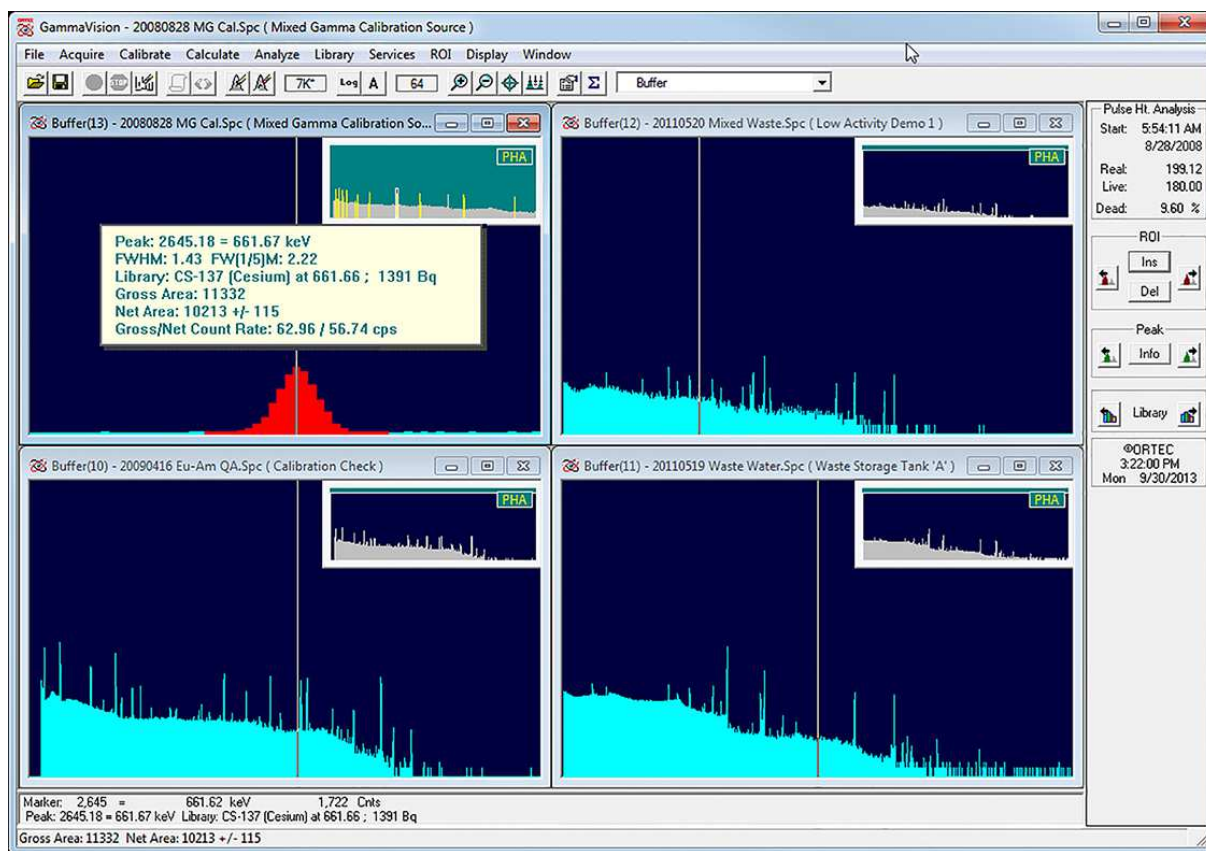


FIG. 9. GammaVision software for spectrum elaboration (Reproduced courtesy of AMETEK/ORTEC).

Long experience with ANGLE utilization in numerous gamma-ray spectrometry laboratories worldwide shows that it is characterized by (i) its wide range of applicability, (ii) its high accuracy, (iii) its ease-of-use, (iv) its short computation times, usually of the order of seconds, (v) its flexibility in respect with input parameters and output data, including easy communication with another software, and (vi) its suitability for teaching/training purposes. The ANGLE architecture also offers (vii) potential for accommodating other efficiency calculation methods of semi-empirical or absolute (Monte Carlo) type. In addition, its current scope of applicability (viii) can readily be extended to further/particular user's needs and/or fields of interest – it can be thus regarded as an ‘open-ended’ computer code. A key aspect (and difference from some other approaches), which greatly enhances practicality is that (ix) no ‘factory characterization’ of the detector response is required. In fact (x) any semiconductor detector may be used as long as some basic information concerning its construction is available.

3. QUALITY OF OUTPUT DATA

3.1. Error segmentation

Utilizing semi-empirical efficiency transfer approach based on effective solid angle calculations, with (realistically) reliable input data, ANGLE produces ε_p results with an estimated uncertainties of 1-2% for point sources, 3-4% for cylindrical ones and 5-7% for Marinelli containers [1, 4, 7]. For low gamma energies (<100 keV) uncertainties may be somewhat larger, mainly due to high error propagation factor of the uncertainty in detector crystal dead layer thickness. In general, the latter parameter is not very well known – it is not directly measurable and is hence usually only estimated by the manufacturer from controlled lithium diffusion conditions during its generation. However, a relatively simple experimental/calculation procedure enables its determination (by the user) with sufficient accuracy [11]. Above 2,000 keV reliable calibration points are scarce, hence results in this region may be poorer too.

When assigning uncertainties to ANGLE calculation results, several uncertainty contributing components should be distinguished, originating from (i) detector manufacturer, (ii) ANGLE user and (iii) ANGLE software itself. Those include:

- Detector data, supplied by the manufacturer;
- Geometrical and compositional (chemical) data of the source, its container vessel and intercepting layers (between the source and the detector), introduced by the user;
- Reference efficiency curve, created or chosen by the user;
- Mathematical model and calculation method applied (ANGLE);
- Gamma attenuation coefficients and other physical/chemical parameter data used in calculations (ANGLE).

The above ‘error segmentation’ is often not realized, the complete uncertainty budget being attributed to the software itself – which is obviously wrong. The same observation may be applied to other semi-empirical and absolute efficiency calculation methods/software, namely that sources of uncertainty outside the code itself may dominate the overall uncertainty.

3.2. An intercomparison exercise

In order to help distinguish between the three uncertainty components, i.e. to estimate uncertainty introduced by the ANGLE software itself, recent participation in a software intercomparison exercise proved useful. The exercise was organized within an IAEA topical coordinated research project and conducted by the EC Joint Research Centre IRMM in Geel, Belgium [6]. Nine well-known ET codes (ANGLE included), running in 10 laboratories, took part – four specialized ones and five general Monte Carlo tools adapted for ET. The task was to calculate ET factors in the 20-2,000 keV energy range for ‘virtual counting arrangements’, that is to say for virtual (‘exact’) detector, source and geometrical/compositional data. The reference geometry was given to be a large cylinder with aqueous solution. Sample geometries included point, disc and another large cylinder, the latter one with two different matrices of exactly specified chemical composition. Two detectors included p- and n-type coaxial HPGe. In this way uncertainties in detector, source, geometry, data, etc, were eliminated, leaving the software introduced uncertainties alone.

As a matter of fact, no ‘true’ values of the intercomparison results were known in advance; the results were compared to mean values obtained from all participants’ data submitted. Participants were requested to provide results (ET factors) within 1% uncertainty. Some targeted this figure, the others aimed at lower. ANGLE reported ET values had much better calculation uncertainties ($<0.01\%$), obtained by setting the numerical integration parameter somewhat higher than usual (Gauss-Legendre coefficient, determining the precision). This required a bit more computing time, but was still comfortably fast – not longer than two minutes on a standard PC.

An illustration of the intercomparison results is given in Tables 1 and 2 [6]. Here A and B refer to two detectors considered (p-type and n-type), ‘Point’ stands for the point source, ‘Filter’ for disc-shape source, ‘Soil’ for a large cylindrical source. Participating ET codes (software) obviously agreed very well with each other, within reported uncertainties (there are a few exceptions in very low energy range).

It can be concluded that mathematical models and numerical methods for efficiency calculations – ANGLE included – are themselves minor (even negligible) sources of uncertainty in efficiency calculations, and that the major sources of uncertainty lie elsewhere, i.e. in the detector, sample and counting geometry data. Small differences appearing between the codes (average discrepancy from the mean values for all participants and all data was 0.76%) could be attributed to different attenuation coefficient and cross-section data used in calculations. For ANGLE, the average discrepancy from the mean values was 0.73% (even 0.65% for $E_\gamma > 20$ keV), with no evidence of systematic bias, i.e. of systematic errors, as shown in Table 3. It has to be noted that participants’ individual intercomparison results were not reported in [6]. In the latter reference more details on the exercise can be found.

TABLE 1. STANDARD DEVIATIONS OF THE POPULATION OF ET FACTORS, AS PERCENT OF ITS MEAN, FOR ALL PARTICIPATING CODES [7]

Energy	Point A	Point B	Soil A	Soil B	Filter A	Filter B
20		1.4		2.5		1.2
45	0.5	0.9	0.9	0.5	0.9	0.8
60	0.6	0.5	0.9	0.9	1.0	0.5
80	0.6	0.4	0.9	0.7	0.8	0.5
120	0.5	0.4	0.7	0.5	0.6	0.6
200	0.7	0.7	0.6	0.6	0.6	0.8
500	0.8	0.9	0.8	0.3	0.6	0.9
1,000	0.7	1.1	0.5	0.5	0.8	0.9
2,000	0.7	1.0	0.7	0.6	0.8	0.8

TABLE 2. MAXIMUM DEVIATIONS OF THE POPULATION OF ET FACTORS FROM ITS MEAN, AS PERCENT OF THE MEAN, FOR ALL PARTICIPATING CODES [7]

Energy	Point A	Point B	Soil A	Soil B	Filter A	Filter B
20		3.1		7.6		3.4
45	1.2	1.7	3.1	1.3	2.2	1.4
60	1.2	1.1	1.9	2.3	2.5	1.0
80	1.2	1.0	2.0	1.6	2.0	1.1
120	0.9	0.8	1.8	1.6	1.2	1.1
200	1.1	1.4	1.2	1.6	1.2	1.4
500	1.4	1.9	1.7	0.5	1.1	1.5
1,000	1.6	2.0	0.9	1.2	1.4	1.5
2,000	1.9	1.9	1.5	0.9	1.4	1.3

TABLE 3. ANGLE DEVIATIONS FROM MEAN ET FACTORS, AS PERCENT OF THE MEAN

Energy	Point A	Point B	Soil A	Soil B	Filter A	Filter B
20		1.7		2.9		1.5
45	0.1	0.9	-0.8	0.2	0.1	0.7
60	0.1	0.5	0.0	0.9	0.2	0.5
80	0.0	0.3	0.1	0.8	0.3	0.4
120	-0.7	-0.4	-0.1	0.6	0.3	0.7
200	-0.9	-1.3	-0.1	0.7	0.8	1.1
500	-1.1	-1.9	-0.4	0.0	1.0	1.2
1,000	-0.9	-2.0	-0.5	-0.1	0.8	1.1
2,000	-1.1	-1.9	-0.7	-0.1	0.9	1.1

3.3. Few practical concerns

Detector data

The quality of the available detector constructional data is nowadays much better than previously (both for completeness and accuracy), especially when requested by the customer. However, expectations of manufacturers in this sense should not go too far – to some extent uncertainties in the data will remain, due to the nature of the detector manufacturing process. This is particularly valid for (i) dead layer thickness (‘our’ critical detector parameter), and partly also for (ii) vacuum thickness and (iii) coaxial positioning of the crystal in the end-cap. Fortunately, simple experimental methods to determine these factors with sufficient accuracy (‘tuning’) – utilizing ANGLE efficiency calculations – are known or can readily be performed [10, 11].

From the ANGLE users’ side, insisting on accurate detector specifications from the manufacturer is crucial. Generally these specifications should be requested at the time of purchase of a new detector: for existing detectors, the data may be incomplete, inaccurate, lost or may never have been measured/recorded. Care should be further paid to accurately determining (or carefully estimating) geometrical characteristics (dimensions) and chemical composition of (i) the source, (ii) its container vessel and (iii) intercepting layers (e.g. source support/holder, protecting foils, etc) between the source and the detector end-cap. This is normally not a significant problem.

Reference efficiency curve

Some more care (time and effort) remains to be paid to obtaining *the reference efficiency curve* (REC), $\varepsilon_{p,ref}$ versus E_γ . The user should be aware of the fact that all further ANGLE results for the given detector will be relative to REC with an error propagation factor of 1 (that is to say 100% of the uncertainty in the REC is added in quadrature to the other sources of uncertainty). Investment of care in determining the REC is very important.

One REC per detector is enough, in principle. It is recommended to construct it by counting a number of calibrated point sources at a large distance from the detector (e.g. 20-30 cm), avoiding true coincidences and matrix effects. Also, absolutely calibrated point sources are often certified to better accuracy than voluminous ones. It is generally more prudent to use several single nuclide sources, than a single multi-nuclide one.

However, in order to additionally exploit the ET error compensation effect, one might consider constructing more RECs for the same detector. For instance, the same point sources counted at large distance could also be counted on the detector top, yielding another REC. Calibrated cylindrical and Marinelli sources could produce additional RECs.

In ideal case, using any of several RECs in ε_p calculations would produce the same result for the actual sample, i.e. result should be independent on the choice of REC. Given the fact that all input data (detector, source, and geometry) are inaccurate to some extent, choosing a REC geometry similar to the actual sample geometry should eventually produce better (more accurate) results – due to larger ET error compensation. In other words, if the REC sample/geometry is closer to the actual sample, results are likely to be better. This in itself is a measure of the accuracy of the various sample and detector parameter choices – if two RECs produce results which are close, the implication is that both sample/geometry and detector are well characterized. ANGLE v2.1 allows multiple RECs to be employed for a given detector. This enables that varying of REC could be one of the elements in the analytical procedure optimization.

4. APPLICABILITY TO IN-SITU CHARACTERIZATION OF CONTAMINATED SITES

ANGLE is readily applicable to radioactivity measurements in the environment. Several possibilities are straightforward at user's disposal:

- 'Regular' radioactivity measurements of (i) voluminous (solid or liquid) samples collected at contaminated sites (either in cylindrical or Marinelli beakers), or (ii) filters collecting air radioactivity by means of air pumps ('disc' sources).

ANGLE supports these cases directly through combination of appropriate entries in Source and Container windows. Activity (A) of a particular nuclide is then simply derived from ANGLE calculated full energy detection efficiency and net gamma peak area (N_p) recorded by multichannel analyzer (MCA) during counting time t_m :

$$A \cdot \varepsilon_p = N_p/t_m \quad (6)$$

- Soil radioactivity can be measured by positioning the detector towards the ground or in a hole.

These cases correspond to infinite cylinder and infinite Marinelli geometry, respectively. In practice, however, only limited area relatively close to the detector contributes on a relevant manner to the measurement – outside that area the contribution is negligible, either because of the distance or attenuation, or both, as illustrated in Fig. 10. One meter source radius (cylinder or Marinelli) usually is a good enough approximation. De Corte et al. [12] showed that even 0.4 m was ‘sufficiently infinite’ even for demanding geochronology purposes (soil type: loess) and high gamma energies (up to 1,460.8 keV for ^{40}K , 1,764.5 keV for ^{214}Bi and 2,614.5 keV for ^{208}Tl). It has to be noted that this model assumes the radioactivity to be homogeneously distributed in the soil. Illustration of data entry for quasi-infinite cylindrical and Marinelli sources are given in Figs. 12 and 13 respectively.

- In case of surface contamination infinite soil surface can be approximated by a large, finite disc.

When surface radioactivity migrates to within a certain depth into the soil, slab geometry can be applied. This corresponds to a large thin cylinder from ANGLE calculations standpoint, as shown in Fig. 11. It has to be noted that a previous example (surface contamination) is, in mathematical terms, a special case of this one (disc being a cylinder with height equal to 0).

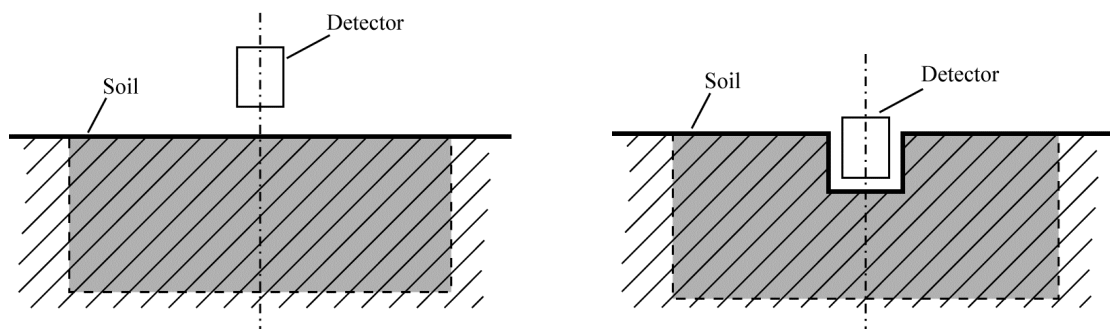


FIG. 10. Very large cylinder and very large Marinelli geometry (replacing quasi-infinite soil source) for in-situ gamma-ray spectrometry using ANGLE software.

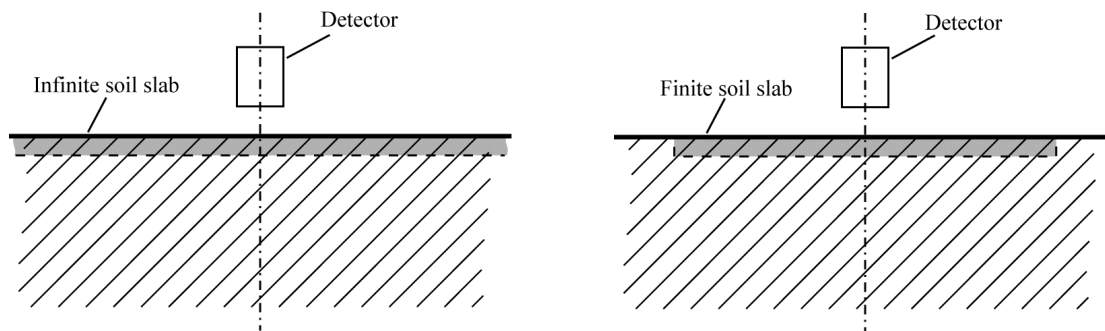


FIG. 11. Infinite and finite soil slab, representing surface contamination which penetrated into the soil to a limited depth.

New container

Container | Container coatings

Container name: Quasi-infinite cylinder

Container type: Cylindrical

Container inside radius: 1000 mm

Container bottom thickness: 0 mm

Container wall thickness: 0 mm

Container foot height: 0 mm

Container material:

Container description: Contaminated soil quasi-infinite cylinder

OK Cancel Help

New geometry

Geometry | Additional intercepting layers

Geometry name: Contamination measurement

For what detector type: Other than well

For what container type: Other than Marinelli

Holder outer radius: 0 mm

Holder cap thickness: 0 mm

Holder cap material:

Holder wall thickness: 0 mm

Holder wall material:

Holder height: 750 mm

Geometry description: Vertically positioned detector above the soil, 75 cm dist

OK Cancel Help

FIG.12. Entering the data for quasi-infinite soil cylinder geometry, effective container radius (upper screen) being given 100 cm, height 100 cm, detector distance from the soil 75 cm (lower screen) (Reproduced courtesy of AMETEK/ORTEC).

New container

Container | Container coatings

Container name: Quasi-infinite soil Marinelli

Container type: Marinelli

Container inside radius: 1000 mm

Marinelli cavity radius: 50 mm

Marinelli cavity depth: 100 mm

Marinelli upper bottom thickness: 0 mm

Marinelli inner side thickness: 0 mm

Marinelli lower bottom thickness: 0 mm

Container material: [Dropdown menu]

Container description: [Text field]

OK Cancel Help

FIG. 13. Entering the data for quasi-infinite soil Marinelli geometry (effective container radius given 100 cm) (Reproduced courtesy of AMETEK/ORTEC).

A few practical arrangements of in-situ gamma-ray spectrometry systems, which accommodate the ANGLE software, are shown in Fig. 14.



FIG. 14. Few practical arrangements of in-situ gamma-ray spectrometry (Reproduced courtesy of AMETEK/ORTEC)

In all above cases, ANGLE will prove helpful not only for activity calculations, but also in counting optimization – to estimate the optimal size of samples to be measured or taken in calculations in place of infinite (e.g. when ‘infinity is reached’ in estimation). Detector calibration (using suitable point or voluminous calibration sources) should be performed prior to ANGLE calculations, as described earlier. For better exploiting efficiency transfer error reduction principle (sample versus calibration source similarity), large calibration sources are preferred.

ANGLE is eligible to expanding its scope of calculation possibilities towards new source geometries and counting arrangements. Even Monte Carlo calculation codes, with some more effort, could be accommodated into ANGLE user friendly and elaborated graphical interface. Both features could be utilized to more complex/demanding quantitative radioactivity measurements of contaminated sites, contributing thus to its characterization.

5. CONCLUSION

ANGLE v3.0 software for semiconductor detector gamma efficiency calculations is presented hereby from theoretical and practical standpoints. Its applicability to in-situ characterization of contaminated sites is shown to be simple and straightforward, as illustrated for in-depth and surface soil contamination. There are possibilities for further ANGLE development and/or adjustments to this particular aim, e.g. within existing or new IAEA coordinated research projects (CRP) or technical cooperation projects (TC) with the University Centre for Nuclear Competence and Knowledge Management (UCNC) of Podgorica in Montenegro. In this sense, a free ANGLE copy could be obtained from UCNC for testing/planning purposes and suggestions/ideas are welcome. ANGLE is commercially available from AMETEK/ORTEC, U.S.A. <http://www.ortec-online.com/software/angle.htm>.

REFERENCES

- [1] MOENS, L., DE DONDER, J., XILEI, L., DE CORTE, F., DE WISPELAERE, A., SIMONITS, A., HOSTE, H., Calculation of the absolute peak efficiency of gamma-ray detectors for different counting geometries, *Nucl. Instrum. Methods Phys. Res.* **187** 2-3 (1981) 451-472.
- [2] ERTEN, H.N., AKSOYOGLU, S., GOKTURK, H., Efficiency calibration and summation effects in gamma-ray spectrometry, *J. Radioanal. Nucl. Chem.* **125** 1 (1988) 3-10.
- [3] LEPY, M-C., ALTZITZOGLOU, T., ARNOLD, D., BRONSON, F., CAPOTE NOY, R., DECOMBAZ, M., DE CORTE, F., EDELMAIER, R., HERRERA PERAZA, E., KLEMOLA, S., KORUN, M., KRALIK, M., NEDER, H., PLAGNARD, J., POMME, S., DE SANOIT, J., SIMA, O., UGLETVEIT, F., VAN VELZEN, L., VIDMAR, T., Intercomparison of efficiency transfer software for gamma-ray spectrometry, *Appl. Radiat. Isot.* **55** 4 (2001) 493-503.
- [4] ABBAS, K., SIMONELLI, F., D'ALBERTI, F., FORTE, M., STROOSNIJDER, M.F., Reliability of two calculation codes for efficiency calibrations of HPGe detectors, *Appl. Radiat. Isot.* **56** 5 (2002) 703-709.
- [5] JACKMAN, K.R., BIEGALSKI, R., Methods and software for predicting germanium detector absolute full-energy peak efficiencies, *J. Radioanal. Nucl. Chem.*, **279** 1 (2009) 355-360.
- [6] VIDMAR, T., CELIK, N., CORNEJO DIAZ, N., DLABAC, A., EWA, I.O.B., CARRAZANA GONZÁLEZ, J.A., HULT, M., JOVANOVIĆ, S., LEPY, M-C., MIHALJEVIĆ, N., SIMA, O., TZIKA, F., JURADO VARGAS, M., VASILOPOULOU, T., VIDMAR, G., Testing efficiency transfer codes for equivalence, *Appl. Radiat. Isot.* **68** 2 (2010) 355-359.
- [7] JOVANOVIĆ, S., DLABAC, A., MIHALJEVIĆ, N., VUKOTIĆ, P., ANGLE: A PC-code for semiconductor detector efficiency calculations, *J. Radioanal. Nucl. Chem.*, **218** 1 (1997) 13-20.
- [8] JOVANOVIĆ, S., DLABAC, A., MIHALJEVIĆ, N., ANGLE v2.1 – New version of the computer code for semiconductor detector gamma-efficiency calculations, *Nucl. Instrum. Methods Phys. Res. Sect. A* **622** 2 (2010) 385-391.
- [9] AMETEK/ORTEC, U.S.A. ANGLE, Advanced Efficiency Calibration Software for High Purity Germanium Detectors, 2008, <http://www.ortec-online.com/software/angle.htm>
- [10] DE WISPELAERE, A., BELLEMANS, F., DE CORTE, F., Proc. International k_0 -Users Workshop–Gent, Astene, Belgium, Sept.30–Oct.2, p.45 (1992).
- [11] VUKOTIĆ, P., MIHALJEVIĆ, N., JOVANOVIĆ, S., DAPCEVIĆ, S., BORELI, F., On the applicability of the effective solid angle concept in activity determination of large cylindrical sources, *J. Radioanal. Nucl. Chem.* **218** 1 (1997) 21-26.

- [12] DE CORTE, F., HOSSAIN, S.M., JOVANOVIĆ, S., DLABAC, A., DE WISPELAERE, A., VANDENBERGHE, D., VAN DEN HAUTE, P., Introduction of Marinelli effective solid angles for correcting the calibration of NaI(Tl) field gamma-ray spectrometry in TL/OSL dating, J.Radioanal. Nucl. Chem., **257** 3 (2003) 551-555.

POSSIBILITIES AND DRAWBACKS OF PORTABLE XRF INSTRUMENTATION FOR CHARACTERIZATION OF METAL CONTAMINATED SITES

E. MARGUÍ

Department of Chemistry, University of Girona
Campus Montilivi s/n, 17071-Girona (Spain)

Email: eva.margui@udg.edu

Abstract

One of the critical factors for successfully conducting characterization of extent of contamination, removal and remedial operations at metal contaminated sites, is a rapid and appropriate response to analyse samples in a timely manner. Rapid, simultaneous, multi-elemental analysis can be performed using X-ray fluorescence spectrometry (XRF), which is a versatile, non-destructive analytical technique commonly used in the environmental field. Field-portable XRF instrumentation (FPXRF) is particularly interesting for such purpose, since it provides near real-time data by in-situ measurements necessary to guide critical field decisions in extent of contamination, removal and remediation actions. Despite that FPXRF analysers have generally less sensitivity than laboratory equipment (i.e. have higher elemental detection limits), the obtained data are in most cases sufficient to meet site action level requirements. However, to obtain in-situ reliable analytical data, a number of factors that may affect FPXRF response must be considered (such as sample matrix effects, accuracy and suitability of calibration standards, sample morphology) and usually, comparison with established laboratory methods and analysis of reference materials are also necessary. The implementation of different configurations of portable XRF spectrometers (benchtop and hand-held systems) for in-situ analysis has been evaluated to achieve reliable analytical results for several types of environmental samples analyses at different scales (from micro to macro). Comparison with established laboratory methods has also been evaluated to test the real capability of portable equipment items for the intended purpose.

1. INTRODUCTION

1.1. In-situ analytical techniques for characterization of metal contaminated sites: The role of field portable X-ray fluorescence spectrometers (FPXRF)

Metal contamination is one of the most ubiquitous, persistent and complex environmental issues, encompassing legacies of the past (e.g. abandoned mines) as well as current anthropogenic activities (e.g. smelting, fuel combustion or electroplating activities). As a consequence, one of the challenges facing society today is the identification, evaluation and remediation of contaminated areas to protect public health and environment quality [1].

Soil Screening Values (SVs) are generic quality standards adopted in many countries to regulate the management of contaminated land. They are usually in the form of concentration thresholds of contaminants in soil (mg/kg soil, expressed as dry weight) above which certain actions are recommended or enforced. The implications of exceeding the soil SVs vary according to national regulatory frameworks [2]. Regulations on limits of concentration for metals in surface waters are also displayed by some international organizations. For instance, the European Water Framework Directive (2008/105/EC) settles the limits of concentration in surface waters of 33 priority substances including Hg, Pb, Cd, Ni and its compounds [3]. Therefore, qualitative and quantitative measurements of the amounts and distribution of metals in the contaminated areas are of significance, leading to the necessity of having appropriate analytical methodologies [4].

The ‘fitness-for-purpose’ of a given analytical technique chosen for the analysis of metal contaminated sites is related to the compliance of some ‘desired’ features, including:

- Multi-elemental capability;
- Simple sample preparation (non-destructive);
- Short term delay in obtaining the measurement results;
- Wide dynamic range;
- High throughput;
- Relatively low investment and operation costs;
- Adequate sensitivity, accuracy and precision of the measurement results.

Field-portable XRF instrumentation (FPXRF) is particularly interesting for such purpose, since it provides near real-time data by in-situ measurements necessary to guide critical field decisions in extent of contamination, removal and remediation actions. The basic components of FPXRF analysers include an excitation source (X-ray tube or radioactive source) to irradiate a sample which in turn fluorescence, and a detection system (usually a semiconductor detector). The entire process is interfaced with a computer that provides general instrument control, data generation, and processing [5]. The most commonly used FPXRF systems have been the so-called ‘hand-held’ analysers that are contained in a single unit and weigh less than 2.5 kg [6]. Such systems are readily adaptable to field operations, though they may be limited by the power capacities of their batteries. Usually they provide a minimum of 8 hours of field use with replacement of batteries. In recent years, the development and commercialization of portable/benchtop tube-powered XRF spectrometers, which offer extreme simplicity of operation in a low-cost compact design, has added the advantage of increasing instrumental sensitivity compared to hand-held instrumentation using isotope sources. It thus improves both precision and productivity and approaches the above-mentioned technique in the environmental field for many analytical problems [7, 8]. However, despite the rapid advances in spectrometer configurations, to obtain in-situ reliable analytical data, a number of factors that may affect FPXRF response must be considered (such as sample matrix effects, accuracy and suitability of calibration standards, sample morphology) and usually, comparison with established laboratory methods and analysis of reference materials are also necessary. For that reason the evaluation of quality assurance and quality control (QA/QC) is of great significance to ensure the data integrity of the field measurements.

1.2. QA/QC considerations for FPXRF measurements

1.2.1. Sample preparation

One of the main advantages of in-situ XRF measurements is that little or no sample preparation is required. However, it has to be taken into account that there are some parameters related to the sample and to the direct XRF measurement that can affect the obtained analytical results. Generally, instrument uncertainty is the least significant source of error in FPXRF analysis. The more significant sources of error are associated to the representativeness of the samples, the sample moisture content, the sample placement and geometry and the physical matrix effects (particle size, heterogeneity, surface condition).

For this reason, even though most FPXRF can measure undisturbed samples directly, a minimal sample preparation protocol is recommended to improve the analytical quality of data. This sample preparation protocol is illustrated in Fig. 1. Ex-situ measurements offer a variety of sample preparation strategies. For instance, a core sampling device may be used to collect the sample to a well-defined depth.

Other sample preparation strategies are based on the preparation of a composite sample of well-ground soil and on its placement in a XRF sample cup for subsequent analysis. The various stages of sample preparation require time and effort, but provide improved measurement accuracy and precision of the results.

1.2.2. Calibration and quantification

In XRF the analytical signal is the intensity of the measured characteristic radiation (in counts per second), which is proportional to the mass fraction of the element in the analysed sample. However, this relationship is not linear in the more general case, since it depends on physical and chemical matrix effects, but also on random and systematic errors due to the spectrometer (detector resolution) and counting procedure employed [9].

Several methods have been described for quantification purposes. Each of those methods has its own advantages and drawbacks, and the choice of the proper method is determined by the particular application and the specific features of the FPXRF instrument. Generally, three types of calibration procedures are used for FPXRF instruments, namely the fundamental parameters calibration (FP), the empirical calibration and the Compton peak normalization. The main advantage of FP over empirical calibration is that no previously collected site-specific samples with confirmed and validated analytical results are necessary. However, the analyst should be aware of the limitations imposed on FP calibration by particle size and matrix effects. The Compton normalization is perhaps one of the methods of choice in FPXRF instrumentation. This method is based on the analysis of a single, certified standard and normalization for the incoherent backscattering of X-ray radiation from the excitation source. Since the Compton peak intensity changes with different matrices, normalizing to the Compton peak can reduce problems with varying matrix effects among samples.

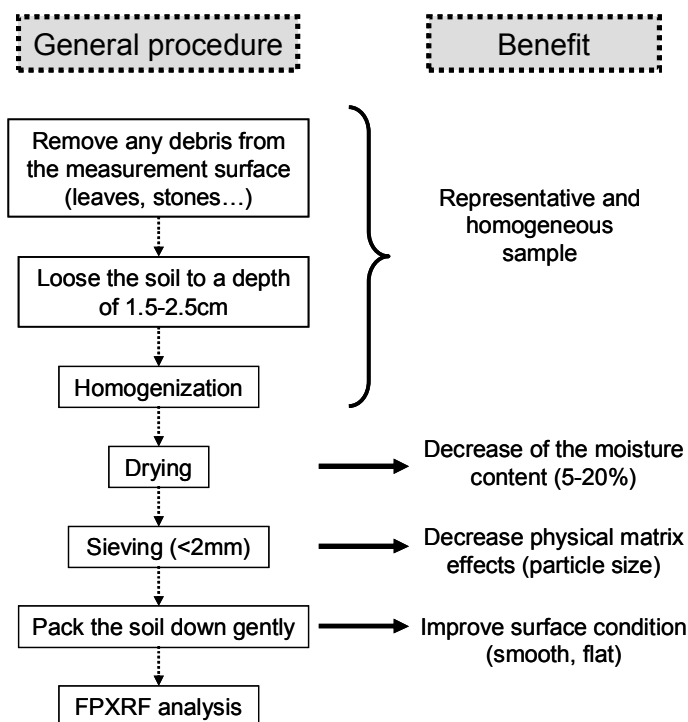


FIG.1. Recommended sample preparation protocol for in-situ soil measurements using FPXRF instrumentation.

The definition of ‘quantitative’ XRF analysis depends, to a large extent, on the application and intended use for the data. For environmental applications, FPXRF results are quantitative when measurement precision is within 20% of the values for each analyte in the analysis of a certified reference material [10].

1.2.3. Limits of detection

Limits of detection (LODs) for the elements of interest have to be carefully determined for each particular application, since, depending on site action levels requirements, FPXRF analysis may not be suitable. LODs are commonly estimated by analysing certified reference materials of the appropriate matrix and within the appropriate calibration range for the application. LODs are highly dependent on the instrument characteristics (excitation source, type of detector), on the sample matrix, on the element itself (fluorescence yield) and on the measuring time. For similar samples the individual LODs improve as a function of the square root of the testing time. For instance, measuring times lower than 50 s are used for ‘hot-spot’ screening, but to meet higher sensitivity requirements, measuring times of 200 to 300 s are used. Limits of detection in the low mg/kg range (10-50 mg/kg) have been reported for the determination of metals (Zn, As, Se) in soils for testing times between 60 and 120 s [11].

1.2.4. Quality assurance

Quality assurance (QA) is a basic requirement of any analytical method. No measurement has value for decision-making process unless its precision and accuracy are known and understood. QA programs generally involve calibration checks at several concentrations (accuracy evaluation) and replicates to assess variation (precision evaluation). Moreover, to determine field data quality, FPXRF results are generally compared to laboratory data using standard methods. In the case of soil analysis, results are compared to laboratory data obtained using a sample digestion procedure [12].

Three equally important QA objectives (QA1, QA2 and QA3) have been defined by the US EPA for assessing and substantiating the field measurements [13]. The characteristics of each of the QA objectives should be evaluated to determine which one or combination thereof fits the data use objectives established for the site. The criteria for characterizing the data quality according to the US EPA are displayed in Table 1.

TABLE 1. CRITERIA FOR CHARACTERIZING DATA QUALITY (ADAPTED FROM US EPA, 1990 [13])

Quality Level	Purpose of the field measurement	Requirement
Q1	Qualitative screening	RSD>20% R ² <0.70 Inferential statistics indicate that the two data sets are statistically different.
Q2	Quantitative screening	RSD<20% R ² =0.70-1 Inferential statistics indicate that the two data sets are statistically different, i.e. relationship y=mx or y=mx+c accepted.
Q3	Definitive	RSD<10% R ² =0.85-1 Inferential statistics (test for slope=1 and y-intercept=0) indicate that the two data sets are statistically similar.

RSD: Relative standard deviation

2. APPLICATION CASES

2.1. Determination of As anomalies in floodplains

The spatial heterogeneity of As concentrations in soils from an area characterized by flooding events, which lead to reducing conditions and As liberation in soils, was studied. Taking into account the high number of soil samples to be analysed ($n>100$), the use of a hand-held FPXRF system to determine As concentrations in soils was considered appropriate. A commercial hand-held Thermo Scientific NITON XLt analyser equipped with a miniature X-ray tube (Ag anode, 40 kV/50 μ A) and a high-performance Peltier-cooled Si-PIN detector were used. To perform the in-situ FPXRF analysis, the sample preparation protocol displayed in Fig. 1 was followed. Compton normalization algorithm was selected as calibration strategy for quantification purposes.

A limit of detection for As of 6 mg/kg was estimated using a measuring time of 120 s. This value was adequate for the planned purpose, since the As content in most of the samples was between 6.9 and 45 mg/kg (the average was 22 mg/kg). Therefore, using a simple in-situ FPXRF method, it was possible to study the As ‘hot-spots’ present in the investigated area. Additionally, the used XRF system provides multi-elemental information that improve the understanding of the controlling factors on As mobility. It was found that As was significantly positively correlated with total Fe and Mn concentrations and it was deduced that As on the floodplain was mainly immobilized by sorption and co-precipitation processes involving Fe and Mn oxides.

To evaluate the quality assurance of the obtained field measurements the precision of the results were evaluated by calculating the relative standard deviation (RSD) of duplicate sample measurements. The calculated RSD values range from 6 to 20%. In addition, a comparability study with laboratory data using a standard method was also carried out. For such purpose, 10% of the total number of samples analysed by in-situ method (n=10) were digested using a microwave oven digestion (EPA Method 3052 [15]) and analysed by ICP-MS. A linear regression model was used to investigate the relationship between both methodologies. As it is shown in Fig. 2, despite a good linear correlation ($R^2=0.9291$) between the two datasets, an underestimation of the As concentrations was found when using the in-situ method. Taking this into account, the in-situ data obtained could be used for quantitative screening purposes according to the criteria for characterizing data quality displayed in Table 1 (RSD<20%, $R^2=0.70-1.0$) [14].

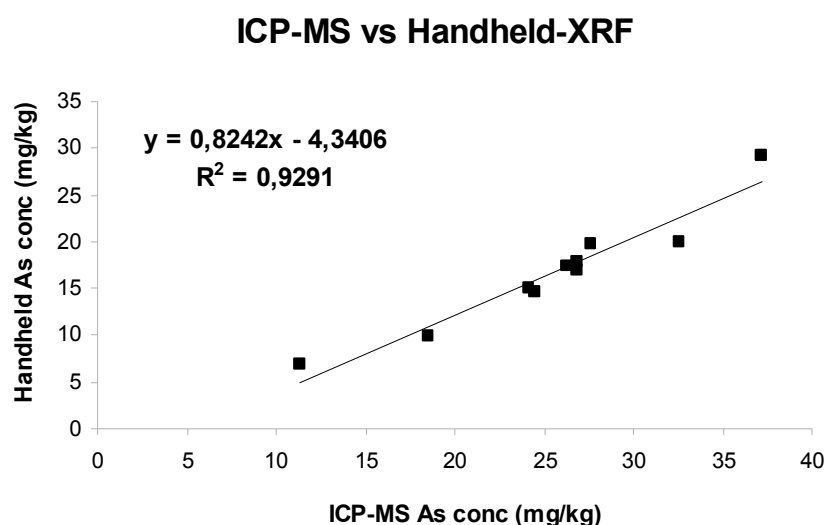


FIG. 2. Relationship between the results obtained with a laboratory standard method (microwave oven digestion + ICP-MS analysis) and those obtained with the in-situ FPXRF method for As determination in soil samples (n=10) [14].

From this study, the hand-held instrumentation proves to be a powerful tool for in-situ determination of As in flood plains, since the limits of detection and the quality of the data obtained were suitable for the intended purpose.

2.2. Environmental impact of past mining activities

Portable XRF systems were also used to evaluate metal contamination in areas affected by past mining activities (determination and distribution of metals in soils and ores) and to study remediation procedures (phytoremediation treatments) of the areas. For such purpose a portable benchtop EDXRF system (XDAL spectrometer from Helmut Fischer GmbH, Germany) was used. The main features of this equipment item are the use of a low power tungsten X-ray tube operating at a maximum power of 50 W, and the possibility to perform the measurements using a small spot X-Ray beam (0.2, 0.6, 1.0 and 2.0 mm). On such type of equipment item, the characteristic radiation emitted by the elements present in the sample is detected by a Si(Pin) diode detector with a energy resolution of 190 eV at 5.89 keV (Mn K_{α} line). A hole mirror located in the path of the primary beam not only allows for a precise selection of the measurement spot using a colour video camera, but also for viewing the area on a PC monitor during the measurement procedure.

Moreover, the use of an XYZ-programmable motorized stage enables fully automatic measurements. Due to the low power X-ray tube and the fact that the instrument works in open-air conditions, it is not necessary to place the sample to be analysed in a cup of fixed external dimensions into a radiation protection chamber. Therefore, the system has no constraints with respect to the dimensions and shape of the samples.

Using this instrument it was possible to study the distribution of regulated pollutants among different mineral phases ore veins. Besides, the evaluation of effects of metal pollution (Pb, Zn) in sediments was performed analysing core samples of metal polluted sediments to a depth of 30 cm. The metal distribution in core samples was studied performing 2D mappings (18x48 points) using a measuring time of 50 s/point and a spot area of 600 μm . The results obtained for Pb and Zn distributions in overbank sediment affected by mining activities are displayed in Fig. 3. From the qualitative information obtained it was found that metals tend to accumulate in the upper layers of the sediment profile. Therefore, XRF-mapping provides interesting data for the assessment of metal mobility along the unsaturated soil zone of metal polluted areas [16]. In this case, to evaluate the quality of the obtained results, cores were split in slices of 2 cm and pellets weighing 5 g of sample and 0.4 g of Elvacite[®] (acrylic resin) were prepared and analysed by means of laboratory WDXRF instrumentation. Good correlation between portable EDXRF signal and concentrations determined by WDXRF was found. This fact demonstrates the suitability of using the proposed methodology for the planned purpose.

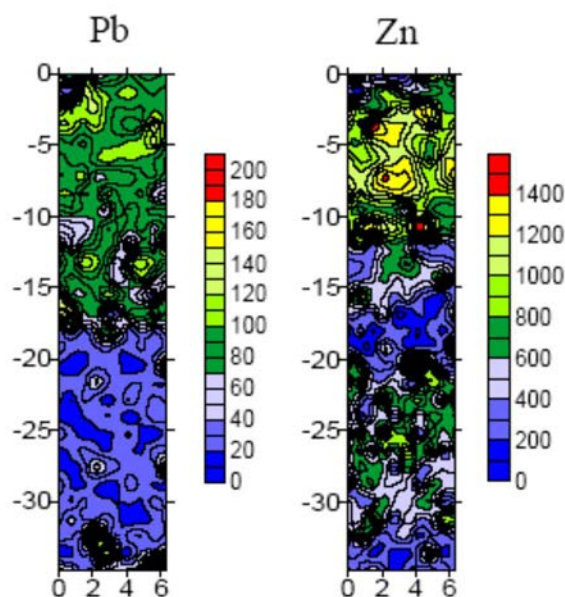


FIG. 3. Two-dimensional Pb and Zn mappings of a soil affected by past mining activities by portable EDXR analyser (Instrument conditions: spot size (600 μm), measuring time (50 s/spot), gridding (18x48 points) [16].

The same FPXRF analyser was used as analytical technique for studying the potential use of sunflowers (*Helianthus annuus*) for the phytoremediation of an abandoned Pb/Zn mining area. The simplicity and ability to operate at room temperature and open-air conditions provide a flexible setup for the rapid analysis of vegetation material without complicated prior sample pre-treatments.

Vegetation specimens were uprooted from the land plots and rinsed with distilled water (to remove superficial dust), placed between several layers of absorbent paper and pressed under a heavy weight until the specimen was free of moisture. The objective of such procedure was to preserve the morphological integrity of the plant and to obtain a straight specimen as required to carry out EDXRF analysis. After that, the vegetation tissues were placed directly into the measurement chamber for subsequent EDXRF analysis.

To study in more detail the translocation of metals from the bottom to the top of sunflowers specimens, the analysis of the leaves along the length of the specimens was carried out. As shown in Fig. 4, metals tended to accumulate with age in the basal part of the sunflowers whereas metal contents in the top part were fairly constant or decreased irregularly. It was found that the contents of Zn and Pb in the leaves nearest to the ground were up to 9 times higher than those close to the tip. It is interesting to remark that this distribution profile along the sunflower leaves was similar for both investigated sampling sites (Zone A and Zone B) but different to that from the control area in which no significant differences were observed between Zn and Pb content in basal and the top part of vegetation specimens.

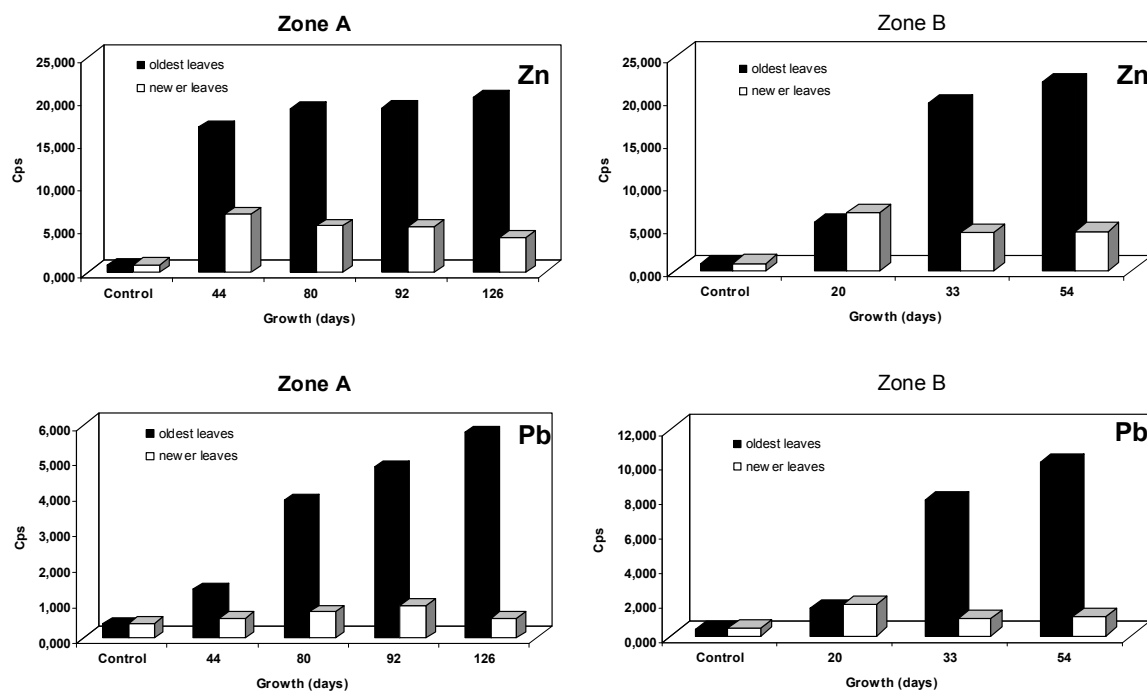


FIG. 4. Metal accumulation in sunflowers collected at two areas affected by mining operations (Zone A and Zone B) over time (Instrument conditions: spot size (1.0 mm), measuring time (300 s)) [8].

To estimate the detection limit and the sensitivity of the proposed methodology for Pb and Zn determination, aerial elemental concentrations ($\mu\text{g}/\text{cm}^2$) were calculated using peak areas intensity versus concentration ratios determined using thin standards prepared at the laboratory. Taking into account the obtained calibration curves for Pb and Zn, the contents in the sunflowers leaves from the mining land spots ranged from $59.7 \mu\text{g}/\text{cm}^2$ (Zone A) to $100.5 \mu\text{g}/\text{cm}^2$ (Zone B) for Pb and from $99.3 \mu\text{g}/\text{cm}^2$ (Zone A) to $108 \mu\text{g}/\text{cm}^2$ (Zone B) for Zn. These concentration values were significantly higher than the values determined in the control area, which were $1.4 \mu\text{g}/\text{cm}^2$ for Zn and $<0.38 \mu\text{g}/\text{cm}^2$ for Pb. This fact demonstrated the great capability of sunflowers to accumulate Pb and Zn and their potential use for phytoremediation of the studied mining area [8].

2.3. Metal content in industrial wastewater effluents

The monitoring of heavy metals in industrial wastewater effluents is nowadays an important activity. The screening of elemental composition of inlet effluents and quantitative analysis of outlet effluents is of particular interest to study the efficiency of the chemical treatment processes to eliminate metals and to comply with current established concentration limits, respectively. In this sense, fast analytical methodologies, which entail simple sample preparation, are desired. Two different analytical strategies based on the use of FPXRF systems were used for this purpose.

In the first case, commercial extraction disks (3M Empore chelating SPE disks) were used as solid sorbent to preconcentrate metals for subsequent FPXRF analysis using a benchtop EDXRF XDAL spectrometer from Helmut Fischer GmbH in Germany. It is important to note that the use of thin targets as preconcentration supports avoids the need of matrix and thickness effect corrections, commonly required in XRF analysis, since, in this case, the attenuation of the incident primary and emergent secondary spectral line radiation is almost negligible and, thus, the intensity of the analyte is proportional to its concentration. An additional advantage of using these materials is the collection of the elements on the solid by means of a simple filtration procedure. Therefore, this analytical strategy can be easily applied for in-situ analysis of the target water samples. A comparison of the results obtained by the analysis of a wastewater sample (outlet effluent) using the proposed methodology and by ICP-MS is presented in Table 2. Good agreement is obtained between the two datasets. Moreover, the calculated limits of detection for FPXRF method prove to be in most cases suitable for the metal determination in this type of water samples.

TABLE 2. COMPARISON OF RESULTS OBTAINED FROM PRECONCENTRATION USING CHELATING DISKS, FPXRF (BENCHTOP EDXRF ANALYSER) AND ICP-MS ANALYSIS OF A WASTEWATER SAMPLE. RESULTS ARE EXPRESSED AS $\mu\text{g/L}$.

Element	FPXRF method			ICP-MS	
	LOD	Mean	SD	Mean	SD
Ni	1.2	351	9	351	7
Cu	2.4	114	3	130	3
Zn	1.7	350	5	400	8
Pb	1.4	n.d	-	n.d	-
Cd	16	n.d	-	n.d	-

In a second study, the possibilities and drawbacks of a benchtop total reflection X-ray fluorescence spectrometer (TXRF) for the rapid and simple determination of some inorganic impurities (As, Ba, Cd, Cu, Cr, Sn, Fe, Mn, Ni, Pb, Se and Zn) in inlet and outlet industrial wastewater effluents from metallurgical and tanning leather factories were tested [17]. For routine and screening analysis of industrial inlet and outlet effluents, TXRF wastewater samples analyses were directly performed depositing 20 μL of the internal standardised sample on a quartz glass reflector and using a measuring time of 500 s. Acceptable results were obtained when applying this methodology for the analysis of the certified reference material SPS-WW2 ('Reference Material for Measurement of Elements in Wastewaters').

The direct analysis of the inlet/outlet effluents by TXRF leads, in most cases, to accurate results compared to the data obtained by ICP-OES/ICP-MS analysis after microwave-assisted digestion, as shown in Table 3. The highest discrepancies were obtained for Fe measurements. The underestimation on Fe concentrations was probably caused by the association of this element within suspended organic matter particles, which could lead to inhomogeneity in the sampling process, and to associated deviation in the quality of the TXRF measurements. Nevertheless, TXRF results obtained for direct analysis of wastewater samples could be considered as acceptable and they could be helpful at least for a fast and simple screening method of heavy metals in this type of complex liquid samples. The fact that the analysis could be performed directly on the raw wastewaters entails less sample manipulation and lower amounts of reagents and therefore, cost and time savings for the industrial laboratories.

Additional advantages of the proposed TXRF method are the multi-elemental information of the sample, the easy quantitation through internal standardization and also low operating costs, since the benchtop system does not require any cooling media and gas consumption for its operation.

TABLE 3. COMPARISON OF RESULTS OBTAINED FROM BENCHTOP TXRF ANALYSER AND ICP-MS ANALYSIS OF METALLURGICAL AND TANNING WASTEWATER SAMPLES. RESULTS ARE EXPRESSED AS MG/L

	Inlet effluent		Outlet effluent	
	TXRF method	ICP-MS	TXRF method	ICP-MS
	Mean/SD	Mean/SD	Mean/SD	Mean/SD
Metallurgical wastewater				
Cr	12.5/0.3	12.6/1.0	n.d	n.m
Fe	88.9/0.9	99.0/2.0	n.d	n.m
Ni	93.8/0.8	82.0/3.0	0.22/0.02	0.17/0.04
Cu	27.1/0.3	27.9/0.8	n.d	n.m
Zn	453.3/3.1	389.0/2.0	0.62/0.03	0.59/0.02
Pb	0.93/0.03	n.m	n.d	n.m
Tanning wastewater				
Cr	5.1/0.3	4.00/0.05	n.d	0.156/0.002
Fe	0.77/0.02	1.50/0.02	3.0/0.1	3.65/0.01
Ni	0.11/0.01	0.093/0.001	n.d	n.m
Cu	0.25/0.03	0.279/0.001	0.37/0.08	0.261/0.006
Zn	0.21/0.01	0.19/0.02	n.d	n.m
Pb	0.93/0.01	0.768/0.005	n.d	n.m

3. CONCLUSIONS AND RECOMMENDATIONS

FPXRF analysers have proven to be a viable, cost- and time-effective approach for in-situ analysis of a variety of environmental samples. FPXRF provides both qualitative and quantitative information about site contamination. Although FPXRF analysers have generally less sensitivity than laboratory equipment (i.e. have higher elemental detection limits), the obtained data are, in most cases, sufficient to meet site action level requirements and to map out contamination patterns, and to assess spatial distribution. However, to obtain in-situ reliable analytical data, a number of factors that may affect FPXRF response must be considered (sample matrix effects, accuracy and suitability of calibration standards, sample morphology) and usually, comparison with established laboratory methods and analysis of reference materials are also necessary.

A summary of the advantages and limitations of using FPXRF for characterization of metal contaminated sites over the laboratory analysis is presented in Table 4.

TABLE 4. ADVANTAGES AND LIMITATIONS OF USING FPXRF OVER LABORATORY ANALYSIS

Advantages	Limitations
<ul style="list-style-type: none"> ▪ Screening tool to design a targeted sampling strategy; ▪ Multi-elemental information; ▪ Minimal sample preparation; ▪ On-site decision (remediation strategies); ▪ Allow prioritization of sample analysis; ▪ Relatively low investment and operational costs; ▪ Versatility (solid, liquid samples). 	<ul style="list-style-type: none"> ▪ Need for laboratory analysis check; ▪ Detection limits require careful consideration; ▪ More reliable for some metals than for others; ▪ Heterogeneity of sample may affect the measurement results.

4. ACKNOWLEDGMENTS

This work was supported by the Spanish “Consolider Ingenio 2010” Program (Project ref. CSD2006-00044) and the Spanish National Research Program (Project ref. CGL2007-66861-C4). E. Marguí gratefully acknowledges the research contract from the Spanish Council for Scientific research (CSIC, JAE-Doc Program contract).

The author would like to thank the following institutions that have collaborated in the presented work: Laboratory of X-ray analytical applications (LARX, ICTJA-CSIC, Spain), Department of Chemistry of the University of Girona (Spain), Micro and Trace Analysis Center (University of Antwerpen, Belgium) and Département Analyse Surveillance Environnement (CEA, Bruyères-le-Chatel, France), Laboratoire de Géophysique Interne et Tectonophysique (LGIT-OSUG, University of Grenoble-I, Grenoble, France).

Instrumentation trade names are included for the benefit of the reader and do not imply an endorsement of or a preference for the products listed.

REFERENCES

- [1] MANAHAN, S.E., Environmental Chemistry. Lewis Publishers, seventh edition (2002).
- [2] CARLON, C., Derivation methods of soil screening values in Europe. A review and evaluation of national procedures towards harmonization. European Commission, Joint Research Centre, Ispra. EUR22805-EN, 306pp. (2007).
- [3] Directive 2008/105/EC of the European Parliament and of the Council of 16 December 2008 on environmental quality standards in the field of water policy and amending. Official Journal of the European Union (EN 24.12.2008)
- [4] WISE, D.L., TRANTOLO, D.J., Remediation of hazardous waste contaminated soils. Marcel Dekker, Inc. (1994).
- [5] KALNICKY, D.J., SINGHVI, R., Field portable XRF analysis of environmental samples. J. Hazard. Mater. **83** (2001) 93.
- [6] “The ideal screening tool for environmental testing”. NITON XLt / XLp/Xli700. (<http://www.niton.com/environmental-analysis.aspx?sflang=en>).
- [7] MARGUI, E., TAPIAS, J.C., CASAS, A., HIDALGO, M., QUERALT, I. Analysis of inlet and outlet industrial wastewater effluents by means of benchtop total reflection X-ray fluorescence spectrometry, Chemosphere **80** (2010) 263.
- [8] MARGUI, E., JURADO, A., HIDALGO, M., PARDINI, G., GISPERT, M., QUERALT, I. Application of small-spot energy dispersive X-ray fluorescence instrumentation in phytoremediation activities around metal mines. Appl. Spectrosc. **63** (2009) 1396.

- [9] VAN GRIEKEN R., MARKOWICZ, A., Handbook of X-ray Spectrometry. Marcel Dekker, Inc. New York (2002) (ISBN:0-8247-0600-5).
- [10] Field portable X-ray fluorescence spectrometry for the determination of elemental concentrations in soil and sediment. EPA Method 6200 (2007).
- [11] NITON[®] XLt 700 Series Instruments. Elemental limits of detection in soils, mg/kg. NITON LLC (2004).
- [12] RADU, T., DIAMOND, D., Comparison of soil pollution concentrations determined using AAS and portable XRF techniques, J. Hazard. Mater. **171** (2009) 1168.
- [13] Quality Assurance/Quality control guidance for removal activities. Sampling QA/QC plan and data validation procedures. EPA/540/G-90/004. OSWER Directive 9360.4-01 (1990).
- [14] PARSON, C., MARGUI, E., PILI, E., FLOOR, G.H., ROMAN-ROSS, G., CHARLET, L. Quantification of trace arsenic in soils by field-portable X-ray fluorescence spectrometry: Considerations for sample preparation and measurement conditions, J. Hazard. Mater. **62** (2013) 1213.
- [15] Sample digestion methods: Microwave assisted digestion of siliceous and organically based matrices. EPA Test Methods on-line (SW-846)
<http://www.epa.gov/epawaste/hazard/testmethods/sw846/pdfs/3052.pdf>
- [16] GONZALEZ-FERNANDEZ, O., QUERALT, I. Fast elemental screening of soil and sediment profiles using small-spot energy dispersive X-ray fluorescence: Application to mine sediments geochemistry, Appl. Spectrosc. **64** (2010) 1100.
- [17] MARGUI, E., TAPIAS, J.C., CASAS, A., HIDALGO, M., QUERALT, I. Analysis of inlet and outlet industrial wastewater effluents by means of benchtop total reflection X-ray fluorescence spectrometry, Chemosphere **80** (2010) 2630.

ENVIRONMENTAL RADIOACTIVITY MONITORING PLAN IN URUGUAY

M. DEL R. ODINO MOURE, E. REINA, L. PIUMA, A. GABRIELLI

Dirección Nacional de Energía y Tecnología Nuclear; ²Dirección Nacional de Minería y Geología, Montevideo, Uruguay

Email: rosario.odino@miem.gub.uy

Abstract

Natural radionuclides are present in many natural resources. The study of natural radioactivity and radioactive contamination of territories is an important and necessary condition for the correct understanding and investigation of how the exposure to sources of radiation could affect the environment and the population. Uruguay's economy relies heavily on trade, particularly in livestock production and agricultural exports. Today, agriculture contributes roughly to 15% of the country's Gross Domestic Product (GDP). This work describes the aim of the radioactivity monitoring plan in Uruguay, how it was implemented, the sampling sites, type of samples, the analytical and measurement methods and the quality control used. The activity concentrations of ⁴⁰K, natural radionuclides of the ²³⁸U and ²³²Th series, and ¹³⁷Cs were measured. The representative results of the environmental samples and of the principal Uruguayan food products are reported. The obtained results show that in all analysed food products (meat, milk, cheese, butter and rice), ¹³⁷Cs activity concentrations are below the detection limit. In environmental samples, no significant values of ¹³⁷Cs are present in soil samples. All the values obtained are not different from the values of the natural background. According to the ALARA principle for protection of the population, exposure should be 'as low as reasonably achievable'. Uruguay is working in the regulatory framework to establish national regulations based on the results of its environmental radioactivity monitoring plan.

1. INTRODUCTION

Uruguay is located in the southern hemisphere on the Atlantic seaboard of South America between 53 and 58 west longitude, and 30 and 35 south latitude. It is surrounded on the west by Argentina, on the north and north-east by Brazil, and on the south-east by the Atlantic Ocean. Montevideo is the capital and major port of the Río de la Plata. Uruguay is a water-rich land. It is inhabited by 3.5 million people, of whom 1.4 million live in the capital Montevideo and its metropolitan area. It has an area of 176,214 km² of continental land and 142,199 km² of jurisdictional water. With respect to the climate, Uruguay is located entirely within the temperate zone, Uruguay has a climate that is fairly uniform nationwide. Seasons are fairly well defined. Uruguay's economy relies heavily on trade, particularly in livestock production and agricultural exports. Today, agriculture contributes roughly to 15% of the country's GDP and is still the main foreign exchange earner. For that reason it is very important to recognize and certify the quality of those products [1].

Since more than fifteen years, with the purpose to know the natural and artificial radioactivity in the environment and food products, samples of livestock meat, milk, milk powder, cheeses, and soils, superficial and subterranean water, etc, were analysed by high-resolution gamma-ray spectrometry, but without a formal program. In 2001 the authorities of the Ministry of Industry, Energy and Mines – National Direction of Energy and Nuclear Technology considered the importance of determining the radioactivity levels of the Uruguayan territory, whether natural levels, anthropogenic/fallout levels and to establish a radiation background of the country. With the support of the IAEA, in the frame of the technical cooperation project URU/9/008 "Environmental Radioactivity Monitoring Plan in Uruguay", a program was established and it began to operate in March 2003.

In the frame of the project an automatic monitoring station for air particulate matter was installed. It began to operate in March 2004; it is operating a monitoring Station (Berthold Brand) in real-time, 24 hours a day, in order to determine the alpha, beta and gamma emissions, natural and artificial radiation. It also measures the concentration of radon gas (natural origin radiation) and determines the dose-rate. At the end of the project, a gamma-ray spectrometry laboratory was installed and continues since then to work in the frame of the national program. The analysed samples are soils, sediments, waters, milk products and meat produced domestically. The results obtained in soils, milk products and meat are presented.

3.1. Radioactivity monitoring plan

Most of the radiation dose comes naturally from the environment. Smaller portions come from medicine, consumer products and other sources. The main external source of irradiation to the human body is the gamma radiation emitted from naturally occurring radioisotopes, such as ^{40}K and the radionuclides from the ^{232}Th , ^{235}U and ^{238}U series and their decay products [2, 3]. The study of natural radioactivity and radioactive contamination of territories is an important and necessary condition for the correct understanding and investigation of how the exposure to sources of radiation could affect the environment and the population. Therefore for the safety of the population it is important to know the levels of radioactivity to which the population is exposed [4, 5].

3.2. Some considerations related with the activities of the project URU/9/008

In relation to the activities of the project URU/9/008, the following considerations were taken into account:

- For the study (measurement/analysis) of environmental levels of radioactivity it was necessary to upgrade the facilities of the laboratories. For this purpose, a new Germanium detector, an electronic chain and new software were acquired.
- The samples to be collected were properly selected: soil, sediments, meat, milk products, grains – especially rice, waters, and particulate matter.
- The radionuclides to be analysed were properly selected: natural radionuclides: ^{40}K ; ^{238}U and ^{232}Th series (^{226}Ra and ^{228}Ra), anthropogenic radionuclide: ^{137}Cs
- A suitable sampling frequency and geographical distribution was established.

2. EXPERIMENTAL CONSIDERATIONS

The activity concentrations of ^{40}K and natural radionuclides of the ^{238}U and ^{232}Th series (^{226}Ra and ^{228}Ra) and anthropogenic ^{137}Cs were measured. Because of the secular equilibrium conditions reached between ^{232}Th and ^{238}U and their decay products, the ^{232}Th activity concentration was determined from the average concentrations of ^{212}Pb (238.63 keV) and ^{228}Ac (911.07 keV). The activity concentration of ^{238}U (^{226}Ra) was determined from the average concentrations of the ^{214}Pb (351.92 keV) and ^{214}Bi (609.31 keV) decay products. ^{40}K was measured directly at its line (1,460.75 keV) and ^{137}Cs was determined at its line (661.66 keV) [6].

2.1. Sampling sites and frequency

Uruguay is divided in nineteen departments. Soils samples are taken once a year in different departments since 2004 consisting of 1 m² soil/sediment with 5 cm depth; the coordinates of the sampling sites are detailed in Table 1. In order to obtain representative samples of rice, milk products and meat from all the departments of the country, a program was developed in cooperation with the Ministry of Livestock, Agriculture and Fisheries. The monitoring station for air particulate matter is located in Colonia, 80 km from the nuclear facilities of the neighbouring country; it works 24 hours a day, since March 2004.

TABLE 1. SAMPLING SITES

Department	Coordinates
Artigas	30° 37' S 56° 56' W
Canelones	34° 35' S 55° 53' W
Cerro Largo	32° 26' S 54° 19' W
Colonia	34° 10' S 57° 41' W
Durazno	33° 02' S 56° 01' W
Flores	33° 33' S 26° 53' W
Florida	33° 47' S 55° 49' W
Lavalleja	33° 55' S 54° 57' W
Paysandu	32° 03' S 57° 19' W
Rivera	31° 28' S 55° 15' W
Rio Negro	32° 47' S 57° 26' W
Rocha	34° 00' S 53° 59' W
Salto	31° 18' S 57° 02' W
San José	34° 20' S 56° 43' W
Soriano	33° 31' S 57° 45' W
Tacuarembó	32° 06' S 55° 45' W
Treinta y Tres	33° 03' S 54° 13' W

2.2. Sample preparation

The soil samples are dried at $(60 \pm 5)^{\circ}\text{C}$ to constant weight. The samples are sieved through a 2 mm sieve and the fractions below 2 mm are homogenized and used for the direct determination of gamma-ray emitting radionuclides. The fractions above 2 mm are stored. Marinelli geometry (1 kg) is used [7]. Food products samples are dried at $(55 \pm 5)^{\circ}\text{C}$ for 24 hours and then measured directly in a 1 kg Marinelli geometry for 64,800 s [7].

3. ANALYSIS AND MEASUREMENT

The samples are measured using a gamma-ray spectrometry system, consisting in a coaxial Ge detector (model Canberra GC3020), equipped with a vertical dipstick, and its resolution and efficiency are shown in Table 2, Fig. 1 and Fig. 2.

TABLE 2. RESOLUTION OF GERMANIUM DETECTOR

E (keV)	FWHM (keV)
1,332	1.85
122	0.842
661	1.22

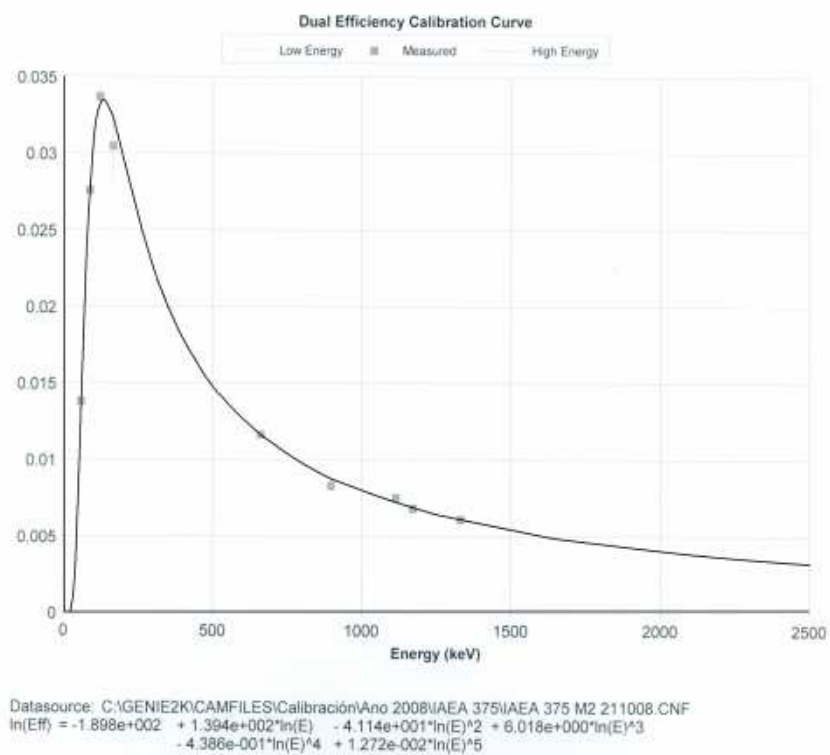


FIG. 1. Efficiency curve for IAEA-375 Soil Certified Reference Material.

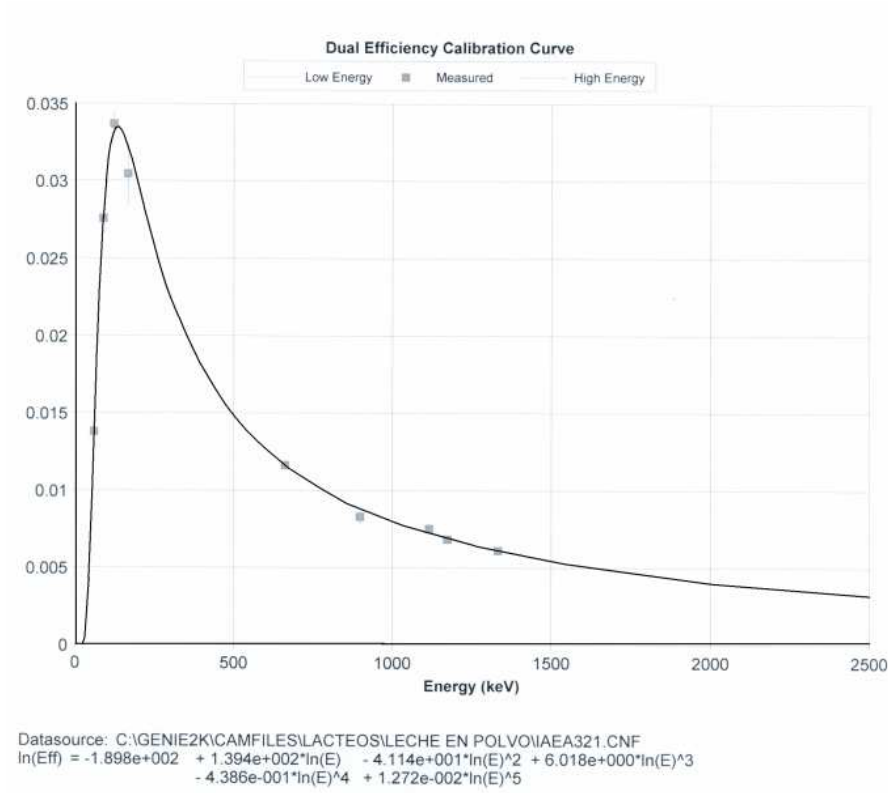


FIG. 2. Efficiency curve for IAEA-321 Milk Powder Certified Reference Material.

The detector is lead shielded. The software Genie 2000 is used to evaluate the spectra and for calculations of the activity concentrations. Detection limits (LD) are calculated using the Currie formula [8].

The uncertainties are calculated using the following formulas [9]:

$$\text{Uncertainty in } A: \frac{u_c(A)}{A} = \sqrt{\left(\frac{u(m)}{m}\right)^2 + \left(\frac{u(N)}{N}\right)^2 + \left(\frac{u(\gamma)}{\gamma}\right)^2 + \left(\frac{u(\varepsilon)}{\varepsilon}\right)^2 + \left(\frac{u(K)}{K}\right)^2}$$

Where $K = K_1 \cdot K_2 \cdot K_3 \cdot K_4 \cdot K_5$

$$\text{Uncertainty in } K: \frac{u(K)}{K} = \sqrt{\left(\frac{u(K_1)}{K_1}\right)^2 + \left(\frac{u(K_2)}{K_2}\right)^2 + \left(\frac{u(K_3)}{K_3}\right)^2 + \left(\frac{u(K_4)}{K_4}\right)^2 + \left(\frac{u(K_5)}{K_5}\right)^2}$$

Certified Reference Materials IAEA-375 and IAEA-SOIL 6 are used as control samples for soils, and IAEA-321 as control sample for milk products. The measured and recommended values for the activity concentration of ^{137}Cs are in good agreement. The samples are measured in the same manner as those in the monitoring program. The laboratory participates also in laboratory intercomparison exercises [10].

4. RESULTS

The activity concentrations in soils of the radionuclides of the ^{238}U series (^{226}Ra), ^{232}Th series (^{228}Ra and ^{232}Th), ^{40}K and ^{137}Cs are expressed in Bq/kg of dry matter, and are presented in Tables 3 and 4.

TABLE 3. RADIONUCLIDES IN URUGUAYAN SOILS - YEAR 2009

Coordinates	Departments	^{40}K (Bq/kg)	^{226}Ra (Bq/kg)	^{232}Th (Bq/kg)	^{137}Cs (Bq/kg)
		1,054.1 ±			
32° 26'S 54° 19'W	Cerro Largo	100.0	19.3 ± 1.5	75.4 ± 7.0	2.1 ± 0.5
34° 10'S 57° 41'W	Colonia	340.5 ± 30.5	14.1 ± 1.0	19.1 ± 1.5	2.2 ± 0.5
31° 18'S 57° 02'W	Salto	89.5 ± 5.0	7.2 ± 0.5	10.5 ± 1.0	<DL
34° 20'S 56° 43'W	San José	439.5 ± 40.0	23.2 ± 2.0	50.5 ± 5.0	3.2 ± 0.5

TABLE 4. RADIONUCLIDES IN COLONIA SOILS FROM 2004 TO 2009

Year	^{40}K (Bq/kg)	^{226}Ra (Bq/kg)	^{232}Th (Bq/kg)	^{137}Cs (Bq/kg)
2004	491.6 ± 45.0	19.2 ± 1.5	8.6 ± 0.5	2.3 ± 0.5
2005	560.0 ± 50.5	21.6 ± 2.0	35.8 ± 30.5	1.8 ± 0.2
2006	495.0 ± 45.0	20.5 ± 2.0	35.0 ± 30.0	1.2 ± 0.2
2007	255.0 ± 20.5	7.7 ± 0.5	9.4 ± 0.5	1.7 ± 0.2
2009	340.5 ± 30.0	14.1 ± 1.0	19.1 ± 1.5	2.2 ± 0.5

The obtained results for the Uruguayan soils analysed from 2004 to 2009, show the following ranges:

^{226}Ra in Bq/kg: $7.2 \pm 0.5 - 23.2 \pm 2.0$

^{40}K in Bq/kg: $89.5 \pm 5.0 - 1,054.1 \pm 100.0$

^{232}Th in Bq/kg: $5.5 \pm 0.5 - 75.4 \pm 5.0$

^{137}Cs in Bq/kg : $< \text{DL} - 3.4 \pm 0.2$

The percentage distributions of food products analysed during 2009 are shown in Fig. 3. The mean (n=30) activity concentrations of the radionuclides of the ^{238}U series (^{226}Ra), ^{232}Th series (^{228}Ra and ^{232}Th), ^{40}K and ^{137}Cs in food products are expressed in Bq/kg of dry matter, and are presented in Tables 5 and 6.

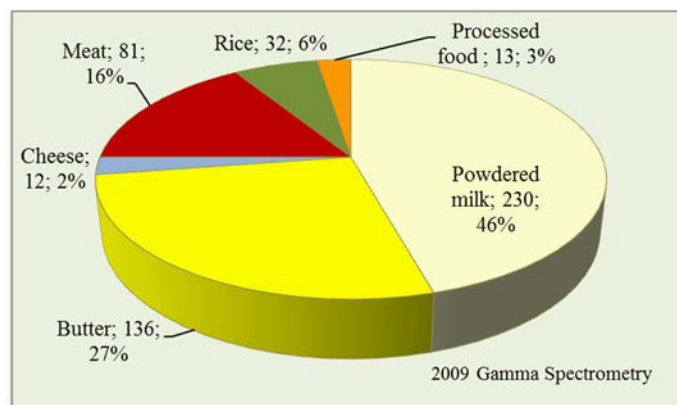


FIG. 3. Type of samples analysed by gamma-ray spectrometry in 2009.

TABLE 5. RADIONUCLIDES IN URUGUAYAN FOOD PRODUCTS FOR THE YEAR 2009

FOOD	^{40}K (Bq/kg)	^{226}Ra (Bq/kg)	^{232}Th (Bq/kg)	^{137}Cs (Bq/kg)
Milk	465.0 ± 40.0	1.5 ± 0.5	1.1 ± 0.5	<DL
Butter	48.4 ± 45.5	1.5 ± 0.5	0.7 ± 0.1	<DL
Cheese	72.0 ± 5.0	1.4 ± 0.5	0.6 ± 0.1	<DL
Meat	133.0 ± 10.5	0.8 ± 0.1	0.7 ± 0.1	<DL
Rice	60.9 ± 5.5	0.9 ± 0.1	0.7 ± 0.1	<DL

The obtained results in powdered milk analysed during 2009, show the following ranges:

^{226}Ra in Bq/kg: < DL – 6.9 ± 0.5

^{40}K in Bq/kg: 240.0 ± 20.0 – 645.3 ± 60.5

^{232}Th in Bq/kg: < DL – 2.9 ± 0.2

Food products ^{137}Cs in Bq/kg: < DL

TABLE 6. RADIONUCLIDES IN URUGUAYAN MEAT FOR THE YEAR 2009

	Departments	^{40}K (Bq/kg)	^{226}Ra (Bq/kg)	^{232}Th (Bq/kg)	^{137}Cs (Bq/kg)
32° 26' S 54° 19' W	Cerro Largo	142.6 ± 10.5	0.8 ± 0.1	0.5 ± 0.1	<DL
34° 10' S 57° 41' W	Colonia	134.9 ± 10.0	1.0 ± 0.1	0.6 ± 0.1	<DL
33° 33' S 26° 53' W	Flores	143.3 ± 10.5	0.6 ± 0.1	<DL	<DL
33° 47' S 55° 49' W	Florida	152.8 ± 15.0	0.9 ± 0.1	0.7 ± 0.1	<DL
33° 55' S 54° 57' W	Lavalleja	162.0 ± 15.5	0.6 ± 0.1	<DL	<DL
32° 03' S 57° 19' W	Paysandú	142.5 ± 10.5	0.7 ± 0.1	<DL	<DL
31° 28' S 55° 15' W	Rivera	140.3 ± 10.0	0.8 ± 0.1	<DL	<DL
32° 47' S 57° 26' W	Río Negro	126.2 ± 10.0	0.7 ± 0.1	<DL	<DL
31° 18' S 57° 02' W	Salto	147.3 ± 10.5	1.5 ± 0.2	0.5 ± 0.1	<DL
33° 31' S 57° 45' W	Soriano	133.9 ± 10.0	0.7 ± 0.1	<DL	<DL
33° 03' S 54° 13' W	Treinta y Tres	162.4 ± 15.0	1.2 ± 0.2	0.7 ± 0.1	<DL

5. DISCUSSION

In the case of ^{40}K , the observed activity concentration is the most significant of all the natural radionuclides measured in soils and in food products, especially when it is measured in milk powder. In the case of the other natural radionuclides of the ^{238}U and ^{232}Th series the activity concentrations in soils and in food products are significantly lower than for ^{40}K and in soils samples higher than in food products. In the case of ^{137}Cs , for all analysed samples by gamma-ray spectrometry of Uruguayan food products, it is not possible to distinguish between the signal and the background, therefore the activity concentrations of ^{137}Cs are lower than the detection limit. In the environmental samples analysed, only in soils it is possible to quantify ^{137}Cs and the values obtained are between: $< \text{DL} - 3.4 \pm 0.2$ in Bq/kg of dry matter. The detection limit for ^{137}Cs is 0.5 Bq/kg for a counting time of 64,800 s.

6. CONCLUSIONS

The environmental radioactivity monitoring plan in Uruguay has been expanded every year, and its goal is to obtain environmental samples from all departments of the country. The plan aims to install an automatic monitoring station in Montevideo, the most populated place in the country, in order to generate a small network, with the already existing station, located near the nuclear facilities of the neighbouring country.

Up to now, Uruguay doesn't have nuclear power plant facilities and it does not have nuclear research reactors. In 2006, the President of Uruguay appointed a Commission to study the possibility of a nuclear facility related to energy production. The Commission followed the guidelines and recommendations of the IAEA.

The obtained results for food products show that the values are not higher than the values of the natural background. It confirms that the concept taken by the government to be a 'natural country' is real from the radioactive point of view. According to the ALARA principle for protection of the population, exposure should be 'as low as reasonably achievable'. Uruguay is working in the regulatory framework to base national regulations on the results of its environmental radioactivity monitoring plan.

The obtained results in soils show that the activity concentrations of ^{137}Cs are low and can be attributed to the atmospheric fallout.

7. ACKNOWLEDGEMENTS

We want to thank the Intendencia Municipal de Colonia and Intendencia Municipal de San José and Ms. Carmen Villasante from Cerro Largo for providing support in sampling, the IAEA for assistance in the design of the environmental radioactivity monitoring plan in Uruguay.

REFERENCES

- [1] INSTITUTO NACIONAL DE ESTADISTICA, Uruguay en Cifras 2009, <http://www.ine.gub.uy/biblioteca/uruguayencifras2009/>.
- [2] L' ANNUNZIATA, M., Handbook of Radioactivity Analysis, 2nd edn, Academic Press, California (2003).
- [3] FRIEDLANDER, G., KENNEDY, J.W., MACIAS, E.S., MILLER, J.M., Nuclear and Radiochemistry, 3rd Edition, New York (1981).

- [4] THE COMMISSION OF THE EUROPEAN COMMUNITIES, Commission Recommendation on the Application of Article 36 of The Euratom Treaty Concerning the Monitoring of the Levels of Radioactivity in the Environment for the Purpose of Assessing the Exposure of the Population as a Whole, 2000/473/Euratom, Brussels (2000).
- [5] INTERNATIONAL ATOMIC ENERGY AGENCY, Environmental and Source Monitoring for Purposes of Radiation Protection, IAEA Safety Standards for protecting people and the environment, Safety Guide No.RS-G-1.8, IAEA, Vienna (2005).
- [6] INTERNATIONAL ATOMIC ENERGY AGENCY, Measurement of Radionuclides in Food and the Environment, a Guidebook, Technical Report Series No295, IAEA, Vienna (1989).
- [7] INTERNATIONAL ATOMIC ENERGY AGENCY, Manual de Procedimientos Técnicos Armonizados para la Determinación de la Contaminación Radiactiva en Alimentos (2005).
- [8] CURRIE, L.A., Limits for Qualitative Detection and Quantitative Determination, Anal. Chem. **40** 3 (1968) 586-593.
- [9] EURACHEM/CITAC GUIDE CG 4, Quantifying Uncertainty in Analytical Measurement, 2nd ed. (2000).
- [10] KONIECZKA, P., NAMIESNIK, J., Quality Assurance and Quality Control in the Analytical Chemical Laboratory, IAEA - TECDOC 619 validación IAEA BSS 115 (2009).

RECENT ADVANCES IN HAND-HELD XRF FOR SITE REMEDIATION

J.I.H. PATTERSON

Bruker, Kennewick, Washington, U.S.A.

Email: John.Patterson@Bruker.com

Abstract

Hand-held XRF has become a standard tool for site analysis when studying the level of hazardous elements in soil and mapping the extent of contamination. In recent years the implementation of Silicon Drift Detectors (SDD) as an alternative to SiPIN detectors, has yielded dramatic improvements in count rate and resolution, enhancing the performance of these systems for soil analysis. Among the improvements is the ability to measure realistic levels of light elements such as Si, S, P, Cl and improving the detection limit for K and Ca all of which are common components in soil. This allows not only quantification of these elements, but substantially improves the overall analysis by providing extended direct measurement of total elemental content. In addition to light element detection, SDD technology provides better resolution and peak-to-background, thus contributing to lower detection limits for most hazardous elements such as Cd, Pb, Hg and Sr. Beyond discussing new detector technology, site specific calibrations, which allow the addition of elements not typically measured in standard soil analyses, are discussed. Calibrations, including elements such as Cs and U, and type standardization allow 'tuning' of a factory calibration to specific locations. Finally, the concepts of limit of detection and limit of quantification are discussed.

1. INTRODUCTION

Hand-held XRF has long been accepted as a method for monitoring environmental contamination. In 1998 the US EPA published EPA Method 6200 Field Portable X-Ray Fluorescence Spectrometry for the Determination of Elemental Concentrations in Soil and Sediments [1]. This method provided guidance on the use of XRF in the field for the determination of heavy metal contamination. Table 1 gives examples of the limits of detection, which were achieved using that method. :

TABLE 1: EPA 6200 DETECTION LIMITS

EPA 6200	
LOD	
mg/kg	
Arsenic (As)	40
Cadmium (Cd)	100
Chromium (Cr)	150
Lead (Pb)	20
Mercury (Hg)	30
Silver (Ag)	70
Strontium (Sr)	10

In addition, the IAEA has had an active program regarding the use of XRF as a measurement technique for the determination of elemental composition in soil and other site remediation.

In the years since EPA Method 6200 became available major changes have occurred to the measurement equipment and accessories, which make the measurement much more sensitive and easier to interpret. The two major hardware changes, which have occurred since EPA 6200 was first published, are the incorporation of miniature X-ray tubes to replace the radioactive sources and the introduction of Silicon Drift Detectors. As miniature X-ray sources have been available for many years they will not be discussed in any detail. The introduction of Silicon Drift Detectors however is recent and will be discussed in some detail. In addition the incorporation of GPS and mapping capabilities has been more recent and provides a capability, which will be discussed briefly.

2. SILICON DRIFT DETECTORS

The introduction of the Silicon Drift Detectors (SDD) to hand-held XRF represents a major step in the improvement of the performance of such devices. The classic detector for hand-held XRF has been the SiPIN detector. The SiPIN detector is basically a small piece of silicon with metal electrodes on both sides of the device. When X-rays enter the silicon, they cause electrons to be generated, which are then collected at the electrodes. Due to the nature of the construction of SiPIN detectors, the capacitance of the detector will increase with the area of the detector. This capacitance impacts the performance of the detector. As the capacitance increases, the count rate, which can be achieved, decreases and the resolution of the detector degrades.

The SDD has a completely different construction. In a SDD, instead of two solid contacts as used in the SiPIN detector, one side of the device is patterned with a series of rings. These rings allow an electric field to be applied to the device, which cause the electrons generated by the X-rays to be directed to the middle of the device and to be collected in a small central contact on the device. This change dramatically reduces the capacitance of the detector and thus improves the resolution of the detector and greatly increases the count rate, which the pulse processor connected to the device can process.

In the Bruker X-Flash™ SDD the FET is built directly in the device. This construction has the advantage that the resolution remains essentially constant over a very large range of count rates. The advantage of the improved resolution and count rate is that improved limits of detection can be achieved in a fixed period of time. As the detection limit is related to the square root of the number of counts in a peak, increasing the count rate by a factor of nine will improve the limit of detection by a factor of three.

In addition, the SDD is capable of measuring lower atomic number elements due to dramatically improved low energy resolution and careful instrument design. When using SiPIN detectors, the lowest atomic number element, which is considered detected is $Z=22$ or Titanium. In some systems, a vacuum or helium environment is used to improve the lower atomic number sensitivity. In the case of SDDs, the electrode on the ‘back’ of the device, i.e. the side in which the X-rays enter, is made as thin as possible. In addition, the Be window of the detector is made as thin as possible. Finally, the geometry of the sample to detector is kept as tight as possible in order to enable SDD-based analysers to ‘detect’ lighter elements such as Al and Si. Typical LOD for the lower atomic number elements are shown in Table 2. The incorporation of a vacuum system is possible to improve the detection of the low atomic number elements. It must be noted that elements with atomic number less than 12 (e.g. Na, F and C) cannot be detected using current generation hand-held XRF analysers.

TABLE 2. EXAMPLES OF LIMIT OF DETECTION FOR LOW Z ELEMENTS

AN	Element	LOD
		mg/Kg
12	Mg	6600
13	Al	1050
14	Si	790
16	S	90
20	Ca	50
30	Zn	4

The ability to measure the matrix of the sample greatly improves the accuracy of the analysis of the contaminant in the sample as the entire composition of the sample can be measured. Further, the ability to measure the lighter elements allows the selection of the calibration, which is most appropriate for the matrix of the sample. For example, in most calibrations for soil samples, a SiO_2 matrix is assumed. If this is incorrect and the actual matrix is a Al_2O_3 -, K- or Ca-rich matrix, this assumption can lead to substantial error.

3. MAPPING

Easy-to-use global positioning systems (GPS) have recently been implemented in hand-held XRF analysers. This allows the position of each sample to be recorded simultaneously with the assay. Current differential GPS systems allow spatial resolution of about 10 cm, so it is possible to very accurately know the location of each sample. By using this information with a good mapping software, it is possible to very easily visualize the contamination pattern.

Figure 1 represents a typical map of environmental contamination.

This map shows the grid used for the measurements and color-codes the level of contamination determined. With appropriate mapping software this level of detail is easy to achieve.

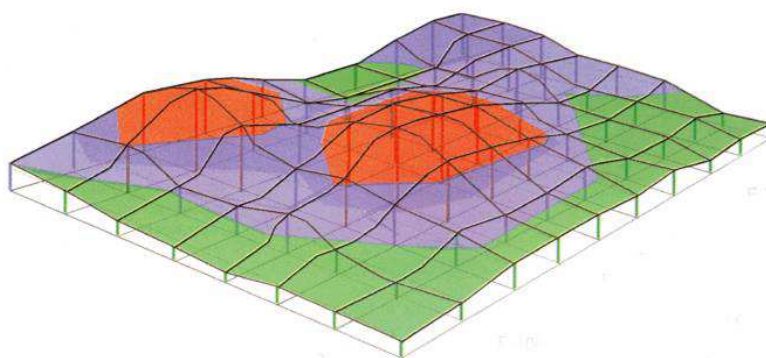


FIG.1 Map of environmental contamination with 'hot-spots' highlighted.

4. SAMPLING

When considering the use of hand-held XRF in the field, the first issue, which must be considered, is the nature of the sampling and the preparation of the sample to be performed before the analysis is made. The preparation of the sample can be as simple as removing any debris from the soil surface and placing the XRF instrument on the surface and making the measurement (e.g. in-situ sampling). Alternatively a representative sample can be removed from the area (typically a 10x10x2.5 cm³ area), dried, ground and well prepared before being put into a sample cup for XRF analysis (e.g. intrusive analysis). In all studies, the exact nature of the sample preparation will be determined by the data quality objectives of the study. Simple in-situ sampling with averaging of multiple points will provide a good general understanding of the nature and extent of the contamination. However, it will most likely result in substantial variability of the results from location to location. Factors such as moisture in the sample and particle size can cause variations in the results and affect the accuracy of the results. On the other hand, intrusive sampling followed by proper sample drying, grinding and preparation will provide a very consistent set of results with good precision and accuracy. In either case it is essential that about 5% to 10% of the samples analysed by hand-held XRF are sent to the laboratory for complete chemical analysis to ensure that accurate analysis is being done and to confirm the relationship between the results generated by the hand-held XRF and the laboratory results.

5. SITE SPECIFIC CALIBRATION AND TYPE STANDARDIZATION

The nature of the sample matrix and physical condition can have a substantial impact on the accuracy of the results obtained using hand-held XRF. Therefore, it may be desirable to perform a site specific calibration for the study. In addition, if an element of interest is not contained in the manufacturer's factory supplied calibration, this may be the only way to add the desired element to the calibration of the analyser. Site specific calibration is achieved by performing an empirical calibration using a set of samples, which have been carefully analysed in the laboratory.

The known samples are measured using the analyser and the concentration information is an input to the calibration program for the specific analyser being used. The software for the analyser then determines the relationship between the peak area and the concentration of the various elements. In addition, any matrix effects and inter-element interferences can be taken into account. This approach, which can be quite time consuming in both the collection and measurement of known samples and measuring those samples on the analyser, will in most cases provide the most accurate results.

An alternative, which is implemented on some hand-held XRF analysers, is the use of type standardization. In most commercial analysers available today, the environmental calibration is a fundamental parameter calibration. That means that the calibration is based on information specific to the analyser and basic theoretical understanding of X-ray physics. This approach gives good results, but may not be correct for any specific location because of differences in the matrix, particle size, moisture content in the sample or other sample-related factors. In most cases these factors will cause an error, which is linearly related to the concentration of the sample being measured. If this is the case, a simple linear correction as follows will provide a more accurate analysis of the sample.

$$\text{Actual Assay} = \text{Slope} \times \text{Measured Assay} - \text{Offset}$$

In this case, a number of samples, which cover the concentration range of interest, can be analysed in the laboratory and the correlation can be an input to the type standardization of the analyser. All results generated by the analyser will then be corrected and will compare well with the laboratory analysis. The spreadsheet, shown in Table 3, shows an example of this type of relationship.

TABLE 3. EXAMPLES OF TYPE STANDARDIZATION

Element 1	Ni	
SLOPE	0.6917	
OFFSET	3.5507	
CORRELATION	99.7%	
Reference values	S1 Meas. Results	Adjusted S1 Result
0	0	3.55
100	131.1	94.24
180	219.45	155.35
500	792.17	551.53
1,000	1,404.84	975.33

In order to determine if such a relationship exists for a specific situation, the XRF values for a set of samples can simply be compared with the laboratory results. If the correlation is greater than about 90%, this method can be used.

6. DETECTION LIMITS

As a result of competitive pressure and to make the calculation as easy as possible most XRF manufacturers report Limits of Detection (LOD), which are calculated as follows:

$$\text{LOD} = 3 \times \sqrt{\text{BKG}} \times \text{Sens}$$

With:

BKG the background, i.e. the average counts in region of interest in counts/second;

Sens the sensitivity, i.e. the slope of calibration curve in ppm/cps.

This calculation represents the signal, which can be statistically distinguished from the background expressed as a concentration. However, if a sample with exactly this concentration is measured repeatedly, the result would only be detected about 50% of the time. This is a very unrealistic representation of the capabilities of the equipment. The only meaningful use of this value is the comparison of one instrument with another. A much better representation of the concentration, which can be measured accurately, is the Limit of Quantification (LOQ), which is three times the limit of detection. This value represents the minimum level of the analyte, which can be quantified in a meaningful way.

Table 4 shows the LOD and LOQ for 180 s measurements (Note: the LOD and LOQ will get better as measurement time is extended, as the sensitivity increases linearly with time while the noise increases as the square root of the measurement time). This table represents the values achieved using the Bruker S1 TITAN hand-held analyser; however, these values are representative of the state-of-the-art in SDD-based analysers available in the market today. When evaluating the various options, many factors affect the exact LOD for each element and some analysers will have lower LODs for some elements and higher for others, so careful evaluation of the LOD for the elements of interest is required.

TABLE 4. CURRENT LOD AND LOQ

	EPA 6200	Current	Current
	LOD	LOD	LOQ
	mg/kg	mg/kg	mg/kg
Arsenic (As)	40	5	15
Cadmium (Cd)	100	17	51
Chromium (Cr)	150	14	42
Lead (Pb)	20	11	33
Mercury (Hg)	30	6	18
Silver (Ag)	70	13	39
Strontium (Sr)	10	5	15

7. CONCLUSIONS

The modern hand-held XRF analyser with a Silicon Drift Detector and current modern software capabilities provides an excellent method of performing fast and accurate analysis of environmental samples. The measurable limits for most heavy metals are in the order of about 10 to 20 mg/kg.

REFERENCE

- [1] United States Environmental Protection Agency, Method 6200 Field Portable X-Ray Fluorescence Spectrometry for the Determination of Elemental Concentrations in Soil and Sediments, Washington DC, USA (1998).

CONTRIBUTORS TO DRAFTING AND REVIEW

Ceccatelli, A.	International Atomic Energy Agency
Karydas, A.G.	International Atomic Energy Agency
Margui, E.	University of Girona, Spain
Mauring, A.	International Atomic Energy Agency
Pitois, A.	International Atomic Energy Agency
Tsabaris, C.	Hellenic Centre for Marine Research, Greece



IAEA

International Atomic Energy Agency

No. 25

ORDERING LOCALLY

In the following countries, IAEA priced publications may be purchased from the sources listed below or from major local booksellers.

Orders for unpriced publications should be made directly to the IAEA. The contact details are given at the end of this list.

CANADA

Renouf Publishing Co. Ltd

22-1010 Polytek Street, Ottawa, ON K1J 9J1, CANADA

Telephone: +1 613 745 2665 • Fax: +1 643 745 7660

Email: order@renoufbooks.com • Web site: www.renoufbooks.com

Bernan / Rowman & Littlefield

15200 NBN Way, Blue Ridge Summit, PA 17214, USA

Tel: +1 800 462 6420 • Fax: +1 800 338 4550

Email: orders@rowman.com Web site: www.rowman.com/bernan

CZECH REPUBLIC

Suweco CZ, s.r.o.

Sestupná 153/11, 162 00 Prague 6, CZECH REPUBLIC

Telephone: +420 242 459 205 • Fax: +420 284 821 646

Email: nakup@suweco.cz • Web site: www.suweco.cz

FRANCE

Form-Edit

5 rue Janssen, PO Box 25, 75921 Paris CEDEX, FRANCE

Telephone: +33 1 42 01 49 49 • Fax: +33 1 42 01 90 90

Email: formedit@formedit.fr • Web site: www.form-edit.com

GERMANY

Goethe Buchhandlung Teubig GmbH

Schweitzer Fachinformationen

Willstätterstrasse 15, 40549 Düsseldorf, GERMANY

Telephone: +49 (0) 211 49 874 015 • Fax: +49 (0) 211 49 874 28

Email: kundenbetreuung.goethe@schweitzer-online.de • Web site: www.goethebuch.de

INDIA

Allied Publishers

1st Floor, Dubash House, 15, J.N. Heredi Marg, Ballard Estate, Mumbai 400001, INDIA

Telephone: +91 22 4212 6930/31/69 • Fax: +91 22 2261 7928

Email: alliedpl@vsnl.com • Web site: www.alliedpublishers.com

Bookwell

3/79 Nirankari, Delhi 110009, INDIA

Telephone: +91 11 2760 1283/4536

Email: bkwell@nde.vsnl.net.in • Web site: www.bookwellindia.com

ITALY

Libreria Scientifica "AEIOU"

Via Vincenzo Maria Coronelli 6, 20146 Milan, ITALY

Telephone: +39 02 48 95 45 52 • Fax: +39 02 48 95 45 48

Email: info@libreriaaeiou.eu • Web site: www.libreriaaeiou.eu

JAPAN

Maruzen-Yushodo Co., Ltd

10-10 Yotsuyasakamachi, Shinjuku-ku, Tokyo 160-0002, JAPAN

Telephone: +81 3 4335 9312 • Fax: +81 3 4335 9364

Email: bookimport@maruzen.co.jp • Web site: www.maruzen.co.jp

RUSSIAN FEDERATION

Scientific and Engineering Centre for Nuclear and Radiation Safety

107140, Moscow, Malaya Krasnoselskaya st. 2/8, bld. 5, RUSSIAN FEDERATION

Telephone: +7 499 264 00 03 • Fax: +7 499 264 28 59

Email: secnrs@secnrs.ru • Web site: www.secnrs.ru

UNITED STATES OF AMERICA

Bernan / Rowman & Littlefield

15200 NBN Way, Blue Ridge Summit, PA 17214, USA

Tel: +1 800 462 6420 • Fax: +1 800 338 4550

Email: orders@rowman.com • Web site: www.rowman.com/bernan

Renouf Publishing Co. Ltd

812 Proctor Avenue, Ogdensburg, NY 13669-2205, USA

Telephone: +1 888 551 7470 • Fax: +1 888 551 7471

Email: orders@renoufbooks.com • Web site: www.renoufbooks.com

Orders for both priced and unpriced publications may be addressed directly to:

Marketing and Sales Unit

International Atomic Energy Agency

Vienna International Centre, PO Box 100, 1400 Vienna, Austria

Telephone: +43 1 2600 22529 or 22530 • Fax: +43 1 2600 29302 or +43 1 26007 22529

Email: sales.publications@iaea.org • Web site: www.iaea.org/books

